RECOVERY OF KRAFT BLACK LIQUOR INCLUDING DIRECT CAUSTICIZATION

by

XUEJUN ZOU

A Thesis Submitted to the Faculty of Graduate Studies and Research in Partial Fulfillment of the Requirements for the Degree of Doctor of Philosophy

Department of Chemical Engineering
McGill University
Montrel, Quebec, Canada

August 1991

ACKNOWLEDGEMENTS

This work would not have been possible without the guidance and support of **Drs. Avedesian and van Heiningen.** Their confidence in my abilities and timely suggestions made my time spent at McGill University both enjoyable and fruitful.

The discussions with **Drs. Kubes and Li,** were always constructive and valuable.

I am also indebted to a number of members of our **CRISP** group: **Yonghao, Pritham, Aliye, Paul, Victor,** and **Mr. A. K. Tiwari,** for their help and friendship.

Special thanks to Mr. **J. Dumont** at the Departmental Stores for his kind help with the selection and purchasing of the equipment and materials, and to **Dr. E. Milanova, Mr. J. Ing,** and **Ms. G. de Silveira** at PAPRICAN for their help with respectively thermal, chemical and microscopic analyses. I would also like to thank **Ms. McGuinness, Ms. McCaffrey,** and **Ms. Shaie** for their help on various occasions.

I am also grateful to the **Chinese Academy of Science** and **PAPRICAN** for the awarded scholarships.

Finally, I would like to thank my family for the moral support they have given me throughout my academic career; my parents who always understood me, and my wife and little son for their patience and love.

ABSTRACT

The direct causticization of kraft black liquor is investigated both thermodynamically and experimentally. A comprehensive thermodynamic analysis is performed to identify suitable causticizing metal oxides and process configurations. TiO_2 is found to be the only metal oxide which can be used for kraft black liquor recovery. Of two possible process configurations, the two-step combustion and reduction process is selected for further experimental study in the present work.

The kinetics of the direct causticization reaction between Na_2CO_3 and TiO_2 in a mixture with Na_2SO_4 are studied in a tube furnace from 750 to 925°C. It is found that complete conversion of Na_2CO_3 can easily be achieved when using a TiO_2/Na_2CO_3 molar ratio of at least 1.25, leading to the formation of $4Na_2O{\cdot}5TiO_2$. The formation kinetics of $4Na_2O{\cdot}5TiO_2$ are well described by a reaction model with product layer control. Insoluble $Na_2O{\cdot}3TiO_2$, obtained from hydrolysis of $4Na_2O{\cdot}5TiO_2$, can be recycled and reused for CO_2 release from fresh Na_2CO_3.

The influence of TiO_2 addition on kraft black liquor combustion is investigated using thermoanalytical techniques. The combustion of kraft black liquor is improved despite the large mass fraction of TiO_2. The melting point of the combustion product of a mixture of kraft black liquor and TiO_2 is much higher than that of pure kraft black liquor. Similar to the experiments with the model mixtures, it is also found that complete conversion of Na_2CO_3 during kraft black liquor combustion can easily be achieved when the TiO_2/Na_2CO_3 molar ratio is at least 1.25. The presence of TiO_2 reduces the sulfur loss during combustion. A high causticizing efficiency is obtained with recycled $Na_2O{\cdot}3TiO_2$.

The kinetics of the reduction of sodium sulfate mixed with sodium titanate by both CO and H_2 are studied in a thermogravimetric system. The H_2 reduction kinetics are described by the nucleation and growth model up to 60% conversion and by the shrinking core model for higher conversions. The CO reduction kinetics are described by nucleation and growth model up to 95%. Both the H_2 and CO reduction are accelerated by the initial presence of Na_2S and are catalyzed by iron oxide. The influence of H_2 and CO concentrations, H_2O and CO_2 concentrations and mass fraction of sodium titanate is also investigated. The combustion product of a mixture of kraft black liquor and TiO_2 is even faster reduced by H_2 and CO than the model mixtures.

RESUME

La caustification directe de la liqueur noire Kraft a été l'objet d'une étude thermodynamique et expérimentale. Une analyse thermodynamique éxaustive fut accomplie pour identifier les oxydes métalliques convenables et choisir les procédés adéquats. TiO_2 s'est avéré le seul oxyde métallique qui peut être utilisé avec la liqueur noire Kraft. Parmi deux configurations de procédés possibles, celle de la combustion et réduction à deux étapes est sélectionnée pour être utilisée dans la partie expérimentale de ce travail.

La cinétique de caustification directe entre Na_2CO_3 et TiO_2 dans un mélange avec Na_2SO_4 est etudiée dans un four cylindrique entre 750 et 925°C. Il s'est avéré que la conversion complète de Na_2CO_3 en $4Na_2O{\cdot}5TiO_2$ s'achève facilement quand le rapport molaire de TiO_2/Na_2CO_3 est au moins égale à 1.25. La cinétique de formation de $4Na_2O{\cdot}5TiO_2$ est bien décrite par une réaction modèle avec un contrôle de phases. $Na_2O{\cdot}3TiO_2$ insoluble, produit de l'hydrolyse de $4Na_2O{\cdot}5TiO_2$, peut être recyclé et réutilisé pour libérer de CO_2 à partir de Na_2CO_3 frais.

L'influence de l'addition de TiO_2 durant la combustion de la liqueur noire est étudiée en utilisant des techniques thermogravimétriques.

Le point de fusion du produit de la combustion du mélange (liqueur noire et TiO_2) est beaucoup plus élevé que celui de la liqueur noire pure. Egalement, pour des mélanges modèles, l'expérience a monté que la conversion de Na_2CO_3 durant la combustion s'achève facilement quand le rapport molaire TiO_2/Na_2CO_3 est au moins égale à 1.25. La presence de TiO_2 reduit la perte du soufre durant la combustion. Un haut rendement de caustification est obtenu après recyclage de $Na_2O{\cdot}3TiO_2$.

La cinétique de la réduction du mélange sulfate et titanates de soduim par CO et H_2 est etudiée par un système thermogravimètrique. Deux modéles cinétiques sont adoptés; formation et croissance des noyaux et contractions des noyaux, le premier est appliqué durant la réduction avec H_2 pour des conversions allant jusqu'à 60%, le second est utilisé pour des conversions plus élevées. Pour la réduction avec CO, seulement le premier modéle est applique. La réaction de réduction par H_2 et CO est accélérée par la presence de Na_2S initial et catalysée par l'oxyde de fer. L'influence des concentrations de H_2, CO, H_2O, CO_2 et des fractions massiques de titanates de soduim est aussi examinée. Le produit de combustion du mélange liqueur noire et TiO_2 est reduit plus rapidement que celui du mélange modèle.

TABLES OF CONTENTS

CHAPTER 4 KINETICS OF DIRECT CAUSTICIZING REACTION BETWEEN SODIUM CARBONATE AND TITANIUM DIOXIDE

CHAPTER 5 KRAFT BLACK LIQUOR COMBUSTION AND DIRECT CAUSTICIZATION WITH TITANIUM DIOXIDE

CHAPTER 6 HYDROGEN REDUCTION OF SODIUM SULFATE MIXED WITH SODIUM TITANATE

CHAPTER 7 CO REDUCTION OF SODIUM SULFATE MIXED WITH SODIUM TITANATE

CHAPTER 8 GENERAL CONCLUSIONS

LIST OF FIGURES

CHAPTER 4

CHAPTER 5

CHAPTER 6

CHAPTER 7

LIST OF TABLES

CHAPTER 1

INTRODUCTION

INTRODUCTION

In conventional kraft pulping, the major chemical pulping process, wood fibers are liberated at elevated temperature and pressure with an aqueous solution of NaOH and Na_2S or white liquor (Casey, 1980 and Smook, 1986). The spent cooking solution, called kraft black liquor, contains 50% of the dissolved wood and most of the pulping chemicals. After evaporation to about 70% solids concentration, black liquor is burned in the recovery furnace. The inorganic salts leave the bottom of furnace as a smelt. After dissolving the smelt, a so-called green liquor is obtained containing mostly Na_2CO_3 and Na_2S. The green liquor is sent to the causticizing process where Na_2CO_3 is converted into NaOH with slaked lime so that the resulting white liquor can be reused in the pulping process.

Although the objective of chemical recovery is adequately achieved in present commercial operations, several major drawbacks are associated with conventional recovery, such as a very high capital cost, the smelt-water explosion hazard, the corrosive nature of the smelt and the complicated and energy-consuming character of the causticizing step. For more than two decades the industry has been investigating alternative chemical recovery processes to overcome these problems. The alternative processes can be roughly divided into two groups according to their principal aims. The first group consists of methods which replace the conventional recovery furnace and eliminate the smelt explosion hazard. Examples of these alternatives are wet combustion, (Pradit, 1969), fluidized bed combustion (Lea, 1969), hydropyrolysis (Timpe, 1973) and the SCA-Billerud process (Horntwedt, 1968). The second group deals with the elimination of the lime cycle. Examples of this group are autocausticization and direct causticization using amphoteric oxides for sodium carbonate conversion (Janson, 1977; Kiiskila, 1979) and gasification using a plasma reactor (Bernhard, 1985). The difference between autocausticization and direct causticization is that in autocausticization, the amphoteric oxide also serves as caustic cooking chemical, which causticizes itself in a combustion process. However, in direct causticization, the amphoteric oxide is not a cooking chemical but causticizes Na_2CO_3 during combustion. After immersion in water, the insoluble metal oxide is separated and recycled for renewed causticization of Na_2CO_3. Among the second group, only the direct causticizing process employing the metal oxide, Fe_2O_3, is presently in operation for recovery of soda liquor (Maddern, 1987).

The ultimate objective of the present research is to produce white liquor by applying the direct causticizing technology to the recovery of kraft black liquor.

DESCRIPTION OF CAUSTICIZING PROCESSES

I. Conventional Causticizing Process

In the conventional causticizing process, sodium carbonate is converted into sodium hydroxide, and various impurities introduced with the wood are removed. As shown in Figure 1, the operation starts with dissolving the furnace smelt in weak liquor to form green liquor. The green liquor is then clarified to remove "dregs". It subsequently reacts with lime (CaO) to form white liquor. The white liquor is clarified by precipitation of "lime mud" ($CaCO_3$), and is then ready to be used for cooking. Auxiliary operations include washing of both the dregs and lime mud for soda recovery, and the calcining (reburning) of lime mud to regenerate lime.

The causticizing reaction occurs in two steps. Lime first reacts with water to form calcium hydroxide, which in turn reacts with sodium carbonate to form sodium hydroxide as:

$$\text{i)}\quad CaO + H_2O = Ca(OH)_2 \qquad (1)$$

$$\text{ii)}\quad Ca(OH)_2 + Na_2CO_3 = 2\ NaOH + CaCO_3\downarrow \qquad (2)$$

The completeness of the second reaction is known as causticizing efficiency. A high conversion is desirable to reduce the dead load of inert sodium carbonate in the liquor cycle. Typically, the causticizing efficiency can vary from 80 to 90%, depending on alkali concentration, sulfidity level and excess of lime.

Although the causticizing process is a routine commercial operation, it is also complex and suffers from high capital cost and some operating problems. The lime causticizing process has the following fundamental drawbacks:

i) The causticizing reaction is incomplete. The considerable sodium carbonate dead load has a negative impact on the energy consumption in the digester, evaporator, recovery furnace and lime kiln.

ii) Some calcium carbonate contaminates the sodium hydroxide stream.

iii) The lime kiln is the principal energy consumer in the causticizing

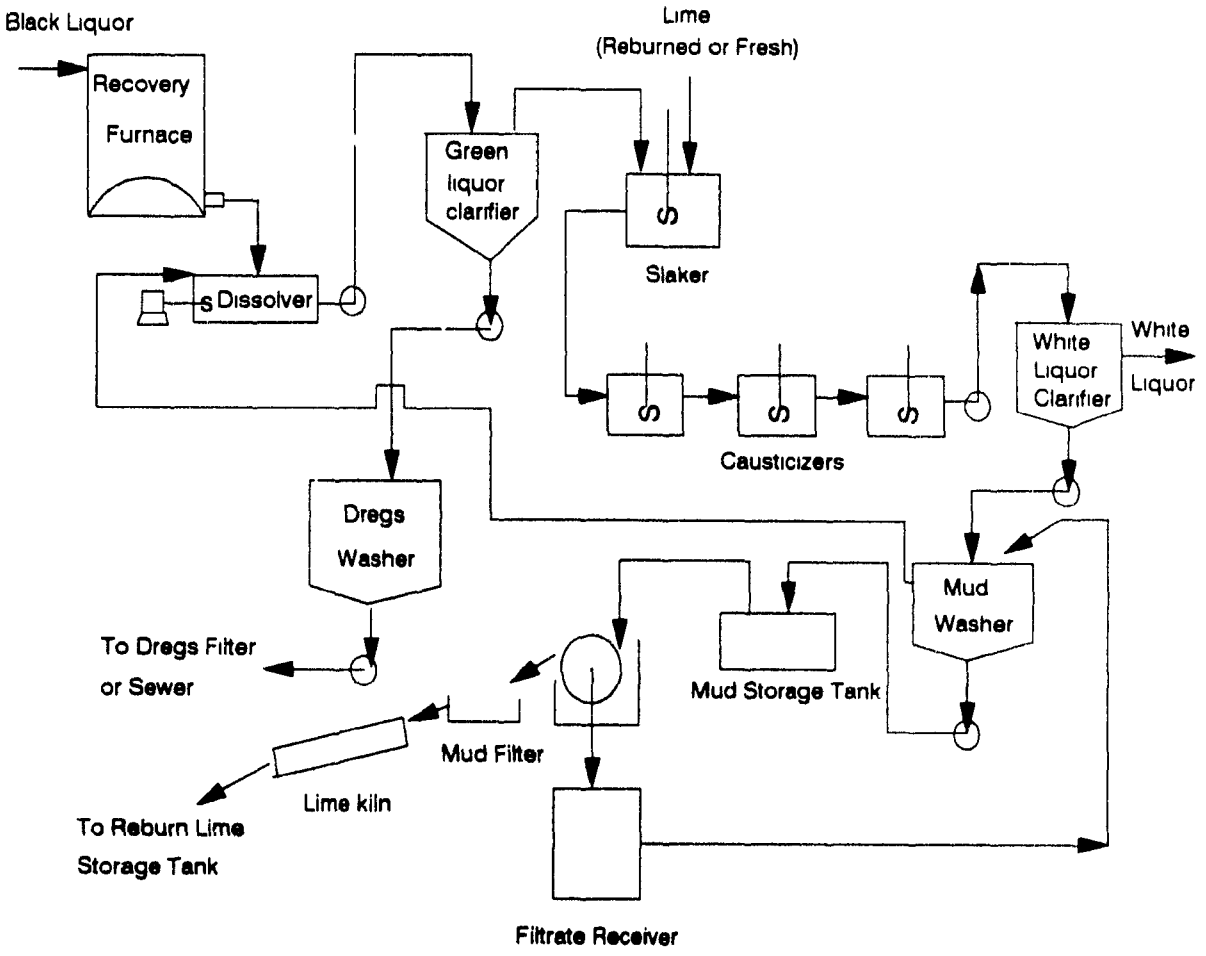

Figure 1 Conventional causticizing process

operation and is, in fact, the major consumer of external fuel in a pulp mill.

iv) The generation of lime dregs creates a disposal problem.

These problems form the impetus for the research to develop an improved method to causticize sodium carbonate.

II. Alternative Causticizing Processes

Spontaneous dissociation of sodium carbonate above its melting point is prevented in the conventional recovery furnace by the presence of a high partial pressure of carbon dioxide. If certain amphoteric or acidic oxides are present in the system, they can react with sodium carbonate to form a mixed oxide and liberate carbon dioxide. The mixed oxide forms a sodium hydroxide solution when contact with water. This series of reactions is called autocausticization or direct causticization, and eliminates the need for the lime cycle. The amphoteric oxides are divided into two main groups according to their behavior in the dissolving stage, and are discussed separately in the sections below.

Causticization with a soluble mixed oxide (Autocausticization)

This group of oxides consists of chemicals which form an alkaline solution in which the amphoteric oxides are at least partly soluble. The inorganic salts formed by this group of oxides are able to liberate carbon dioxide under conditions such as those in a recovery furnace. They are also sufficiently alkaline to replace sodium hydroxide during pulping and bleaching. In general, the autocausticizing process with an amphoteric oxide, Y, may be formulated as (Janson and Pekkala, 1977 and 1978):

Liberation of carbon dioxide:

$$Na_2CO_3 + n\ Y = Na_2Y_nO + CO_2 \qquad (3)$$

Dissolution:

$$Na_2Y_nO + H_2O = Na_2H_2Y_nO_2\ (aq.) \qquad (4)$$

Protolysis:

$$Na_2H_2Y_nO_2\ (aq.) = 2\ NaOH + n\ Y\ (aq.) \qquad (5)$$

Since the autocausticizing agent is water soluble, it accompanies the cooking chemicals in the whole liquor cycle. The agent therefore can be regarded as part of the cooking alkali. The oxides in this group include BO_3, P_2O_5, and SiO_2. A considerable amount of fundamental work has been done in Finland with BO_3 as causticizing chemical (Janson, 1977, Janson and Pekkala, 1977 and 1978). It was estimated that there will be a net reduction in investment cost for a new mill using this technology, rather than the conventional soda or kraft process configurations

However, even though soluble autocausticizing agents eliminate the causticizing cycle, they also change the characteristics of the white liquor produced. The impact of the presence of autocausticizing agents in white liquor on the pulping and recovery operation is not yet fully understood. Several other disadvantages can be identified in this process, such as the higher viscosity of black liquor at high solids concentration (Janson and Pekkala, 1978) and the almost double inorganic load as compared to the conventional recovery system that must be carried through the recovery cycle.

Causticization with an insoluble metal oxide (Direct causticization)

The second group of chemicals are metal oxides which can be precipitated to form sodium hydroxide solutions during the dissolving stage. The principle of direct causticizing using an insoluble oxide, M_xO_y, can be illustrated by the general reaction (Kiiskila, 1979):

$$a\ Na_2CO_3 + b\ M_xO_y = aNa_2O{\cdot}bM_xO_y + a\ CO_2 \uparrow \qquad (6)$$

The oxides proposed in literature are iron oxide, titanium dioxide and alumina.

The oxide circulation system is based on the general hydrolysis reaction:

$$aNa_2O{\cdot}bM_xO_y + (a+z)\ H_2O = 2a\ NaOH + bM_xO_y\ zH_2O \downarrow \qquad (7)$$

The precipitated causticizing agent $bM_xO_y{\cdot}zH_2O$, is separated from the white liquor and can be reused for direct causticization. The concept of direct causticization along with conventional causticization is shown in Figure 2

The direct causticizing process has the following advantages compared to the conventional causticizing process:

i) The elimination of the lime cycle reduces the energy, equipment and

manpower requirements.

ii) Since sodium hydroxide is directly obtained by dissolution of a double salt, a high concentration NaOH solution can easily be obtained. This favorably affects the water balance of the pulping process and accordingly superior heat economy can be expected.

iii) A causticizing efficiency of more than 90% can be easily obtained. Therefore, the dead load of Na_2CO_3 will be greatly reduced.

The potential disadvantages associated with this process are the price of causticizing agents, particularly of TiO_2; the accumulation of non-process elements in the liquor cycle; and the dead load of metal oxides in the oxide circulation system.

The applicability of the direct causticizing technology to the kraft recovery process depends on the stability of the metal oxides under reducing conditions. Fe_2O_3 is generally thought to be only applicable to the soda recovery process. TiO_2 and Al_2O_3 are potentially applicable to both soda and kraft recovery processes.

OBJECTIVES AND STRATEGY

The objective of the present study is to develop the direct causticizing technology for kraft black liquor recovery as an alternative to the conventional recovery process. More specifically, the objectives are to identify feasible process configurations with TiO_2 as causticizing chemical, and to obtain the rate equations and mechanisms of the key gas-solid and solid-solid reactions which occur in a direct causticizing process of kraft black liquor with TiO_2.

First, previous work on direct causticization and the general literature on gas-solid and solid-solid reaction kinetics are reviewed. Secondly, comprehensive thermodynamic calculations at high temperatures are performed to identify suitable process configurations for direct causticizing of kraft black liquor. Then, the mechanism and kinetics of the key reactions are determined experimentally with salt mixtures representative of those which would be obtained in the various stages of direct causticizing of kraft black liquor. The kinetic equations are then tested for actual black liquor or salt mixtures prepared from black liquor. The key reactions are: the direct causticizing reaction between Na_2CO_3 and TiO_2, the hydrolysis of $Na_2O{\cdot}xTiO_2$, and the reduction of sodium sulfate by CO and H_2 in the presence of

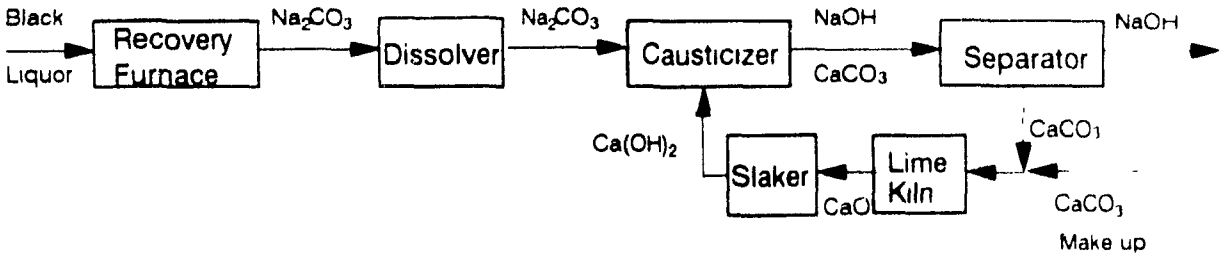

(a) Conventional causticization

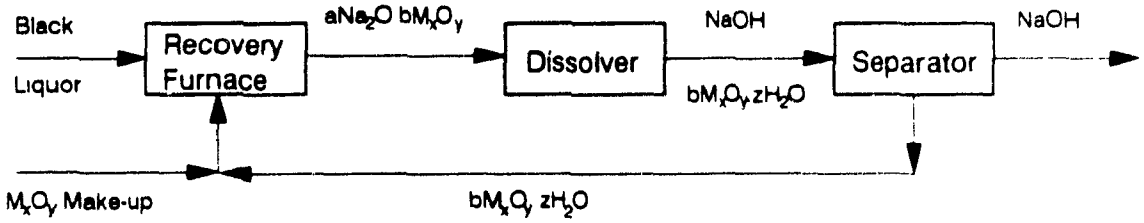

(b) Direct causticization

Figure 2 Comparison of conventional causticization with direct causticization

$Na_2O{\cdot}xTiO_2$. The kinetic study of the direct causticizing reaction is performed in a tube furnace system and conversion is determined from the CO_2 concentration in the exhaust gas. The reduction of Na_2SO_4 is determined in a thermogravimetric analysis system.

OUTLINE OF THE THESIS

This thesis is a fundamental investigation of the application of the direct causticizing technology to kraft black liquor recovery. After identification of TiO_2 as the only suitable direct causticizing chemical for kraft black liquor recovery, the rate processes and mechanisms of the various chemical reactions involved were studied. All experiments are performed with model compounds and actual black liquor solids in either a thermogravimetric or tube furnace system.

In chapter 2, the literature on direct causticizing and on gas-solid and solid-solid reaction kinetics is reviewed

The results of thermodynamic calculations are presented in Chapter 3. It is concluded that only TiO_2 is technically viable for kraft black liquor recovery and a two-step process including combustion and reduction is identified for further experimental study.

The kinetics and mechanism of the reaction between Na_2CO_3 and TiO_2 are presented in Chapter 4. The reaction is very fast if sufficient TiO_2 is available for formation of $4Na_2O{\cdot}5TiO_2$. The conversion data are analyzed following solid-solid reaction kinetics. The influence of temperature, CO_2 concentration and Na_2SO_4 molar fraction is determined.

In Chapter 5, the influence of TiO_2 addition on kraft black liquor combustion is studied. The results are presented in terms of characteristic combustion properties and the melting point of combusted product. The conversion of Na_2CO_3 in the direct causticizing reaction with TiO_2 during the combustion and the hydrolysis of the combustion product are also discussed.

The H_2 reduction kinetics of Na_2SO_4 in the presence of sodium titanate are presented in Chapter 6. The influence of the H_2 concentration, steam concentration, Na_2SO_4 molar fraction fraction, initial presence of Na_2S, and addition of Fe_2O_3 as a catalyst is investigated. The results obtained with kraft black liquor are compared with those of a model mixture. The reaction data are described by nucleation and growth kinetics. A reaction mechanism is proposed to explain the experimental data.

The CO reduction kinetics of Na_2SO_4 in the presence of sodium titanate are presented in Chapter 7 similar to that of the H_2 reduction kinetics in Chapter 6.

The general conclusions, suggestions for further work and the contributions to knowledge are presented in Chapter 8

The work described in Chapters 3, 4, 5, 6, and 7 has been written as self-contained papers suitable for publication with little or no further modifications. Thus each chapter has its own abstract, nomenclature, and references. As far as possible, uniform and standard symbols are used throughout the thesis. The major content in several chapters has been presented or will soon be presented at technical conferences. Specifically,

Chapter 3: presented at 1990 TAPPI Alkaline Pulping Conference, Toronto, Canada, Oct., 1990.

Chapter 4: will be presented at 1991 AIChE Annual Meeting, Los Angeles, USA, Nov., 1991.

Chapter 5: will be presented at 1991 TAPPI Alkaline Pulping Conference, Orlandor, USA, Oct., 1991.

Chapter 6: presented at 1990 Canadian Chemical Engineering Conference, Halifax, Canada, July, 1990.

Chapter 7: will be presented at 1991 Canadian Chemical Engineering Conference, Vancouver, Canada, Nov., 1991.

REFERENCES

Bernhard, R and Martenson, J., "Plasma Gasification of Kraft Black Liquor", *Proceedings of the 1985 International Chemical Recovery Conference*, p.245-247, TAPPI Press, Atlanta.

Casey, J.P., editor, *Pulp and Paper*, Vol.1, 3rd edition, John Wiley & Sons, New York, 1980.

Horntwedt, E., "The SCA-Billerud Recovery Process" *Proceedings of the Symposium on Recovery of Pulping Chemicals, IUPC EUCEPA*, Helsinki, p.687-700, 1968.

Janson, J., "The Use of Unconventional Alkali in Cooking and Bleaching — Part 1, A New Approach to Liquor Generation and Alkalinity", *Paperi ja Puu-Papper och. Trà*, 1977, 59, p.425-430.

Janson, J. and O. Pekkala, "The Use of Unconventional Alkali in Cooking and Bleaching — Part 2, Alkali Cooking of Wood with the Use of Borate",

Paperi ja Puu-Papper och Trà, 1977, 59, p.546-577.

Janson, J. *and* O. Pekkala, "The Use of Unconventional Alkali in Cooking and Bleaching — Part 3, Oxygen-Alkali Cooking and Bleaching with the Use of Borate, *Paperi ja Puu-Papper och Tra.*, 1978, 60, p.349-352.

Janson, J. and O Pekkala, "The use of Unconventional Alkali in Cooking and Bleaching — Part 4, Kraft Cooking with the Use of Borate", *Paperi ja Puu-Paper o Tra* , 1978, 60, 349-357

Kiiskila, E., "Recovery of Sodium Hydroxide from Alkaline Pulping Liquors by Autocausticizing: Part 1, General Aspects", *Paperi ja Puu-Papper och Tra*, 1979, 61, p.505.

Lea, D.C. and J.M. Tomlinson, "Incineration of Kraft Liquor by the Fluidized Bed Process", *Proceedings of the 24th TAPPI Engineering Conference*, San Francisco, Sept., 1969, p.1-26, TAPPI Press, Atlanta.

Maddern, K.N., "Mill Scale Development of the DARS — Direct Causticizing Process", *Pulp & Paper Canada*, 1987, 10, p.78-82.

Pradit, L. A., "New Soda Plant Used at Eucalyptus Pulp Mill", *Pulp Paper Int.*, 1969, 11, 56-57.

Smook, G.A., *Handbook for Pulp and Paper Technologists*, CPPA, Montreal, 1986.

Timpe, W.G. and W.J. Evers, "The Hydrolysis Recovery Process–A New Approach to Kraft Chemical Recovery", *TAPPI*, 1973, 56(8), p.100-103.

CHAPTER 2

LITERATURE REVIEW

INTRODUCTION

The basic principle of the process to produce sodium hydroxide by reacting Na_2CO_3 with Fe_2O_3 and subsequently to hydrolyze the formed sodium ferrite was patented by Lowig as early as 1883 (Lowig, 1883). Nagano introduced this concept under the name **Direct Causticization** for the recovery of alkali from waste pulping liquor in 1976 (Nagano et al., 1976). Since then it has been widely studied as a means to eliminate the causticizing plant from the present alkaline pulping recovery processes. A literature review was conducted to establish the "state of the art" of this new technology. Since direct causticization involves a number of gas-solid and solid-solid reactions, the literature on the kinetic models of these two reaction system was also reviewed.

PART I DIRECT CAUSTICIZCATION

The patented process of Nagano et al. (1976) of Toyo Pulp Company was the first reference to direct causticization of black liquor with an insoluble metal oxide. In this process, black liquor is premixed with the metal oxide and the combustion and causticization are carried out in one step in a single reaction vessel. Since then the process was investigated and patented by various researchers in Australia, Finland, Japan and USSR (Covey, 1978; Kiiskila, 1979a, 1979b; Kishigami, 1987; Nepenin, 1986).

Fundamental Studies

Causticizing reactions

With Fe_2O_3 as causticizing chemical, the following single reaction with Na_2CO_3 takes place:

$$Na_2CO_3 + \alpha\text{-}Fe_2O_3 \rightleftarrows \beta\text{-}Na_2O{\cdot}Fe_2O_3 + CO_2 \qquad (1)$$

However it is known from the literature dealing with the synthesis of sodium titanates (Belyaev et al, 1968; Safiulin and Belyaev, 1968; Anderson and Wadsley, 1962; Kurolin and Vulikh, 1965; Belyaev, 1969 and 1976; Mitsuhashi and Fujiki, 1985) that the reaction between Na_2CO_3 and TiO_2 may lead to the formation of other mixed oxide compounds besides $Na_2O{\cdot}TiO_2$ according to the

general reaction:

$$x\ Na_2CO_3 + y\ TiO_2 \rightleftarrows xNa_2O{\cdot}yTiO_2 + x\ CO_2 \qquad (2)$$

There is, however, disagreement on the existence of some of these titanates. According to Belyaev (1968), at least six sodium titanates can be synthesized besides $Na_2O{\cdot}TiO_2$, namely, $2Na_2O{\cdot}TiO_2$, $4Na_2O{\cdot}5TiO_2$, $Na_2O{\cdot}2TiO_2$, $Na_2O{\cdot}3TiO_2$ and $Na_2O{\cdot}6TiO_2$. Older literature (Gmelins, 1951) included $2Na_2O{\cdot}3TiO_2$, $Na_2O{\cdot}5TiO_2$ and $6Na_2O{\cdot}TiO_2$ but their existence has been questioned in later references. A partial phase diagram of Na_2O-TiO_2 system using XRD data is shown in Figure 1(a) and 1(b) (Bouaziz and Mayer, 1971; Gicquel et al., 1972). $Na_2O{\cdot}2TiO_2$, $2Na_2O{\cdot}3TiO_2$ and $Na_2O{\cdot}5TiO_2$ are absent in this diagram because they were not observed by Bouaziz and Mayer (1971). Anderson and Wadsley (1961) found that the X-ray diffraction (XRD) data given for $Na_2O{\cdot}2TiO_2$ in literature were actually for $Na_2O{\cdot}3TiO_2$ because of sodium loss during the preparation of $Na_2O{\cdot}2TiO_2$. Furthermore Hill et al. (1985) concluded that the XRD data for $3Na_2O{\cdot}2TiO_2$ (Card No. 28-1154) were those of the γ-polymorph of $Na_2O{\cdot}TiO_2$. *The Joint Committee on Powder Diffraction Standard (JCPDS) Powder Diffraction Files* (1984) lists still other sodium titanates whose existence is questionable. Glasser and Marr (1979) concluded that Card No. 11-291 corresponds to $4Na_2O{\cdot}5TiO_2$ instead of $Na_2O{\cdot}TiO_2$, and that card No. 11-289 corresponds to a mixture of $Na_2O{\cdot}3TiO_2$ and $Na_2O{\cdot}6TiO_2$ rather than $Na_2O{\cdot}5TiO_2$. Recently the situation regarding the existence of some of the above compounds was clarified by Bamberger and Begun (1987) who used Raman spectra in addition to X-ray diffraction. Bamberger and Begun (1987) successfully synthesized $2Na_2O{\cdot}TiO_2$, $Na_2O{\cdot}TiO_2$, $4Na_2O{\cdot}5TiO_2$, $Na_2O{\cdot}3TiO_2$, and $Na_2O{\cdot}6TiO_2$ in the temperature range of 800 to 1200°C. However their attempts to prepare $Na_2O{\cdot}2TiO_2$ and $Na_2O{\cdot}5TiO_2$ were not successful, confirming that these compounds did not exist, and earlier identifications probably involved mixtures rather than single compound.

A series of kinetic studies have been conducted by Kiiskila (1979a, 1979b) on direct causticization of Na_2CO_3 with Fe_2O_3, TiO_2 and ilmenite concentrate (43.32 wt.% TiO_2, 39.60 wt.% FeO, 9.28 wt% Fe_2O_3 and 7.80 wt.% impurities). Since sulfur is absent these results are relevant to soda liquor recovery. Kiiskila found that the causticizing efficiency with Fe_2O_3 was very little influenced by the temperature above the melting point of sodium carbonate (856°C). The causticizing efficiency was also not very sensitive to

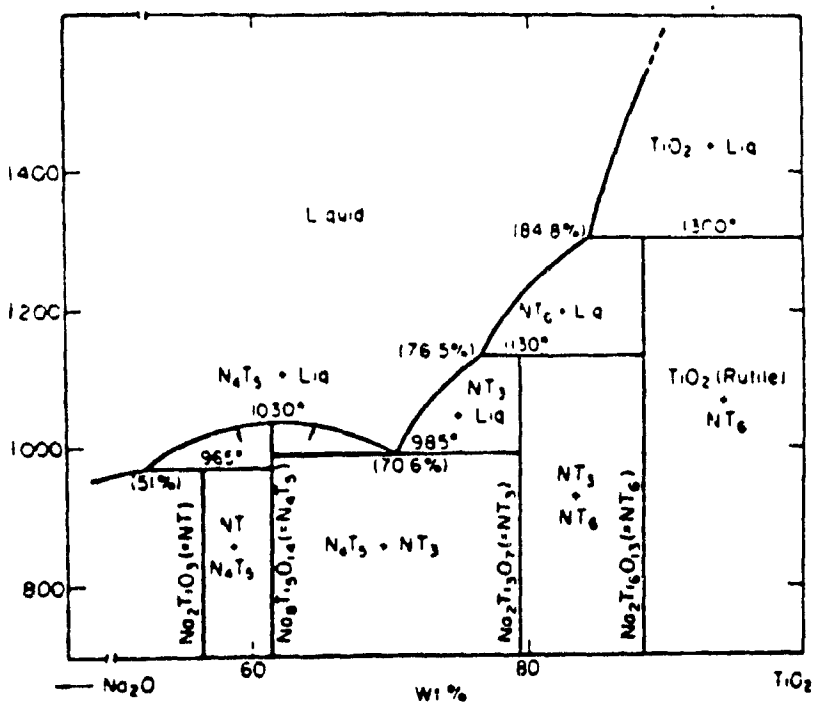

(a) From Bouaziz and Mayer (1971)

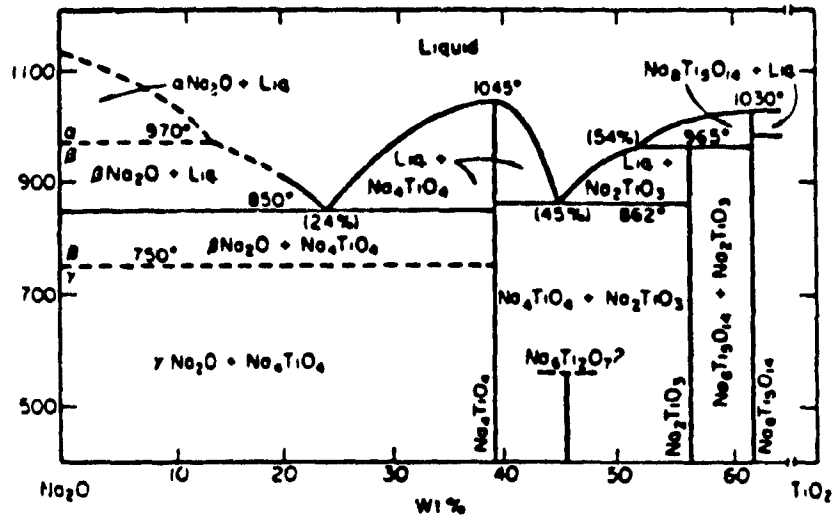

(b) From Gicquel, Mayer and Bouaziz (1972)

Figure 1 System of Na_2O-TiO_2

the CO_2 partial pressure over the temperature range studied (900-1100°C).

The causticizing efficiency with TiO_2, however, increased with increasing temperature up to 1100°C. Also in the absence of CO_2, Kiiskila (1979b) reported that the direct causticization with TiO_2 was very effective, with Na_2CO_3 stabilized in the smelt up to a Na_2O/TiO_2 molar ratio of 1.4 at 1000°C. However, the most Na_2O-rich sodium titanates ($2Na_2O \cdot TiO_2$ and $Na_2O\ TiO_2$) were converted to $4Na_2O \cdot 5TiO_2$ in an atmosphere of CO_2. Because of the presence of TiO_2, Kiiskila (1979c) also found that the causticizing efficiency of ilmenite concentrate was dependent on the temperature and CO_2 concentration.

Direct causticization of Na_2CO_3 is more difficult with Al_2O_3 than Fe_2O_3 or TiO_2 (Janson, 1979), and a much higher temperature is needed to complete the CO_2 liberation from Na_2CO_3 with Al_2O_3 (Kovalenko and Bukun, 1978). The use of Al_2O_3 as causticizing agent was patented in Japan by Abe (1984) and in South African by Davis and Boehmer (1987).

It should be noticed that all of the above studies were conducted at 850-1200°C, i.e., above the melting point of Na_2CO_3 (856°C). Also the experimental results were not analyzed in terms of a chemical kinetic model.

Hydrolysis

The studies by Kiiskila (1979a) of the hydrolysis of causticized smelt showed that sodium ferrite can be effectively decomposed to sodium hydroxide at temperatures above 30°C according to the reaction:

$$Na_2O \cdot Fe_2O_3 + H_2O = 2\ NaOH + Fe_2O_3 \qquad (3)$$

Sodium titanates decomposed only partially and it was shown that the amount of sodium oxide in the undissolved TiO_2 residue was almost independent of the Na_2O/TiO_2 ratio of the causticizing smelt. The insoluble fraction of sodium oxide decreased the efficiency and the capacity of TiO_2 to stabilize sodium oxide in the smelt. A similar influence was also observed for ilmenite.

Comparison of TiO_2, ilmenite and Fe_2O_3 showed that the chemical load for direct causticization at 900°C in the presence of CO_2 is the lowest for Fe_2O_3. At higher temperatures or in the absence of CO_2, the causticizing efficiency of TiO_2 increases so that the chemical load of TiO_2 becomes lower than that of Fe_2O_3 despite the incomplete hydrolysis of the former (Kiiskila, 1979b).

Al_2O_3 is not stable in a caustic solution and therefore not suitable for recovery of alkaline pulping liquor.

Application of Direct Causticizing Technology

An Australian company, APM Ltd., using the patent of the Toyo Pulp Company (Nagano et al., 1976), developed a direct causticizing process based on Fe_2O_3. This process known as the Direct Alkali Recovery System (DARS) is shown in Figure 2 (Covey et al., 1979 and 1984; Covey, 1982, Maddern, 1985). Fe_2O_3 is added to concentrated soda black liquor prior to combustion in a fluidized bed reactor at 850-950°C. Fe_2O_3 reacts with sodium carbonate producing sodium ferrite ($Na_2O{\cdot}Fe_2O_3$) and carbon dioxide. No smelt is formed because sodium ferrite has a high melting point (1050°C). When water is added to the cooled sodium ferrite, a solution of sodium hydroxide and a precipitate of Fe_2O_3 are produced. Fe_2O_3 is recycled to the fluidized bed (Covey et al, 1988). The Fe_2O_3 make-up requirement is 10-30 kg/ton pulp and the causticizing efficiency can reach 94%. This is substantially higher than 85% normally obtained with the lime causticizing cycle. Safety of operation, 30% reduction in capital cost and a 20% increase in steam production are other advantages of the process. This process has been successfully tested since 1980 with pine, eucalyptus and non-wood fiber feeds in a 5-10 ton/d pilot plant by APM Ltd. at Maryvale, Australia. A commercial scale DARS process is operating with partial success in Burnie, Tasmania and Fredericia, Danmark. Similar processes have been proposed and studied in a pilot scale by Japanese investigators (Babcock-Hitachi Co., 1983; Kishigami, 1987; Nagai et al., 1989).

The DARS process is limited to the recovery of soda or soda-AQ black liquor. It is not applicable to kraft black liquor recovery because Fe_2O_3 reacts with sulfur species and is reduced under the conditions required for formation of Na_2S, the other pulping chemical in the kraft pulping process.

Direct Causticization of Kraft Black Liquor

The application of the direct causticizing technology to kraft black liquor recovery was patented by Nguyen in 1985 (Nguyen, 1985). In his patent, kraft black liquor is first combusted with Fe_2O_3 or TiO_2. The product (Na_2SO_4 and $Na_2O{\cdot}Fe_2O_3$ or $Na_2O{\cdot}TiO_2$) is then reduced by H_2 and/or CO. The stability of the formed mixed oxides and the metal oxides themselves under reducing conditions is not addressed in Nguyen's patent. No further publications have appeared on the application of direct causticizing technology to kraft black

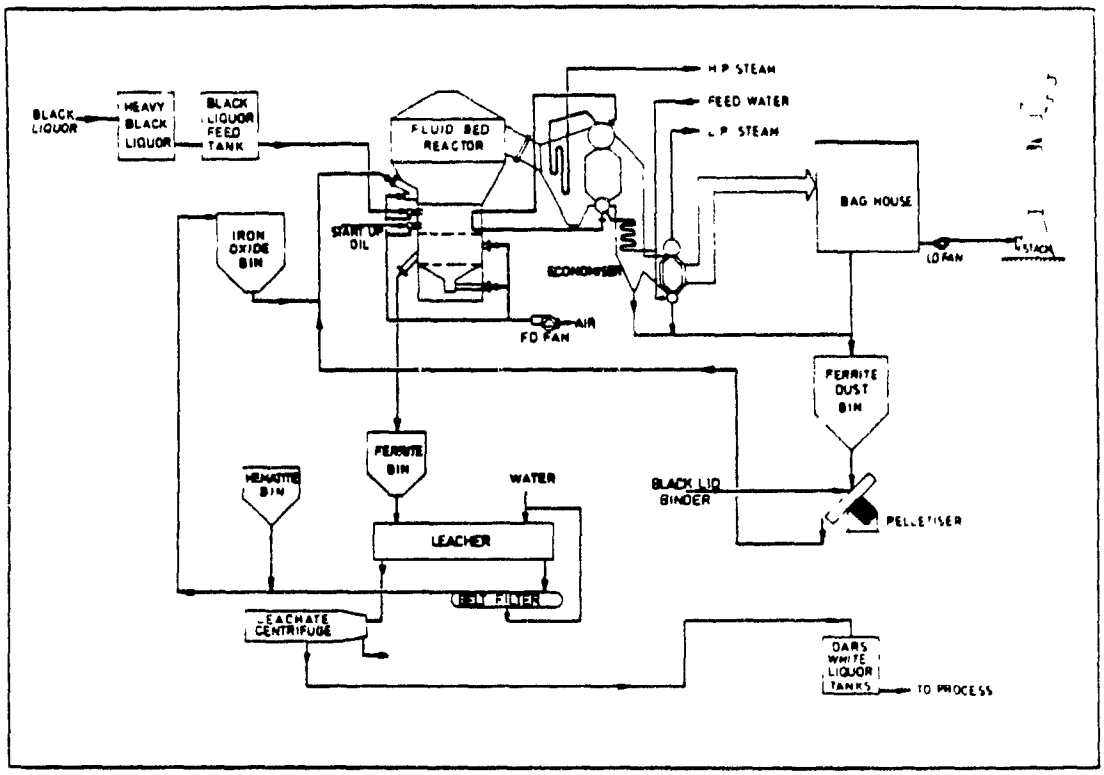

Figure 2 Direct alkali recovery system (DARS)

liquor recovery.

PART II GAS-SOLID AND SOLID-SOLID REACTION KINETICS

The direct causticizing technology applied to kraft black liquor mainly involves gas-solid and solid-solid reactions such as combustion of black liquor, the direct causticizing reaction between Na_2CO_3 and a metal oxide and the reduction of sodium sulfate. In order to establish the reaction mechanism, the proper kinetic model must be selected for data analysis. Therefore the main phenomenological gas-solid and solid-solid reaction kinetic models will be reviewed here.

Gas-Solid Reactions

Non-catalytic gas-solid reactions constitute an important class of heterogeneous reactions. Examples can be abundantly found in chemical and metallurgical processes such as decomposition of solids, reduction, gasification and combustion. Since these reactions are considerably affected by heat and mass transport, any kinetic analysis must take into account these transfer processes.

Most heterogeneous reactions can be represented by

$$A(g) + b\ B(s) \longrightarrow r\ R(g) + s\ S(s) \qquad (4)$$

The following elementary steps may be involved in the conversion process:

i) Mass transfer of reactant and product gases through the film surrounding the sample.

ii) Diffusion of these gases through the product layer in the sample.

iii) Simultaneous diffusion of cations and anions between the bulk of the sample and the reaction interface.

iv) Chemical reaction between the gas and solids at the reaction interface.

The slowest step or a combination of slow steps will determine the overall reaction rate. The conversion-time (X-t) behavior for this type of chemical reactions can be crudely classified into two cases. The first corresponds to formation and subsequent growth of product nuclei, while in the second case a uniform product layer is formed which grows inward. The two

cases are shown schematically in Figure 3(a) and 3(b). In Figure 3(a), the reaction interface increases until the growing nuclei overlap extensively and then decreases, resulting in a sigmoidal X-t curve. This model is known as the nucleation and growth model. In the second model, the entire reactant surface is covered with a thin product layer soon after contact with the reactant gas, and the reaction boundary then advances inward as the reaction proceeds. This model is the well-known shrinking core model (Levenspiel, 1962; Harrison, 1969). It should be noticed that the later stage of the nucleation and growth model may also be well described by the shrinking core model.

Shrinking core model

In deriving the equations for the time dependence of conversion the following assumptions are made: a sharp reaction interface, isothermal conditions, uniform spherical particles, equimolar counter diffusion of gaseous reactants and products, pseudo-steady state, and a first-order irreversible reaction. Depending on the rate controlling step, the following X-t relationships are obtained (Levenspiel, 1962):

i) Gas film diffusion control, $X = k_f t$ (5)

ii) Product layer diffusion control, $1-3(1-X)^{2/3}+2(1-X)=k_s t$ (6)

iii) Chemical reaction control, $1-(1-X)^{1/3}=k_r t$ (7)

where

$$k_f = \frac{3bk_g C_{Ab} M_B}{\rho_B R}$$

$$k_s = \frac{6D_e bC_{Ab} M_B}{\rho_B R^2}$$

$$k_r = \frac{k_s bC_{Ab} M_B}{\rho_B R}$$

k_s: Surface reaction rate constant,

k_g: Gas film transfer coefficient, m/s.

C_{Ab}: Bulk gas concentration, mol/m^3.

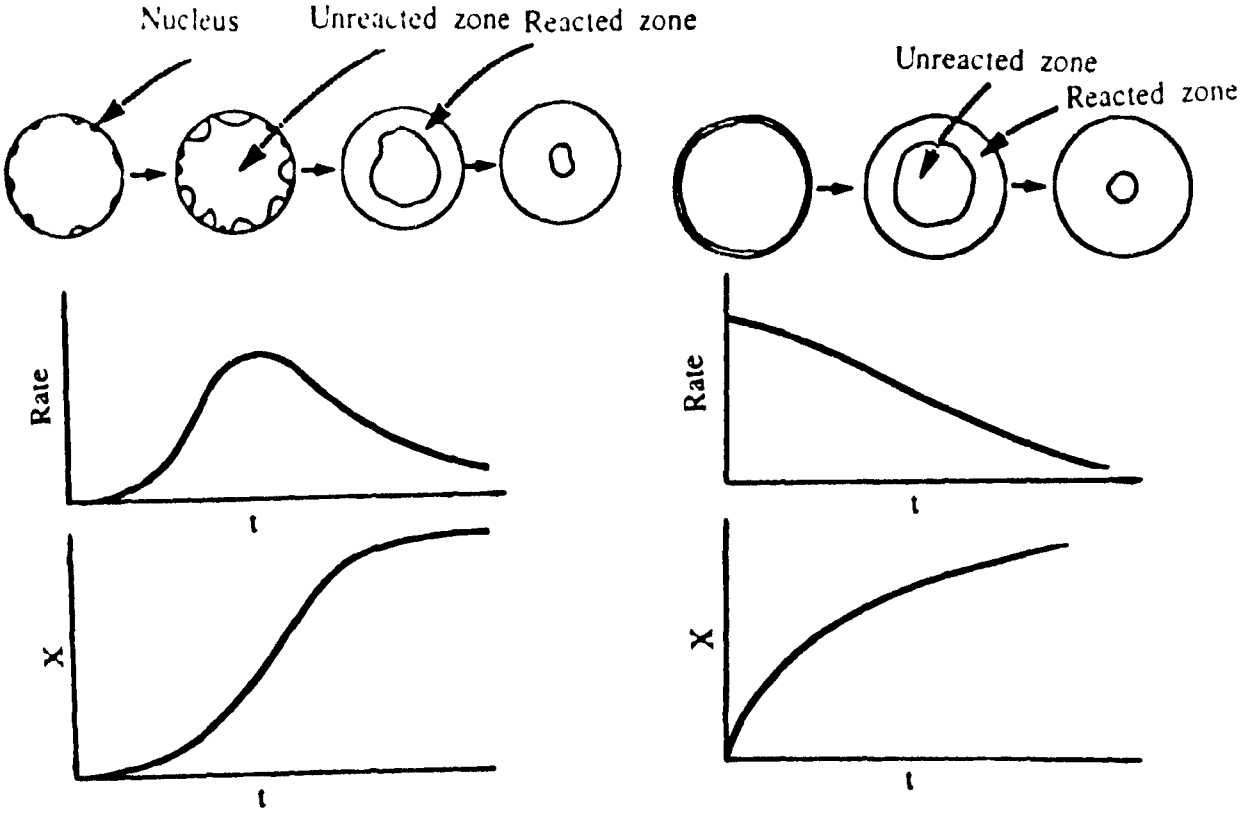

(a) Nucleation and growth model (b) Shrinking core model

Figure 3 gas-solid reaction models

M_B: Molecular weight of solid B, kg/mol.

b: Stoichiometric coefficient of Eq.(4).

ρ_B: Density of solid B, kg/m^3.

R: Diameter of solid particles, m.

$\mathbb{D}_e$: Effective diffusivity of gas in solid, m^2/s.

Since the resistances are in series and linear processes, simple addition gives an overall X-t expression (Sohn, 1978; Rao et al., 1979):

$$\frac{R}{3k_g} X + \frac{R^2}{6\mathbb{D}_e} [1-3(1-X)^{2/3} + 2(1-X)] + \frac{R}{k_s} [1-(1-X)^{1/3}]$$

$$= \frac{bC_{Ab}M_B}{\rho_B} t \qquad (8)$$

Eq.(8) can also be expressed as:

$$t = t_M + t_{DP} + t_R \qquad (9)$$

where t_M, t_{DP} and t_R are the times required to achieve a given conversion when the process is completely controlled by respectively external mass transfer, product layer diffusion and chemical reaction. The usefulness of Eq.(8) is twofold. It can predict the conversion as a function of time for a system in which all the parameters are known. Alternatively, it can be used to interpret experimental data of gas-solid reactions with the objective to identify the rate controlling step and to obtain the model parameters.

The shrinking core model has been applied to a number of systems, such as the oxidation of nickel (Carter, 1961), reduction of iron oxides (Kawasaki et al., 1962), combustion of coke (Weisz and Goodwin, 1963), and oxidation of zinc sulfide (Gokarn and Doraiswamy, 1971). The validity of the various assumptions made in developing the model is discussed by Bischoff (1963), Luss (1968) and Wen (1968).

Nucleation and Growth Model

Although more common in solid-solid reactions, nucleation effects can also be significant in some gas-solid reactions such as the reduction of metallic oxides and inorganic salts. Typical X-t curves show three stages: (a) an induction period, (b) an acceleratory period, and (c) a deceleratory period, These stages are the result respectively, of (a) formation of nuclei

at localized sites on the sample surface, (b) growth of these nuclei and (c) overlap of the growing nuclei and a decrease in reaction interface. The length of the induction period is determined by the rate of formation of nuclei. Following nucleation, the surface of the product grows equiaxially into the unconverted solid. The important assumption is that the reactant gas is able to penetrate the product layer without a significant diffusion resistance.

The mathematical description of the nucleation and growth model was formulated many years ago for the decomposition of austenite (Avrami, 1939, 1940 and 1941; Cahn, 1956). The conversion-time equation depends on the mechanism of nucleation as well as on the texture of the product and substrate. Since an excellent discussion of the model may be found in the book of Bamford and Tipper (Harrison, 1969; Brown et al., 1980 and Kago and Harrison, 1982), only the problem statement and the main derivation steps of the general conversion-time equation will be presented here.

The volume of a nucleus at time t, V(t), is given by the general expression:

$$V(t)=\int_0^t V(t,t_j)\left(\frac{dN}{dt}\right)_{t=t_j} dt_j \qquad (10)$$

where dN/dt is the rate of nucleation and V(t,tj) is the volume occupied by a nucleus formed at time t_j. Eq.(10) may be integrated for any combination of nucleation rate and type of growth. For a linear growth rate, the following equation can be obtained from Eq.(10) when taking into consideration the overlap of nuclei:

$$-\ln(1-X)=(K_g K_1^2 k_n N_o/V_o)\int_0^t (t-t_j)^m e^{-k_n t_j} dt_j \qquad (11)$$

where K_g is a shape factor, k_n a nucleation rate constant, V_o the volume of the product at complete conversion, N_o the number of potential nucleus forming sites initially present in the solid sample, and m is the number of dimensions in which the nuclei are growing. The growth rate constant, K_1, is equal to $k_s V_2^o P_g$ where k_s is the intrinsic rate constant for the interfacial reaction, V_2^o the molar volume of the product and P_g the partial pressure. Integrating Eq.(11) with, for example, m=2 gives:

$$-\ln(1-X)=\frac{K_g K_1^2 N_o}{k_n^2 V_o}\left[1-2\,e^{-(k_n t)} - k_n t + (k_n t)\right]^2 \qquad (12)$$

For large values of $k_n t$, a condition normally valid in the deceleration period, Eq.(12) simplifies to:

$$-\ln(1-X) = (K_g K_1^2 N_o/V_o)\, t^2 \qquad (13)$$

Designating $(N_o/V_o)=n_o$, $K_g=2\pi$ (for a spherical particle), Eq.(13) can be transformed to.

$$-\ln(1-X)=(2\pi n_o K_1^2)\, t^2 = (k_1 t)^2 \qquad (14)$$

It can be shown (Harrison, 1969) that for m=1, 2 or 3, the general result of this model is:

$$[-\ln(1-X)]^{1/m} = k_1\, t \qquad (15)$$

This is the so called Avrami-Erofe'ev equation, where n depends on the number of growth dimensions of the nuclei, and the nuclei formation rate. The value of the Erofe'ev rate constant, k_1, can be determined from the slope of a log-log plot of [-ln(1-X)] versus t over the appropriate range of X. The above derivation shows that the rate constant k_1 is not only a function of temperature, but also depends on the concentration of potential nuclei forming sites initially present and on the gas composition.

It should be noted that the deceleration stage of the nucleation and growth model is sometimes also well described by the shrinking core model. Thus the shrinking core model is appropriate for those cases whereby the nucleation and growth time is small compared to the total reaction time. This situation would be favored when the surface to volume ratio of the solids is small, i.e., large particles, or when the reaction temperature is high. However, for very small solid particles and relatively low temperatures, the nucleation and growth model may describe the kinetics up to complete conversion.

Solid-Solid Reactions

As is the case for other heterogeneous system, solid-solid reactions are also controlled by one or several steps involved in the overall reaction process. In essence, in any mixed-powder reaction, the different solid

particles should contact one another and at least one of them must then diffuse through a growing product shell in the other solid. This situation gives rise to the following possibilities for the rate controlling step (Tamhankar and Doraiswamy, 1979):

1. Product growth controlled by diffusion of reactants through a continuous product layer.
2. Product growth controlled by nucleation and nuclei growth.
3. Product growth controlled by phase-boundary reactions.
4. Product growth controlled by homogeneous reactions.

The main features of the different models based on these controlling mechanisms, as well as a few other models, are outlined below.

i) Product-layer diffusion control

Models based on product-layer diffusion control involve three basic assumptions:

1. The reactant particles are spheres.
2. Surface diffusion rapidly covers the reactant particles with a continuous product layer during the initial stages of the reaction.
3. Further reaction is controlled by bulk diffusion of a mobile reactant species through the product layer.

Jander (1927) first derived the following conversion-time expression based on this model:

$$[1-(1-X)^{1/3}]^2 = kt \qquad (16)$$

This expression as well as others for product layer diffusion control can be found in a review paper by Tamhankar and Doraiswamy (1979).

ii) Nucleation and growth model

The general form of the X-t equation for the nucleation and growth model is the same as that presented previously in the review of gas-solid reactions, i.e. Eq. (15) (Harrison, 1969).

iii) Phase-boundary reaction control

When the kinetics are controlled by reaction at the interface between the solid phases, identical expressions as those derived for gas-solid reactions are valid. Thus, for a sphere reacting from the surface inward, the conversion

versus time expression is (Jach, 1963):

$$1-(1-X)^{1/3}=kt \qquad (17)$$

For a cylinder the relation is (Jach, 1963):

$$1-(1-X)^{1/2}= kt \qquad (18)$$

and for a contracting cube (Sharp et al., 1968):

$$8k^3t^3-12k^2t^2+ 6kt = X \qquad (19)$$

iv) Kinetic expressions based on the concept of a homogeneous reaction

The general rate equation for a nth-order homogeneous reaction is (Taplin, 1974):

$$\frac{1}{n-1}\left[\frac{1}{(1-X)^{n-1}}-1\right] = kt \qquad (20)$$

Apart from the models presented above, empirical models (Blum and Li, 1961; Patai et al., 1961 and 1962) and a stochastic model developed by Waite (1960) have been proposed to describe the kinetics of mixed-powder reactions.

Interpretation of Kinetic Data

It has been pointed out in literature that the description of a given set of (X,t) values by a particular kinetic expression does not necessarily prove that the governing mechanism of the kinetic model is valid. Kinetic interpretations should always be supported by independent evidence. Microscopic observations in particular can be very valuable as supporting evidence for a certain mechanism.

The following effects can reduce the validity of the interpretation of kinetic data: (i) the reaction rate is inhomogeneous within the reactant mass, (ii) the mechanism changes during reaction, (iii) the importance of different resistances changes with progressive conversion, (iv) particle size effects, reactant pretreatment, etc..

CONCLUDING REMARKS

From the literature review, it can be concluded that further study of the direct causticization of kraft black liquor is needed. Specifically, the reaction kinetics and mechanism of the direct causticizing reaction and the reduction of sodium sulfate are very important for the development of this new recovery process. For the interpretation of the kinetic data one should be aware of the large number of kinetic models available in the chemical engineering literature for gas-solid and solid-solid reactions.

NOMENCLATURE

b =Stoichiometric coefficient of reaction (4).

C =Gas concentration, mol/m^3.

D_e =Effective diffusion coefficient, m^2/s.

k =Reaction rate constant, s^{-1}.

k_1 =Reaction rate constant in nucleation and growth kinetics, s^{-1}.

k_a =Rate constant with gas film diffusion, s^{-1}.

k_f =Rate constant with product layer diffusion control, s^{-1}.

k_g =Gas film mass transfer coefficient, m/s.

k_n =Nucleation rate constant, s^{-1}.

k_r =Rate constant with chemical reaction control, s^{-1}.

k_s =Surface reaction rate constant, s^{-1}.

K_g =Shape factor.

K_1 $=k_s V_2^o P_g$.

M =Molecular weight, kg/mol.

m =Number of dimensions.

n_o $=N_o/V_o$.

n =Order of reaction.

N =Number of nuclei.

N_o =Number of potential nucleus forming sites.

P_g =Partial pressure, N/m^2.

R =Diameter of the solid particle, m.

t =Time, s.

$V(t)$ =Volume of a nucleus at time t, m^3.

V_o =Volume of nucleus at complete conversion, m^3.

V_2 =Molar volume of product, m^3/mol.

X =Conversion.

Greek letters

ρ_B =Density of solid B, kg/m^3

REFERENCES

Abe, Z., "Recovery of Sodium Hydroxide via Alumina in Paper and Pulp Industry Waste Water", *Jap. Pat. Kokai*, 182,226/84, Oct. 1984.

Anderson, S. and A.D. Wadsley, "The Crystal Structure of $Na_2Ti_3O_7$", *Acta Cryst.*, 1961, 14, p.1245.

Anderson, S. and A.D. Wadsley, "The Structures of $Na_2Ti_6O_{13}$ and $Rb_2Ti_6O_{12}$ and the Alkali Metal Titanates", *Acta Cryst.*, 1962, 15, p.194-201.

Avrami, M., "Kinetics of Phase Change, I. General Theory", *J Chem. Phys*, 1939, 7, p.1103.

Avrami, M., "Kinetics of Phase Change, I. Transformation-Time Relations for Random Distribution of Nuclei", *J. Chem. Phys*, 1940, 8, p.212.

Avrami, M., "Kinetics of Phase Change. III. Granulation, Phase Change, and Micro Structure", *J. Chem. Phys.*, 1941, 9, p.177.

Babcock-Hitachi Co., "Direct Causticization with a Fluidized-Bed Furnace", *Jap. Pat. Kokai*, 132,193/83, 1983.

Bamberger, C.E. and G.M. Begun, "Sodium Titanates: Stoichiometry and Raman Spectra", *J. Am. Ceram. Soc.*, 1987, 70(3), c48-51.

Belyaev, E.K., N.Sh. Safiullin and N.M. Panasenko, "Reaction of Titanium Dioxide with Sodium Carbonate", *Izv. Akad. Nauk. Neorg Mater.*, 1968, 4, p.97-103.

Belyaev, E.K., "The Formation of Sodium Metatitanate in Sodium Carbonate—Titanium Dioxide Mixtures", *Russ. J. Inorg. Chem.*, 1976, 21, p.830-833.

Bischoff, K.B., "Accuracy of the Pseudo Steady State Approximation for Moving Boundary Diffusion Problem", *Chem. Eng. Sci.*, 1963, 18, 711.

Blum, S.L. and P.C. Li, "Kinetics of Nickel Oxide Ferrite Formation", *J. Am Ceram. Soc.*, 1961, 44, p.661.

Bouaziz, R. and M. Mayer, "On Some Sodium Titanate", (in Fr.), *C.R. Hebd. Seances Acad. Sci.*, Ser. C., 1971a, 272C, p.1773.

Bouaziz, R. and M. Mayer, "The Binary Sodium Oxide-Titanium Dioxide" (in Fr.), *C.R. Hedb. Seances Acad. Sci.*, Ser. C., 1971b, 272C, p.1874.

Cahn, J.W., "Transformation Kinetics during Continuous Cooling", *Acta. Metall*

1956, 4, p.572-575.

Brown, W.E., D. Dollimare and A.K. Galwey, "Reactions in Solid State", in *Comprehensive Chemical Kinetics*, Vol. 22, Bamford C.H. and C.F.H. Tipper Ed., Elsevier, Amsterdam, 1980.

Carter, R.E., "Kinetics of Model for Solid-State Reactions", *J. Chem Phys*, 1961, 34, p.2010.

Covey, G.H. and K.H. Algar, "Alkali Regeneration Process", *Aus. Pat* 519,156, Nov. 16, 1979.

Covey G.H., "Development of Direct Alkali Recovery System and Potential Application", *Pulp and Paper Canada*, 1982, 82(12), p.92-96.

Covey, G.H., "Direct Alkaline Recovery Process", Notes provided at the *Pacific Section of TAPPI-the Thirty Seventh Annual Seminar*, Sept. 1984, p.13-14.

Covey, G.H., K.N. Maddern, B.A. Stoddart, and J. Scukovic, "Leaching of Sodium Ferrite in DARS", *Appita*, 1988, 41(1), p.22-26.

Davis, C.J., and V.J. Boehmer, "Direct Recovery of Sodium Hydroxide from Spent Pulping Liquors", *So. African Pat.* 6,715/86, April, 1987.

Dunwald, H. and C. Wagner, "Measurement of Diffusion Rate in the Process Dissolving Gases in Solid Phases", *Z. Phys. Chem.* (Leipzig), 1934, B24, p.53.

Gicquel, C., M.M. Mayer and R. Bouaziz, "On Some Oxygenerated Compounds of Titanium and the Alkali Metals (Na, Li): Study of Binaries M_2O-TiO_2 in the Alkali Oxide-Rich Zones", (in Fr.), *C.R. Hebd. Seances Acad. Sci.*, Ser. C., 1972, 275C, p.1427.

Glasser, F.P. and J. Marr, "Phase Relation in the System Na_2O-TiO_2-SiO_2", *J. Am. Ceram. Soc.*, 1979, 62(1-2), p.42.

Gmelins Handbuch Der Anorganisschen Chemie, Titan, System-Nummer 41, 8th Ed., p.383, Verlag Chemie GMBH, Weinhein, Germany, 1951.

Gokarn, A.N. and L.K. Doraiswamy, "A Model for Solid-Gas Reactions", *Chem. Eng. Sci.*, 1971, 26, p.1521.

Harrison, L.G.,"Reaction Kinetics in Solid State", in *Comprehensive Chemical Kinetics*, Vol. 2, Bamford C.H. and C. F. H. Tipper Eds., Elsevier, Amsterdam, 1969, Chapter 5.

Hill, W.A., A.R. Moon and G. Higginbotham, "Alkali Oxide Rich Titanates", *J. Am. Ceram. Soc.*, 1985, 68, 10, c-266.

Jach, J., "The Thermal Decomposition of $NaBrO_3$, Part I — Unirraduated Material", *J. Phys. Chem. Solids*, 1963, 24, p.63.

Jander, W., "Reactions in Solid State at High Temperatures: I", *Z. Anorg.*

Allgem. Chem., 1927, 163, p.1.

Janson, J., "The Use of Unconventional Alkali in Cooking and Bleaching, Part 5, Autocausticizing Reactions", *Paperi ja Puu—Papper och Trà* , 1979, 1, p.20-30.

Joint Committee for Powder Diffraction Standards (JCPDS), 1984 Powder Diffraction File, International Center for Diffraction Data, Swarthmore, PA 19081.

Kago, Y. and L.G. Harrison. "Reactions of Solids with Gases Other than Oxygen", in *Comprehensive Chemical Kinetics, Chapter 2*, Bamford C.H. and C.F.H. Tipper Ed., Elsevier, Amsterdam, 1982.

Kawasaki, E., J. Sanscranite and T.J. Walsh, "Kinetics of Reduction of Iron Oxide with Carbon Monoxide and Hydrogen", *AIChE J.*, 1962, 8, p.48.

Kiiskila, E., "Recovery of Sodium Hydroxide from Alkaline Pulping Liquors by Smelt Causticizing, Part II, Reaction Between Sodium Carbonate and Titanium Dioxide", *Paperi ja Puu-Papper och Trà*, 1979a, 61(5), p.393.

Kiiskila, E., "Recovery of Sodium Hydroxide from Alkaline Pulping Liquors by Smelt Causticizing, Part III, Alkali Distribution in Titanium Dioxide Causticizing", *Paperi ja Puu-Papper och Trà*, 1979b, 61(6), p.453-464.

Kiiskila, E., "Recovery of Sodium Hydroxide from Alkaline Pulping Liquors by Smelt Causticizing, Part V, Causticizing of Molten Sodium Carbonate by Ilmenite", *Paperi ja Puu-Papper och Trà*, 1979c, 61(9), p.564-577.

Kishigami, K., "Direct Causticizing of Black Liquor", *Jap. Pat. Kokai*, 181,392/85, Sept. 17, 1987.

Kovalenko, V.I. and H.G. Bukun, "Reaction of Sodium Carbonate with Different Forms of Aluminum Oxide", *Rus. J. of Inorg. Chem.*, 1978, 23(2), p.158.

Kurolin, S.A. and A.I. Vulikh, "The Proceeding of the International Conference on Sintering and Related Phenomena", Gordon and Breach, New York, N.Y., 1965, p.75

Levenspiel, O., *Chemical Reaction Engineering*, John Wiley, New York, 1962, Chapter 12.

Lowig, A., *US Patent* 274,619, March 27, 1883.

Luss, D. and N.R. Amundson, "Maximum Temperature Rise in Gas-Solid Reactions", *AIChE J.*, 1969, 15, p.194.

Maddern, K.N., "Mill Scale Development of the DARS - Direct Causticizing Process", *Pulp and Paper Canada*, 1987, 10, p.78-82.

Mitsuhashi, T. and Y. Fujiki, "The Preparation of Alkali-Metal Titanates in Vacuum", *Russ. J. Inorg. Chem.*, 1965, 10, p.74-77.

Nagai, C., S. Matsumoto and H. Hattori, "Development of Fluidized Bed Chemical Recovery Boiler", *1989 Int. Chem Recov Conf.*, April, 1989, p.195.

Nagano, T., S. Miayo and N. Niimi, "Method of Recovering Sodium Hydroxide from Sulfur Free Pulping or Bleaching Waste Liquor Prior to Burning", U.S. Pat. 4,000,264, 1976, 28, 12.

Nepenin, Yu. N., "Method of Regenerated Black Liquor from Soda Cooks", *USSR Pat.* 1,278,372, Dec. 1986.

Nguyen, X.T., "Process to Regenerate Kraft Black Liquor", *Canadian Patent* No. 1,193,406, 1985.

Patai, S., M. Albeck and H. Cross, "Reactions between Solids", *J. Appl. Chem.* 1962, 12, p.217.

Patai, S., M. Albeck and H. Cross, "Kinetics of Oxidation of Solid Organic Substances by Solid Oxidants at High Temperature", *Proc. 4th Int. Symp.*, Reactivity of Solids, 1961, p.138.

Rao, Y.K., S.K. El-Rahaiby and M.M. Al-Kahatany, "The Discussion of Law of Additive Reaction Time in Fluid-solid Reactions", *Met. Trans.*, 1979, 10B, p.295.

Safiullin, S.A. and E.K. Belyaev, "Mechanism of Formation of Sodium Titanates, *Thermochimica Acta*, 1985, 88, p.177-184.

Sharp, J.H., G.W. Brindley and B.N.N. Achar, "Numerical Data for Some Commonly Used Solid State Reaction Equations", *J. Am. Ceram. Soc.*, 1966, 49, p.379.

Sohn, H.Y., "The Law of Additive Reaction Times in Fluid-Solid Reactions", *Met. Trans.*, 1978, 9B, p.89.

Tamhankar, S.S. and L.K. Doraiswamy, "Analysis of Solid-Solid Reactions: A Review", *AIChE J.*, 1979, 25, p.56.

Taplin, J. H., "Index of Reaction — A Unifying Concept for the Reaction Kinetics of Powders", *J. Am. Ceram. Soc.*, 1974, 57, p.140.

Waite, T.R., "Biomolecular Reaction Rates in Solids and Liquids", *J. Chem. Phys.*, 1960, 32, p.21.

Weisz, P.B. and R.D. Goodwin, "Combustion of Carbonaceous Deposits within Porous Catalyst Particles, I. Diffusion Controlled Kinetics", *J. Catal.*, 1963, 2, p.397-404.

Wen, W.Y., D.R. Janson and M. Doie, "A Second-Order Diffusion Controlled Reaction, Decay of Allyl Free Radial in Irradiated Polyethlene", *J. Phys. Chem.*, 1974, 78, p.1798.

CHAPTER 3

DIRECT CAUSTICIZATION OF KRAFT BLACK LIQUOR: PROCESS IMPLICATIONS BASED ON CHEMICAL EQUILIBRIUM CALCULATIONS

ABSTRACT

Chemical equilibrium calculations have been performed with the program F*A*C*T to evaluate process configurations and conditions for direct causticization of kraft black liquor with metal oxides, Fe_2O_3, Al_2O_3 and TiO_2. It is found that Fe_2O_3 is unsuitable, since reducing conditions lead to formation of Fe, FeO and FeS. Al_2O_3 is also unsuitable as direct causticizing chemical because some of its hydrates are soluble in white liquor. However TiO_2 can be used, because itself or its causticizing products are stable under high temperature reducing conditions, and the insoluble hydrolysis product can be reused in the direct causticization process. The equilibrium calculations showed that it is not feasible to recover kraft black liquor with TiO_2 in the conventional recovery furnace. However a *combustion-reduction* or *gasification-sulfur recovery* two-step process involving direct causticization of kraft black liquor with TiO_2 is thermodynamically possible.

INTRODUCTION

The alkaline pulping chemical recovery process presently makes use of lime causticization in order to convert sodium carbonate to sodium hydroxide. This method has a number of drawbacks in terms of economy and safety. In order to eliminate these drawbacks, a number of processes, collectively referred to as direct causticization, have been investigated. Direct causticization is a technology of regenerating pulping chemicals by using amphoteric oxides which directly leads to the formation of caustic. During combustion of kraft black liquor with amphoteric oxides the following generalized reaction takes place:

$$a\ Na_2CO_3 + b\ M_xO_y = aNa_2O{\cdot}bM_xO_y + a\ CO_2 \qquad (1)$$

which after hydrolysis yields caustic and regeneration of the oxide as:

$$aNa_2O{\cdot}bM_xO_y + (a+z)\ H_2O = 2a\ NaOH + bM_xO_y{\cdot}zH_2O \qquad (2)$$

Many patents and a number of papers have been published in the past two decades (Kiiskila, 1978; Maddern, 1986; Tsukamoto, 1986; Tsukamoto and Nakura, 1987), all concerning the direct causticization of soda pulping liquor. No work has been published on direct causticization of kraft black liquor because it is more complicated due to potential reactions between the metal oxide and sulfur and/or reducing agents.

Chemical equilibrium calculations constitute a fundamental part of research and development in high temperature chemical and metallurgical processing because they can be used to identify the possible reaction products and establish the influence of operating variables on the maximum conversion of all possible reactions. For example, Bauer and Dorland (1954) predicted that the volatile sodium species in the conventional kraft black liquor recovery furnace are Na, Na_2, and NaOH. Warnqvist and Norrstrom (1976) showed that although the equilibrium assumption is somewhat unrealistic in practice, the equilibrium calculations provide a good indication of the chemical species present in the furnace and the trends caused by operating variables. Detailed thermodynamic equilibrium calculations for the inorganics in the kraft recovery furnace have been made by Pejryd and Hupa (1984). Results obtained for the sulfur species by Pejryd and Hupa were found to be in good agreement

with industrial data.

In this chapter the latest thermodynamic data are used to establish the equilibrium composition for combustion and gasification of kraft black liquor in the presence of direct causticizing metal oxides. The objective is to establish the feasible process configurations which will then form the basis for further experimental studies.

DESCRIPTION OF THE F*A*C*T PROGRAM PACKAGE

The F*A*C*T program developed by Thompson et al. (1985) is a package which includes a chemical equilibrium calculation program (EQUIL), a Pourbaix (or redox potential-pH) program (EPH) for aqueous solutions, a database program (DATABASE) to store thermodynamic data and other useful programs for chemical systems. EQUIL is a modified version of SOLGASMIX developed by Eriksson (1975). The program determines the equilibrium composition by minimization of the Gibbs free energy of a chemical system. The Gibbs free energy of a chemical system is expressed by the following formula:

$$(G/RT) = \sum n_i [(g^o/RT)_i + \ln a_i] \qquad (3)$$

In this equation:
- G represents the total free energy;
- R the gas constant;
- T the temperature;
- n_i the moles of substance i;
- g^o the standard chemical potential;
- a_i the activity of substance i

The algorithm is described as being non-stoichiometric; This means that no chemical equations are used as part of the solution. The additional constraint that is introduced is the mass balance relationship:

$$\sum_{p=1}^{q+s+1} \sum_{i=1}^{m_p} a_{pij}\, n_{pi} = b_j \qquad (4)$$

In this equation: a_{pij} represents the number of atoms of the jth element in

a molecule of the substance i in the pth phase.

b_j the number of moles of the jth element;

q the number of pure phases;

s the number of of condensed phases;

m_p the total number of substances

The algorithm proceeds by the method of undetermined multipliers and a Taylor's expansion about an arbitrary starting point (an estimate of the equilibrium and an initial guess of the undetermined multipliers). The solution is then found iteratively by solving the linear equations generated and then using the new estimate of the n_i's. Convergence of this linear system will represent the equilibrium of the chemical system being modeled.

The particular advantage of the EQUIL program is its ability to handle a number of condensed phases, both mixtures and solutions. Each of the condensed phases is added to the system in turn. The set of phases that gives the lowest free energy, while obey ; phase rule, is selected as the equilibrium set. In the systems examined the condensed phase is of primary importance.

The standard enthalpy, standard entropy and heat capacity as function of temperature for all chemical compounds are stored in DATABASE of the F*A*C*T package. All the data, except Na_2S are taken from "Thermochemical Properties of Inorganic Substances" by Barin and Knacke (1973 and 1977). The melting point T_m, standard enthalpy ΔH_{298} and melting enthalpy ΔH_m for Na_2S listed in this reference are 1251 K, -374.468 kJ/mol and 26.359 kJ/mol respectively. It has been reported by Warnqvist (1980) that those values were inaccurate because they were obtained with impure Na_2S. With better experimental techniques, Warnqvist reported that T_m, ΔH_{298} and ΔH_m are respectively 1443±10 °K, -386.6 kJ/mol and 30.1 kJ/mol. By replacing the former data with Warnqvist's data in essentially the same program as EQUIL, Backman (1989) calculated the phase diagram for the system Na_2CO_3-Na_2S-Na_2SO_4, and obtained a very good agreement with experimental results of Andersson (1982). Therefore, Warnqvist's data were used in the present calculations just as was done recently by Li (1989) for thermodynamic analysis of the gasification of black liquor char with CO_2 and steam.

All of the thermodynamic calculations were performed at the total pressure of one atmosphere.

THE CONSEQUENCES OF ASSUMING EQUILIBRIUM

The validity of assuming that a system is in thermodynamic equilibrium is based primarily on the following two considerations:

i) *Complete mixing of reactants is assumed* — This assumption can lead to error, as the majority of the reactions that will be considered are between condensed molten salts and a gas phase, and all of the condensed phase may not be accessible to the gas.

ii) *The effect of kinetics is ignored* — Chemical thermodynamics indicate the potential for a reaction to occur, but that potential may not be realized due to kinetic limitations. In a non-equilibrium system one reaction may proceed faster than another and limit the extent of the slower reaction. In a high temperature system, kinetic effects can usually be ignored since the reaction rates are quite high, and equilibrium is usually obtained.

RESULTS AND DISCUSSION

Evaluation of Direct Causticizing Agents

From a review of the literature (Kiiskila, 1978), it appears that iron oxide, titanium dioxide and alumina are the only water-insoluble oxides suitable for direct causticization. Soluble direct causticizing compounds were not considered in the present study because of their impact on the pulping process. First, calculations were done to determine the temperatures for initial and complete reaction between the metal oxides and sodium carbonate in an inert atmosphere, respectively T_i and T_c. The results listed in Table 1 show that the lowest temperature for complete conversion is achieved with Al_2O_3 at 470°C, followed by TiO_2 at 700°C and Fe_2O_3 at 930°C. It should be noted that the latter temperature compares well with experimental results of Kiiskila (1979) who only obtained complete conversion of Fe_2O_3 above 900°C.

Table 1 T_i and T_c for Different Metal Oxides

Temperature (°C)	Al_2O_3	TiO_2	Fe_2O_3
T_i	330	350	700
T_c	470	700	930

In order to evaluate the influence of sulfur and reducing conditions on direct causticization, equilibrium calculations were performed for the system Na_2CO_3-Na_2S-metal oxide, in an inert or a reducing atmosphere. The calculations show that:

1) Under inert conditions at 900°C iron oxide reacts with Na_2S to form FeS. More importantly, Fe_2O_3 and causticized product $Na_2O{\cdot}Fe_2O_3$ (or $Na_2Fe_2O_4$) are easily reduced to Fe and FeO by reducing agents such as C, H_2 and CO at temperatures as low as 500°C.

2) The presence of sulfur does not influence the direct causticizing reaction between Na_2CO_3 and TiO_2 or Al_2O_3, and no metal sulfides are formed. Also TiO_2 or Al_2O_3 and their causticized products, $Na_2O{\cdot}TiO_2$ (or Na_2TiO_3) and $Na_2O{\cdot}Al_2O_3$ (or $NaAlO_2$) respectively, are stable under reducing conditions at temperatures below 1000°C.

From these results it can be concluded that only TiO_2 and Al_2O_3 are suitable as potential direct causticizing metal oxides for kraft black liquor recovery.

The hydrolysis of the causticized products such as $Na_2O{\cdot}Al_2O_3$ and $Na_2O{\cdot}TiO_2$ was also studied thermodynamically. The results showed that hydrolysis of sodium titanate $Na_2O{\cdot}TiO_2$ proceeds according to following overall reaction:

$$3\ Na_2O{\cdot}TiO_2 + 2\ H_2O = 4\ NaOH + Na_2O{\cdot}3TiO_2(s) \qquad (5)$$

i.e., the solid product $Na_2O{\cdot}3TiO_2$ instead of TiO_2 is obtained. This is consistent with experimental results of Kiiskila (1979) who showed that the maximum yield of NaOH after hydrolysis is about 66.7%. This indicates that hydrolysis of sodium titanate is limited by thermodynamics, and that $Na_2O{\cdot}3TiO_2$ rather than TiO_2 must be recycled in a commercial process. This does not represent a technical problem in a potential direct causticizing process, because $Na_2O{\cdot}3TiO_2$ reacts with Na_2CO_3 to form $Na_2O{\cdot}TiO_2$. However, it is an economic disadvantage since the recycle of TiO_2 must be increased by 50% to account for the fact that in such a continuous direct causticization process the internal sodium recycle is equal to one half of the sodium input into the process.

Hydrolysis of $Na_2O \cdot Al_2O_3$ produces NaOH and $Al_2O_3 \cdot H_2O$ according to the following reaction:

$$Na_2O \cdot Al_2O_3 + 2\ H_2O = 2\ NaOH + Al_2O_3 \cdot H_2O \qquad (6)$$

Since $Al_2O_3 \cdot H_2O$ is only stable in water over a certain pH range, a Pourbaix diagram is calculated. The results in Figure 1 show that $Al_2O_3 \cdot H_2O$ is dissolved above pH=9.4 because of the overall oxidation reaction:

$$Al_2O_3 \cdot H_2O + 2\ OH^- + 2\ H_2O = 2\ Al(OH)_4 + 2\ e \qquad (7)$$

Since the pH of white liquor will be about 14, no solid precipitate will be obtained. Thus the solubility behavior of Al_2O_3 makes this metal oxide unsuitable for direct causticization of kraft black liquor. Based on the above analysis it is concluded that TiO_2 is the only technically viable direct causticizing metal oxide for kraft black liquor recovery.

Combustion and Gasification of Kraft Black Liquor with TiO_2 Addition

The chemical species considered and elementary composition of kraft black liquor used in the equilibrium calculations are given in Table 2 and 3 respectively.

Upon complete combustion of the present kraft black liquor, assuming no sulfur or sodium loss, a mixture of Na_2CO_3 and Na_2SO_4 in a molar ratio of Na_2CO_3:Na_2SO_4= 0.7386:0.2614 is obtained. Variables investigated are the temperature, TiO_2/Na_2O molar ratio and percentage of stoichiometric air.

The percentage of stoichiometric air is defined as the percentage of air required for complete combustion of kraft black liquor to CO_2, H_2O, Na_2CO_3 (or $Na_2O \cdot TiO_2$), and Na_2SO_4.

The chemical equilibrium calculations for combustion and gasification of kraft black liquor at 900°C without TiO_2 addition are shown in Figure 2(a) and 2(b) for the gas and condensed phase respectively. These results, which serve as a reference for the combustion and gasification results with TiO_2, are identical to those obtained by Pejred and Hupa (1984). It can be seen that the main components between 30-80% of stoichiometric air are liquid sodium carbonate and sodium sulfide, and H_2S is the main gaseous sulfur species,

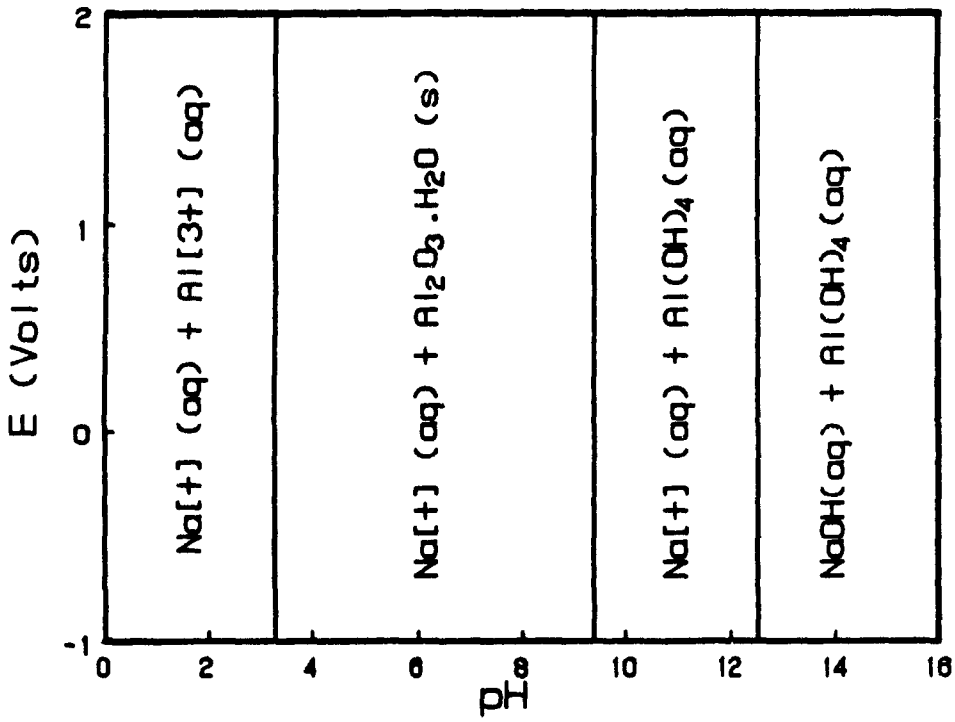

Figure 1 Pourbaix diagram for Na-Al-H_2O system at 90°C

Table 2 Chemical Species Included in the Equilibrium Calculations

Gases

CH_4, CO, CO_2, COS, CS_2, H_2, H_2O, H_2S, HCN, N_2, NH_3, NO, N_2O, NO_2, Na, Na_2, NaH, NaOH, NaCN, $Na_2(CN)_2$, O_2, S_2, S, SO_2, SO_3.

Liquids

Na_2S, Na_2S_2, Na_2S_3, NaS_2, Na_2SO_3, Na_2SO_3, NaOH, Na_2CO_3, Na_2O, TiO_2, TiO, Ti, TiS_2, TiS, TiH_2, TiN, TiC, $Na_2O{\cdot}TiO_2$, $Na_2O{\cdot}2TiO_2$, $Na_2O{\cdot}3TiO_2$.

Solids

Na_2S, Na_2S_2, Na_2S_3, NaS_2, Na_2SO_3, Na_2SO_4, NaOH, Na_2CO_3, Na_2O, TiO_2, $Na_2O{\cdot}TiO_2$, $Na_2O{\cdot}2TiO_2$, $Na_2O{\cdot}3TiO_2$, TiO_2, TiO, Ti, TiS_2, TiS, TiH_2,TiC, TiN, C.

Table 3 The Composition of Kraft Black Liquor Solids

Element	C	H	O	S	Na
Weight percentage	38.8	3.9	35.2	3.4	18.7

accounting for only a small fraction of the total sulfur in the system. Above 100% stoichiometric air, all the sulfur is in the form of liquid sodium sulfate. Apart from elementary carbon there is no solid phase present at 900°C below 20% stoichiometric air.

The results of the chemical equilibrium calculations with TiO_2 added at a TiO_2/Na_2O molar ratio of 0.85 are shown in Figure 3. The TiO_2/Na_2O molar ratio of 0.85 corresponds to a TiO_2/Na_2CO_3 molar ratio of 1.15. Between 20 and 80% stoichiometric air, the main species in the condensed phase are $Na_2S(l)$, $Na_2O{\cdot}TiO_2$, $Na_2O{\cdot}2TiO_2$, $Na_2O{\cdot}3TiO_2$ (collectively called $Na_2O{\cdot}xTiO_2$) and $Na_2CO_3(l)$. $Na_2O{\cdot}2TiO_2$ and $Na_2O{\cdot}3TiO_2$ represent only a small fraction of $Na_2O{\cdot}xTiO_2$, and $Na_2O{\cdot}xTiO_2$ is mostly in solid form. The small amount of $Na_2CO_3(l)$ remaining shows that Na_2CO_3 is almost completely converted to

$Na_2O\,xTiO_2$. Above 100% stoichiometric air all the sulfur is in the form of Na_2SO_4(l). The molar fraction of Na_2S(l) for air ratios between 30 and 80% is only about half of that of Na_2SO_4 above 100% stoichiometric air because of volatilization of sulfur, mainly as H_2S.

When the percentage of stoichiometric air is kept below 100%, the main sulfur gases are H_2S, COS, SO_2 and S_2. The COS concentration is about ten times smaller than that of H_2S, and the SO_2 and S_2 concentrations become significant only at air ratios between 80 and 100%. No sulfur is lost to the gas phase above 100% stoichiometric air, with all sulfur remaining as Na_2SO_4(l). Under reducing conditions, some sodium appears as Na and NaCN in the gas phase.

Compared with Figure 2, it is found that the addition of TiO_2 reduces the concentration of sodium vapor. Since sodium vapor is formed by reaction between Na_2CO_3 and reducing species, the reduction in sodium emission with TiO_2 can be explained by the large reduction in the molar fraction of Na_2CO_3 due to the direct causticization reaction:

$$Na_2CO_3 + x\ TiO_2 = Na_2O{\cdot}xTiO_2 + CO_2 \qquad (8)$$

However, under reducing conditions the addition of TiO_2 leads to higher concentrations of H_2S and COS which are at least ten times larger than those obtained in Figure 2, and a considerable reduction in the molar fraction of Na_2S.

The increased sulfur emission and reduced Na_2S yield can be explained by direct causticization reaction (8) and the following sulfur emission reactions:

$$Na_2S + 2\ CO_2 = Na_2CO_3 + COS \qquad (9)$$

$$Na_2S + CO_2 + H_2O = Na_2CO_3 + H_2S \qquad (10)$$

With the addition of TiO_2, Na_2CO_3 is converted into sodium titanate, and as a result the equilibrium of the sulfur emission reactions is shifted to the right. With excess air, all the sulfur is in the form of Na_2SO_4, and the equilibrium composition is the same as that without TiO_2 addition, except that sodium titanate instead of sodium carbonate is present as shown in Figure

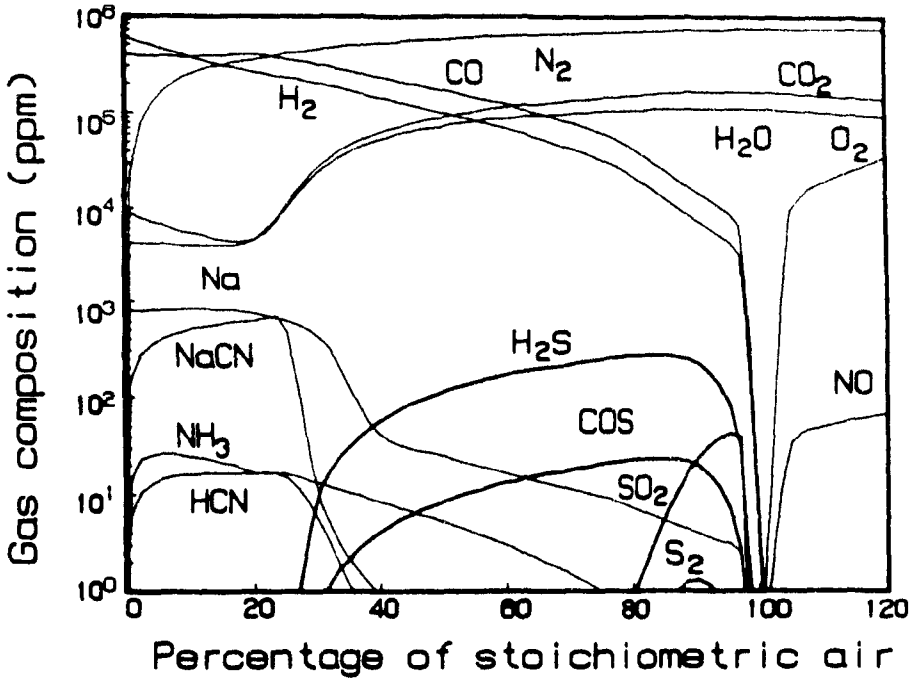

(a)

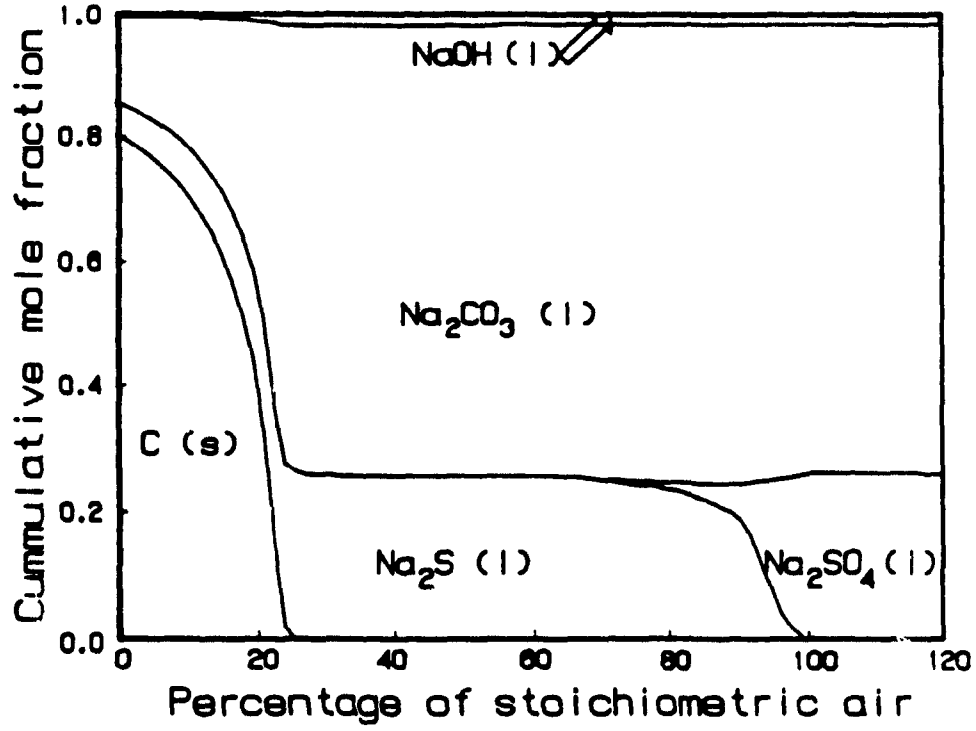

(b)

Figure 2 Equilibrium composition as function of air ratio at 900°C. No TiO_2 added

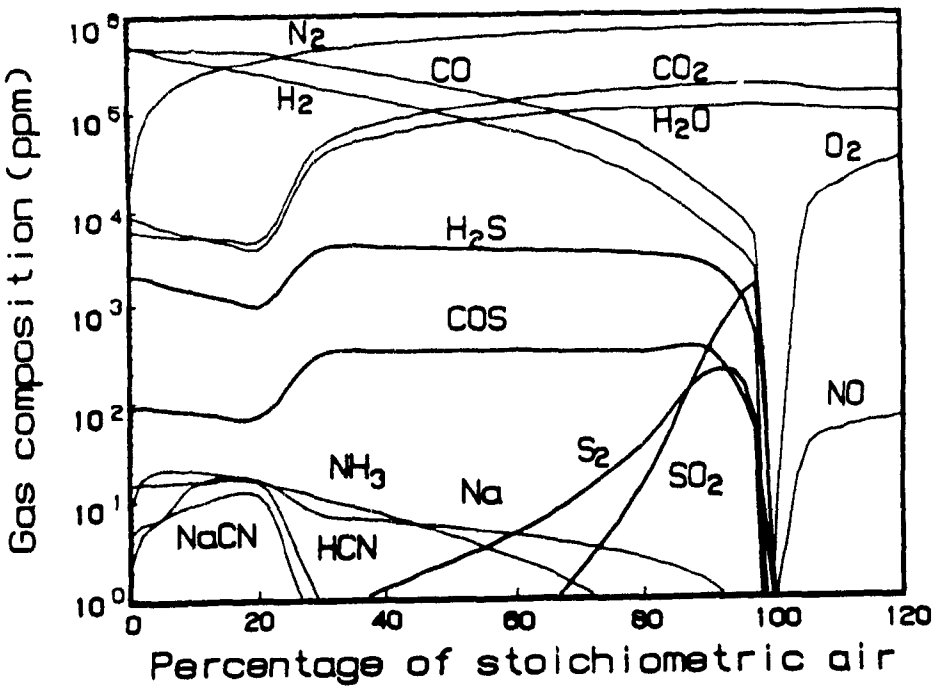

(a)

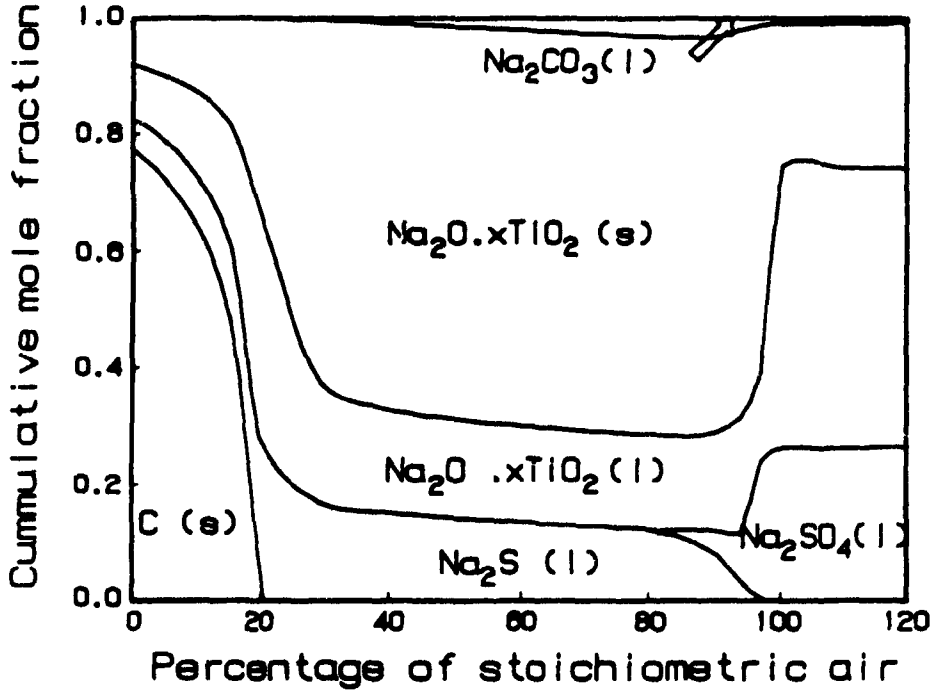

(b)

Figure 3 Equilibrium composition as function of air ratio at 900°C and TiO_2/Na_2O = 0.85 mol/mol

3(b).

The results in Figure 3 suggest that it is not feasible to make white liquor by adding TiO_2 to kraft black liquor in the recovery furnace, because the reducing conditions in the char bed will lead to a large increase in sulfur emission and solid $Na_2O \cdot xTiO_2$ will accumulate at the bottom of the furnace.

The influence of temperature on the equilibrium composition of kraft black liquor combustion with 70% stoichiometric air and a TiO_2/Na_2O molar ratio of 0.85 is shown in Figure 4(a) and 4(b). The H_2S and COS concentrations remain approximately constant with varying temperatures, while the SO_2 and S_2 concentrations increase with increasing temperature. As a result the molar fraction of Na_2S in the condensed phase is also relatively insensitive to the temperature at a level well below 0.2614, the value which would be obtained without volatilization of sulfur. When the temperature is increased, a molten phase is formed at about 800°C and the last solid phase, $Na_2O \cdot TiO_2$, disappears just below 1000°C.

Under oxidizing conditions, an increase in temperature only leads to an increase in the concentration of NO in the gas phase as shown in Figure 5(a). In the condensed phase shown in Figure 5(b), initial melting occurs at 760°C and all salts are molten above 930°C.

The results of the influence of TiO_2/Na_2O molar ratio at 900°C and 70% stoichiometric air are shown in Figure 6(a) and 6(b). The concentrations of H_2S and COS increase considerably with increasing TiO_2/Na_2O molar ratio and all sulfur appears in the gas phase when TiO_2/Na_2O is larger than 1.0, as can be seen from the absence of Na_2S in the condensed phase under these conditions in Figure 6(b). In effect, all sodium sulfide is converted to $Na_2O \cdot xTiO_2$, H_2S and COS via the sulfur emission reactions (9) and (10) and by direct causticization reaction (8). It is important to note that the sodium emission is negligible and only solid products remain when the TiO_2/Na_2O molar ratio is larger than 1.0.

Since the TiO_2/Na_2O molar ratio does not have any influence on the gas composition under oxidizing conditions, only its effect on the composition of the condensed phase at 120% stoichiometric air is displayed in Figure 7. It shows that sodium carbonate is almost completely converted at $TiO_2/Na_2O>0.76$ and that all sulfur is in the form of molten Na_2SO_4. At higher TiO_2/Na_2O ratios, solid TiO_2 appears as a new phase. Contrary to Figure 6(b), some

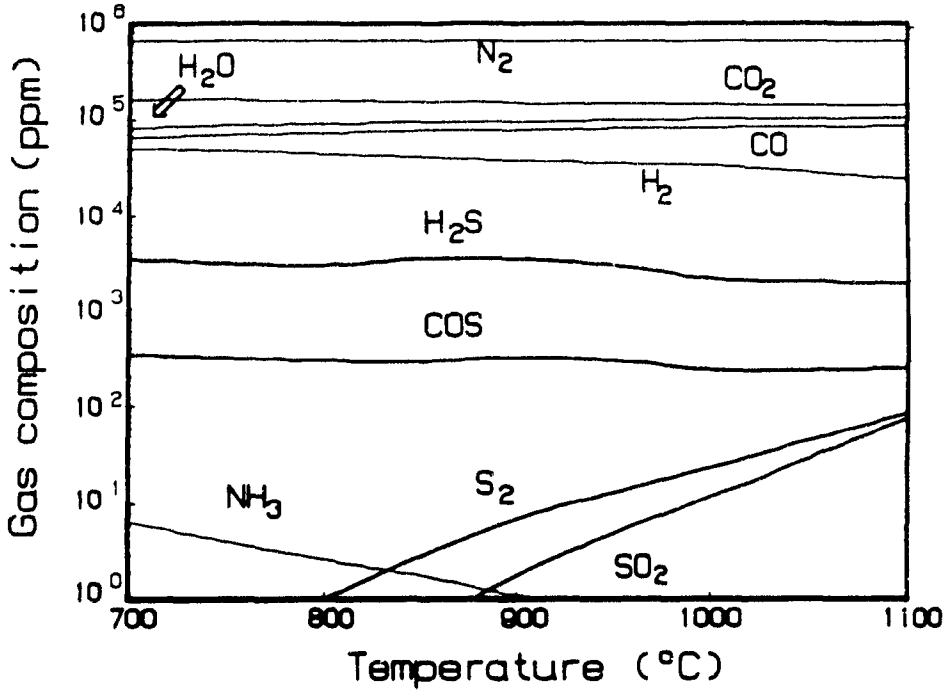

(a)

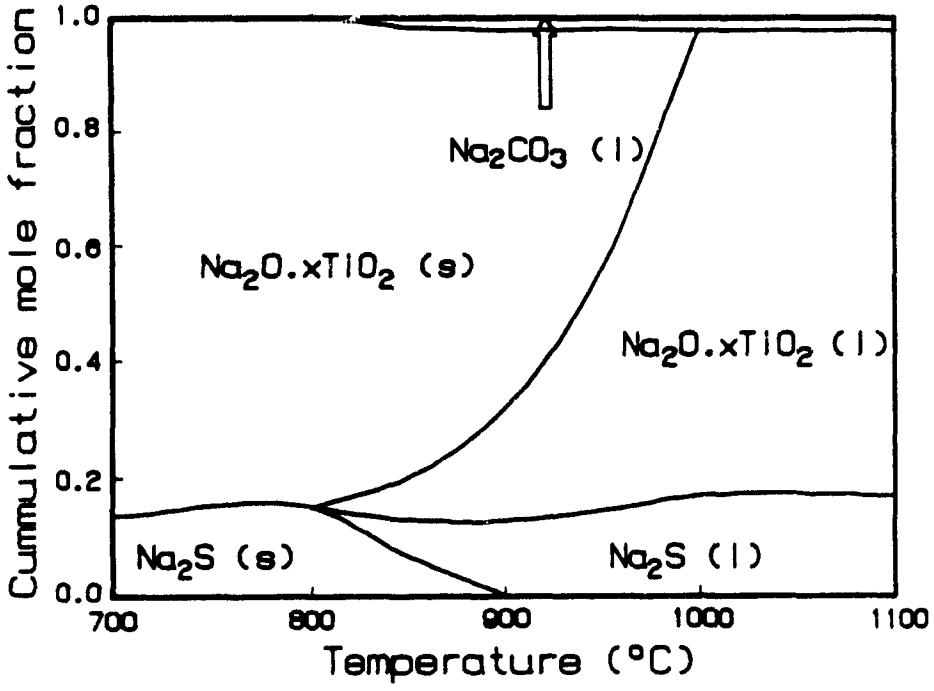

(b)

Figure 4 Equilibrium composition as function of temperature 70% stoichiometric air, TiO_2/Na_2O = 0.85 mol/mol

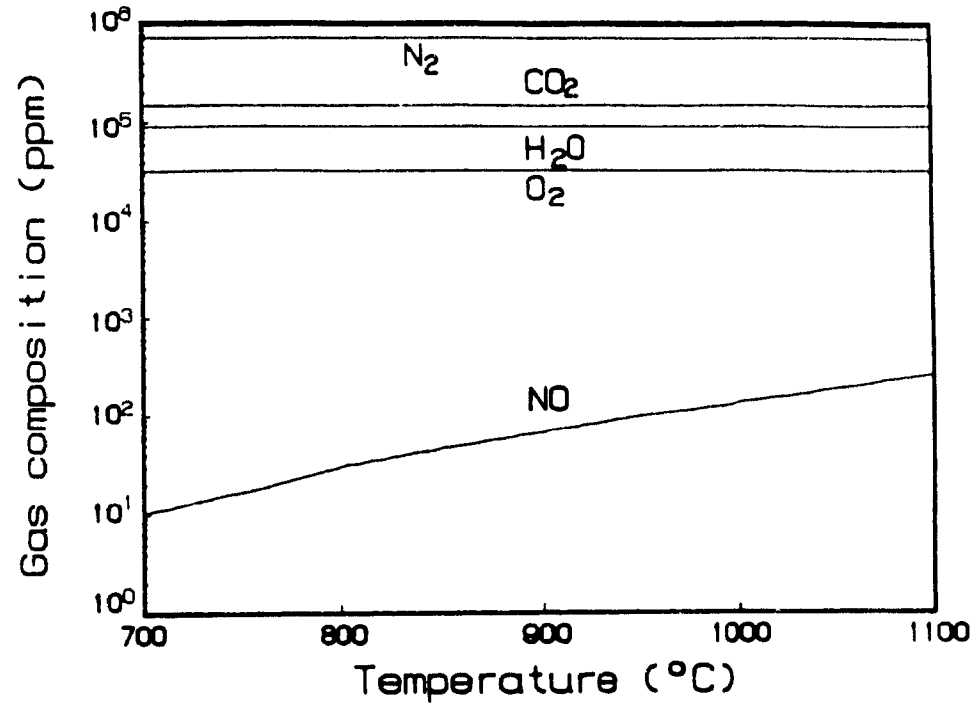

(a)

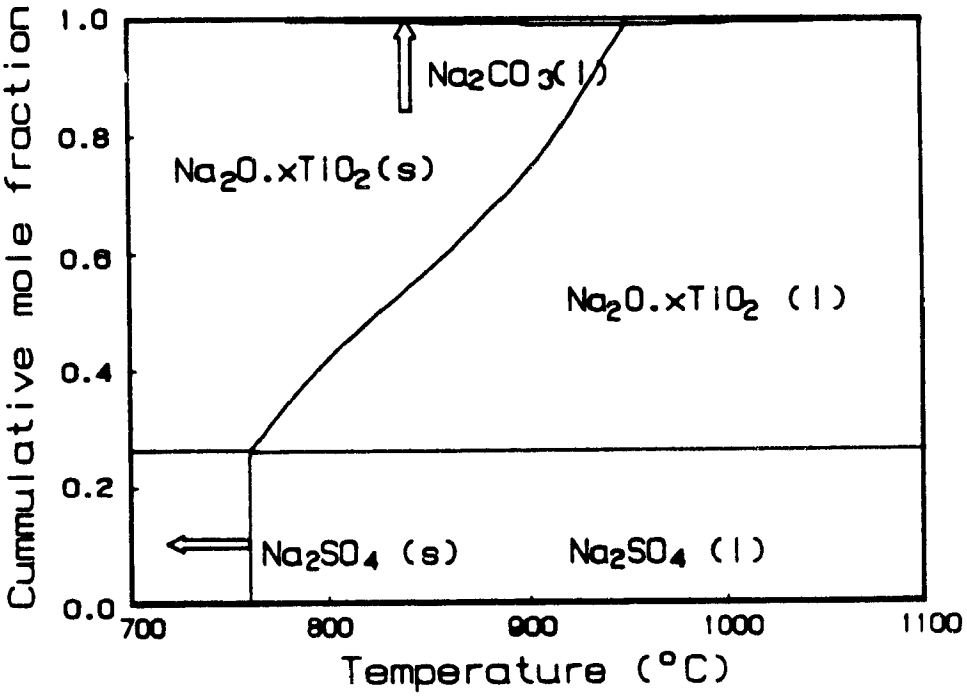

(b)

Figure 5 Equilibrium composition as function of temperature 120% stoichiometric air, TiO_2/Na_2O = 0.85 mol/mol

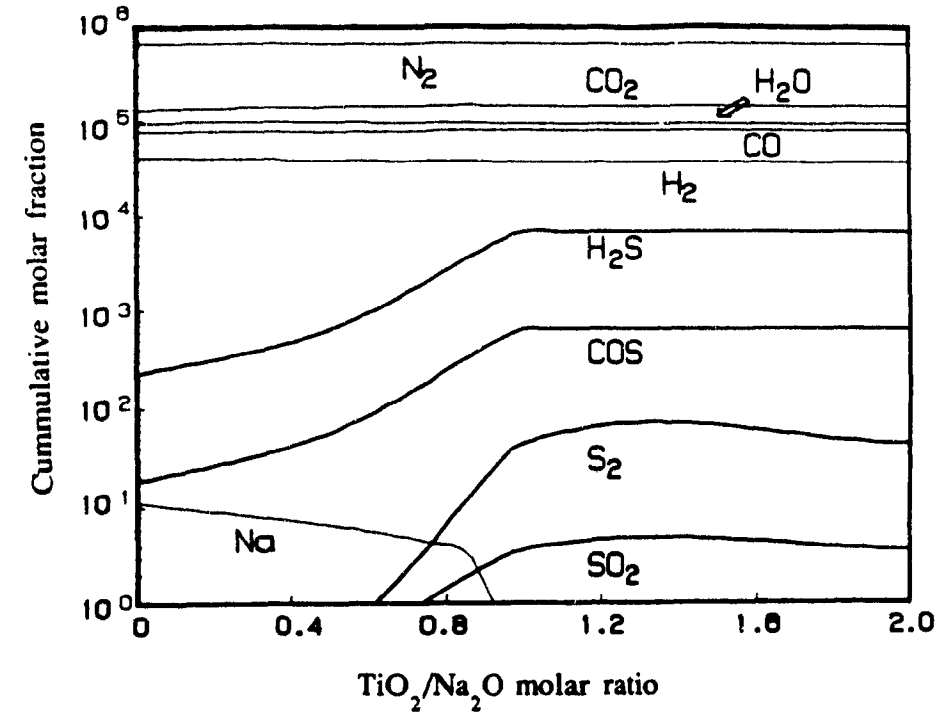

(a)

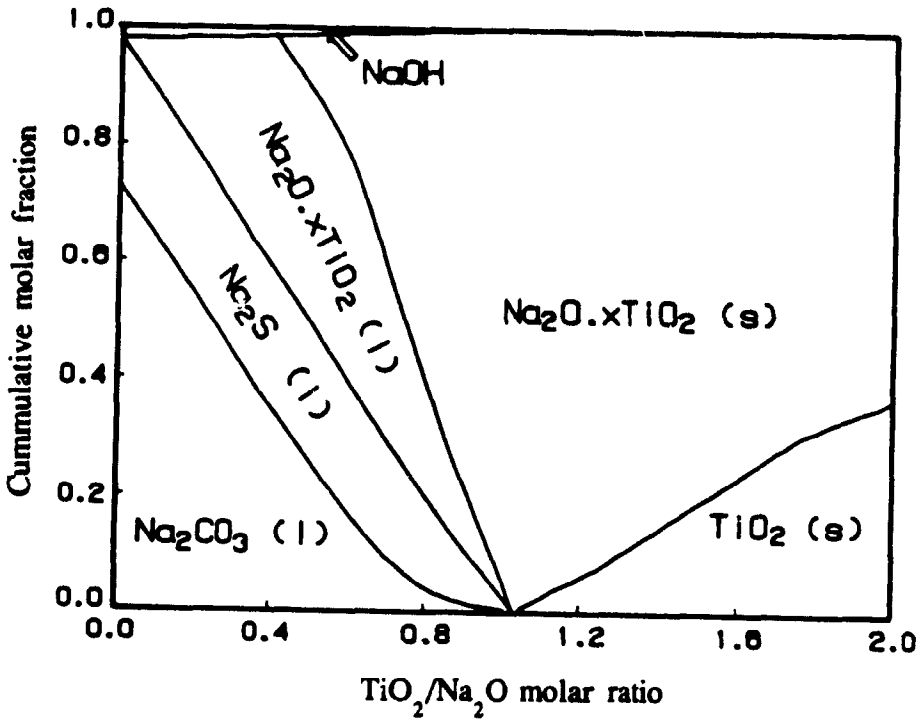

(b)

Figure 6 Equilibrium composition as function of TiO_2/Na_2O molar ratio T = 900°C, 70% stoichiometric air.

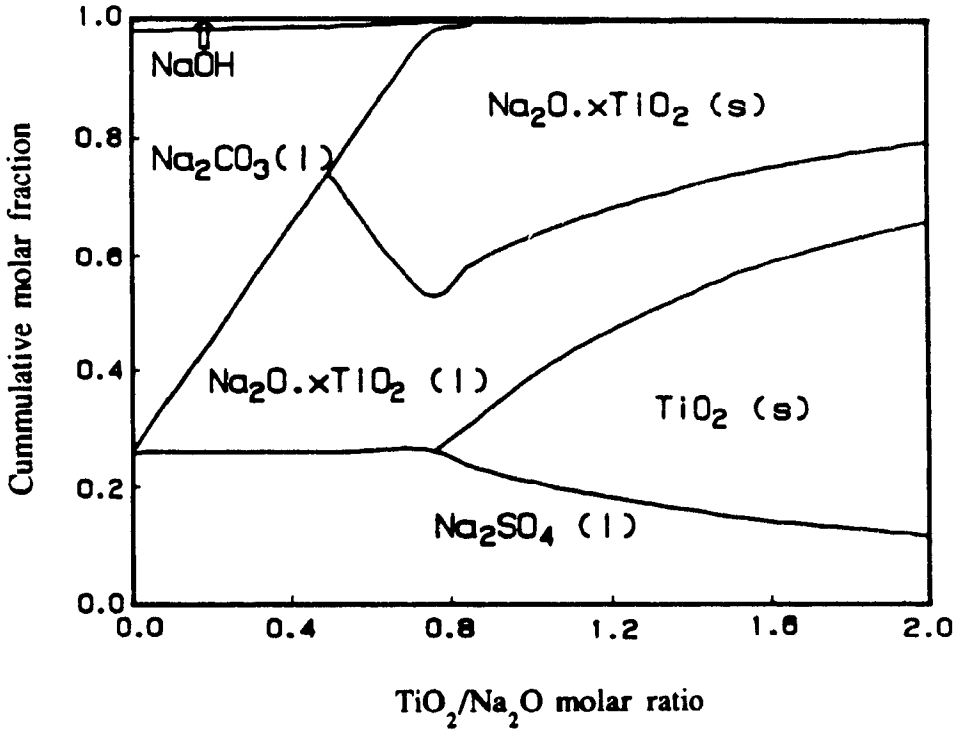

Figure 7 Equilibrium composition as function of TiO_2/Na_2O molar ratio T=900°C, 120% stoichiometric air

molten $Na_2O \cdot xTiO_2$ is found under oxidizing conditions at high TiO_2/Na_2O molar ratios because of the presence of liquid Na_2SO_4.

The results in Figures 6 and 7 suggest two interesting process configurations for alternative recovery of kraft black liquor. In the first configuration, kraft black liquor is combusted with TiO_2 at less than 100% stoichiometric air (i.e., gasification) and a molar ratio of TiO_2/Na_2O larger than 1.0. Upon dissolution of the solid residue in water a caustic solution, solid $Na_2O \cdot 3TiO_2$ and NaOH are obtained. H_2S must be selectively removed from the gasification gas by standard techniques employed in the petrochemical industry, and then absorbed in the caustic solution to form white liquor. This concept is similar to the gasification process (without TiO_2 addition) presently under development in the USA by MTCI (Durai-swamy et al., 1989) and in Finland (McKeough and Saviharju, 1991). A schematic graph to describe this process is shown in Figure 8(a). Advantages of the present concept are that white liquor is produced, no significant sodium vapor is formed and that higher gasification temperatures can be used without melt formation. The latter allows a fluid bed gasifier to operate at significantly higher temperatures. This in turn will lead to a much smaller residence time and thus reactor volume, and more complete gasification of organic sulfur compounds produced during pyrolysis of kraft black liquor. A disadvantage is however that expensive TiO_2 must be used so that only small losses are allowed in the TiO_2 recycle.

The second process configuration involves combustion of kraft black liquor with excess TiO_2 in an oxidizing atmosphere, and subsequent reduction of Na_2SO_4 in the mixture of Na_2SO_4, $Na_2O \cdot xTiO_2$ and TiO_2. This is similar to the DARS process (Maddern, 1986) for soda black liquor, which operates with Fe_2O_3 as direct causticizing chemical, and plus an additional reduction step, as shown in Figure 8(b).

In order to establish the thermodynamic feasibility of the latter process configuration, equilibrium calculations were performed for the reduction step.

Reduction of Direct Causticized Product

The condensed combustion product of kraft black liquor and TiO_2 is a mixture of sodium titanates and sodium sulfate. Sodium sulfate needs to be reduced for its reuse in the pulping process. Reduction of sodium sulfate was

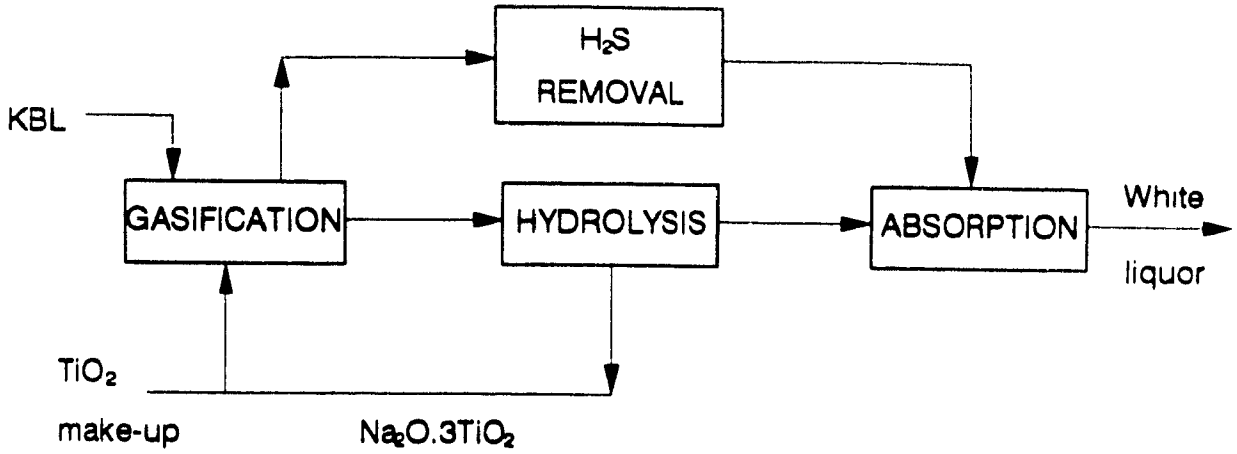

(a)

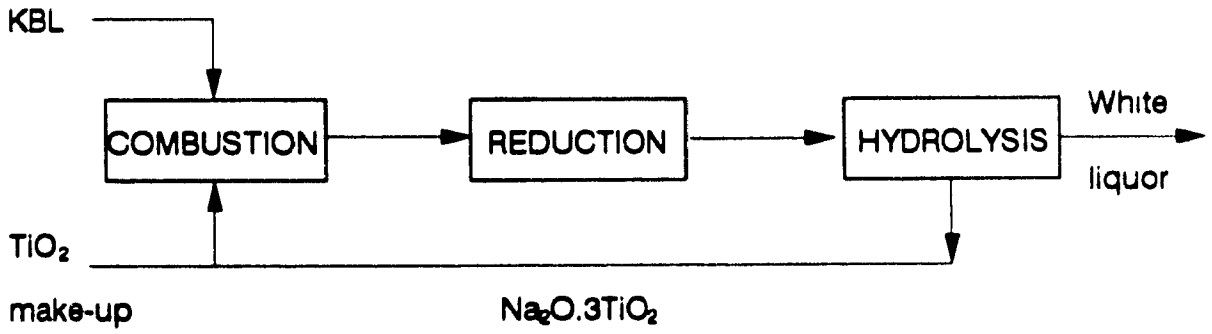

(b)

Figure 8 Proposed two process configurations

usually realized by some reducing agents. H_2 and CO were believed as the most effective ones. Therefore equilibrium calculations have been performed for the following system:

$$0.26 \text{ mole } Na_2SO_4 + 0.74 \text{ mole } Na_2O{\cdot}xTiO_2 + 5 \text{ mole } H_2 \text{ and/or } CO_2$$

i.e., the molar ratio of reducing agents H_2 and/or CO to Na_2SO_4 is 19.23. The influence of temperature on the reduction with pure hydrogen is shown in Figure 9(a) and 9(b). $Na_2O{\cdot}xTiO_2$ is chemically inert under these conditions. The H_2S and Na concentrations increase with temperature due to reaction between Na_2S and H_2. However this reaction does not lead to a significant loss of Na_2S when Na_2S is still solid. At higher temperatures, some of the molten Na_2S is converted into NaOH due to reaction with steam. These results imply that the direct causticized mixture of Na_2SO_4 and $Na_2O{\cdot}xTiO_2$ can be reduced with hydrogen without melt formation at temperatures below about 870°C.

With pure CO the reduction results are shown in Figure 10(a) and 10(b). Although $Na_2O{\cdot}xTiO_2$ is again chemically inert, its molar fraction decreases considerably at lower temperatures because of formation of large amounts of carbon by the CO disproportionation reaction:

$$CO = CO_2 + C \qquad (11)$$

The produced CO_2 reacts with Na_2S via reaction (9) so that a large amount of COS is formed at low temperatures. This also explains the sodium carbonate found in the solid phase under these conditions. Since the CO disproportionation reaction is unfavorable above about 760°C, the COS concentration is relatively small above 760°C. Because a molten phase appears above 850°C, it follows that pure CO can be used for reduction of the direct causticized mixture in the temperature range of 750-850°C.

The results for reduction with an equimolar gas mixture of CO and H_2 (CO/H_2=1:1 mol/mol), are shown in Figure 11(a) and 11(b). High concentrations of H_2S and COS are found below 700°C because presence of both H_2O and CO_2 leads to a large conversion of reaction (10). With increasing temperature the concentrations of H_2S and COS are reduced significantly and become constant above about 700°C At low temperatures a significant amount of CH_4 is formed because of the following reaction:

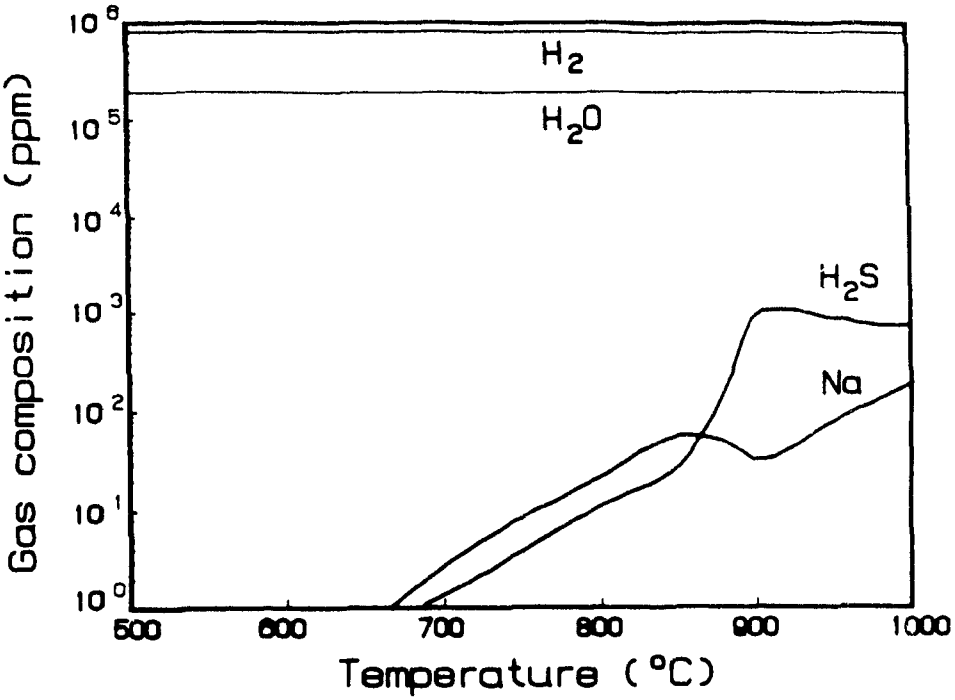

(a)

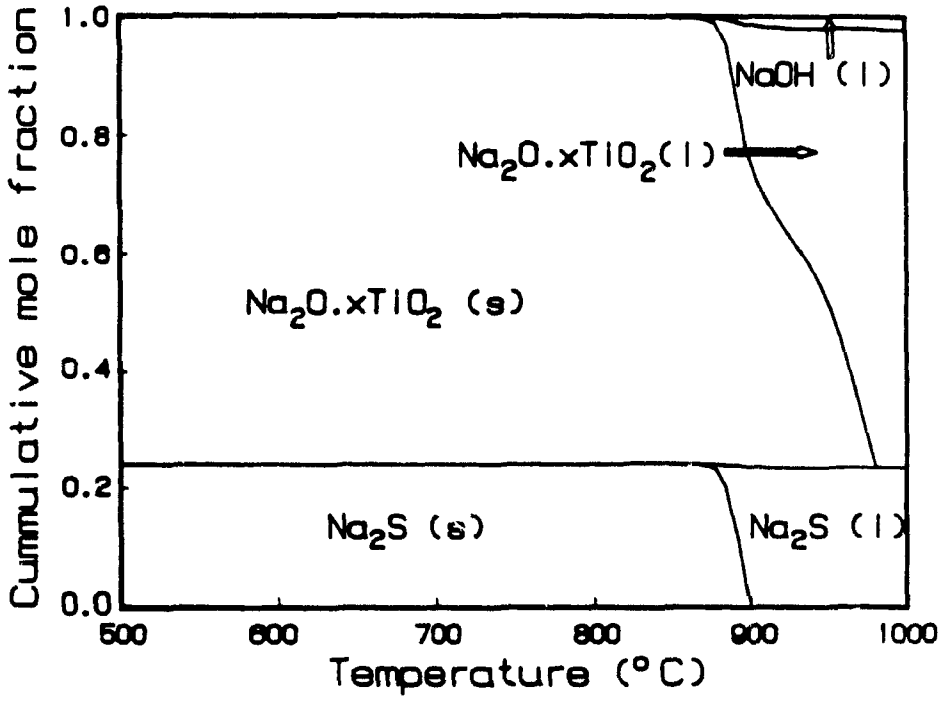

(b)

Figure 9 Reduction of sodium sulfate by H_2
H_2/Na_2SO_4=19.23 mol/mol

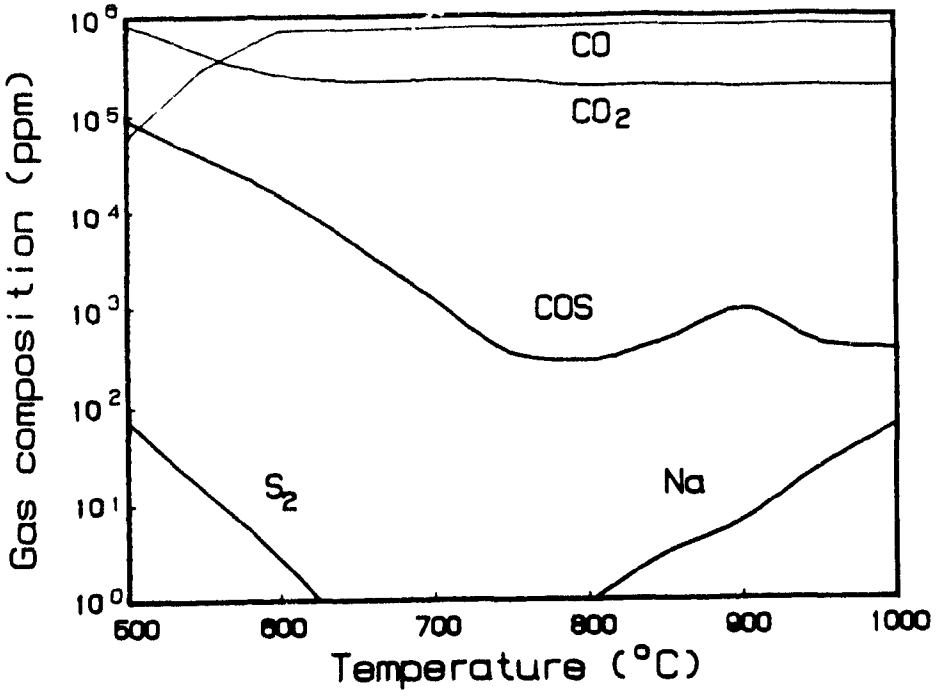

(a)

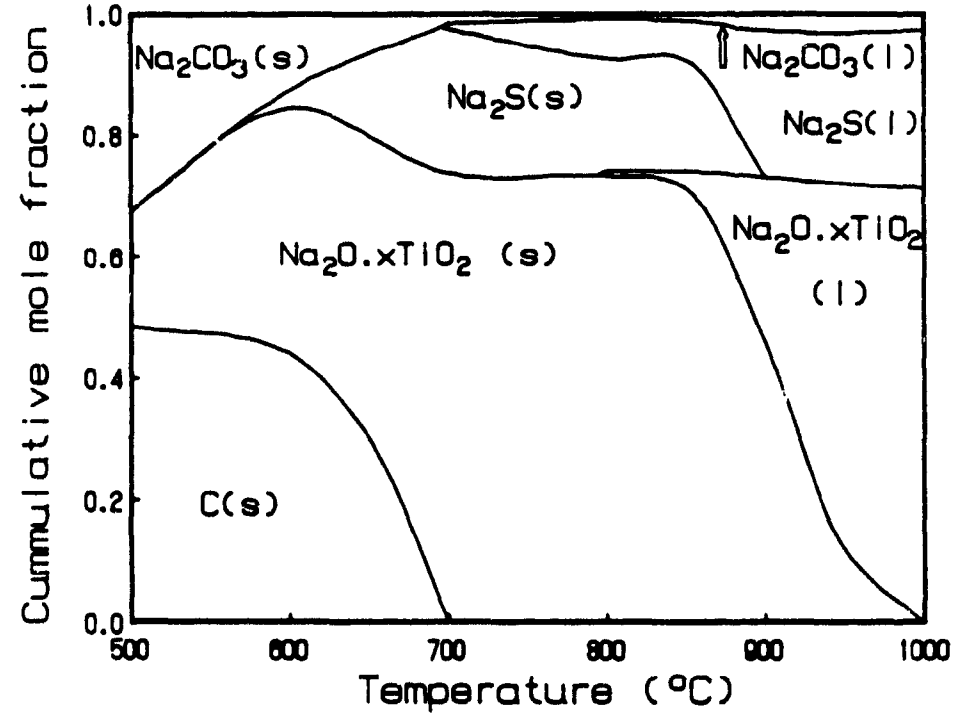

(b)

Figure 10 Reduction of sodium sulfate by CO

CO/Na_2SO_4 = 19.23 mol/mol

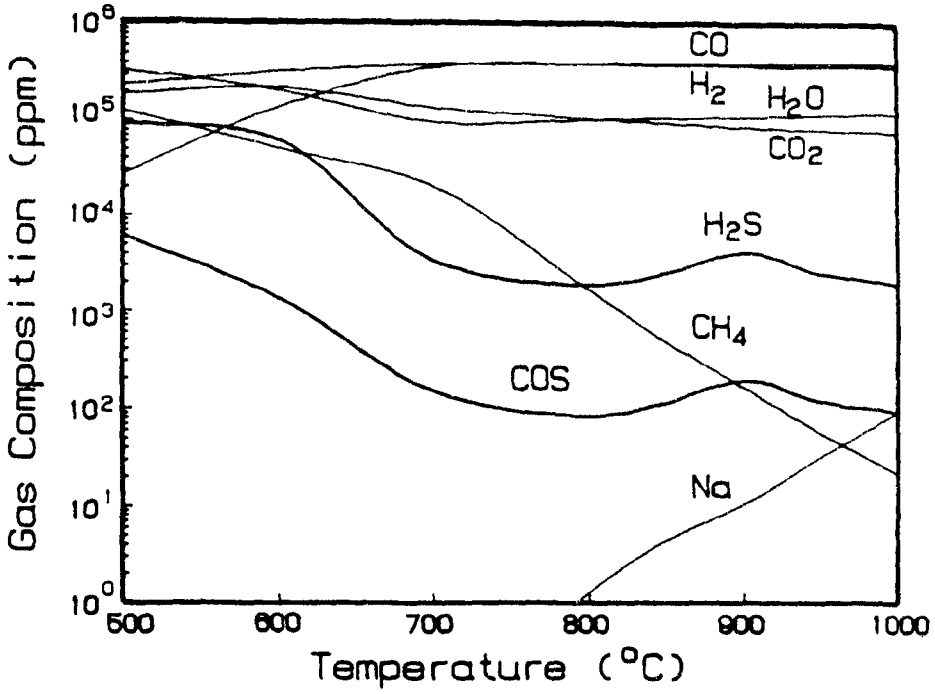

(a)

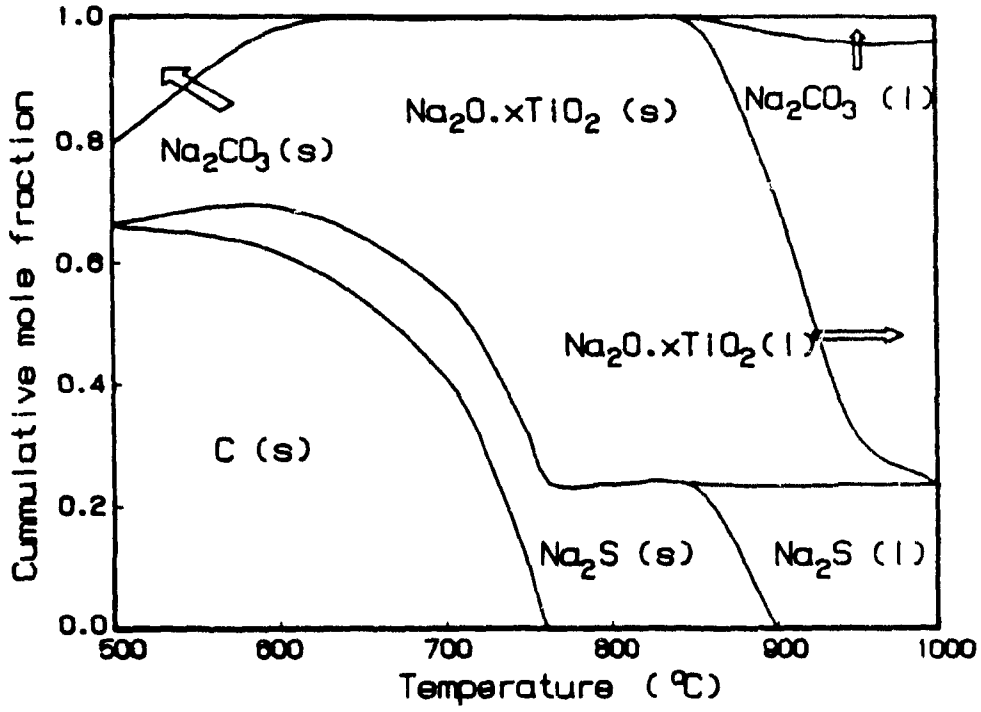

(b)

Figure 11 Reduction of sodium sulfate by a mixture of CO and H_2 $(CO+H_2)/Na_2SO_4$=19.23 mol/mol, CO/H_2=1 mol/mol

$$CO + 3\ H_2 = CH_4 + H_2O \qquad (12)$$

At high temperature the CH_4 concentration is considerably reduced. This suggests that according to thermodynamics CH_4 plus steam may also be used for reduction of the direct causticized mixture at higher temperature. The results for the condensed phase are similar to those obtained for reduction with CO.

Thus a mixture of CO and H_2 can also be used for reduction in the temperature range of 700-850°C, although the sulfur emission as H_2S is now approximately 4-5 times larger than the COS emission obtained with reduction by CO alone.

CONCLUSION

A computer program called F*A*C*T was used to perform thermodynamic calculations for direct causticization of kraft black liquor. It is concluded that only TiO_2 is suitable as water-insoluble metal oxide for kraft black liquor recovery. The combustion/gasification of kraft black liquor with TiO_2 was analyzed thermodynamically for different operating conditions. Based on these calculations, two potential process configurations have been proposed. It is also concluded that the solid combustion product of a mixture of kraft black liquor and TiO_2 can be reduced in the solid state by H_2 and/or CO.

NOMENCLATURE

a_i =Activity of substance i.

a_{pij} =Number of atoms of the jth element in a molecule of the substance i in the pth phase.

b_j =Number of moles of jth element.

g^o_i =Standard chemical potential, J/mol.

G =Total free energy, J.

ΔH_{298} =Formation enthalpy, J/mol.

ΔH_m =Melting enthalpy, J/mol.

m_p =Total number of substances.

n_i =Moles of substance i, mol.

q =Number of pure phases.

R =Universal gas constant, J/(mol.K).

s =Number of condensed phases.

T =Temperature, K.

T_c =Temperature for complete reaction,°C.

T_i =Temperature for initial reaction,°C.

T_m =Melting temperature,°C.

REFERENCES

Andersson, S., "Study on phase diagrams of Na_2S-Na_2SO_4,Na_2CO_3-Na_2S-Na_2SO_4, Na_2CO_3-Na_2SO_4-NaOH and Na_2CO_3-Na_2S-NaOH",*Chemica Scripta*, 1982, 20, p.164.

Backman, R., "Calculations on the System Na_2CO_3-Na_2S-Na_2SO_4", *Academic Dissertation*, part VI, Åbo. Akademi, Finland, March 1989

Barin, I. and S. Knacke, *Thermodynamic Properties of Inorganic Substances*, Springer, Berlin, 1973, (Supplement incl., Kubaschewski O . 1977).

Bauer, T.W. and R.M. Dorland, "Thermodynamics of the Combustion of Sodium-Base Pulping Liquors", *Canadian Journal of Chemical Technology*, 1954, 32(3), p.91.

Durai-Swamy, K., D.W. Warren and M.N. Mansour, "Pulse-Enhanced Indirect Gasification for Black Liquor Recovery", *Proceeding of the 1989 International Chemical Recovery Conference*, p.127-221, CPPA/TAPPI, May, 1989, Ottawa.

Eriksson, G., "Thermodynamic Studies of High Temperature Equilibria, SOLGASMIX", *Chemica Scripta*, 1975, 8, p.100.

Li, J. "Rate Processes during Gasification and Reduction of Kraft Black Liquor Char", *Ph D Dissertation*, McGill University, Montreal, 1989.

Kiiskila, E., "Recovery of Sodium Hydroxide from Alkaline Pulping Liquors By Smelt Causticizing—Part I", *Paperi ja puu—Paper o Tra*, 1978, 60, p.129-132.

Kiiskila, E., Recovery of Sodium Hydroxide from Alkaline Pulping Liquors By Smelt Causticizing—Part II", *Paperi ja puu—Paper o Tra*, 1979, 61, p.394-401.

Kiiskila, E., "Recovery of Sodium Hydroxide from Alkaline Pulping Liquors By Smelt Causticizing—Part IV", *Paperi ja puu—Paper o Tra*, 1979, 61, p.505-510.

Maddern, K.N., "Mill-Scale Development of the DARS — Direct Causticization

Process", *Pulp and Paper Canada*, 1986, 87(10), p.78-82.

McKeough, P., and K. Savıharju, "Novel Energy Production Process for Pulp Mill", *Kemıa - Kemi*, 1991, 18(2), p.102-106.

Pejryd, L. and Hupa, M., "Bed and Furnace Gas Composition in Recovery Boiler — Advanced Equilibrium Calculations", *Proceeding of TAPPI Pulpings Conference 1984*, TAPPI, Atlanta Ga, USA, 1984.

Thompson, W.T., A. D., Pelton and C.W. Bales, *Facility for the Analysis of Chemical Thermodynamics - Guide to Operation*, McGill University, May 1985.

Tsukamoto, H., "Direct Causticizing Technology", *Japan TAPPI*, 1986, 40(1), p.44-50.

Tsukamoto, H. and M. Nakura, "Total Process in Direct Causticizing Technology", *Japan TAPPI*, 1987, 41(1), p.68-73.

Warnqvist, B., "Comments on the Thermodynamical Data and Fusion Temperature for Pure Sodium Sulfide, *Thermochemica Acta.*, 1980, 37, p.343.

Warnqvist, B. and Norrstrom, H., "Chloride in the Recovery Boiler and a Mechanism for Chloride Removal", *TAPPI*, 1976, 59(1), p.59.

CHAPTER 4

KINETICS OF THE DIRECT CAUSTICIZING REACTION BETWEEN SODIUM CARBONATE AND TITANIUM DIOXIDE

ABSTRACT

The kinetics of CO_2 release from the solid (or melt)-solid reaction between Na_2CO_3 and TiO_2 are studied in a tube furnace from 750 to 925°C. It is found that complete conversion of Na_2CO_3 can easily be achieved when using a TiO_2/Na_2CO_3 molar ratio of at least 1.25, leading to the formation of $4Na_2O{\cdot}5TiO_2$. The influence of CO_2 partial pressure and the presence of Na_2SO_4 on the direct causticization of Na_2CO_3 with TiO_2 is also investigated. The kinetic data of the formation of $4Na_2O{\cdot}5TiO_2$ are well described by a reaction model with product layer diffusion control. The activation energy of the formation reaction of $4Na_2O{\cdot}5TiO_2$ in solid state is 216 kJ/mol. Insoluble $Na_2O{\cdot}3TiO_2$ from hydrolysis of $Na_2O{\cdot}TiO_2$ and $4Na_2O{\cdot}5TiO_2$ can be recycled and fully used for CO_2 release from fresh Na_2CO_3.

INTRODUCTION

The direct causticizing method of recovering sodium hydroxide from kraft black liquor with metal oxides was discussed in Chapter 1 and 2. Based on thermodynamic analysis it was shown in Chapter 3 that TiO_2 is the only metal oxide which can be used for direct causticization of kraft black liquor. In the two-step process proposed in Chapter 3, kraft black liquor is first combusted in the presence of TiO_2 and $Na_2O{\cdot}3TiO_2$, leading to the release of CO_2 from Na_2CO_3 by the reactions:

$$Na_2CO_3 + TiO_2 = Na_2O{\cdot}TiO_2 + CO_2 \qquad (1)$$

and

$$2\ Na_2CO_3 + Na_2O{\cdot}3TiO_2 = 3\ Na_2O{\cdot}TiO_2 + 2\ CO_2 \qquad (2)$$

The combusted mixture also contains Na_2SO_4, which is converted into Na_2S in a subsequent reduction step. Because of the weak bond between Na_2O and TiO_2, $Na_2O{\cdot}TiO_2$ decomposes in water to form NaOH according to the reaction:

$$3\ Na_2O{\cdot}TiO_2 + 2\ H_2O = 4\ NaOH + Na_2O{\cdot}3TiO_2 \qquad (3)$$

$Na_2O{\cdot}3TiO_2$ is insoluble in an alkaline solution and can easily be separated from the solution of NaOH and Na_2S or white liquor. The dried $Na_2O{\cdot}3TiO_2$ is recycled to the kraft black liquor combustion step.

Previous studies of the reaction between Na_2CO_3 and TiO_2 were mainly concerned with synthesis and identification of the sodium titanates (Belyaev et al., 1968; Safiulin and Belyaev, 1968; Andersson and Wadsley, 1962; Kurolin and Vulikh, 1965; Mitsuhashi and Fujiki, 1985). The confusions regarding the existence of some of the titanates and the X-ray diffraction (XRD) data in the literature were recently resolved by Bamberger and Begun (1987). They synthesized the compounds by heating stoichiometric quantities of Na_2CO_3 and TiO_2 in the temperature range of 800 to 1200°C. Using Raman spectroscopy, Bamberger and Begun (1987) positively identified $2Na_2O.TiO_2$, α-, β-, γ-$Na_2O{\cdot}TiO_2$, $4Na_2O{\cdot}5TiO_2$, $Na_2O{\cdot}3TiO_2$, and $Na_2O{\cdot}6TiO_2$. However they were not able to synthesize $Na_2O{\cdot}2TiO_2$ and $Na_2O{\cdot}5TiO_2$, previously identified in the literature. More detailed information on the XRD data can be found in Chapter 2. The generally accepted phase diagrams of the system Na_2O-TiO_2 reported by Bouaziz and Mayer (1971) and Gicquel et al. (1972) are reproduced in Chapter

2.

The only relevant kinetic studies are those by Kiiskila (1979a, 1979b) who investigated the reaction between pure Na_2CO_3 and TiO_2 without the presence of Na_2SO_4 from 850-1200°C, i.e., above the melting point of Na_2CO_3 (856°C). Kiiskila reports that the decomposition of sodium carbonate at 850-950°C is due to the formation of solid $4Na_2O\,5TiO_2$ which reacts further with sodium carbonate to yield solid $Na_2O{\cdot}TiO_2$ at low CO_2 partial pressure. Above 1000°C the reaction between sodium carbonate and TiO_2 proceeds in the molten state and the Na_2O/TiO_2 ratio in the melt increases above 1.0. In all cases the sodium titanates could not completely be hydrolyzed, and the insoluble TiO_2 residue contained about 0.33 moles Na_2O per mole TiO_2. Kiiskila did not analyze the conversion-time data in terms of a kinetic model. In the thermodynamic analysis presented in Chapter 3, $Na_2O{\cdot}3TiO_2$ was identified as the insoluble TiO_2 residue obtained during the hydrolysis of sodium titanate.

The objective of the present study is to determine the kinetics and mechanism of the direct causticizing reaction between TiO_2 and Na_2CO_3 from 750-925°C, i.e., below the melting point of the sodium titanate products. The influence of the presence of Na_2SO_4 on the kinetics of the direct causticizing reaction and the reactivity of $Na_2O{\cdot}3TiO_2$ for direct causticization of Na_2CO_3 is also investigated.

EXPERIMENTAL

Experimental apparatus and procedures

A thermogravimetric analysis/differential thermal analysis (TGA/DTA) system of Netsch thermal analyser (model STA 409) was used in the constant heating rate mode (5-40°C/min) to characterize the reaction between Na_2CO_3 and TiO_2 in a flow of 60 ml/min of air or pure carbon dioxide. In addition a TGA system with data acquisition system at McGill University was also used for some experiments. The weight of the sample in the alumina pan was about 20 mg. The sample temperature, sample weight, and the temperature difference between the sample and a reference were continuously recorded.

The TGA/DTA system was not suitable for kinetic study because even at its maximum heating rate of 40°C/min, a significant conversion was obtained before stabilization at the desired measurement temperatures varying from 750 to 925°C. Therefore isothermal kinetic experiments were performed in a tube furnace system (Lindberg type 55035, Oven length: 34 cm) shown schematically

in Figure 1. The reaction between Na_2CO_3 and TiO_2 was followed by measuring the CO_2 concentration continuously by an IR analyzer (A.D.C. type SB-305). A platinum sample pan was fixed to the support of a thermocouple and its junction was in contact with the sample. The thermocouple and the sample pan could be moved smoothly from one end of the furnace to its center by moving the support rod through a tightly fitted hole in a rubber stopper at that end of a quartz tube (I.D. 2.5 cm) inside the furnace. Initially the sample pan was kept near the end of the tube furnace at a temperature of about 500°C. After the reactor system was flushed with 1000 ml/min N_2 (99.99% purity) for half an hour and the CO_2 concentration was less than 1 ppm, the sample was quickly pushed to the center of the tube furnace and the CO_2 liberation was subsequently recorded. It took generally about 30 seconds to reach the preset reaction temperature. The temperature of the furnace could be controlled with ±3°C during the experiments. The sample size was varied from 3 to 10 mg in order to keep the maximum CO_2 concentration below 1000 ppm, the optimum range for the IR analyzer. The samples for XRD analysis were prepared in the tube furnace using a large sample of about 1000 mg.

The sodium sulfate and carbonate content of the solid reaction product was determined by ion chromatography (IC). The sodium titanates were identified by X-ray diffraction (XRD). A scanning electron microscope (SEM) was used to characterize the morphological changes of the reaction product.

Sample preparation

The reagents used were anhydrous sodium carbonate of 99.95% purity, anhydrous sodium sulfate of 99.0% purity and titanium dioxide of 99.975% purity (d_p<10 μm). Pure Na_2CO_3 or 3 moles of Na_2CO_3 and one mole of Na_2SO_4 were dissolved in water and subsequently dried to obtain a model compound mixture. The latter closely simulates the combustion product from kraft black liquor. The mixtures were ground to a particle size of less than 25 μm and again dried in air at 500°C for 1 hour.

Solid $Na_2O.3TiO_2$ for the recycling experiments was obtained as follows: Na_2CO_3 (d_p<25 μm) and TiO_2 (d_p<10 μm) at a molar ratio of 1:1 were ground together, and the mixture was placed in a tube furnace at 900°C for 6 hours (melting point of Na_2CO_3, 858°C). Complete hydrolysis of the product $Na_2O{\cdot}TiO_2$ to $Na_2O{\cdot}3TiO_2$ and NaOH was achieved after 4 hours in 90°C distilled water in a glass flask equipped with a magnetic stirrer. The degree of hydrolysis was measured by titrating the formed sodium hydroxide. After washing, the solid

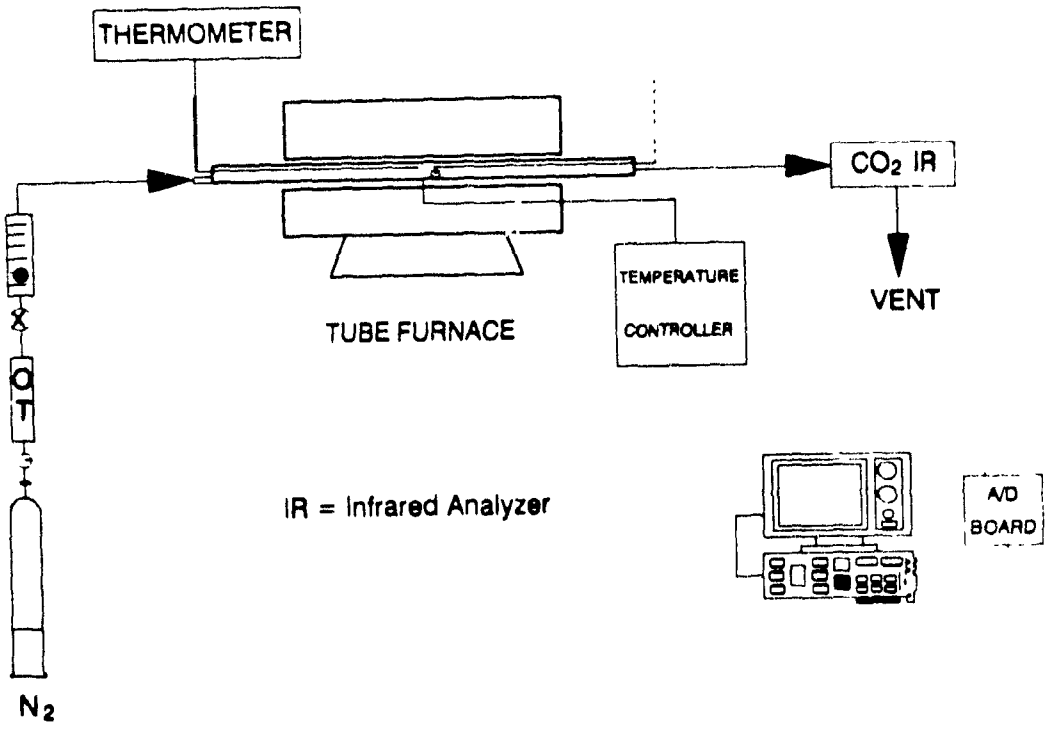

Figure 1 Tube furnace reactor system

filtrate, $Na_2O{\cdot}3TiO_2$, was heated at 500°C before further use.

RESULTS AND DISCUSSION

Thermogravimetric and Differential Thermal Analysis

It is well known that sodium carbonate decomposes at elevated temperature according to the following reaction:

$$Na_2CO_3 \triangleq Na_2O + CO_2 \qquad (4)$$

The thermogravimetric results in Figure 2 show that the decomposition of pure Na_2CO_3 starts in air at about 820°C. In a CO_2 atmosphere, Na_2CO_3 is stable up to 1000°C. These results are consistent with those found by Kiiskila (1979a). Therefore the presence of CO_2 will strongly retard the decomposition, and a causticizing agent will be needed to liberate CO_2 from Na_2CO_3.

The TGA/DTA results for a mixture of pure sodium carbonate and titanium dioxide at a molar ratio of 1.0 are shown in Figure 3. Three DTG and DTA peaks are observed at 655°C, 750°C and 985°C, respectively. According to the older literature (Belyaev et al., 1968; Safiullin and Belyaev, 1968), $Na_2O{\cdot}2TiO_2$ is formed initially at 600°C via the reaction:

$$Na_2CO_3 + 2\ TiO_2 = Na_2O{\cdot}2TiO_2 + CO_2 \qquad (5)$$

However, the existence of $Na_2O{\cdot}2TiO_2$ could not be demonstrated in recent literature (Bouaziz and Mayer, 1971; Bamberger and Begun, 1987). A more likely explanation for the first weight loss shown in Figure 3 may be the formation of the known sodium trititanate, $Na_2O{\cdot}3TiO_2$, via reaction:

$$Na_2CO_3 + 3\ TiO_2 = Na_2O{\cdot}3TiO_2 + CO_2 \qquad (6)$$

The theoretical weight loss associated with the complete conversion of TiO_2 according to reaction (6) is indicated by ΔW_1 in Figure 3. It can be seen that ΔW_1 corresponds approximately to the weight loss at completion of the first DTG peak, thus giving support to the formation of $Na_2O{\cdot}3TiO_2$ rather than $Na_2O{\cdot}2TiO_2$. When the second DTG peak is complete, the total weight loss is equivalent to a CO_2 release by about 80% of Na_2CO_3. This suggests that

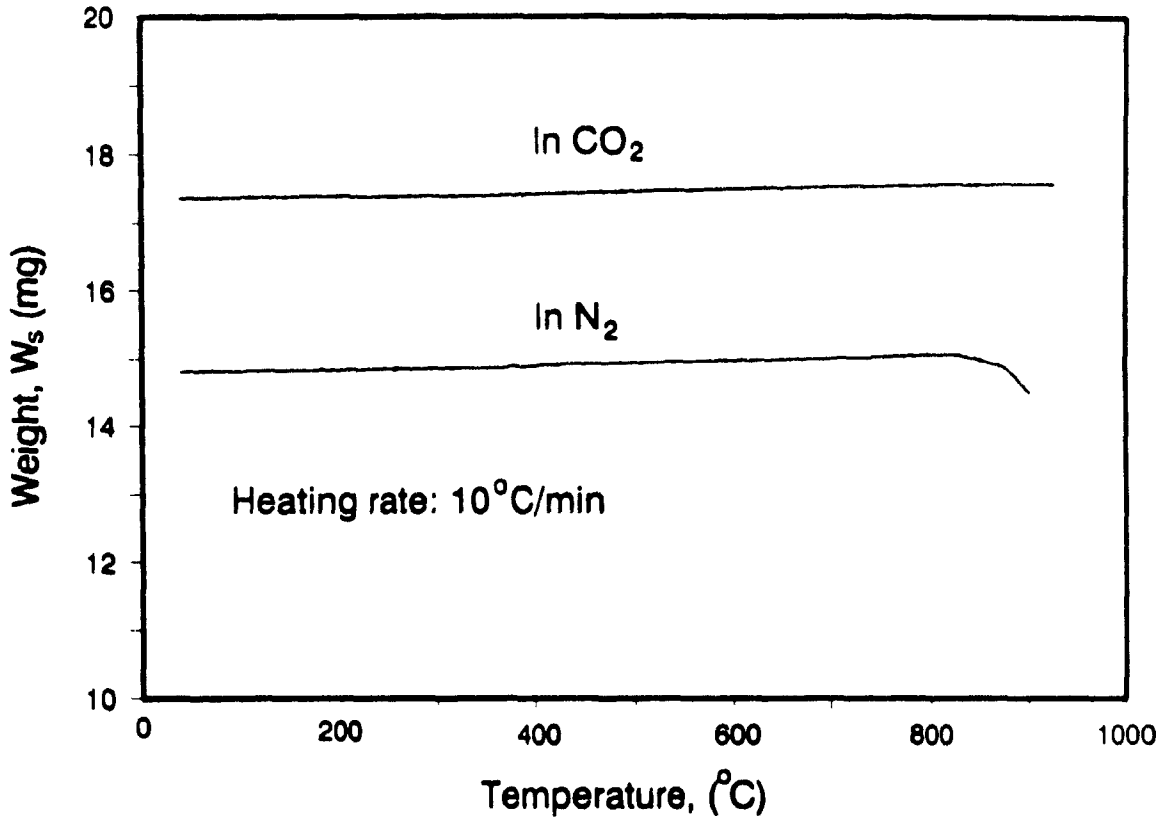

Figure 2 Decomposition of sodium carbonate

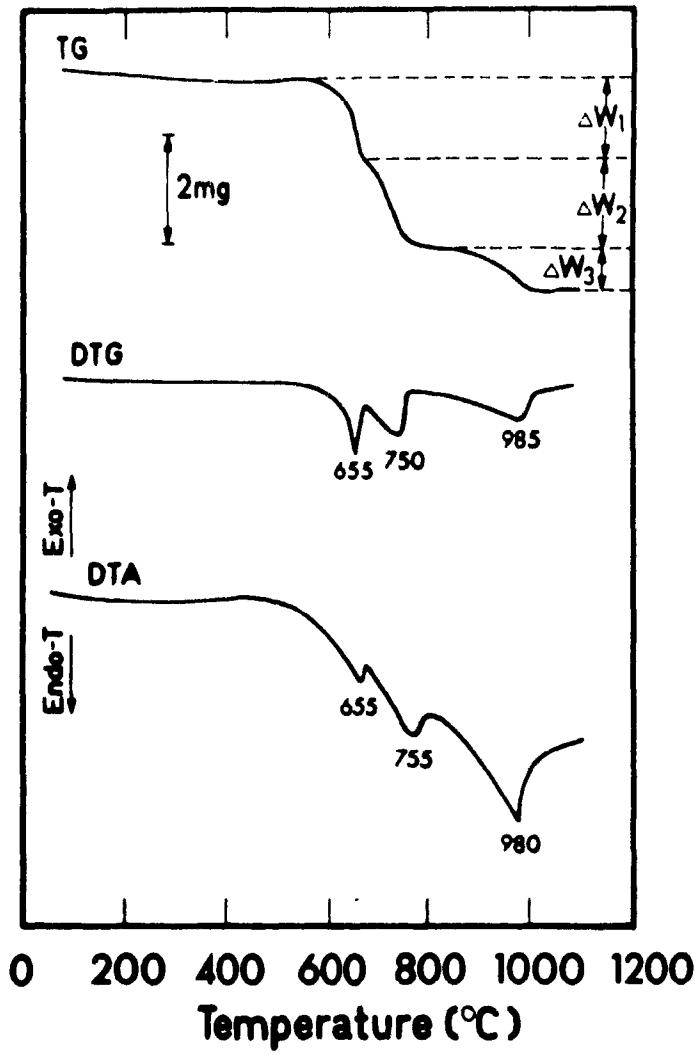

Figure 3 TGA and DTA results for a mixture of pure Na_2CO_3 and TiO_2
TiO_2/Na_2CO_3=1.0 mol/mol, Heating rate: 10°C/min
Initial sample weight: 16.8 mg

$Na_2O{\cdot}3TiO_2$ reacts further with Na_2CO_3 to form $4Na_2O\,5TiO_2$ according to the overall reaction:

$$5\ (Na_2O{\cdot}3TiO_2) + 7\ Na_2CO_3 = 3\ (4Na_2O{\cdot}5TiO_2) + 7\ CO_2 \quad (7)$$

The theoretical weight loss due to complete conversion of $Na_2O{\cdot}3TiO_2$ according to reaction (7) is indicated by ΔW_2 in Figure 3. The combination of reactions (6) and (7) can be written as:

$$4\ Na_2CO_3 + 5\ TiO_2 = 4Na_2O{\cdot}5TiO_2 + 4\ CO_2 \quad (8)$$

The formation of $4Na_2O{\cdot}5TiO_2$ for a sample heated at 900°C was confirmed by X-ray diffraction analysis, using the most recent XRD data. At a molar ratio of TiO_2/Na_2CO_3=1.0 and 1.25, the formation of $4Na_2O{\cdot}5TiO_2$ after 5 minutes at 900°C is clearly observed from XRD analysis shown in Figure 4, in agreement with the observation of Kiiskila (1979a). After melting of Na_2CO_3 at about 850°C, another weight loss is seen in Figure 3. Based on the size of this weight loss, literature evidence (Belyaev et al., 1968) and the XRD analysis in Figure 5, $Na_2O{\cdot}TiO_2$ is formed according to the following reaction:

$$4Na_2O{\cdot}5TiO_2 + Na_2CO_3 = 5\ Na_2O{\cdot}TiO_2 + CO_2 \quad (9)$$

The theoretical weight loss associated with complete conversion of reaction (9) is shown as ΔW_3 in Figure 3. The combination of reactions (6), (7) and (9) can be written as:

$$Na_2CO_3 + TiO_2 = Na_2O{\cdot}TiO_2 + CO_2 \quad (10)$$

and therefore the sum of ΔW_1, ΔW_2, and ΔW_3 corresponds to 100% conversion of Na_2CO_3 when charged with an equimolar amount of TiO_2. It must be noted, however, that the three steps are not completely sequential but occur simultaneously to some degree so that the theoretical weight loss does not always exactly correspond to the experimental weight loss. The experimental results in Figure 3 also show that a very high temperature of about 1000°C is required for completion of reaction (9). Furthermore, the wide temperature range needed for completion of ΔW_3 compared to that of ΔW_2, suggests that the apparent activation energy of reaction (9) is lower than that of reaction (7).

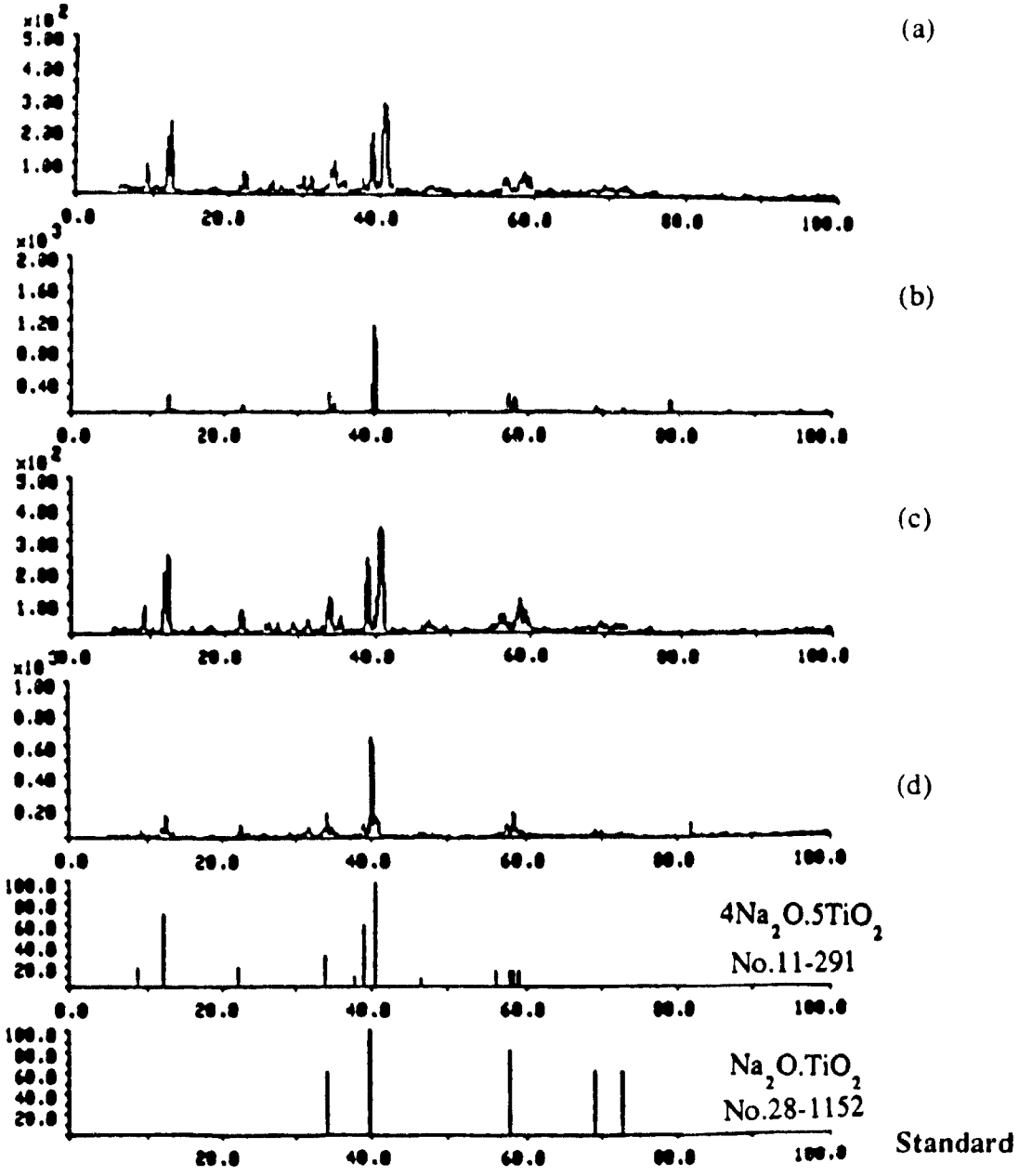

Figure 4 Results of X-ray diffraction analysis
Mixture of pure Na_2CO_3 and TiO_2 after heating at 900°C,
(a) TiO_2/Na_2CO_3=1.0, t=5 min.; (b) TiO_2/Na_2CO_3=1.0, t=60 min.;
(c) TiO_2/Na_2CO_3=1.25, t=5 min.;(d) TiO_2/Na_2CO_3=1.25, t =60 min.

Since the results in Figure 3 show that reaction (7) is fast and can be completed below the melting point of Na_2CO_3 (856°C), the reaction between TiO_2 and pure Na_2CO_3 was investigated at a TiO_2/Na_2CO_3 molar ratio of 1.25. The TGA and DTA results are shown in Figure 5. The theoretical weight losses associated with complete conversion of TiO_2 via reactions (6) and (7) are indicated as ΔW_1 and ΔW_2, respectively. The total weight loss, $\Delta W_1+\Delta W_2$, is also equivalent to 100% conversion of Na_2CO_3. Therefore, similar to Kiiskila's (1979a) experiments for TiO_2/Na_2CO_3 molar ratios larger than 2.0, it is shown in the present study that complete conversion of Na_2CO_3 can be obtained with the reactants and products in the solid state when the TiO_2/Na_2CO_3 molar ratio is larger than 1.25. The CO_2 release rate is faster in the present study compared to that of Kiiskila (1979a and 1979b) because smaller TiO_2 particles (10 μm versus 250 μm, respectively) and a smaller sample size (respectively about 20 mg and 2 g) are used.

The influence of CO_2 was also checked by changing the atmosphere from N_2 to CO_2. It was found that reaction (8) is somewhat affected by the change-over to CO_2 and however the temperature to complete the conversion of Na_2CO_3 is very close to that in N_2 as shown in Figure 6. In another experiment with $Na_2O{\cdot}TiO_2$ as the initial sample, it is seen in Figure 7 that $Na_2O\,TiO_2$ reacts with CO_2 to form $4Na_2O{\cdot}5TiO_2$ at 810°C according to the following reaction:

$$5\ Na_2O{\cdot}TiO_2 + CO_2 = 4Na_2O{\cdot}5TiO_2 + Na_2CO_3 \qquad (11)$$

The results agree with those of Niggli (1916), who reported that $Na_2O{\cdot}TiO_2$ is not formed at temperature below 1000°C in a CO_2 atmosphere, and with those of Bennington and Brown (1973), and Mitsuhashi and Fujiki (1985), who found that $Na_2O{\cdot}TiO_2$ decomposes to $4Na_2O{\cdot}5TiO_2$ at temperatures of 910-1100°C. Thus, the above results indicate that reaction (11) is a reversible reaction.

Chemical Reaction Kinetics of the Formation of $4Na_2O{\cdot}5TiO_2$ and $Na_2O\,TiO_2$

I Reaction between TiO_2 and Na_2CO_3 mixed with Na_2SO_4

The sample temperature and CO_2 concentration in the product gas for a typical kinetic experiment are shown in Figure 8. A mixture of 75% Na_2CO_3 and 25% Na_2SO_4 (molar percent) was always used in the kinetic part of this study. The conversion of Na_2CO_3, X, can be calculated from the released amount of CO_2 by the following equation:

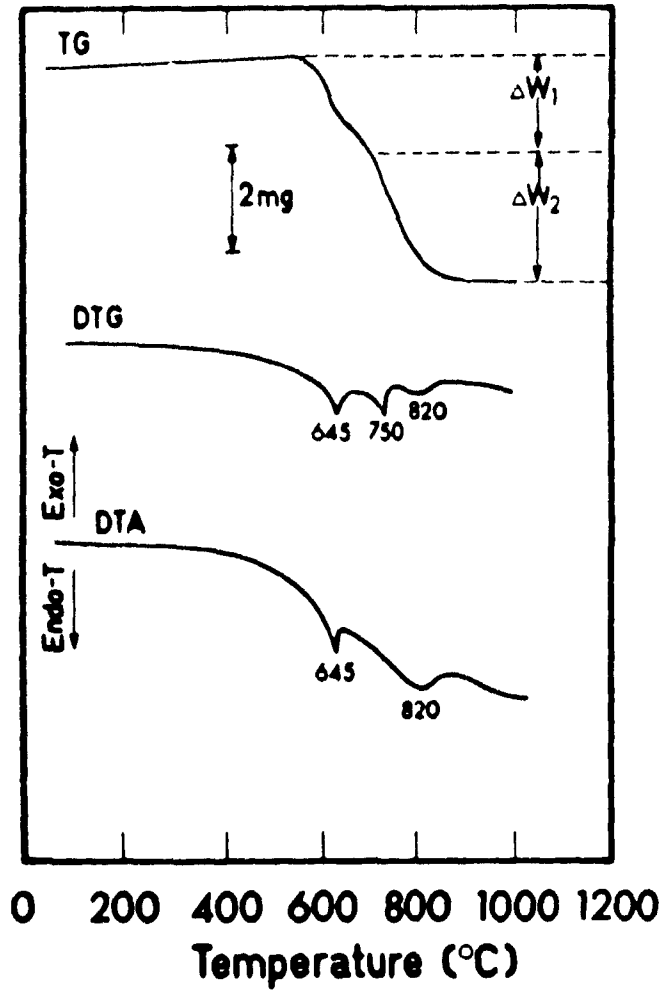

Figure 5 TGA and DTA results for a mixture of Na_2CO_3 and TiO_2
TiO_2/Na_2CO_3=1.25 mol/mol, Heating rate: 10°C/min
Initial sample weight: 20.1 mg

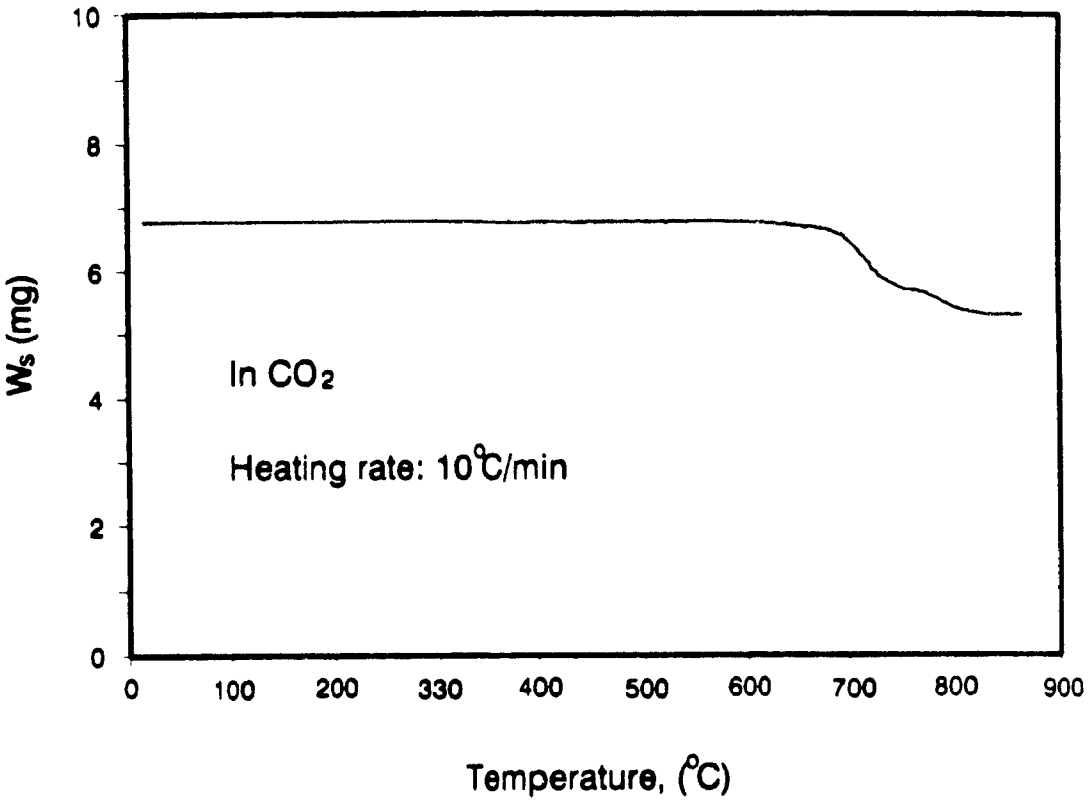

Figure 6 Reaction between Na_2CO_3 and TiO_2 in atmosphere of CO_2
TiO_2/Na_2CO_3=1.25 mol/mol

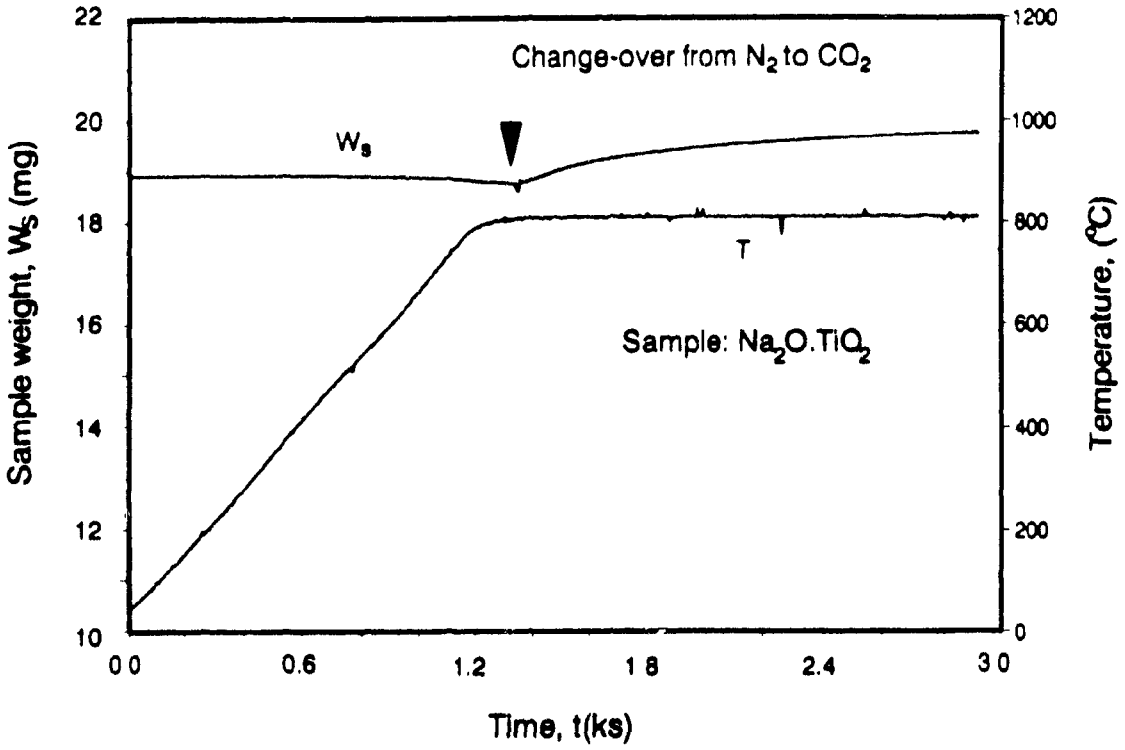

Figure 7 Reaction between CO_2 and $Na_2O.TiO_2$

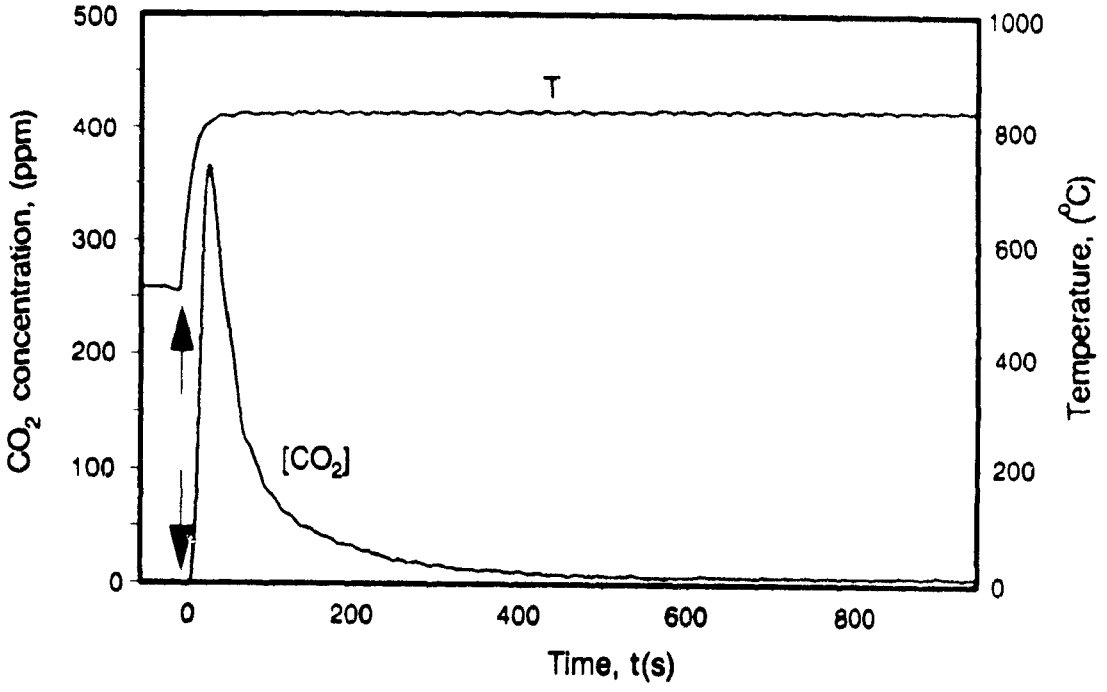

Figure 8 Typical raw data for a kinetic experiment

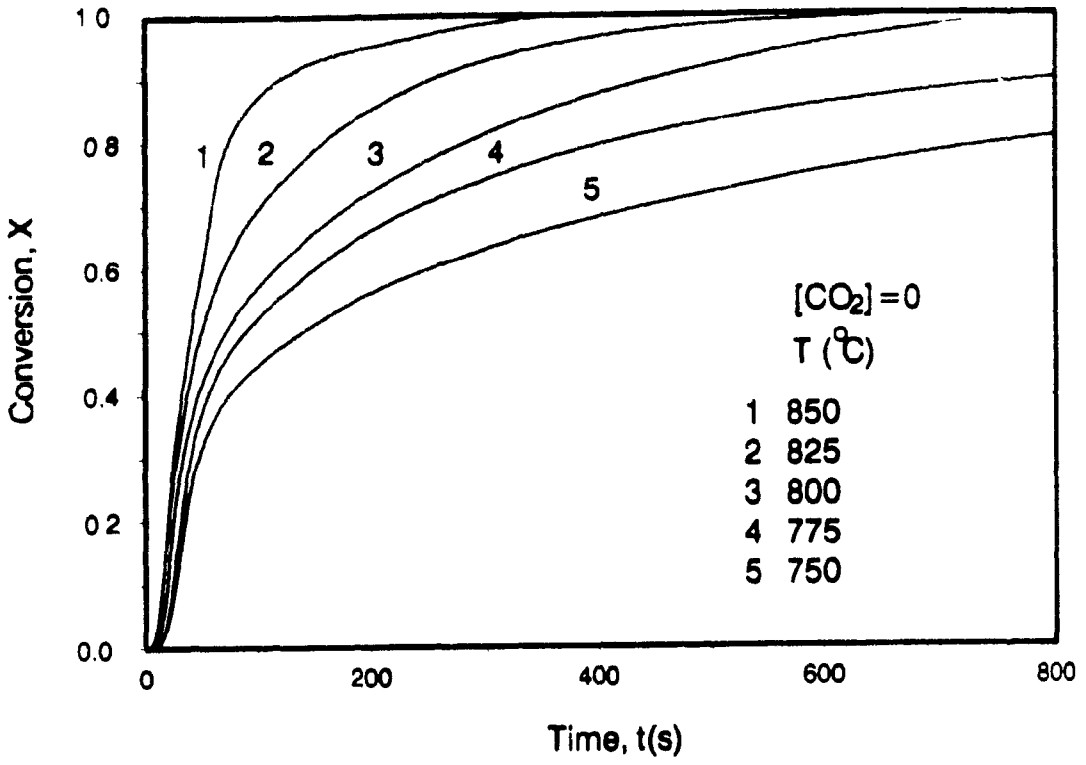

Figure 9 Kinetic data from mixture of TiO_2/Na_2CO_3=1.25 mol/mol

$$X = \frac{\int_0^t \frac{QM}{RT} Pco_2(t)\, dt}{[Wco_2]_i} \qquad (12)$$

where $[Wco_2]_i$ is the theoretical weight of CO_2 which can be released from the initial sample upon complete decomposition of Na_2CO_3; Q is the flow rate, R is the universal gas constant, T is the temperature; M is the molecular weight of CO_2 and Pco_2 is the partial pressure measured by the IR analyzer. Preliminary experiments showed an excellent agreement with differences of about 1% between the conversion calculated from Eq.(12) and the conversion calculated from the measured weight loss. This was also confirmed by measuring the amount of Na_2CO_3 remaining in the sample by ion chromatography. The amount of sulfate before and after CO_2 release was unchanged, confirming that Na_2SO_4 is inert during the direct causticizing reaction.

Influence of temperature

The different conversion-time (X-t) curves obtained for a molar ratio of TiO_2/Na_2CO_3 of 1.25 at 750 to 850°C are shown in Figure 9. Complete conversion of Na_2CO_3 is achieved in a relatively short time above 800°C, while the initial conversion is extremely fast. These results are in agreement with the earlier finding that the formation of $Na_2O{\cdot}3TiO_2$ is very rapid, and that further reaction to $4Na_2O{\cdot}5TiO_2$ can be accomplished in the solid state.

The melting point of the present Na_2CO_3-Na_2SO_4 mixture is about 830°C (Gitlesen and Motzfeldt, 1964). The melting point of TiO_2 is 1800°C, i.e., much higher than that of the mixture of Na_2CO_3 and Na_2SO_4. Therefore it is likely that Na_2CO_3 diffuses through the reaction product formed on the TiO_2 particles rather than TiO_2 diffusing into the Na_2CO_3-Na_2SO_4 particles. Since the product, $4Na_2O{\cdot}5TiO_2$, is a refractory which forms a barrier for diffusion of Na_2CO_3, internal transport of Na_2CO_3 will likely become the rate-determining step for further reaction. This effect increases in significance with increasing particle size of TiO_2. Thus one might expect that the following X-t relationship:

$$[1-(1-X)^{1/3}]^2 = \frac{2k'A}{r^2}\, t = kt \qquad (13)$$

derived by Jander (1927) for a diffusion controlled solid-solid reaction, and discussed in Chapter 2 will be applicable. In Equation (13), k' is a constant,

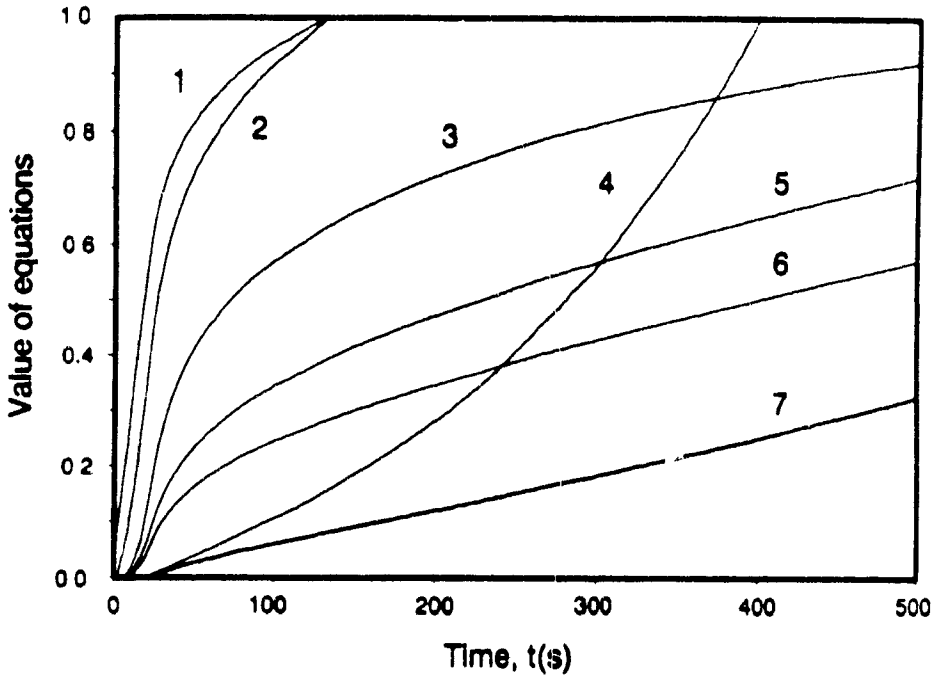

1 $[-\ln(1-X)]^{1/3}=kt$

2 $[-\ln(1-X)]^{1/2}=kt$

3 X

4 $\left[\frac{1}{(1-X)^{1/3}} - 1\right]^2 = kt$

5 $1-(1-X)^{1/3}=kt$

6 $1-(1-X)^{1/2}=kt$

7 $[1-(1-X)^{1/3}]^2=kt$

Figure 10 Comparison of different model fittings
T=800°C, TiO_2/Na_2CO_3=1.25 mol/mol

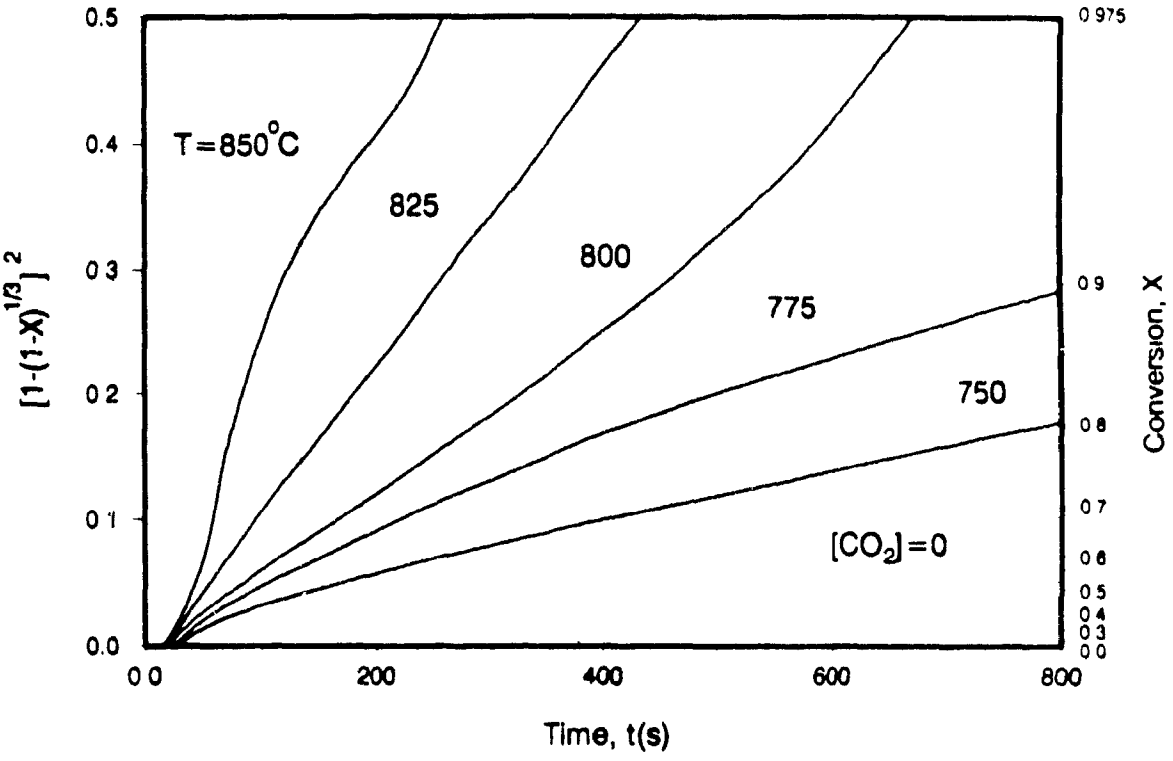

Figure 11 $[1-(1-X)^{1/3}]^2$ vs. t
TiO_2/Na_2CO_3=1.25 mol/mol
(Data from Figure 9)

A is the cross-sectional area and r is the initial radius of the spherical TiO_2 particles. The X-t data obtained in Figure 9 at 800°C were plotted in Figure 10 according to Eq (13) as well as according to the other solid-solid reaction models reviewed in Chapter 2. The comparison shows that the experimental results are indeed best represented by Jander's model because only with that model a linear relationship is obtained between the left hand side of the model equation and reaction time, t. The fiting by these models was also conducted for data at other temperatures and demonstrated that Jander's model gives the best fitting. Figure 11 shows the left-hand side of Eq.(13), $[1-(1-X)^{1/3}]^2$, *vs* time for all the data of Figure 9 obtained at different temperatures. A reasonable linear fit is obtained for the conversion between 40 to 90% at all temperatures except 775°C. The inapplicability of Eq.(13) at conversions below 40% could be explained by that the initial reaction between Na_2CO_3 and TiO_2 is kinetically controlled. This was also observed for the reaction between $BaCO_3$ and SiO_2 where the mechanism changed from being controlled by reaction at the interface to the product layer diffusion control (Yamaguchi et al., 1972). Also most of the initial delay time for conversion of Na_2CO_3 is the result of the heat-up time of about 30 seconds. The rate constants were calculated from the linear fitting in Figure 11 with a correlation coefficient higher than 0.98. An Arrhenius plot of the rate constants obtained from Figure 11 gives an activation energy of 246 kJ/mol in Figure 12. The somewhat higher rate constant at 850°C might be due to melting of the Na_2SO_4-Na_2CO_3 mixture. Thus a regression analysis is made without the data point at 850°C. A better straight line correlation is obtained as shown in Figure 12 with an activation energy of 216 kJ/mol. The activation energy of 216 kJ/mol is comparable to those published for similar systems with product layer control, for example, 217 and 210 kJ/mol for the Na_2CO_3-Fe_2O_3 and Li_2CO_3-Fe_2O_3 systems respectively (Gallagher and Johnson, 1976), 226 kJ/mol for the $BaCO_3$-SiO_2 system (Yamaguchi et al., 1972) and 250 kJ/mol for the Na_2CO_3-Al_2O_3 system (Christie et al., 1978).

SEM pictures of the samples before and after complete conversion of Na_2CO_3 by TiO_2 (TiO_2/Na_2CO_3=1.25 mol/mol) are shown in Figure 13. The larger particles in the original sample are Na_2CO_3 and the agglomerates of the smaller particles are TiO_2. After treatment at 770 and 900°C, the Na_2CO_3 particles have disappeared and the TiO_2 agglomerates appear to be solid but distinct particles. The explanation for the latter is that TiO_2 and the products $Na_2O{\cdot}3TiO_2$, $4Na_2O{\cdot}5TiO_2$ and $Na_2O{\cdot}TiO_2$ do not melt (melting points

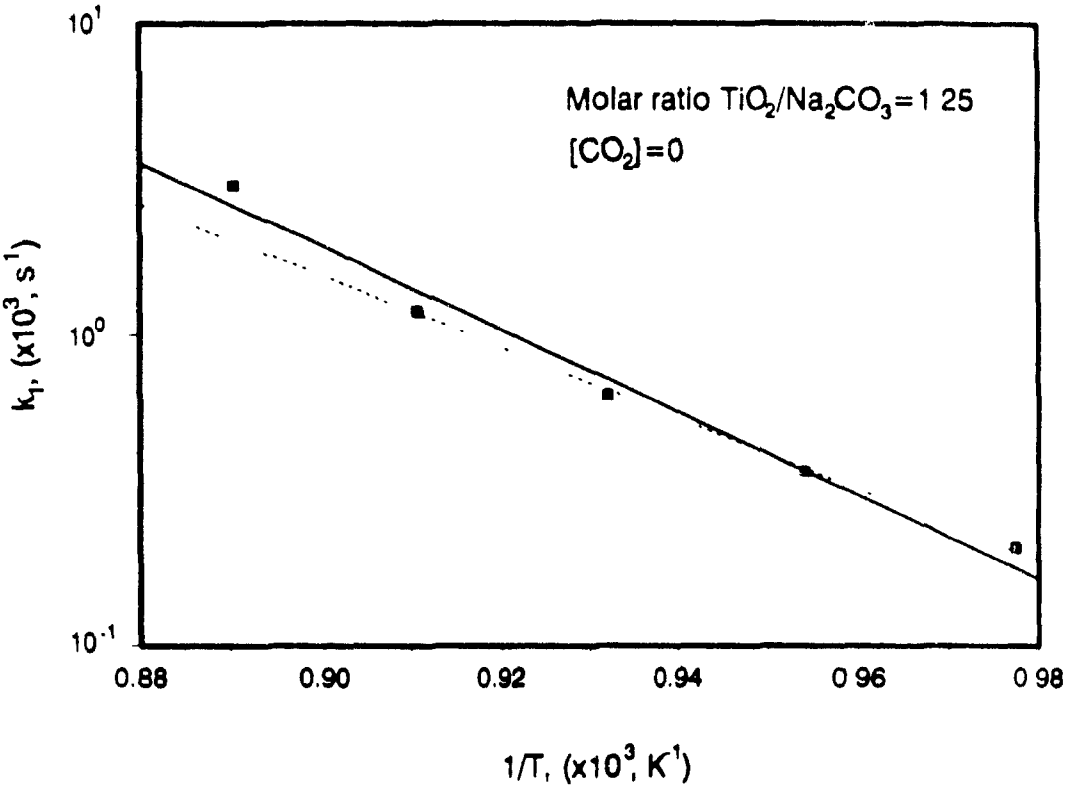

Figure 12 Arrhenius plot of rate constants

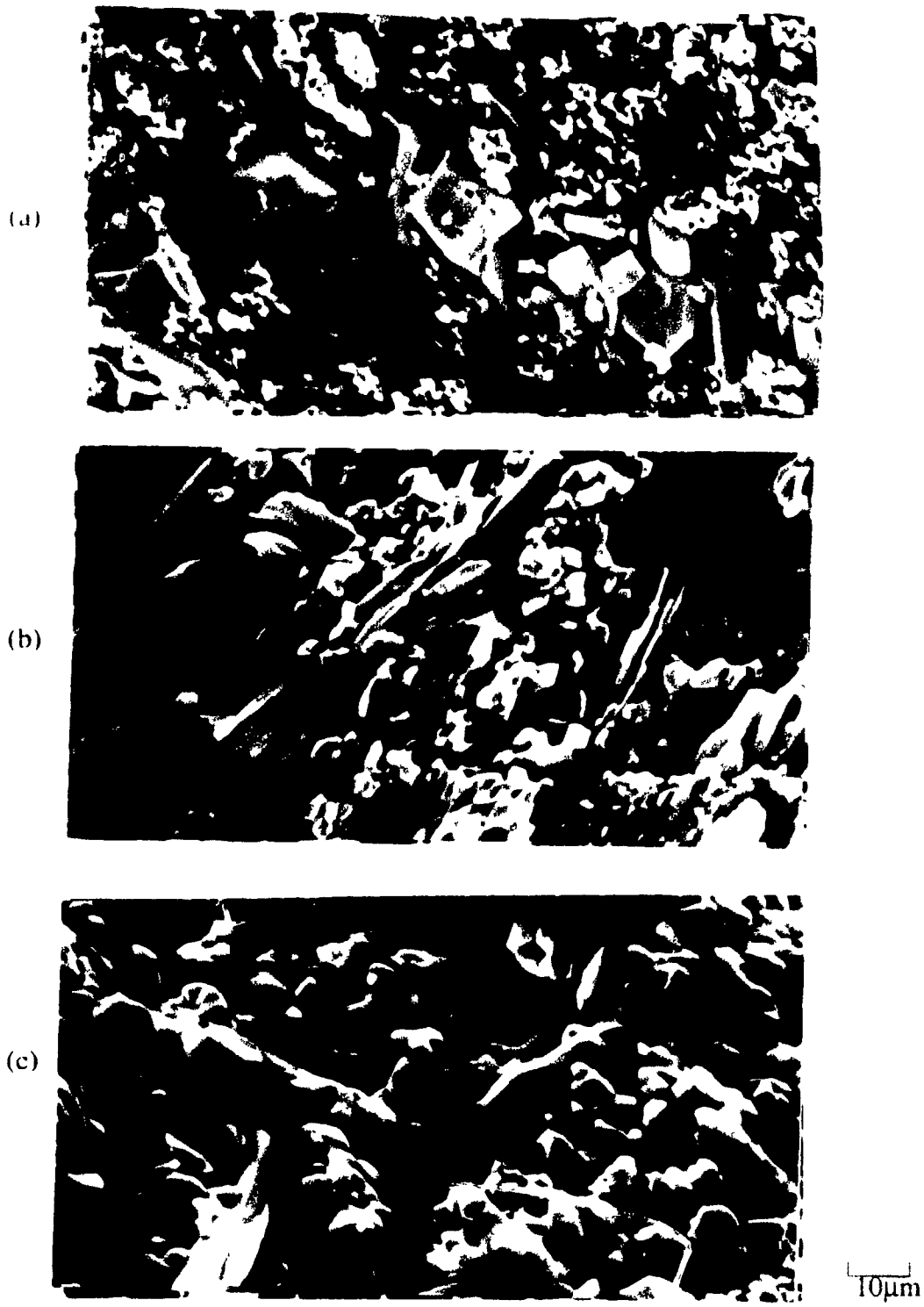

(a) before treatment; (b) Treated at 770°C for 70 minutes;
(c) Treated at 900°C for 12 minutes.

Figure 13 SEM pictures of the reaction sample
(TiO_2/Na_2CO_3=1.25 mol/mol)

respectively of 1840, 1130, 1030 and 965°C, Bouaziz and Mayer, 1971) under the present conditions, and that the molar volume of the sodium titanates (31.5 and 41.3 cm^3/mole TiO_2 for respectively $Na_2O{\cdot}3TiO_2$ and $Na_2O\ TiO_2$, Shomate, 1946) is much larger than that of TiO_2 (18.8 cm^3/mole TiO_2). As a result, the micron sized particles making up the agglomerates swell upon reaction with Na_2CO_3. When Na_2CO_3 is completely converted, each agglomerate is transferred into a solid fused particle with many protuberances which is larger than the original agglomerate. Since only some of these complicated phenomena are included in Jander's model, it might also explain why Eq (13) is only partially successful in representing the present data for conversions higher than 90%.

Finally some speculations can be made regarding the nature of the diffusing species. Data reported in literature (Kuczynski, 1965) showed that diffusion-controlled activation energies of ~250 kJ/mol were observed for similar systems, e.g., the diffusion of nickel ions through $NiAlO_2$ and through $NiCr_2O_4$, and atomic oxygen through $NiCr_2O_4$. A much higher activation energy was found for the diffusion of metal ions through metal oxides. For example, about 500 kJ/mol was reported for the diffusion of aluminum ions through Al_2O_3. On other hand it was found that the activation energy for the diffusion of oxygen ions through a metal oxide such as NiO, WO_3, Al_2O_3 or TiO_2 is about 250 kJ/mol. Thus it appears likely that for the Na_2CO_3-TiO_2 system, Na and O ions, or combined as Na_2O, are the diffusing species. In the similar system of Li_2CO_3-Fe_2O_3, it was observed that the activation energy is 210 kJ/mol for the Li and O ions diffusing through Fe_2O_3 (Gallagher and Johnson, 1976). Thus it is suggested that since Na_2CO_3 is mobile at the temperatures used in present study, it can migrate to cover the TiO_2 particles. Na_2CO_3 then reacts with TiO_2 to release CO_2 with the rate-limiting step being the diffusion of Na and O ions or Na_2O through the product layer of $4Na_2O{\cdot}5TiO_2$.

The kinetic data for a Na_2CO_3/TiO_2 molar ratio of 1.0 are shown in Figure 14(a) and 15(a) for the temperature ranges of respectively 750 to 825°C, and 850 to 925°C. As for a TiO_2/Na_2CO_3 molar ratio of 1.25 (Figure 9), the initial reaction is again relatively fast, but then the reaction rate slows considerably. At the highest temperature of 925°C, the Na_2CO_3 conversion approaches 80% during the rapid initial phase and then slowly approaches 100% at longer times, indicative of a rapid formation of $4Na_2O{\cdot}5TiO_2$ and a slow consecutive reaction to $Na_2O{\cdot}TiO_2$. The representation of the data by Jander's model in Figure 14(b) and 15(b) shows a distinct change in the slope of

$[1-(1-X)^{1/3}]^2$ *vs* t at 70-80% conversion, in agreement with the completion of reaction (8) and start of reaction (9). No reaction rate constants were determined for the data in Figure 14(b) and 15(b) because of the difficulty to identify a linear region. The much faster reaction below 80% conversion at 850°C compared to 825°C (Figure 14) can be explained by melting of the mixture of Na_2SO_4-Na_2CO_3 at about 830°C.

However, if the data in Figure 14(a) and 15(a) are replotted according to a newly defined conversion, X', of TiO_2 to $4Na_2O{\cdot}5TiO_2$ instead of X for Na_2CO_3 to $Na_2O{\cdot}TiO_2$, (*Note X' can be more generally defined as the conversion as the fraction of the maximum amount of* $4Na_2O{\cdot}5TiO_2$ *which can be formed The maximum amount depends on which of the two components* Na_2CO_3 *or* TiO_2 *is the least available for formation of* $4Na_2O{\cdot}5TiO_2$ *Only when the molar ratio is* $TiO_2/Na_2CO_3=1.25$ *then it does not make a difference; otherwise it does*), a rather good linear relationship could be obtained below 85% conversion as shown in Fig 17(a) and 17(b). This again shows that Jander's model is suitable to describe the kinetics of formation of $4Na_2O{\cdot}5TiO_2$. The deviations above 85% conversion may be the results of formation of $Na_2O{\cdot}TiO_2$ from $4Na_2O{\cdot}5TiO_2$ which proceeds simultaneously with the formation of $4Na_2O{\cdot}5TiO_2$. From the linear portion of the straight lines below 85% conversion in Figure 16, rate constants at different temperature are obtained (correlation coefficient higher than 0.99) and plotted against the inverse of temperature in Figure 17. It is very interesting to see a break in this Arrhenius plot near the melting temperature of the mixture of Na_2SO_4-Na_2CO_3. From the slope of the two straight line sections, activation energies of 208 kJ/mol and 151 kJ/mol are obtained for solid-solid and solid-liquid state reaction, respectively. In fact, the difference between the two activation energies may be directly related to the heat of melting of the Na_2SO_4-Na_2CO_3 mixture. The rate constants at a molar ratio of TiO_2/Na_2CO_3 of 1.25 are also plotted in Figure 18. It can be seen that the rate constants at a molar ratio of 1.25 agree very well with those obtained at a molar ratio of 1.0 below 825°C. Consequently the activation energies for the solid-solid reaction at the molar ratios of 1.25 and 1.0 are also very close (216 *vs.* 208 kJ/mol respectively).

The present kinetic model was tested for the experimental data obtained by Kiiskila (1979b) for a mixture of pure Na_2CO_3 and TiO_2 (i.e., no Na_2SO_4 present) at a TiO_2/Na_2CO_3 molar ratio of 1.325. Kiiskila used much larger particles of 250 μm for both TiO_2 and Na_2CO_3. Kiiskila's original data are shown in Figure 18(a) and the fit of the model is shown in Figure 18(b). It

can be seen that the experimental data are very well presented by Jander's model. From the slope of the straight line fits of the data at 850, 900 and 950°C in Figure 18(b), reaction rates are calculated and plotted in Figure 17. The rate constants obtained from Kiiskila's data are much smaller than those obtained in the present study for TiO_2 particles less than 10 μm and with Na_2SO_4 present. It illustrates the large influence of particle size on the rate of the direct causticizing reaction. With increasing TiO_2 particle size, the initial reaction (6) consumes a decreasing fraction of TiO_2 before the outer shell of $4Na_2O{\cdot}5TiO_2$ is established and diffusion through this layer becomes the rate limiting step. This might explain the fact that the large particle size data of Kiiskila (1979b) are better represented by Eq. (13) than the present data. In effect, in the present work the conversion, X, should be corrected for the initial conversion of TiO_2 via reaction (6). An activation energy of 268 kJ/mol is obtained when Kiiskila's results of Figure 18(b) are plotted in Figure 17, which is higher than 216 kJ/mol obtained in the present work.

Influence of TiO_2/Na_2CO_3 molar ratio

The influence of the TiO_2/Na_2CO_3 molar ratio on the Na_2CO_3 conversion is shown in Figure 19(a). The results show that with increasing molar ratio the Na_2CO_3 conversion is completed in a shorter time. It also shows that the reaction rate remains high up to high conversions when the TiO_2/Na_2CO_3 molar ratio is larger than 1.25. There is a very little difference between the results obtained with molar ratios of 1.25 and 2.00 for X<85%. However, for X>85%, the sodium carbonate conversion with a molar ratio of 2.00 is faster probably because in the latter case there is an excess amount of TiO_2 for conversion of Na_2CO_3 to $4Na_2O{\cdot}5TiO_2$. In the former case, with a molar ratio just sufficient for the formation of $4Na_2O{\cdot}5TiO_2$, the final conversion is slow because the reaction becomes limited by the availability of TiO_2. Plotting the X-t data according to Jander's model in Figure 19(b) shows that the conversion range of the model fit increases for molar ratios larger than 1.0, i.e., for conditions which favor the formation of $4Na_2O{\cdot}5TiO_2$ as the final product. Results in Figure 19(a) are replotted in Figure 19(c) according to the conversion, X', to $4Na_2O\,5TiO_2$, which is based on complete conversion of either Na_2CO_3 and TiO_2, whichever is in the smallest amount available for formation of $4Na_2O{\cdot}5TiO_2$. The results in Figure 19(c) show that all the curves for a TiO_2/Na_2CO_3 molar ratio larger than 1.0 regroup closely together. This

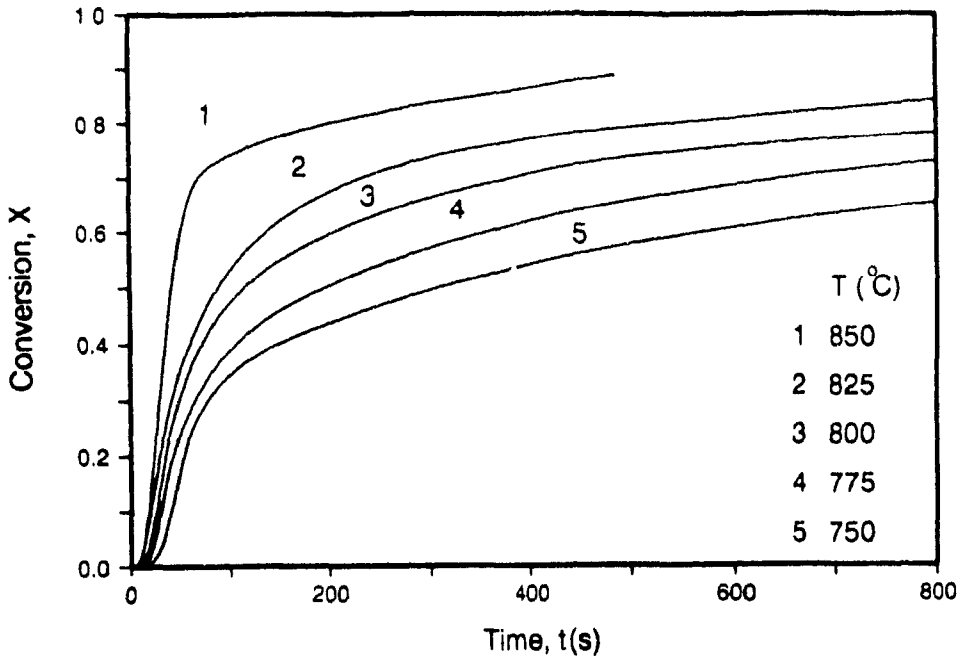

(a) X versus t

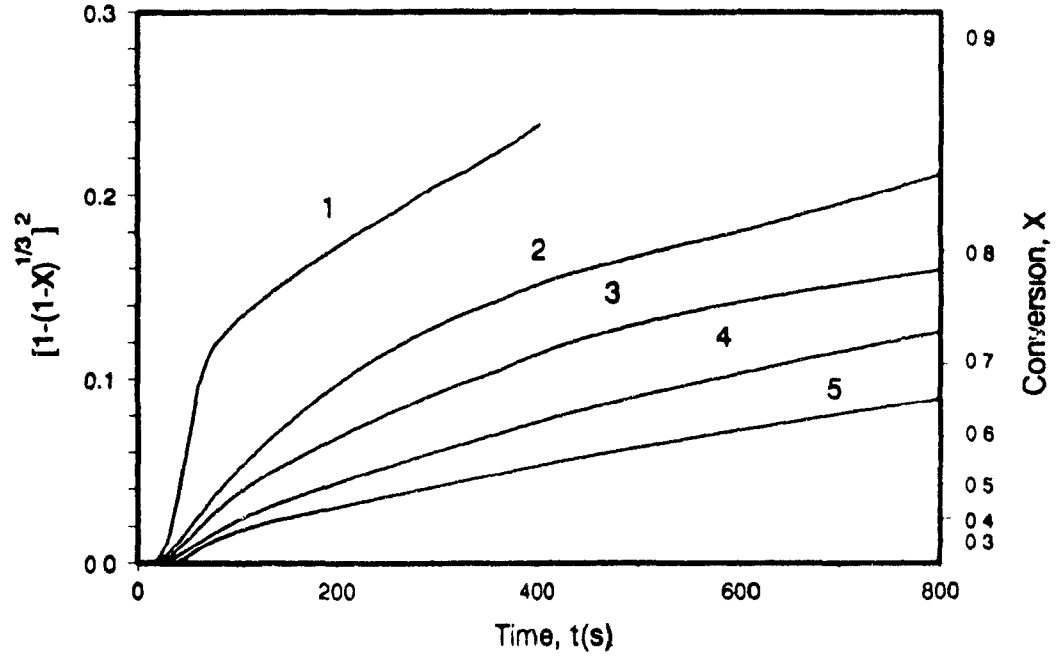

(b) $[(1-(1-X)^{1/3}]^2$ versus t

Figure 14 Kinetic data for a TiO_2/Na_2CO_3 molar ratio of 1.0

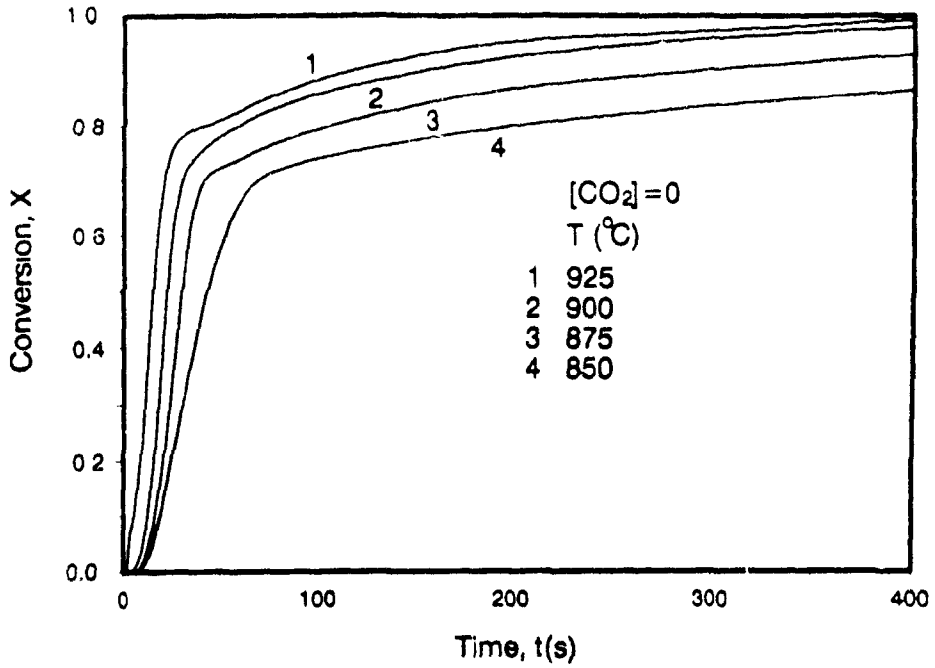

(a) X versus t

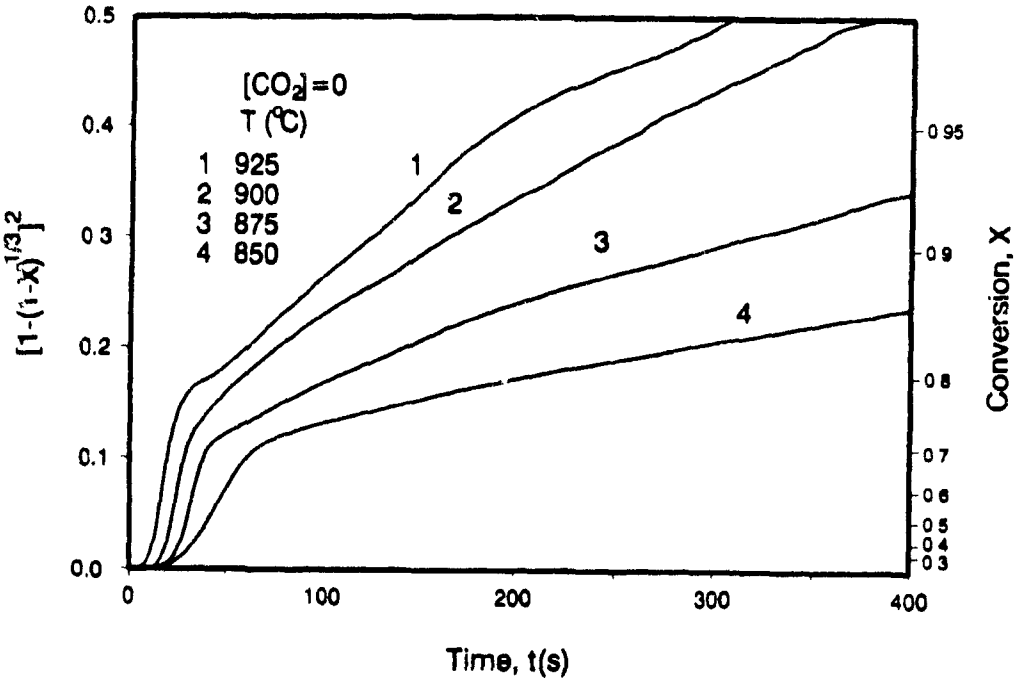

(b) $[1-(1-X)^{1/3}]^2$ versus t

Figure 15 Kinetic data for a TiO_2/Na_2CO_3 molar ratio of 1.0

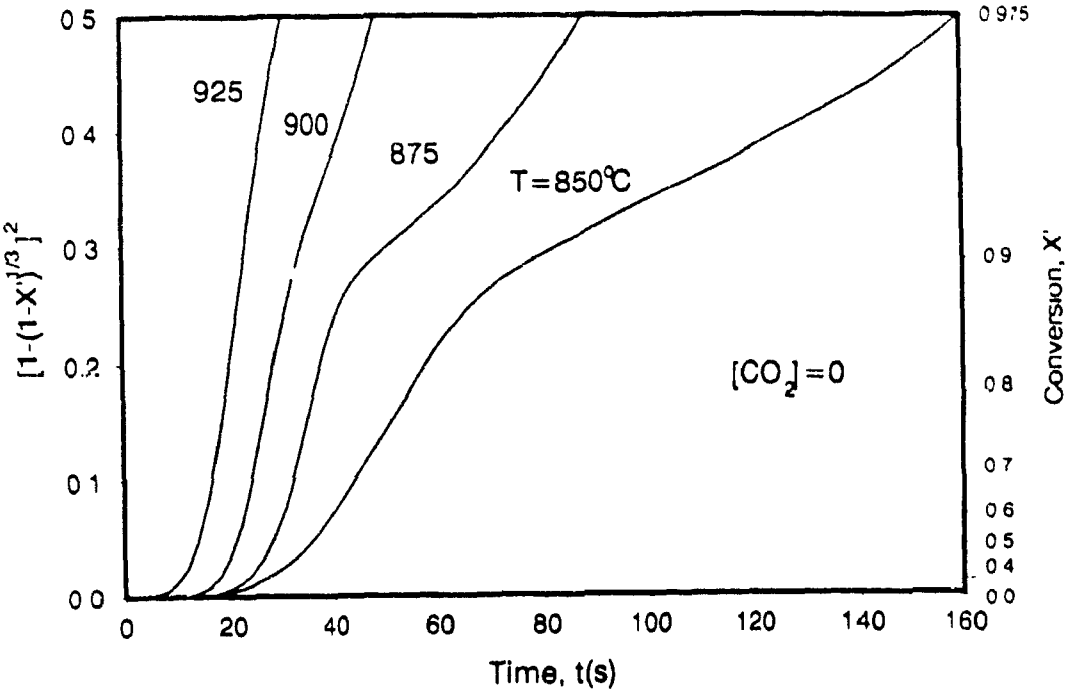

(a)

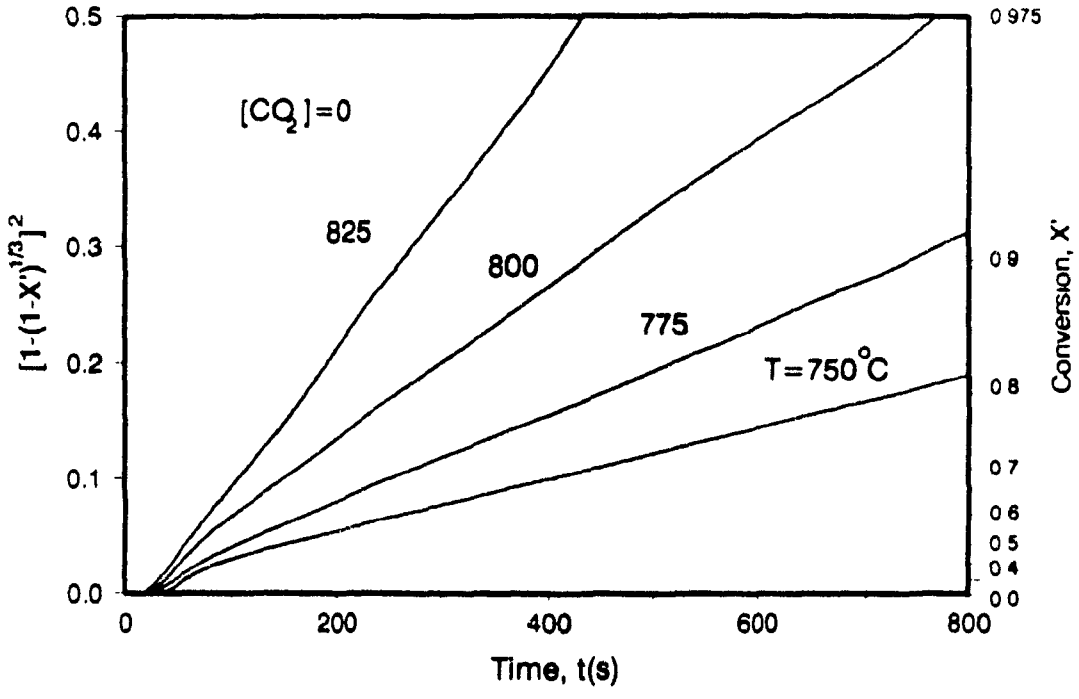

(b)

Figure 16 Replotting of the data in Figure 14(a) and 15(a)

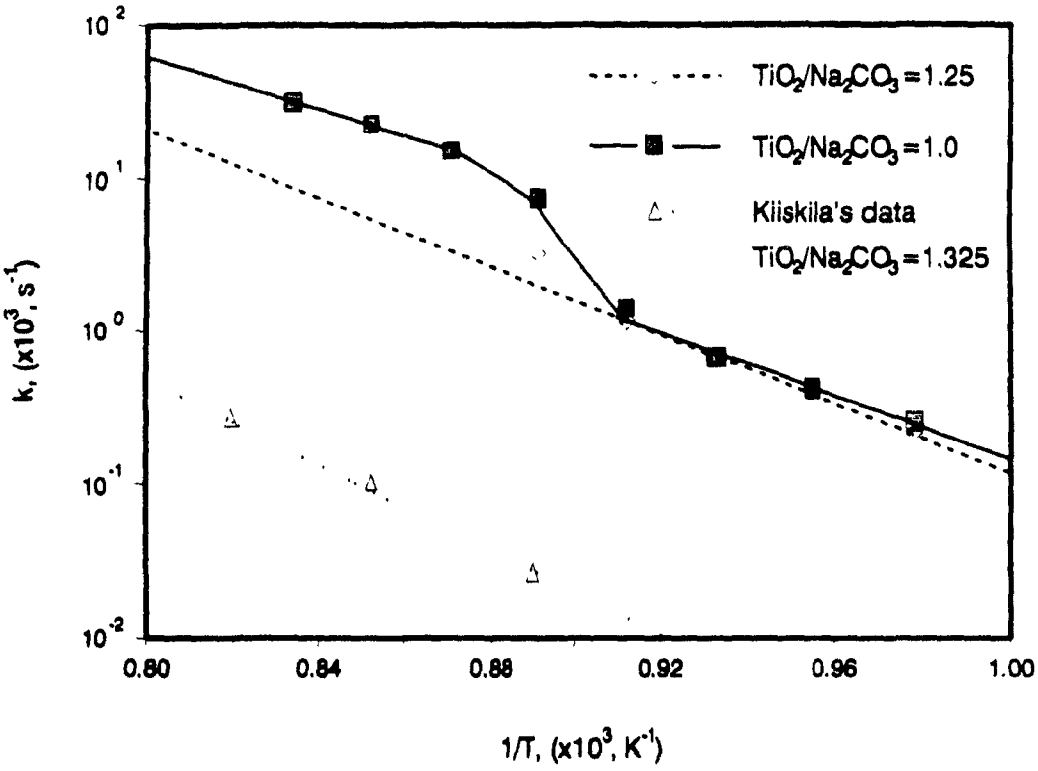

Figure 17 Arrhenius plot of rate constants from Figure 16

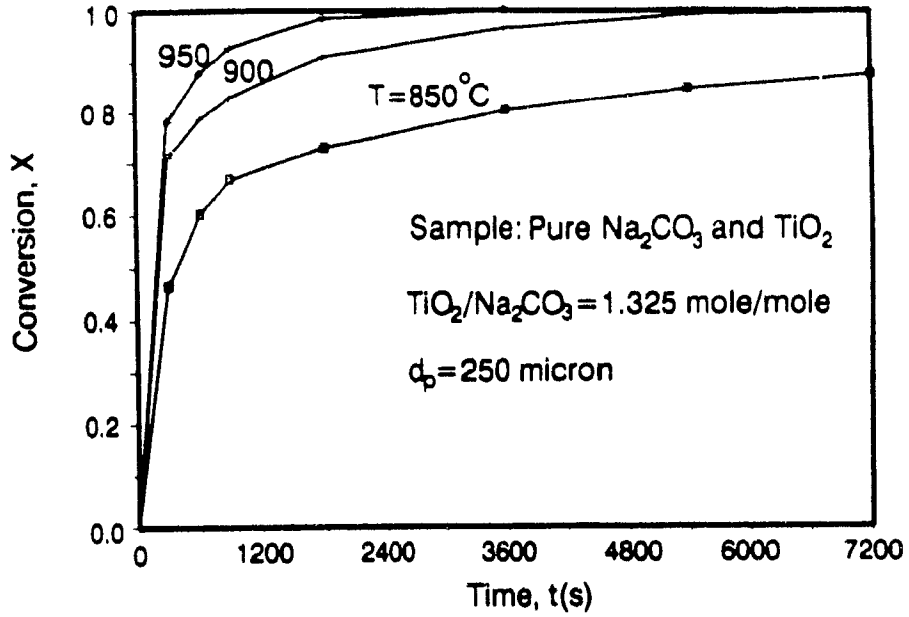

(a) X versus t

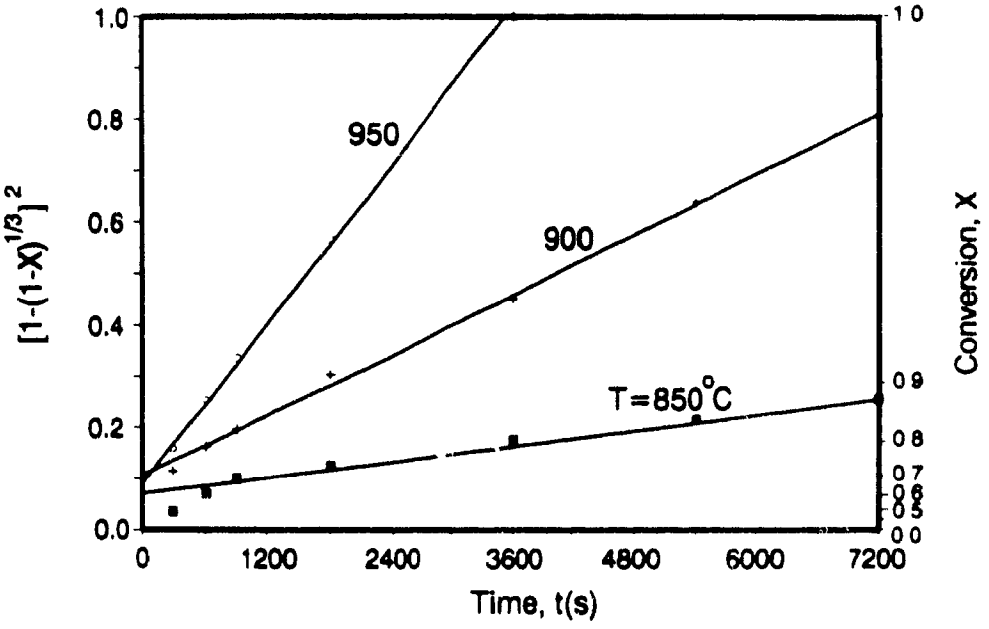

(b) $[1-(1-X)^{1/3}]^2$ versus t

Figure 18 Analysis of the data of Kiiskila (1979b)

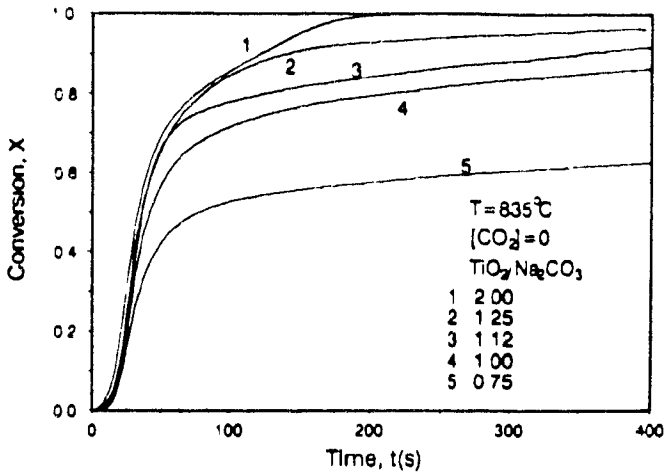

(a) X versus t

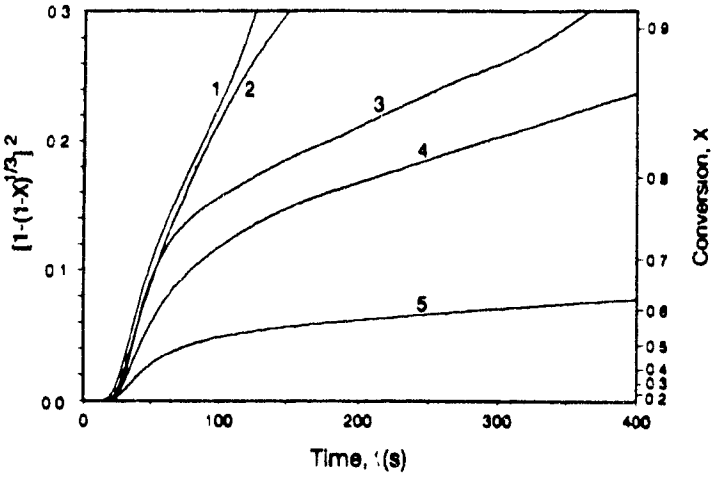

(b) $[1-(1-X)^{1/3}]^2$ versus t

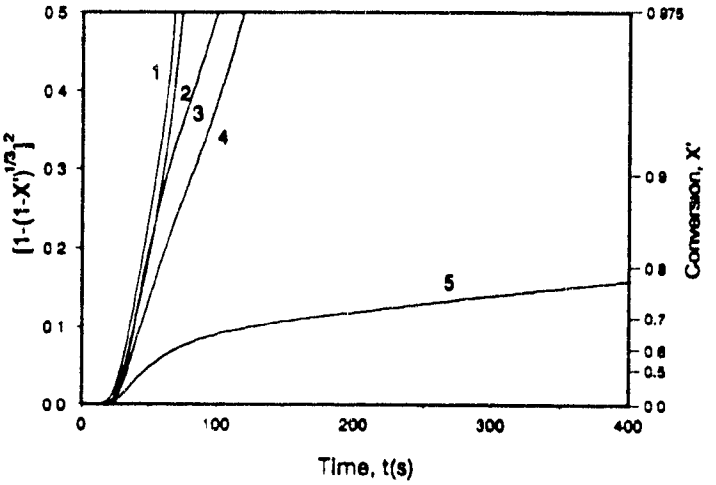

(b) $[1-(1-X')^{1/3}]^2$ versus t

Figure 19 Influence of TiO_2/Na_2CO_3 molar ratio on Na_2CO_3 conversion

indicates that the TiO_2/Na_2CO_3 molar ratio has only a small influence on the formation of $4Na_2O{\cdot}5TiO_2$ when the molar ratio is larger than or equal to 1.0

Influence of sodium sulfate content

All the above results were obtained with a mixture of Na_2CO_3 and Na_2SO_4 at a Na_2CO_3/Na_2SO_4 molar ratio of 3.0. An additional experiment was conducted with 100% Na_2CO_3 and the results are compared in Figure 20. Since the differences are small, it seems likely that Na_2SO_4 acts as an inert material which only has a small influence on the rate of diffusion of the sodium and oxygen containing species through TiO_2.

II Reaction between sodium carbonate and recycled $Na_2O.3TiO_2$

In an industrial process $Na_2O{\cdot}3TiO_2$ will be recycled because it is the hydrolysis product formed in reaction (3). Therefore the kinetics of the direct causticizing reactions between recycled $Na_2O\,3TiO_2$ and sodium carbonate, i.e., reaction (2) and

$$7\ Na_2CO_3 + 5\ Na_2O{\cdot}3TiO_2 = 3(4Na_2O{\cdot}5TiO_2) + 7\ CO_2 \qquad (14)$$

were investigated. Some mixtures were prepared by adding $Na_2O\,3TiO_2$ (for preparation, see **EXPERIMENTAL** section) to the mixture of Na_2CO_3 and Na_2SO_4 (Na_2CO_3/Na_2SO_4 molar ratio of 3.0) at a TiO_2/Na_2O molar ratio of 1.25 (Na_2O in Na_2SO_4 not included). The kinetic results in Figure 21(a) are again reasonably described by Jander's equation (13) in Figure 21(b) with a correlation coefficient higher than 0.98. An activation energy of 365 kJ/mol was obtained in Figure 22 from the Arrhenius plot of the slopes of the linear relationships shown in Figure 21(b). This means that the direct causticizing reactions with recycled $Na_2O{\cdot}3TiO_2$ is more temperature sensitive than with pure TiO_2. Recycled $Na_2O{\cdot}3TiO_2$ is more reactive than pure TiO_2 above 775°C, probably due to the amorphous nature of the recycled $Na_2O{\cdot}3TiO_2$. The amorphous nature of $Na_2O{\cdot}3TiO_2$ is indicated by XRD analysis shown in Figure 23. The solid structure is an important parameter in solid-solid reactions particularly when product layer diffusion is the controlling step. The particle size and shape are also different from the TiO_2 used (Figure 13) as indicated by the SEM picture in Figure 24.

The results with recycled TiO_2 at a TiO_2/Na_2O molar ratio of 1.0 also show a fast formation of $4Na_2O{\cdot}5TiO_2$ and a slow further conversion to

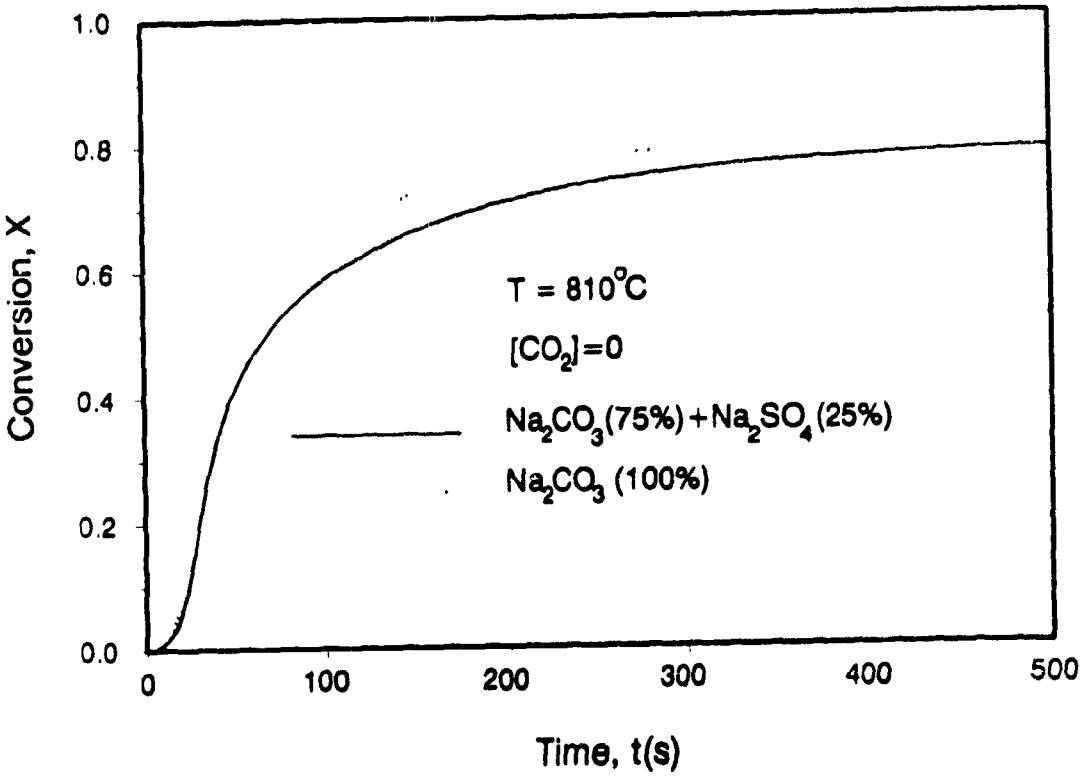

Figure 20 Influence of sodium sulfate content on Na_2CO_3 conversion
TiO_2/Na_2CO_3=1.0 mol/mol

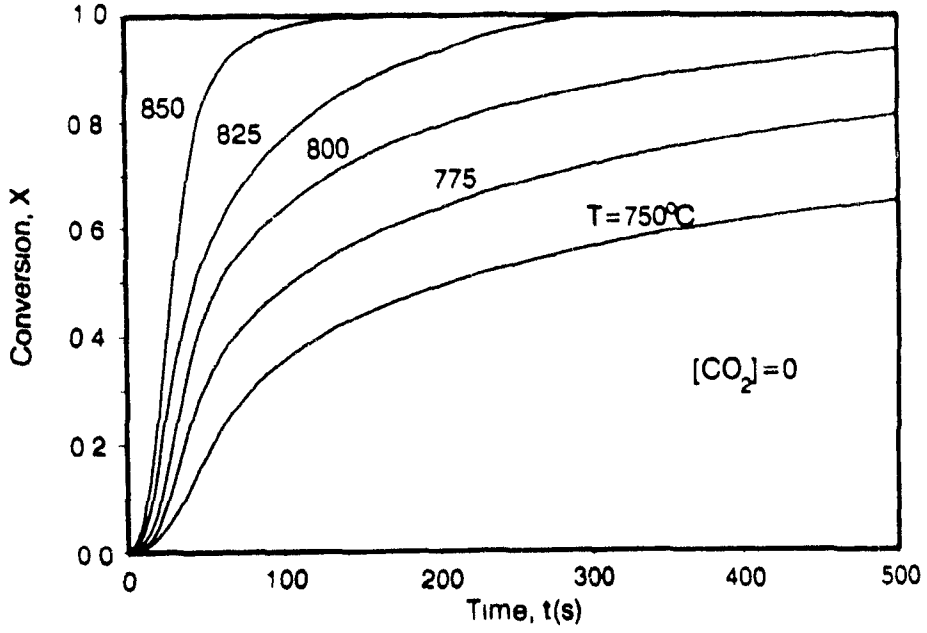

(a) X versus t

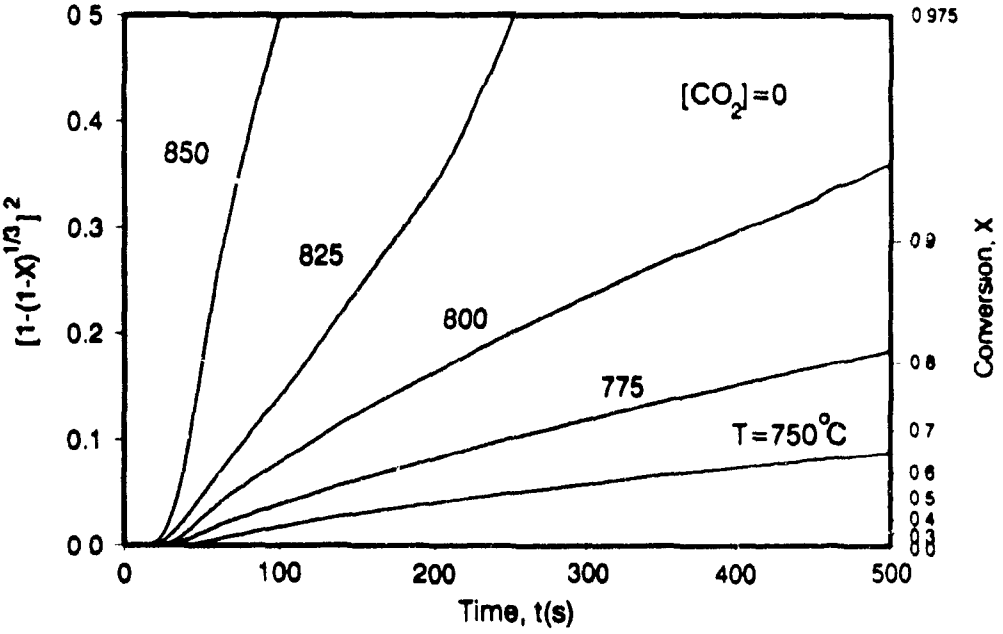

(b) $[1-(1-X)^{1/3}]^2$ versus t

Figure 21 Kinetic data with recycled $Na_2O{\cdot}3TiO_2$
TiO_2/Na_2O=1.25 mol/mol

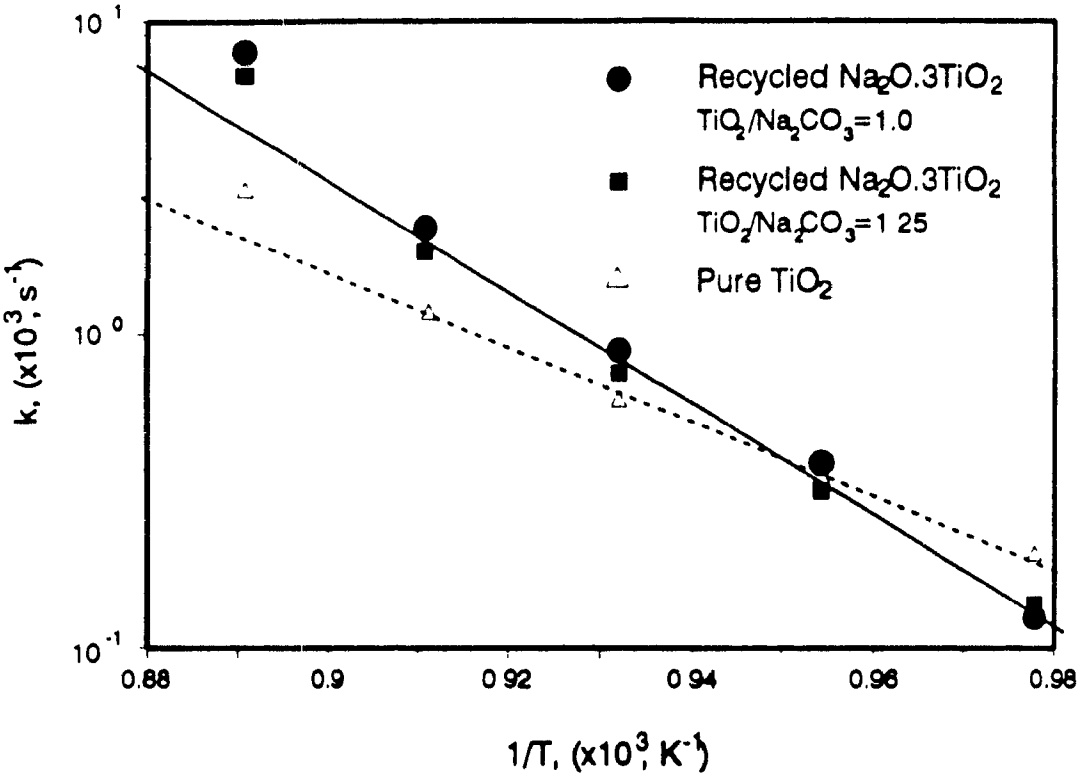

Figure 22 Arrhenius plot of rate constants

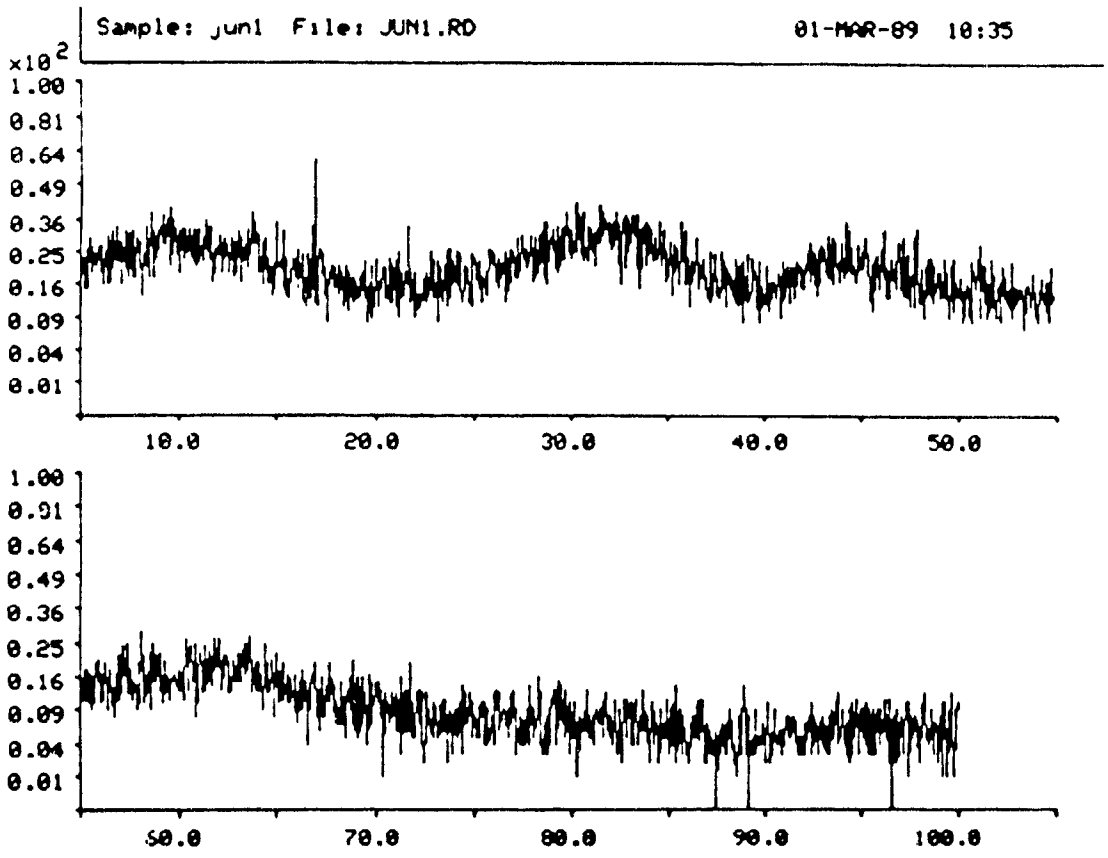

Figure 23 Results from XRD analysis of the precipitate from hydrolysis

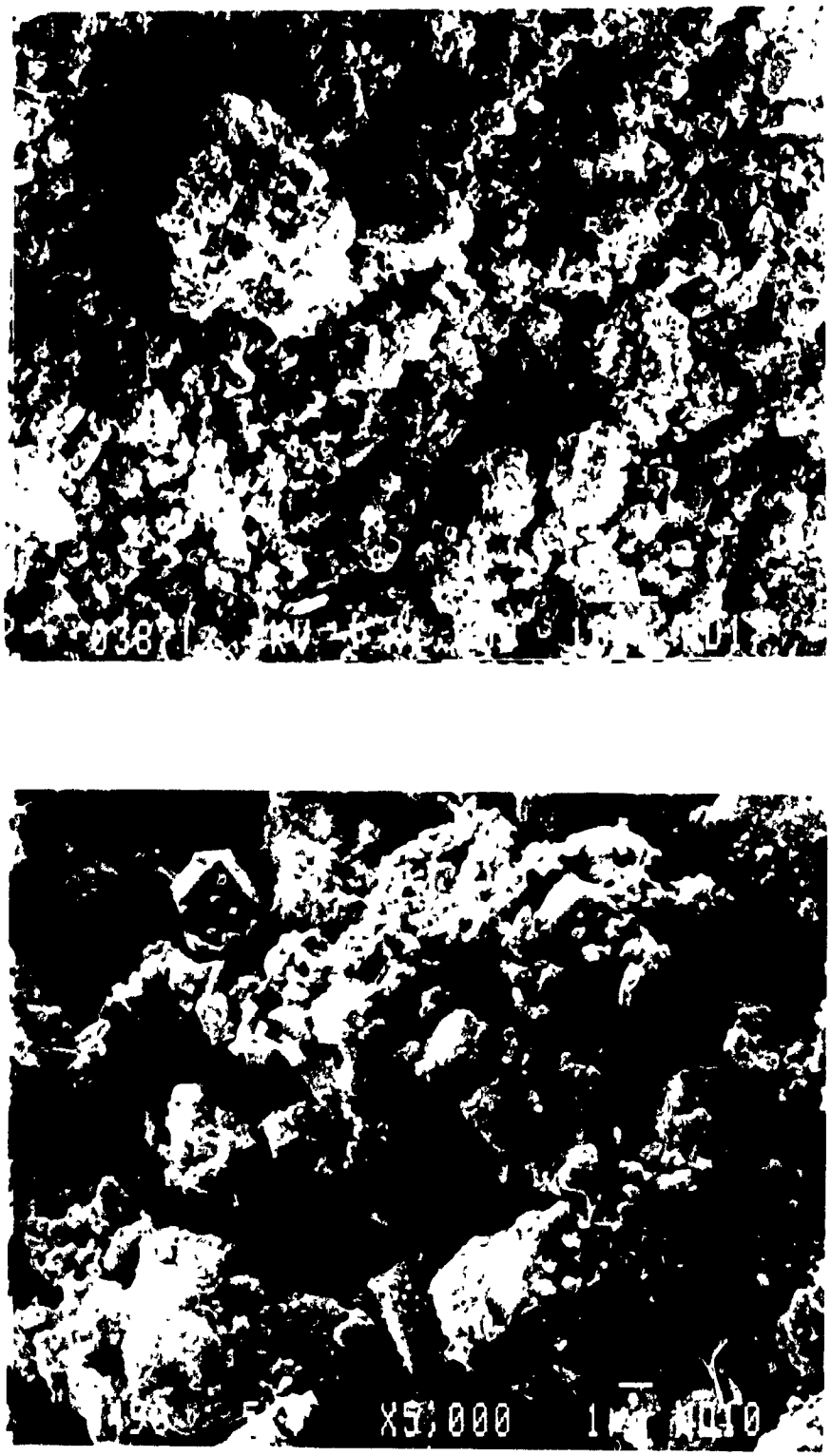

Figure 24 SEM pictures of the precipitate from hydrolysis

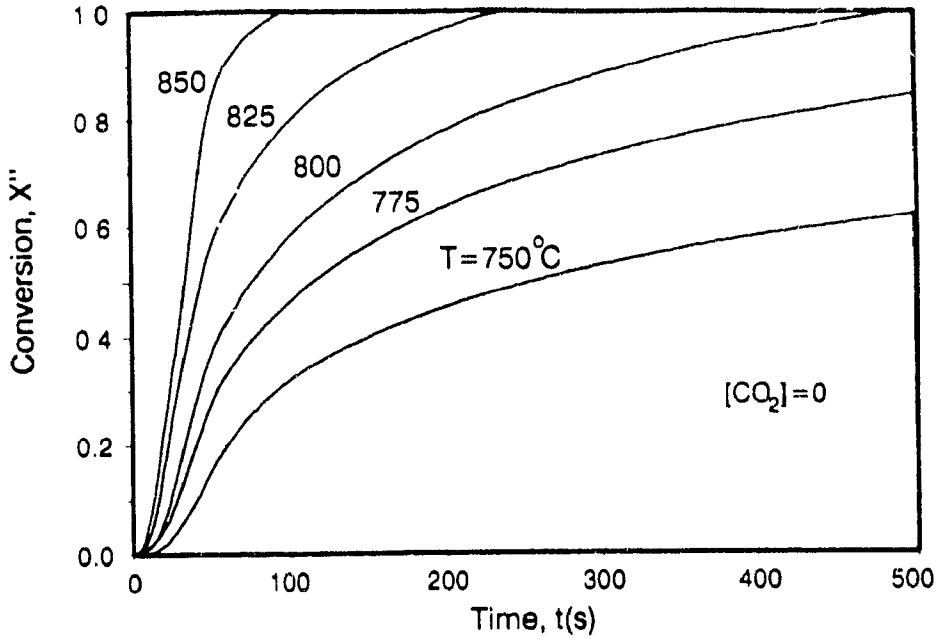

(a) X versus t

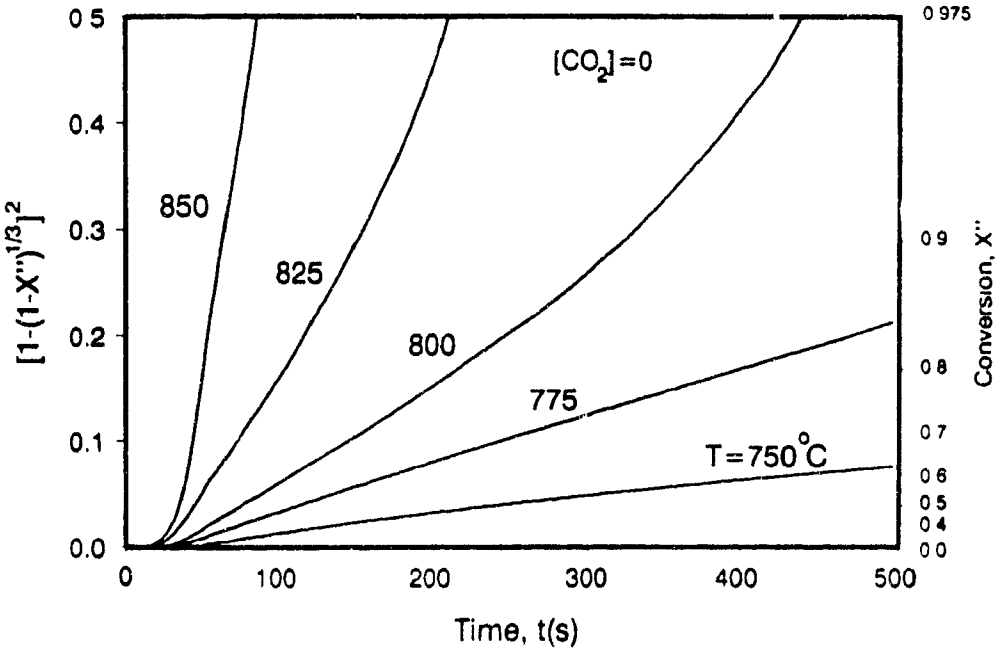

(b) $[1-(1-X'')^{1/3}]^2$ versus t

Figure 25 Kinetic data with recycled $Na_2O{\cdot}3TiO_2$
TiO_2/Na_2O=1.0 mol/mol

$Na_2O\,TiO_2$, similar to those obtained with pure TiO_2. The results are plotted according to X'' versus t in Figure 25(a), where X'' is defined as the conversion of $Na_2O{\cdot}3TiO_2$ to $4Na_2O{\cdot}5TiO_2$. Figure 25(b) again shows the validity of Eq.(13) for the description of the conversion of $Na_2O{\cdot}3TiO_2$ to $4Na_2O\,5TiO_2$. A correlartion coefficient higher than 0.99 is obtained from the linear regression in Figure 25(b). The calculated rate contants from Figure 25(b) are also shown in Figure 22. The rate constants at a TiO_2/Na_2O molar ratio of 1.0 agree very closely with those at a TiO_2/Na_2O molar ratio of 1.25, similar to what was found for pure TiO_2.

CONCLUSION

$4Na_2O{\cdot}5TiO_2$ and $Na_2O{\cdot}TiO_2$ are identified as products of the direct causticizing reaction between Na_2CO_3 and TiO_2 from 750 to 925°C. The formation of $4Na_2O{\cdot}5TiO_2$ is relatively fast and can be accomplished in the solid state. The rate of formation of $4Na_2O{\cdot}5TiO_2$ is controlled by diffusion, most likely of Na and O as ions, or combined as Na_2O through the product layer of $4Na_2O{\cdot}5TiO_2$. The conversion-time data are well described by Jander's kinetic model for solid-solid reactions when X>0.4 with an activation energy of 216 kJ/mol. In the presence of CO_2, $Na_2O{\cdot}TiO_2$ is converted into $4Na_2O{\cdot}5TiO_2$. The presence of Na_2SO_4 has only a minor influence on the direct causticization of Na_2CO_3. Recycled $Na_2O{\cdot}3TiO_2$ is at least as effective as TiO_2 for direct causticization of Na_2CO_3. The activation energy with $Na_2O{\cdot}3TiO_2$ is 365 kJ/mol.

From the experimental results it follows that it is recommended to use a TiO_2/Na_2O (excluding Na_2O in Na_2SO_4) molar ratio of ≥1.25 and small TiO_2 containing particles for relatively fast and complete conversion of sodium carbonate to $4Na_2O{\cdot}5TiO_2$.

NOMENCLATURE

A	=Cross-sectional area of solid particle, m^2.
k	=Rate constant, s^{-1}.
k'	=Rate constant, m^2/s.
M	=Molecular weight, kg/mol.
Pco_2	=Partial pressure of CO_2, N/m^2.
Q	=Flowrate, m^3/s.
R	=Universal gas constant, J/(mol K).

r =Diameter of solid particle, m.

t =Time, s.

T =Temperature, K.

[Wco_2] =Weight of CO_2 released from sodium carbonate, kg.

ΔW =Weight loss, mg.

X =Conversion of sodium carbonate.

X' =Conversion of TiO_2 to $4Na_2O{\cdot}5TiO_2$.

X'' =Conversion of $Na_2O{\cdot}3TiO_2$ to $4Na_2O{\cdot}5TiO_2$.

REFERENCES

Andersson, S. and A.D. Wadsley, "The Crystal Structure of $Na_2Ti_3O_7$", *Acta Cryst.*, 1961, 14, p.1245.

Andersson, S. and A.D. Wadsley, "The Structures of $Na_2Ti_6O_{13}$ and $Rb_2Ti_6O_{13}$ and the Alkali Metal Titanates", *Acta Cryst.*, 1962, 15, p.194-201.

Baker, M.G. and D.J. Wood, "The Preparation and Characterization of the Compounds Na_2TiO_4 and Na_2ZrO_4", *J. Chem. Soc , Dalton Trans ,* 1972, p.2448-2450.

Bamberger, C.E. and G.M. Begun, "Sodium Titanates: Stoichiometry and Raman Spectra", *J. Am. Ceram. Soc.*, 1987, 70(3), C48-C51, p.97-103.

Belyaev, E.K., N. Sh. Safiullin and N. M. Panasenko, "Reaction of Titanium Dioxide with Sodium Carbonate", *Izv. Akad. Nauk. SSSR Nerog Mater ,* 1968, 4, p.97-103.

Belyaev, E.K., "The Formation of Sodium Metatitanate in Sodium Carbonate — Titanium Dioxide Mixtures", *Russ. J. Inorg. Chem.*, 1976, 21, p.830-833.

Bennington, K.O. and R.R. Brown, "Reaction between Sodium Carbonate and Titanium Dioxide", *Int. Bu. of Mines,* PGH., PA. 18591, 1973, p.1-13.

Bouaziz, R. and M. Mayer, "The Binary Sodium Oxide-Titanium Dioxide" (in Fr.), *C.R. Hebd. Seances Acad. Sci.,* Ser. C., 1971, 272C, p.1874.

Bouaziz, R. and M. Mayer, "On Some Sodium Titanates" (in Fr.), *C.R Hebd. Seances Acad. Sci.*, Ser. C., 1971, 272C, p.1773.

Christie, J.R., A.J. Darnell and D.F. Dustin, "Reaction between Sodium Carbonate and Aluminum Oxide", *The Journal of Physical Chemistry*, 1978, 82(1), p.33.

Gallagher, P.K. and D.W. Johnson, "Kinetics of Formation of $LiFeO_2$ from $2Li_2CO_3{\cdot}Fe_2O_3$ Mixtures", *J. Am. Ceram. Soc.*, 1976, 59(34), p.171.

Gicquel, C., M.M. Mayer and R. Bouaziz, "On Some Oxygenated Compounds of

Titanium and the Alkali Metals (Na, Li): Study of Binaries M_2O-TiO_2 in the Alkali Oxide-Rich Zones", (in Fr.), *C R. Hebd Seances Acad Sci*, Ser. C., 1972, 275C, p.1427.

Gitlesen, G. and B. Motzfeldt, "The Phase Diagram of Na_2SO_4-Na_2CO_3 Mixture", *Acta. Chem Scand*, 1964, 18, p.488.

Glasser, F.P. and J. Marr, "Phase Relations in the System Na_2O-TiO_2-SiO_2", *J Am Ceram. Soc*, 1979, 62(1-2), p.42.

Gmelins Handbuch Der Anorganisschen Chemie, Titan,System-Nummer 41,8th ed.; p.383, Verlag Chemie GMBH, Weinhein, Germany, 1951.

Hill, W.A., A.R. Moon and G. Higginbotham, "Alkali Oxide Rich Titanates", *J. Am. Ceram. Soc*, 1985, 68(10), c-266.

Jander, W., "Reactions in Solid State at High Temperatures: I", *Z. Anorg. Allgem. Chem.*, 1927, 163, p.1.

Joint *Committee for Powder Diffraction Standards (JCPDS)*, 1984 Powder Diffraction File, International Center for Diffraction Data, Swarthmore, PA 19081.

Kiiskila, E., "Recovery of Sodium Hydrioxide from Alkaline Pulping Liquors by Smelt Causticizing, Part II, Reactions between Sodium Carbonate and Titanium Dioxide", *Paperi ja—Papper och. Trà*, 1979a, 61(5), p.394-401.

Kiiskila, E., "Recovery of Sodium Hydroxide from Alkaline Pulping Liquors by Smelt Causticizing, Part III, Alkali Distribution in Titanium Dioxide Causticizing", *Paperi ja — Papper och. Trà*, 1979b, 61(6), p.453-464.

Kuczynski et al., Ed., Proceedings of the International Conference on Sintering and Related Phenomena, Gordon and Breach, New York, N.Y., 1965, p.75.

Kurolin, S.A. and A.I. Vulikh, "The Preparation of Alkali Metal Titanates in Vacuum", *Russ. J. Inorg. Chem.*, 1965, 10, p.74-77.

Mitsuhashi, T. and Y. Fujiki, "Thermochemistry of Alkali-Metal Titanates", *Thermochimica Acta*, 1985, 88, p.177-184.

Niggli, P., "Gleichgewicht Zwischen TiO_2 und CO_2, Sowie SiO_2 und CO_2 in Alkali-, Kalk-Alkali und Alkali-Aluminatschmelzen", *Z. Anorg. Allg. Chem.* 1916, 98, p.241-326.

Safiullin, N.S. and E.K. Belyaev, "Mechanism of Formation of Sodium Titanates in Mixtures of Sodium Carbonate and Titanium Dioxide", *Izv. Akad. Nauk. SSSR, Neorg. Mater*, 1968, 4, p.557-562.

Shomate, C.H., "Heat Capacities at Low Temperatures of Na_2TiO_3, $Na_2Ti_2O_5$ and $Na_2Ti_3O_7$", *J Am. Soc. of Chem.*, 1946, 66(8), p.1634.

Taker, M., "Growth and Properties of $Na_8Ti_5O_{14}$ Crystal", *J Mater Sci*, 1976, 11, p.1467-1469.

Yamaguchi, T., H. Fujii and H. Kuno, "Kinetic Studies of the Solid State Reaction Involving Intermediate Phases: System $BaCO_3$-SiO_2", *J Am Soc Chem*, 1972, 34, p.2793-2745.

CHAPTER 5

KRAFT BLACK LIQUOR COMBUSTION AND DIRECT CAUSTICIZATION WITH TITANIUM DIOXIDE

ABSTRACT

The ignition temperature and burning time of kraft black liquor solids with or without TiO_2 admixture are measured by thermoanalytical methods. The ignition temperature is significantly lowered by the presence of TiO_2. The melting point of the combustion product of kraft black liquor mixed with TiO_2 is much higher than that of kraft black liquor alone because of formation of high melting sodium titanates by the direct causticization reaction between TiO_2 and Na_2CO_3. Simultaneous combustion and direct causticization of kraft black liquor with TiO_2 is studied in an isothermal tube furnace. It is found that complete conversion of Na_2CO_3 into sodium titanates such as $Na_2O{\cdot}TiO_2$ and $4Na_2O{\cdot}5TiO_2$ can be achieved in a relatively short time with high TiO_2/Na_2CO_3 molar ratio of 1.25. The presence of TiO_2 reduces the sulfur emission. Hydrolysis of $Na_2O{\cdot}TiO_2$ and $4Na_2O{\cdot}5TiO_2$ produces $Na_2O{\cdot}3TiO_2$ and NaOH.

INTRODUCTION

The alkaline chemical recovery process presently makes use of lime causticization to convert sodium carbonate to sodium hydroxide. This method has a number of drawbacks in terms of economy, safety and environmental impact. In order to eliminate these drawbacks, a number of processes, collectively referred to direct causticization, have been investigated. Direct causticization is a technology of regenerating pulping chemicals by using amphoteric oxides which directly leads to the formation of caustic. Although there are a few amphoteric oxides such as iron oxide, alumina and titanium dioxide available for direct causticization, titanium dioxide was found to be the only suitable oxide for kraft black liquor recovery in Chapter 3

A two step kraft black liquor recovery process which includes direct causticization with TiO_2 has been proposed by Nguyen (1985) and in Chapter 3 of this thesis. In this process, kraft black liquor is combusted in the presence of TiO_2, leading to the release of CO_2 from Na_2CO_3 and the formation of sodium titanates, $xNa_2O{\cdot}yTiO_2$, by the so-called direct causticizing reaction:

$$x\ Na_2CO_3 + y\ TiO_2 = xNa_2O{\cdot}yTiO_2 + x\ CO_2 \qquad (1)$$

The other major remaining inorganic salt is Na_2SO_4. After reduction of Na_2SO_4 in a separated process step, the resulting mixture of Na_2S and sodium titanates is contacted with water to form white liquor and a solid residue, $Na_2O{\cdot}3TiO_2$. NaOH is generated by the hydrolysis reaction:

$$xNa_2O{\cdot}yTiO_2 + (x-\tfrac{y}{3})\ H_2O = 2(x-\tfrac{y}{3})\ NaOH + (\tfrac{y}{3})\ Na_2O{\cdot}3TiO_2 \qquad (2)$$

The TiO_2 containing residue, $Na_2O{\cdot}3TiO_2$, is recycled to the combustion step.

Kiiskila (1979a, 1979b) studied the direct causticization of pure Na_2CO_3 by TiO_2 at 850-1200°C, i.e., both below and above the melting point (950-1000°C) of the sodium titanates produced. In Chapter 4, we investigated the solid state kinetics of the direct causticization reaction of Na_2CO_3 in a mixture with Na_2SO_4 by TiO_2 from 750 to 925°C. It was found that the formation of $4Na_2O{\cdot}5TiO_2$ from Na_2CO_3 and TiO_2 is a fast reaction and further conversion to $Na_2O{\cdot}TiO_2$ is very slow. If the ratio of TiO_2 to Na_2CO_3 is larger than 1.25, the complete conversion of Na_2CO_3 is very fast even in the lower temperature

range of 700 to 850°C. The causticizing reaction between Na_2CO_3 and TiO_2 to form $4Na_2O{\cdot}5TiO_2$ can be described by solid-solid reaction kinetics with product layer diffusion control. A few examples of direct causticization of Na_2CO_3 by TiO_2 in commercial kraft black liquor are given in the Canadian patent of Nguyen (1985). In order to obtain causticizing efficiencies in excess of 95%, Nguyen recommends a TiO_2/Na_2CO_3 molar ratio of up to 2.0 and a reaction time of 10-20 hours at 900°C. This time is one or three orders of magnitude larger than that reported by respectively Kiiskila (1979b) and in our study of a the mixture of model compounds in Chapter 4.

It is likely that the kraft black liquor burning process is affected by the large amount of TiO_2 which must be added in order to causticize all of the Na_2CO_3 formed during combustion. The techniques to investigate pyrolysis and combustion processes, and to characterize the properties of the ash are well known. The most useful methods are differential thermal analysis (DTA) and thermogravimetric analysis (TGA). TGA records the changes in weight that a sample undergoes during heating; DTA characterizes chemical or physical transformations which are accompanied by heat effects. DTA is particularly well suited for fuel analysis, and has been applied extensively in the coal industry (Scott & Baker, 1953) for classifying different kinds of coal and for predicting their behavior during burning (Gamel & Smothers, 1952).

It is the objective of this study to evaluate the combustion process of a mixture of kraft black liquor and TiO_2, and to investigate the melting behavior of the combustion product by thermal analytical methods. The influence of operating conditions such as TiO_2/Na_2CO_3 molar ratio, temperature and reaction time on the direct causticizing efficiency of Na_2CO_3 will be studied. The sulfur loss during isothermal combustion and the effect of recycling of $Na_2O{\cdot}3TiO_2$ will also be investigated.

EXPERIMENTAL

Apparatus

The pyrolysis and combustion experiments were performed with a Netzsch thermal analyzer, Mode STA 409. A specially made cup-type alumina crucible (99.9% purity, about ~5mm I.d.) was used for holding the samples. It was paired with a reference cup-type alumina crucible, having a capacity of about 0.3 ml. A stem carrying the sample crucible and an the inert reference

crucible were located in the center of a ceramic, 100 ml, 26 mm i.d. cylinder placed in a tube furnace. The cylinder was closed at the top. Gas was introduced in the top of the ceramic cylinder, at about the sample level. A second 1 mm I.d. ceramic tube, along the inside of the wall of the ceramic cylinder, introduced inert gas at the top of the cylinder. The gas outlet was at the bottom of the furnace. To minimize back-diffusion of air, the outlet valve was connected to a 8 foot long teflon tube with a restrictor. In all runs the gas pressure within the cylinder cavity was close to atmospheric.

Some isothermal combustion and direct causticization experiments were also conducted in a tube furnace system. When the furnace temperature was stabilized, the sample was quickly pushed to the center of the tube furnace and the combustion and causticizing reaction started immediately. The residue after combustion and direct causticization was analyzed by ion chromatography. The hydrolysis equipment consists of a thermostat and a 500 ml glass flask with mechanical stirrer.

Materials

Spent kraft black liquor was obtained from the brown stock washers of Domtar Inc.'s hardwood kraft mill in Cornwall, Ontario. This black liquor with 15-17% solids was oxidized in a 4 liter autoclave at 90-100°C by oxygen of 1-2.4 l/min during 120 minutes (Sen Gupta, 1986). The kraft black liquor was dried in air at 90°C, ground and the fraction passing a 100 mesh metal screen (d_p <149 μm) was collected. The composition of the dried solids is listed in Table 1. Two types of samples were prepared. In the first, kraft black liquor solids were mechanically mixed with TiO_2 particles of size less than 10 μm. The TiO_2 was rutile with a purity of 99.97%. Another type of sample was prepared by mixing TiO_2 with kraft black liquor, followed by drying under constant stirring. Subsequently, the sample was ground and the fraction passing a 100 mesh metal screen was retained. Different TiO_2/Na_2CO_3 molar ratios were used.

Table 1 Composition of Kraft Black Liquor Solids

Elements	Na	S	C	H	O	Cl	K
wt. (%)	22.90	2.90	31.67	2.64	33.04	0.16	1.46

Recycled TiO_2 was prepared by drying the solid residue obtained after hydrolysis of sodium titanate ($Na_2O \cdot TiO_2$) at 500°C in a tube furnace. Sodium titanate was prepared by heating an equimolar mixture of Na_2CO_3 and TiO_2 in a tube furnace at 900°C for 6 hours.

The combustion products were made by exposing kraft black liquor or a mixture of kraft black liquor and TiO_2 to air at about 900°C for 6 hours in a tube furnace. These conditions are such that both the combustion and direct causticization reactions go to completion. The combustion residue was then ground and the fraction passing a 100 mesh sieve was used.

Procedures

About 10-25 milligrams of kraft black liquor solids were arranged as a "heap" in the center of the crucible of the Netzsch thermal analyzer and heated at a rate of 10°C/min, starting from room temperature. Air was introduced at a flowrate of 56 scc/min. The kraft black liquor solids first pyrolyze at from 200 to 450°C, and, depending on the heating rate and type of sample, also soften and swell. This produces a single mass of char on the alumina crucible for combustion at higher temperatures. Before each test, the sample crucible was thoroughly washed in deionized water in order to remove the fused ash residue from the previous run.

For the isothermal combustion and direct causticization experiments, the tube furnace was preheated to the desired temperature under an air flowrate of 1000 scc/min. The alumina crucible boat with about 500 mg kraft black liquor solids was then quickly pushed into the center of the furnace and the sample started to pyrolyze and burn. After complete combustion and partial direct causticization, the residue was dissolved in deionized water. The remaining solids were then separated by filtration on a filter paper and the solution analyzed by ion chromatography for its content of sodium carbonate and sodium sulfate. In some cases, the combusted solids were immersed in deionized water in a flask used for the hydrolysis tests. Usually 50 ml deionized water was used for 500 mg solid sample. After 60 minutes at 90°C, the solids were filtered off and weighed after drying. The amount of hydroxide formed was determined by titration with 0.1 M HCl standard solution. The dissolved sodium was measured by atomic adsorption spectroscopy (AAS).

RESULTS AND DISCUSSION

Combustion Properties

Two properties which describe the combustion behavior of a material are. the ignition temperature, and the burning time. These two properties depend on experimental conditions, such as gas atmosphere, particle size and heating rate, since these, in turn, determine the heat- and mass-transfer characteristics of the experimental system. The ignition of a char particle is a complex phenomenon and its quantitative analysis is rather involved Generally, it could be said that ignition takes place if the rate of heat production from all reactions is higher than the rate of heat loss to the colder environment. On the other hand, the burning time after ignition is controlled by the transport rate of oxygen within and outside the char. Therefore, a comparison of the ignition temperature and burning time of different materials should be made under identical experimental conditions. A complicating factor for the present mixture of kraft black liquor solids and TiO_2 is that the direct causticizing reaction between Na_2CO_3 and TiO_2 starts at about 600°C and proceeds simultaneously during combustion.

i) *Ignition temperature*: Shown in Figure 1 are the TGA and DTA curves obtained for kraft black liquor solids without TiO_2 in air. The first weight loss is due to pyrolysis of the organics since a modest exothermic peak is recorded by DTA. With further increase in temperature, a sudden change in the slope of the thermogravimetric (TG) curve and a simultaneous release of heat on the differential thermal analysis (DTA) curve were observed. This point, signals the ignition of the char, and is denoted as T_{ig} in Figure 1. The repeatability of the ignition temperature for duplicate experiments was 5°C.

The results obtained for kraft black liquor mixed with different amounts of TiO_2 are shown in Figure 2 and 3. The TiO_2/Na_2CO_3 molar ratios in Figure 2 and 3 are 1.0 and 1.5, respectively. The ignition temperatures determined from Figures 1, 2 and 3 are summarized in Table 2. The ignition temperature of pure kraft black liquor solids found in this study is very close to the values of 650 to 750°C published by Milanova and Kubes (1986). However it is relatively high compared to other solid fuels such as 380-500°C for coals, and 420 to about 620°C for cokes depending on the carbonization temperature (Brame and King, 1967). The high ignition temperature of kraft black liquor char is, in part, due to that the organics are present in the form of their sodium salts

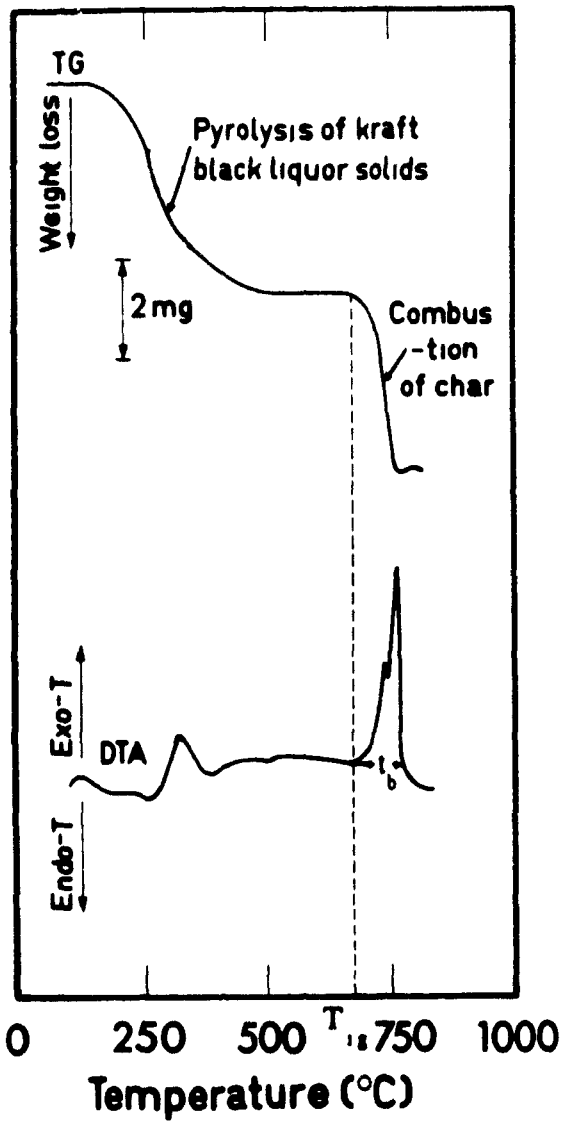

Figure 1 Results from TGA and DTA analysis
(Sample: kraft black liquor solids)

(Milanova and Kubes, 1986).

The results in Table 2 show that the addition of TiO_2 leads to a dramatic decrease in the ignition temperature of kraft black liquor Fe_2O_3 and Al_2O_3 displayed similar results when mixed with kraft black liquor The explanation

Table 2 Ignition Temperatures and Burning Times for Different Samples

Samples	T_{ig} (°C)	t_b (min)
KBL solids	710	9
KBL solids + TiO_2 (TiO_2/Na_2CO_3=1.0)	575	9
KBL solids + TiO_2 (TiO_2/Na_2CO_3=1.5)	510	12

for this behavior may be the catalytic action of TiO_2 on the burning process, as was reported for carbon combustion and gasification (Baker, 1977; Ranish and Walker, 1990). It was found in these studies that during the oxidation of carbon, elements such as Ti, Fe, Ag, Mn, etc., exhibit a pitting catalyst behavior (Thomas, 1965; Walker, 1990). Pitting catalysts produce a pit in the basal plane and accelerate the oxidation rate. The decrease in ignition temperature may also be explained by a larger surface with the adding a large amount of TiO_2, or in combination with the catalytic action of TiO_2

By comparing Figure 2 with Figure 3, it can be seen that the direct causticizing reaction takes place simultaneously with combustion At a TiO_2/Na_2CO_3 molar ratio of 1.5, the direct causticization is completed at 750°C. This is lower than 850°C found for the direct causticization experiments with model mixtures in Chapter 4. The explanation for this behavior may be that the contact between Na_2CO_3 and TiO_2 is very good in the present samples because the kraft black liquor solids form a coating around the TiO_2 particles during pyrolysis. Also the combustion results in a significantly higher particle temperature than the recorded furnace temperature. The continued weight loss in Figure 2 after combustion of the mixture with a TiO_2/Na_2CO_3 molar ratio of 1.0 indicates that the reaction between TiO_2 and Na_2CO_3 is not completed. This is consistent with the results obtained for a mixture of Na_2CO_3 and TiO_2 at a molar ratio of 1.0 in Chapter

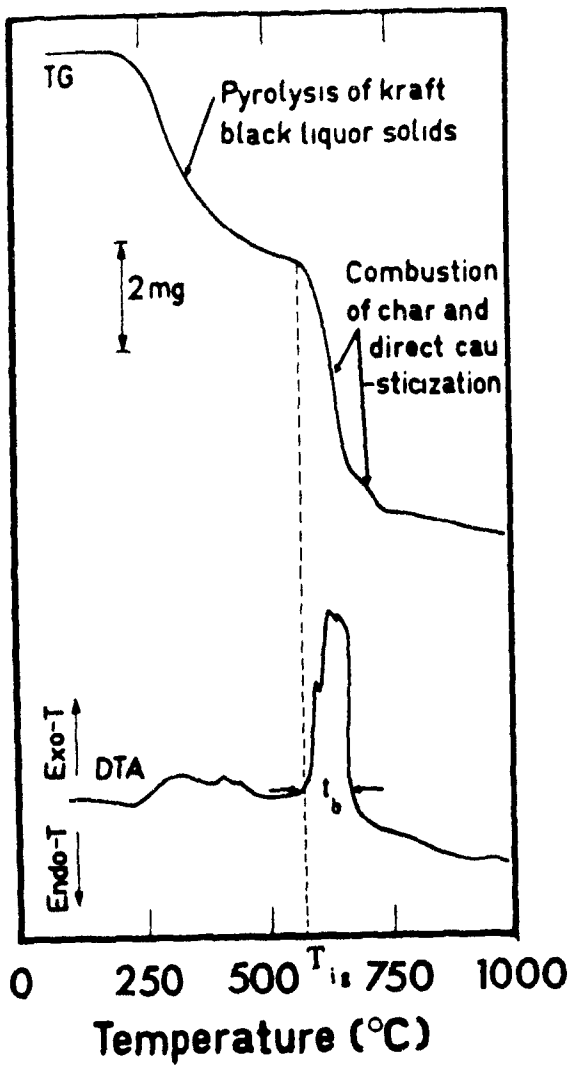

Figure 2 Results from TGA and DTA analysis
(Sample: kraft black liquor solids mixed
with TiO_2, TiO_2/Na_2CO_3=1.0 mol/mol)

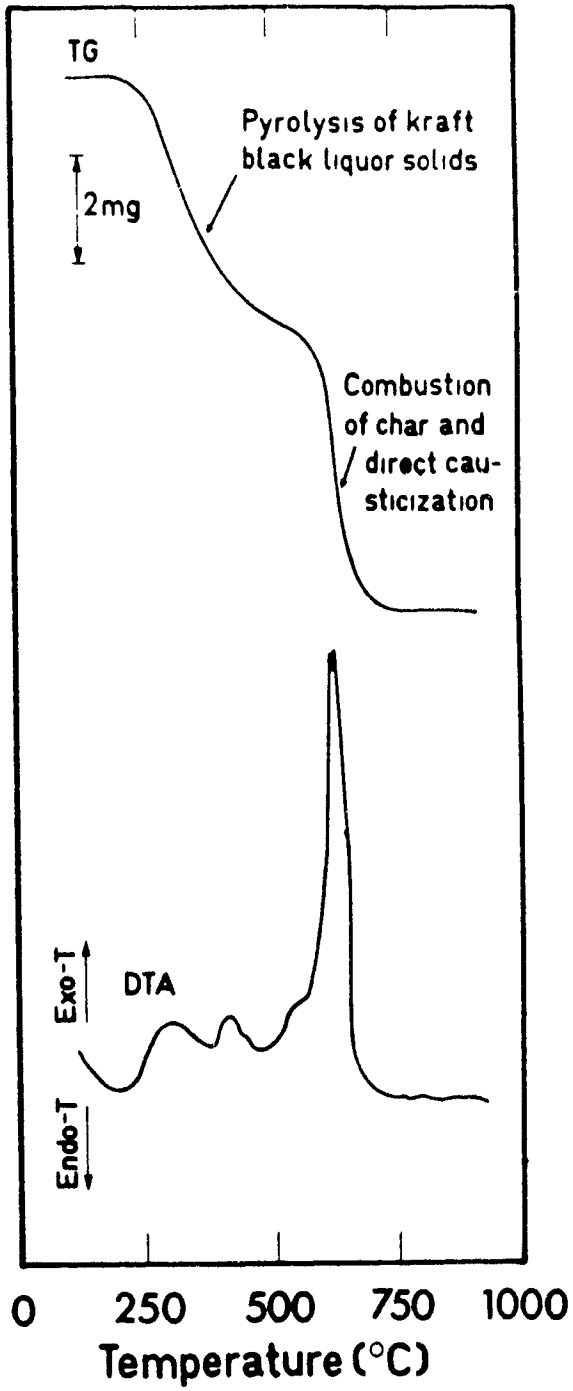

Figure 3 Results from TGA and DTA analysis (Sample: kraft black liquor solids mixed with TiO_2, TiO_2/Na_2CO_3 = 1.5 mol/mol)

4, which showed that the formation of $Na_2O{\cdot}TiO_2$ via reaction

$$4Na_2O.5TiO_2 + Na_2CO_3 = 5\ Na_2O{\cdot}TiO_2 + CO_2 \qquad (3)$$

is slow. At a high TiO_2/Na_2CO_3 molar ratio of 1.5, no tailing was observed in Figure 3 because the formation of $4Na_2O{\cdot}5TiO_2$ by reaction:

$$4\ Na_2CO_3 + 5\ TiO_2 = 4Na_2O{\cdot}5TiO_2 + 4\ CO_2 \qquad (4)$$

is much faster. This again shows that it is important to use a TiO_2/Na_2CO_3 molar ratio larger than or equal to 1.25 in order to obtain complete direct causticization of kraft black liquor at relatively low combustion temperatures.

The sample obtained by suspending TiO_2 particles in kraft black liquor rather than mixing with kraft black liquor solids had an ignition temperature of 650°C, i.e somewhat higher than found for the latter. The explanation for this behavior might be that the dispersion of TiO_2 in the latter sample is not as good as in the former, because the TiO_2 particles are likely to settle during the drying step.

ii) *Burning time*: The burning time of the chars can, in principle, be measured from the TGA curves, but with the present samples this is difficult because of the simultaneous weight loss resulting from the direct causticizing reaction. Therefore, the width of the exothermal DTA peak has been used as a measure of the burning time (t_b). As can be seen in Table 2, the burning times of black liquor are not much influenced by the presence of TiO_2. Since a lower ignition temperature and a shorter burning time (when compared at the same burning temperatures) are generally indicative of a more reactive material, these results suggest that TiO_2 addition to kraft black liquor will improve the combustion process provided that enough heat is supplied or generated by the combustion process to heat up the additional inorganics.

However, it must be stressed that the burning times measured in the present experiments can not be used as values for the calculation of retention times in a furnace; they merely indicate the relative behavior of the different samples.

Melting Point of the Combustion Products

The TGA and DTA curves of the combustion product of a mixture of kraft black liquor and TiO_2 at a TiO_2/Na_2CO_3 molar ratio of 1.5, are shown in Figure 4. The softening point and a melting point temperatures are defined here as the beginning and minimum of endothermic DTA peak, respectively. The softening and melting points obtained for different samples are summarized in Table 3. The melting point of the combustion product of kraft black liquor is 810°C, which is lower than the eutectic melting point of 826°C of a Na_2SO_4-Na_2CO_3 mixture (Gitlesen and Motzfeldt, 1964). This might be explained by the presence of other species such as K and Cl in kraft black liquor. The data in Table 3 shows that TiO_2 addition significantly increases the melting point of the combustion product, and that the melting point increases with increasing TiO_2/Na_2CO_3 ratio. The increase in melting point can be explained by the high melting points of TiO_2 and the formed sodium titanates listed in Table 4.

Table 3 Softening and Melting Points of Combustion Samples

Samples	KBL	KBL + TiO_2 (TiO_2/Na_2CO_3=1.0)	KBL + TiO_2 (TiO_2/Na_2CO_3=1.5)
T_s (°C)	785	880	930
T_m (°C)	810	900	975

Table 4 Melting Points of Pure Compounds

Compound	Na_2CO_3	Na_2SO_4	TiO_2	$Na_2O{\cdot}TiO_2$	$4Na_2O{\cdot}5TiO_2$
T_m (°C)	858	884	1850	965	1030

The implication of the above results is that a fluidized bed reactor operating below 930°C could be used for combustion and simultaneous direct causticization without agglomeration problems when the molar ratio of TiO_2 to Na_2CO_3 is larger than 1.5.

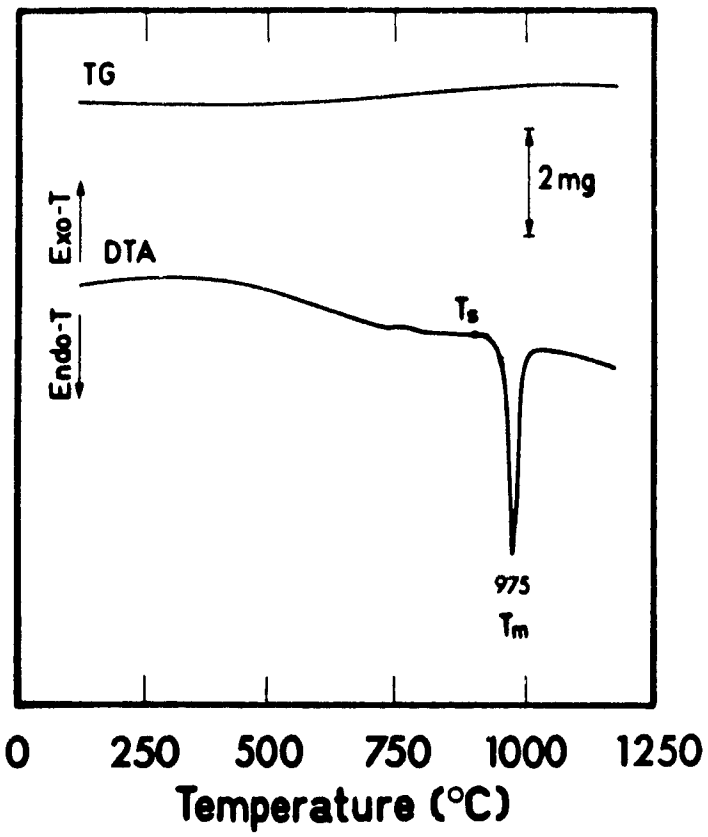

Figure 4 Thermal analysis of the combustion product of a mixture of KBL solids and TiO_2 (TiO_2/Na_2CO_3=1.5 mol/mol)

Isothermal Combustion of Kraft Black Liquor Solids with TiO_2

Isothermal combustion experiments were conducted to study the direct causticization reaction. The conversion was determined by measuring the amount of carbonate remaining in the combusted residue using ion chromatographic analysis. The carbonate content of combusted black liquor without TiO_2 is 45.8% (wt.), which is equal to 19.2 g carbonate/100 g KBL solids based on an ash yield of 41.9%. The Na_2CO_3 conversion, X, was defined as:

$$X = \frac{\text{Carbonate content of combusted mixture of KBL solids and titanium dioxide}}{\text{Carbonate content of combusted KBL solids}} \times 100\% \qquad (5)$$

The carbonate content of both combusted mixtures was based on the weight of the original KBL solids. Shown in Figure 5 are the results for combustion mixtures of two different TiO_2/Na_2CO_3 molar ratios. After only 5 minutes the percent conversion of sodium carbonate is more than 80%. Further conversion of the mixture with a TiO_2/Na_2CO_3 molar ratio of 1.0 is very slow. The conversion after 2 hours is about 85%. This agrees with the results obtained for the model mixtures in Chapter 4, which showed that formation of $4Na_2O{\cdot}5TiO_2$ is fast but further conversion to $Na_2O.TiO_2$ is extremely slow at 825°C. When the TiO_2/Na_2CO_3 molar ratio is increased to 1.5, the Na_2CO_3 conversion is almost complete in about half an hour as shown in Figure 5. Thus it can be concluded that with a high TiO_2/Na_2CO_3 ratio, one can obtain a high degree of direct causticization of kraft black liquor at temperatures below the melting point of the combustion product.

Although it was found by thermodynamic analysis in Chapter 3, that under oxidizing conditions all the sulfur is captured as Na_2SO_4, it is likely that sulfurous gases are emitted during initial oxiditive pyrolysis of kraft black liquor. This was confirmed experimentally by burning kraft black liquor solids with or without the presence of TiO_2. The results in Figure 6 show that about 8% sulfur of the total is lost during combustion of kraft black liquor solids and that all the sulfur is lost in the first minutes when pyrolysis takes place. With the addition of TiO_2 the initial sulfur loss is significantly reduced to about 3%. No significant sulfur loss is detected during direct causticization after the initial pyrolysis and combustion of KBL solids.

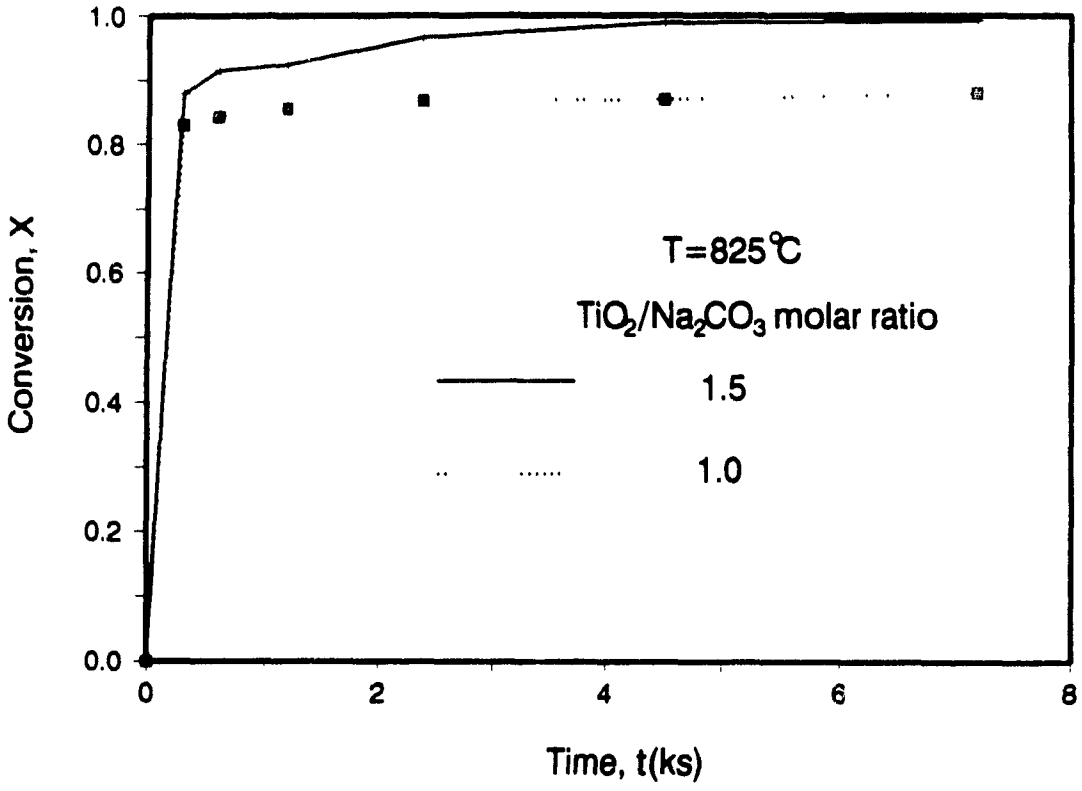

Figure 5 Carbonate conversion during combustion of a mixture of kraft black liquor solids and TiO_2.

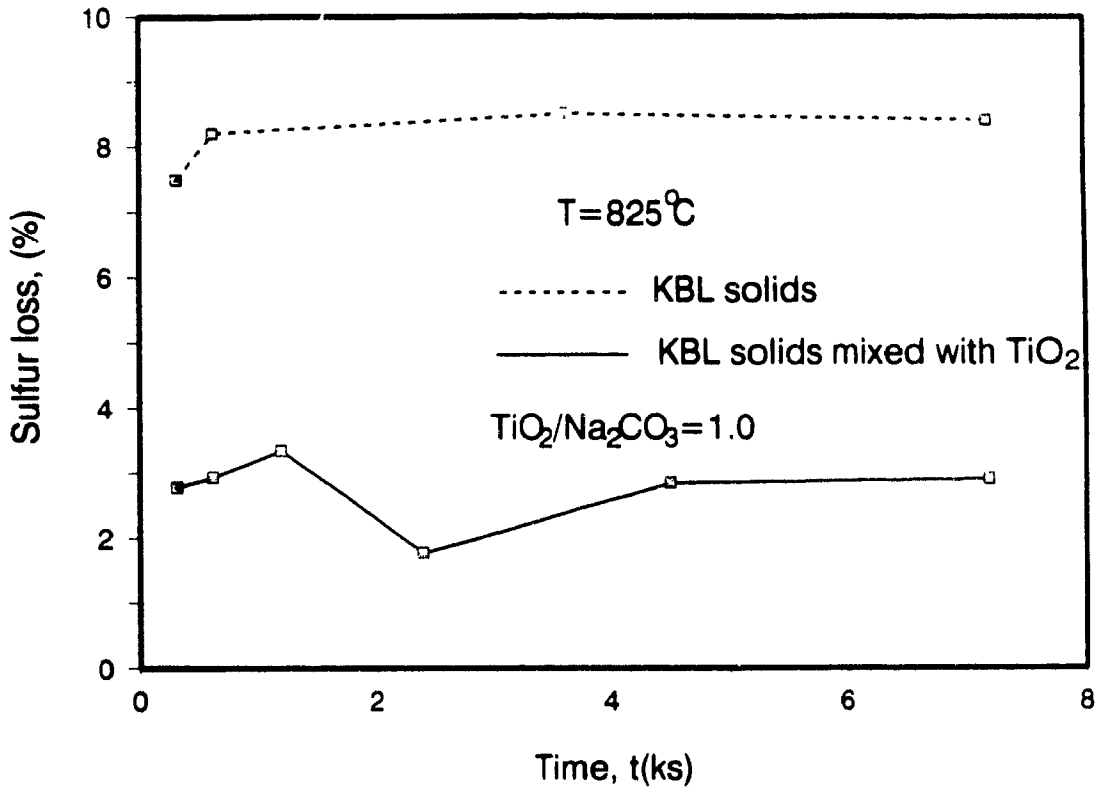

Figure 6 Sulfur loss during the combustion and direct causticization of kraft black liquor solids.

Hydrolysis of the Combustion Product

The residue obtained after combustion and direct causticization of kraft black liquor solids was immersed in water to determine the hydrolysis efficiency. The hydrolysis efficiency, H, is defined as the amount of NaOH formed after hydrolysis, divided by the theoretical amount of NaOH assuming complete decomposition of the sodium titanates into NaOH and TiO_2. A TiO_2/Na_2CO_3 molar ratio of 1.0 was used for combustion except when specified otherwise. The results in Table 5 indicate that the hydrolysis is incomplete even after a 2 hours in 80°C water. This is expected since according to thermodynamics the hydrolysis products are NaOH and $Na_2O{\cdot}3TiO_2$ formed by the reactions:

$$3\ Na_2O{\cdot}TiO_2 + 2\ H_2O = 4\ NaOH + Na_2O{\cdot}3TiO_2 \qquad (6)$$

$$3\ (4Na_2O{\cdot}5TiO_2) + 7\ H_2O = 14\ NaOH + 5\ (Na_2O{\cdot}3TiO_2) \qquad (7)$$

A calculation based on the two chemical reaction equations shows that that the maximum degrees of hydrolysis of $Na_2O{\cdot}TiO_2$ and $4Na_2O{\cdot}5TiO_2$ are 66.7% and 58.3%, respectively. It can be seen from Table 5 that the hydrolysis efficiency is always smaller than 66.7% even when the sample is combusted at 905°C for 60 minutes (Test 6) and most of the sodium titanate is in the form of $Na_2O{\cdot}TiO_2$. The results in Table 5 are similar to those published earlier by Kiiskila (1979a) and Belyaev et al. (1968) for model mixtures.

The precipitate ($Na_2O{\cdot}3TiO_2$) obtained after hydrolysis was filtered from the NaOH solution and reused for combustion and direct causticization of kraft black liquor solids. The results of these recycle experiments performed at a TiO_2/Na_2O molar ratio of 1.25 are shown in Table 6. The causticizing efficiency Y is defined as:

$$Y = \frac{\text{moles of NaOH formed with } TiO_2 \text{ addition}}{\text{moles of } Na_2CO_3 \text{ in combusted KBL solids} \times 50\%} \qquad (8)$$

Both NaOH and Na_2CO_3 are based on kraft black liquor solids. As can be seen in Table 6, the causticizing efficiency of the first cycle performed with pure TiO_2 is only 58%. However, when the recycled TiO_2 was used, a high

Table 5 Kraft Black Liquor Combustion and Direct Causticization with TiO_2 (TiO_2/Na_2CO_3=1.0)

Run No	Combustion and causticizing reaction				Hydrolysis		
	T (℃)	t (min)	W_s (mg)	Na_2CO_3 conversion (%)	T (℃)	t (min)	Hydrolysis efficiency (%)
1	800	30	502 5	83 1	80	60	53 2
2	825	30	498 3	84 5	80	60	54 5
3	860	30	510 5	85 7	80	80	55 7
4	880	30	500 3	86 1	80	120	58 9
5	900	30	498.7	92 1	80	60	62 4
6	905	60	487 4	96 5	80	120	66 6
* 7	900	15	508 3	99 5	80	40	55 8
* 8	800	20	505 5	90.5	80	60	56 5
* 9	825	20	501.3	93 4	80	120	58 4

* TiO_2/Na_2CO_3=1.5 mol/mol

Table 6 Kraft Black Liquor Combustion and Direct Causticization with Recycled $Na_2O.3TiO_2$

Cycle No.	Combustion and Causticization				Hydrolysis		Causticizing efficiency (%)
	W_s (mg)	T (℃)	t (min)	Na_2CO_3 conversion (%)	T (℃)	t (min)	
1 *	507.3	890	60	98.83	80	90	58.05
2 **	502.5	890	60	97.89	80	90	94 35
3 **	503.8	890	60	98.15	80	90	94 88
4 **	498.9	890	60	97.96	80	90	94 50

* Pure TiO_2 used; TiO_2/Na_2CO_3=1.5 mol/mol

** Precipitated $Na_2O{\cdot}3TiO_2$ used; $Na_2O{\cdot}3TiO_2/Na_2CO_3$=0.9 mol/mol

causticizing efficiency of about 95% was obtained. This can be explained by the relevant direct causticization and hydrolysis reactions:

$$Na_2O{\cdot}3TiO_2 + 2\ Na_2CO_3 = 3\ Na_2O{\cdot}TiO_2 + 2\ CO_2 \qquad (9)$$

$$3\ Na_2O{\cdot}TiO_2 + 2\ H_2O = 4\ NaOH + Na_2O{\cdot}3TiO_2 \qquad (10)$$

which together result in the overall reaction:

$$2Na_2CO_3 + 2\ H_2O = 4\ NaOH + 2\ CO_2 \qquad (11)$$

At relatively low combustion temperatures and high TiO_2/Na_2CO_3 molar ratios the equivalent reactions are respectively:

$$5\ (Na_2O{\cdot}3TiO_2) + 7\ Na_2CO_3 = 3\ (4Na_2O{\cdot}5TiO_2) + 7\ CO_2 \qquad (12)$$

$$3\ (4Na_2O{\cdot}5TiO_2) + 7\ H_2O = 14\ NaOH + 5\ (Na_2O{\cdot}3TiO_2) \qquad (13)$$

It should be noted that the present $Na_2O{\cdot}3TiO_2/Na_2CO_3$ molar ratio of 0.9 is much higher than 0.714 required for the stoichiometry of direct causticization reaction (10). However the results in Table 6 show that by recycling $Na_2O{\cdot}3TiO_2$ a causticizing efficiency of about 95% can be achieved in this proposed alternative kraft black liquor recovery process.

CONCLUSION

The effect of the addition of TiO_2 on the ignition temperature and burning time of kraft black liquor solids shows that the presence of TiO_2 would improve rather than retard the combustion process provided that enough heat is supplied for the increased thermal load of the inorganics. The melting point of the combustion product is also increased by the presence of TiO_2 thus allowing higher operating temperatures of an alternative fluid bed combustion process. The sulfur loss during the combustion is significantly reduced by the addition of TiO_2. Almost complete direct causticization of Na_2CO_3 can be obtained by combustion of a mixture of kraft black liquor solids and TiO_2 at molar ratio of 1.5. With recycled $Na_2O{\cdot}3TiO_2$ as direct causticizing chemical, a causticization efficiency of 95% is obtained.

NOMENCLATURE

H	=Hydrolysis efficiency, %.
t	=Time, s
t_b	=Burning time, s.
T	=Temperature, °C
T_{ig}	=Ignition temperature, °C.
T_m	=Melting temperature, °C.
T_s	=Softening temperature, °C.
X	=Na_2CO_3 conversion, %.
Y	=Causticizing efficiency, %.

REFERENCES

Baker, R.T .K., "Controlled Atmosphere Electron Microscopy of Gas-Solid Reactions", in *Chemistry and Physics of Solid Surface* (Edited by R. Vanselow and S.Y. Tong), 1977, Vol.1, p.293, CRC Press, Cleveland.

Belyaev, E. K., N. Sh. Safiullin and N. M. Panasenko, "Reaction of Titanium Dioxide and Sodium Carbonate", *Izv. Akad. Nauk. SSSR Neorg Mater* , 1968, 4, p.97-103.

Brame, J.S.S. and J.G. King, *Fuel: Solid, Liquid and Gaseous*, 6th ed., Arnold, London, 1967.

Gamel, C.M. and W.J. Smothers, "Calorimetric Determination on Semibituminous Coals Using Differential Thermal Analysis", *Anal. Chim. Acta* 1952, 6, p.422.

Gitlesen, G. and K. Motzfeld, "The Phase Diagram of Na_2SO_4-Na_2CO_3 Mixture", *Acta Chem. Scand.*, 1964, 18, p.488.

Kiiskila, E., "Recovery of Sodium Hydroxide from Alkaline Pulping Liquors by Smelt Causticizing, Part II, Reactions between Sodium Carbonate and Titanium Dioxide", *Paperi ja Puu — Paper och. Tra*, 1979a, 61(5), p.129-132.

Kiiskila, E., "Recovery of Sodium Hydroxide from Alkaline Pulping Liquors by Smelt Causticizing, Part III, Alkali Distribution in Titanium Dioxide Causticizing", *Paperi ja — Papper och. Trà*, 1979b, 61(6), p.453-464.

Milanova, E. and G.J. Kubes, "The Combustion of Kraft Black Liquor Chars", *Journal of Pulp and Paper Science*, 1986, 12(6), p.J187-192.

Nguyen, X.T., "Process to regenerate kraft black liquor", *Canadian pat.*

No.1,193,406, 1985.

Ranish, J.M., and P.L. Walker, "Model for Roughening of Graphite in Its Catalyzed Gasification", *Carbon*, 1990, 28(6), p.887-896.

Sen Gupta, K.G., "Oxidation of Sodium Thiosulfate in Weak Kraft Black Liquor", *Master thesis*, McGill University, Montreal, 1986.

Scott, J.B. and O.J. Baker, "Classification of Coal by Thermal Analysis", *Fuel*, 1953, 32, p.415.

Thomas, J.M., "Microscopic Studies of Graphite Oxidation", in *The Chemistry and Physics of Carbon* (edited by P.L. Walker, Jr.), 1965, Vol.1, p.121, Marcel Dekker, New York.

CHAPTER 6

HYDROGEN REDUCTION OF SODIUM SULFATE MIXED WITH SODIUM TITANATE

ABSTRACT

The hydrogen reduction kinetics of solid sodium sulfate mixed with sodium titanate are studied in a thermogravimetric system. The reduction rate is much faster than that of pure sodium sulfate and is well described by the nucleation and growth model up to about 60% conversion. In the deceleratory conversion period, the reduction is controlled by gas diffusion through a product layer. Activation energies of 302 and 179 kJ/mol are obtained respectively for the nucleation and growth, and diffusion limited period. The influence of hydrogen concentration, sodium sulfate fraction, steam concentration, sodium sulfide addition, and iron oxide catalyst is also studied.

The reduction of sodium sulfate in the combusted residue of kraft black liquor mixed with TiO_2 is also investigated. A faster reduction rate is obtained with a lower activation energy, and the kinetic data are also well described by the nucleation and growth model.

INTRODUCTION

The recovery of chemicals and energy from spent pulping liquor is an integral part of modern pulp and paper processes. In the kraft process, the pulping chemicals, NaOH and Na_2S, are recovered from so-called kraft black liquor by combustion and by subsequent conversion of Na_2CO_3 to NaOH with lime in a separate causticizing step. Although the objective of chemical recovery is adequately achieved, several major drawbacks are associated with the present process such as the smelt-water explosion hazard, high capital and operating costs as well as the complicated nature of the causticizing cycle (Hough, 1985; Adams & Frederick, 1988). These form the impetus for on-going research into alternative technologies such as the proposed fluidized bed process in which black liquor is burned with TiO_2 (Nagano, 1976; Nguyen, 1985). TiO_2 functions as causticizing chemical during the recovery process, because CO_2 is released from Na_2CO_3 by following reaction:

$$Na_2CO_3 + TiO_2 \longrightarrow Na_2O{\cdot}TiO_2 \text{ (or } 4Na_2O{\cdot}5TiO_2) + CO_2\uparrow \quad (1)$$

Sodium sulfate in the combustion product is subsequently reduced in the solid state with H_2 and/or CO, giving a mixture of sodium sulfide and sodium titanate. Hydrolysis/leaching of the reduced solids produces a solution of sodium hydroxide and sodium sulfide, and insoluble sodium trititanate, $Na_2O{\cdot}3TiO_2$, according to following reactions:

$$3\ (Na_2O{\cdot}TiO_2) + 2\ H_2O = 4\ NaOH + Na_2O{\cdot}3TiO_2\downarrow \quad (2a)$$

or

$$3\ (4Na_2O.5TiO_2) + 7\ H_2O = 14\ NaOH + 5\ Na_2O.3TiO_2\downarrow \quad (2b)$$

The aqueous solution, called white liquor, is reused for kraft pulping, while sodium trititanate is recycled to the fluidized bed combustion operation.

PREVIOUS WORK

Using carbon monoxide, hydrogen, and carbon as reducing agents, Budnikoff and Shilov (1928) conducted one of the earliest sulfate reduction studies, and reported that the reactivity of H_2 was much greater than that of CO. For several gaseous reducing agents, Nyman and O'Brien (1947) determined that H_2

was the most effective, followed by H_2S, NH_3 and CH_4, respectively. Kunin and Kirillov (1968) also reported that H_2 was the most effective reducing agent followed by C_2H_4, C_3H_8, C_4H_{10}, and CH_4.

Sodium sulfate reduction by H_2 was previously studied mainly in the molten state (in the temperature range of 800-950°C) because the reduction without any catalysts is very slow at temperatures below 750°C (White & white, 1936; Nyman & O'Brien, 1947; Birk et al., 1971). The use of metal compounds (Fe, Ni, Cu), carbon, sodium carbonate, etc as catalysts significantly accelerates the H_2 reduction of sodium sulfate, thus allowing a lower reduction temperature (Budnikoff and Shilov, 1928; Wolf and Mathains, 1957; Puttagunta et al., 1970; Birk et al., 1971). Among the catalysts used, iron was found to be most effective. The catalytic effect of iron in the presence of hydrogen was clearly demonstrated in the work of Nyman and O'Brien (1947) and Birk et al. (1971). The iron oxide catalyzed reduction was studied in a fluidized bed by Puttagunta et al. (1970). They found that fusion and caking occurred at temperatures as low as 650°C, even though the eutectic point of a mixture of Na_2SO_4-Na_2S is 740°C (Andersson, 1982). Highly concentrated Na_2S was produced by Golikova et al. (1976) in a fluidized bed with large particles of Na_2SO_4 at temperatures of 675-700°C. Sulfate reduction with gaseous agents was reported to be autocatalytic by Birk et al. (1971) and Budnikoff and Shilov (1928).

The reduction of sodium sulfate is one of the critical reactions in the direct causticizing process of kraft black liquor described in Chapter 1. The only information available is that in the patent of Nguyen (1985), which shows that it is possible to reduce Na_2SO_4 in the solid state. However there is no information available concerning the mechanism and parameters controlling the reduction Na_2SO_4 in this process. The objective of this study is to obtain the kinetics and reaction mechanism of the hydrogen reduction of sodium sulfate mixed with sodium titanate in the solid state.

THEORETICAL

The rate behavior of gas-solid reactions as a function of time, t, can be crudely classified into two cases as is discussed in Chapter 2 (Koga and Harrison, 1982). The first corresponds to the formation and growth of product nuclei. As shown schematically for the nucleation and growth behavior in Figure 1(a), the size of the reaction interface increases until growing nuclei overlap extensively. Subsequent decrease in reaction surface results in a

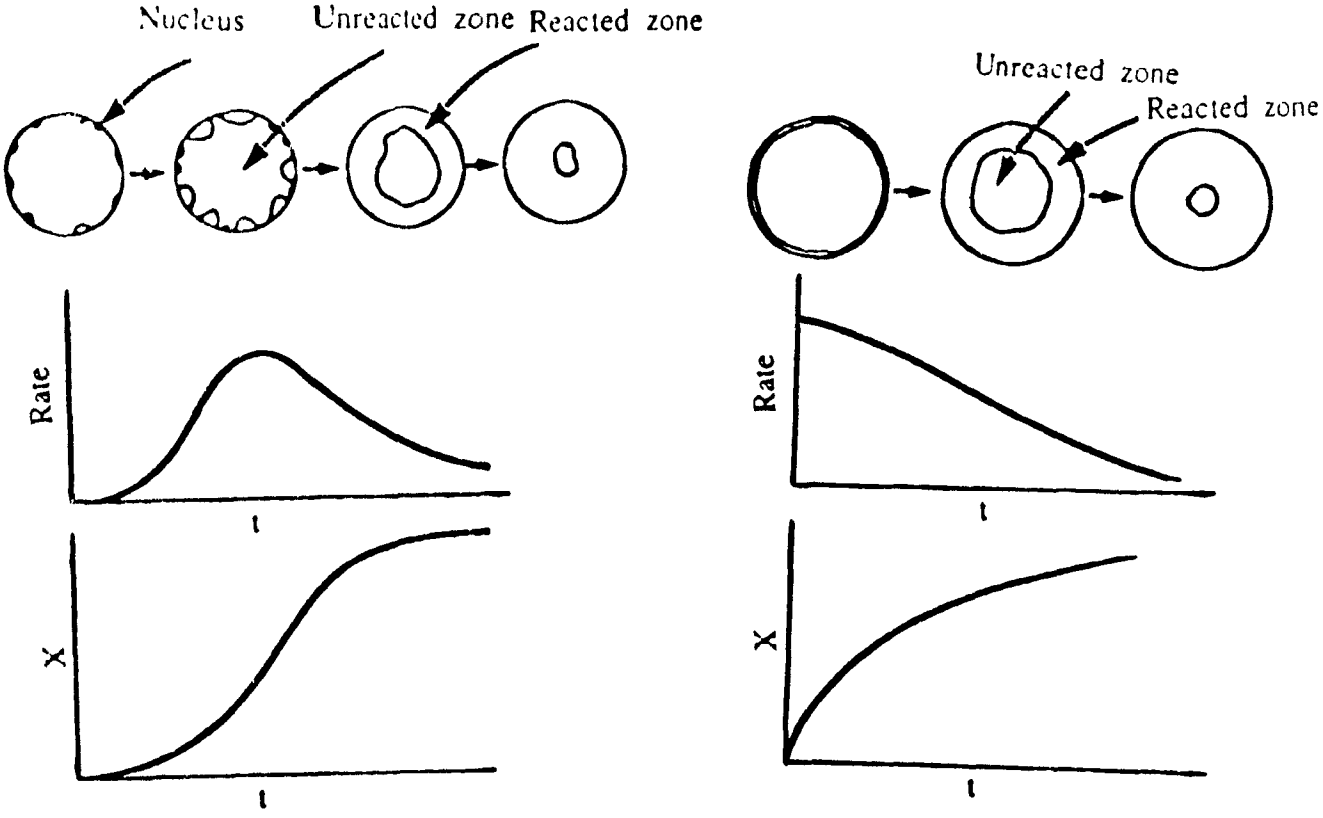

(a) Nucleation and growth model

(b) Shrinking core model

Figure 1 Gas-solid reaction models

sigmoidal shape of the conversion-time (X-t) curve. The type of X-t equation depends on the mechanism of nucleation as well as on the texture of the product nuclei and substrate grains. An excellent discussion of the theory can be found in the book of Harrison (1969).

For relatively rapid nucleation and a linear growth rate of the nuclei, a general conversion versus time equation can be derived as:

$$[-\ln(1-X)]^{1/m} = k_1 t \qquad (3)$$

where m is a constant which depends on the number of dimensional directions of nuclei growth and on the nuclei growth kinetics. The proportionality constant, k_1, in the so-called Avrami-Erofe'ev equation [Eq.(3)] for reduction of spherical particles is

$$k_1 = (2\pi n_o)^{1/2} k_s V_2 [P^o_{H_2} - P^o_{H_2O}/K_e]^a \qquad (4)$$

where n_o is the concentration of nuclei in the product at complete conversion, k_s is the intrinsic rate constant for the interfacial reaction, V_2 is the molar product volume, $P^o_{H_2}$ and $P^o_{H_2O}$ are the partial pressure of hydrogen and steam, a is the order of surface reaction and K_e is the equilibrium constant for the reduction reaction.

In the second case, shown in Fig 1(b), the entire surface of the reactant particle is covered with a thin layer of solid product very soon after contacting the reactant gas. The reaction boundary subsequently advances inward as the conversion increases. This is the well-known shrinking core model (Levenspiel,1962; Harrison,1969). The conversion is controlled by three resistances in series: (i) external mass transfer; (ii) gas diffusion through the reacted zone and (iii) chemical kinetics at the reacting interface. The kinetic equations when one of the three resistances is rate controlling step are respectively:

$$X = t/\tau \qquad (5)$$

$$1 - 3(1-X)^{2/3} + 2(1-X) = t/\tau \qquad (6)$$

$$1 - (1-X)^{1/3} = t/\tau \qquad (7)$$

where τ is the time for complete conversion of a particle. It should be noted

that the last stage of the previous nucleation and growth model when the nuclei completely overlap, is also well described by the shrinking core model. Thus the shrinking core model is appropriate for those cases whereby the nucleation and growth time is small compared to the total reaction time. This model would be favored when the surface to volume ratio of the solids is small, i.e. large particle, or when the reaction temperature is relatively high. However, for very small solid particles and relatively low temperatures, the nucleation and growth period may describe the reaction up to almost complete conversion.

EXPERIMENTAL

Equipment, Sample Preparation and Procedures

Equipment

The experimental apparatus consists of a Cahn TGA 113-DC thermo-gravimetric balance and auxiliary gas preparation system as shown in Figure 2. In addition, a steam generation system was employed and a heating tape was used to trace the gas lines transporting steam to the TGA system. The temperature and sample weight were continuously recorded with a computerized data acquisition system. A gas chromatography (GC) with flame photometric detector was used for analysis of sulfurous gases. The anion content of the solids, such as sulfate, sulfide, carbonate, etc. was measured with a Dionex ion chromatography (IC) equipped with thermal conductivity and electro-chemical detectors.

Sample preparations

i) Model compound mixture: A solution was made of reagent grade sodium sulfate and sodium carbonate (molar ratio =1:3) in deionized water. After evaporation of the water, the resulting solids were ground, sieved, (d_p<25 μm) and mixed with titanium dioxide (d_p<10 μm) at a molar ratio of Na_2CO_3/TiO_2 of 1.0. The mixture was then exposed to air at 910°C for 6-8 hours in a tube furnace. The sample was subsequently ground and sieved (d_p<25 μm). XRD analysis showed the presence of only Na_2SO_4 and $Na_2O{\cdot}TiO_2$, confirming that the direct causticizing reaction (1) was complete. The molar ratio of Na_2SO_4 to $Na_2O{\cdot}TiO_2$ in the mixture is 1:3.

ii) Combusted kraft black liquor with TiO_2: Two types of samples were prepared from kraft black liquor. a) Sample 1: Oxidized kraft black liquor

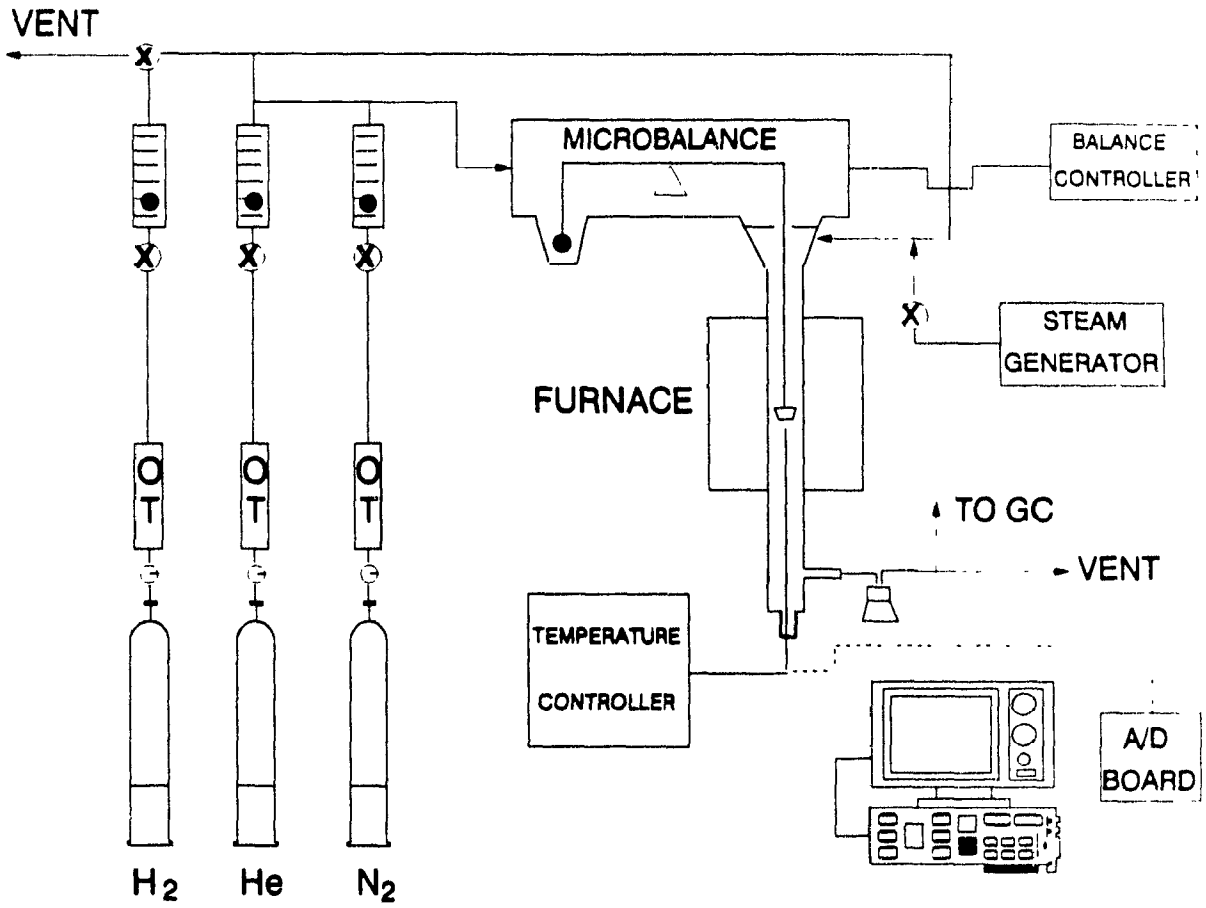

Figure 2 TGA reactor system

solids were mechanically mixed with TiO_2 at a molar ratio of TiO_2/Na_2O of 1.0:, and subsequently burned and kept at 900°C in air in a tube furnace for 6 hours until the causticizing reaction (1) is complete. b) Sample 2: Oxidized kraft black liquor solids were first burned at 900°C in a tube furnace. The residue, mainly Na_2CO_3 and Na_2SO_4, was mechanically mixed with TiO_2 at a molar ratio of TiO_2/Na_2O=1:1, and kept at 900°C in a tube furnace in air for 6 hours. Both mixtures were ground and sieved (d_p<25 μm) before subsequent reduction experiments. The composition of the kraft black liquor solids and pure combusted kraft black liquor is listed in Table 1.

Experimental procedures

With 10-20 mg of the previously described samples, the bed height in the pan of the TGA system is about 1 mm. The furnace temperature was raised at a heating rate of 25°C/min under a N_2 or He flow rate of 300 cm^3/min. Hydrogen was introduced into the reaction tube when the furnace temperature was stabilized at a preselected value. Steam was added by controlled injection of water with a syringe into the heated gas line connected to the TGA system. After completion of the reduction reaction, the hydrogen flow was discontinued and the furnace rapidly cooled to room temperature (about 3 minutes). The reduced sample was immediately dissolved in deairated and deionized water and the residue removed by filtration. The sample handling before analysis by IC was kept at less than 5 minutes in order to minimize oxidation of sodium sulfide. Some solid samples were also immediately analyzed by X-ray diffraction analysis and scanning electron microscopy.

Data Analysis

Preliminary experiments showed that sodium titanate was inert in H_2 below 850°C, and substantial decomposition of sodium titanate by H_2 occured only above 900°C. Thus below 850°C, the conversion, X, of the reduction reaction:

$$Na_2SO_4 + 4\ H_2 = Na_2S + 4\ H_2O \qquad (8)$$

can be calculated from the weight-loss due to the release of oxygen. This was confirmed by the small difference, ΔW_L, in Table 2 between the measured weight loss, W_L, at complete reduction and the calculated weight loss based on the initial sulfate weight, $W^{o}_{SO_4^=}$. The absence of sulfate in the final sample, $W_{SO_4^=}$, shows that the reduction is complete. The small percentage weight

Table 1 Composition of Kraft Black Liquor

(a) Elemental composition of oxidized kraft black liquor solids

Elements	%(wt)
Na	22.90
S	2.90
C	31.67
H	2.64
O	33.04
Cl	0.16
K	1.46
	(ppm)
Al	1700
Si	120
Fe	4
Mn	10
Cr	8
Ti	0

(b) Composition of pure combusted kraft black liquor solids

Ion	wt.(%)
Na^+	38.7
K^+	2.3
$SO_4^=$	14.4
$CO_3^=$	45.8
Cl^-	0.3

(Molar fraction: M_2SO_4, 0.17; M_2CO_3, 0.83. M: Na or K)

difference between the initial and final sulfur content, respectively $W_{SO_4}^{=}$ and $W_S^{=}$, shown as ΔW_s in Table 2, as well as the small sulfur emission (< 2 ppm below 750°C) establishes the accuracy of the sulfur anion analysis.

Table 2 Mass and Sulfur Balances

T (°C)	$[H_2]$ (%)	$[H_2O]$ (%)	$W_{SO_4}^{=}$ (mg S)	$W_S^{=}$ (mg S)	$W_{SO_4}^{=}$ (mg S)	W_L (mg)	ΔW_s (%)	ΔW_L (%)
700	50	0	1.38	1.45	0	2.77	+5.0	+0.4
700	80	0	0.67	0.65	0	1.34	-3.0	0
700	50	10	0.92	0.89	0	1.82	-3.3	-1.1
750	50	0	0.89	0.94	0	1.75	+5.6	-1.7

ROLE OF EXTERNAL MASS TRANSFER

A shallow alumina pan was used in this study for which the external mass-transfer correlations are available (Li, 1989). Although the flow of H_2 was maintained well in excess of starvation levels, it was felt that mass transfer in the film around the sample might offer some resistance to the reduction. To find out to what extend the film mass transfer affects the reduction rate, the following calculations were performed. The rate of transfer of H_2 across the film surrounding the reduction sample is given by:

$$N_{H_2} = \frac{k_g}{RT} [P^o_{H_2} - P^s_{H_2}] \quad (mol/m^2s) \qquad (9)$$

where N_{H_2}: Rate of film mass transfer of H_2, mol/(m^2s).
k_g : Film mass transfer coefficient, m/s.
$P^o_{H_2}$: H_2 pressure in the bulk gas stream, atm.
$P^s_{H_2}$: Equilibrium H_2 pressure at the reaction interface, atm.

The mass transfer coefficient k_g was computed using the mass-transfer correlations for the Sherwood number (Sh), which were obtained experimentally in the present TGA reactor system by Li (1989) via the following equation:

$$k_g = Sh\ \mathbb{D}/d_c \qquad (10)$$

Details of the calculation procedure for k_g can be found in Appendix 1. The film mass-transfer rate, N_{H_2}, is compared in Table 3 with the maximum experimental rates r_{max} at each temperature. The measured maximum reaction rate was expressed according to following equation:

$$r_{max} = W^{s}_{So4} \times \frac{64}{142} \times \left(\frac{dX}{dt}\right)_{max} \times \frac{1}{S} \quad (\text{mol m}^2/\text{s}) \quad (11)$$

where W^{s}_{So4} is the initial weight of sodium sulfate and S is the surface area of sample pan. In order for the film mass transfer resistance to be negligible, N_{H_2} must be at least 20 times as large as the measured reaction rate. i.e.:

$$M_H = \frac{r_{max}}{N_{H_2}} < 5\% \quad (12)$$

Inspection of the data in Table 3 shows that this condition is met below 720°C for model mixtures. However, the mass transfer resistance is significant at 750°C.

Table 3 Evaluation of the Influence of the External Mass-Transfer Resistance

Run No	T (°C)	Carrier gas	k_g (m/s)	N_{H_2} (mol/m²s)	r_{max} (mol/m²s)	M_H (%)
1	630	N_2	0.1094	0.7382	0.0007	0.09
		He	0.1813	1.2230	0.0007	0.06
2	650	N_2	0.1134	0.7487	0.0013	0.18
		He	0.1883	1.2432	0.0013	0.11
3	680	N_2	0.1194	0.7635	0.0041	0.53
		He	0.1985	1.2694	0.0041	0.32
4	700	N_2	0.1239	0.7756	0.0135	1.74
		He	0.2055	1.2868	0.0135	1.05
5	720	N_2	0.1286	0.7879	0.0325	4.26
		He	0.2107	1.2878	0.0336	2.71
6	750	N_2	0.1354	0.8064	0.0831	11.0
		He	0.2123	1.2943	0.0897	7.06

The above calculations indicate that the mass transfer resistance can be

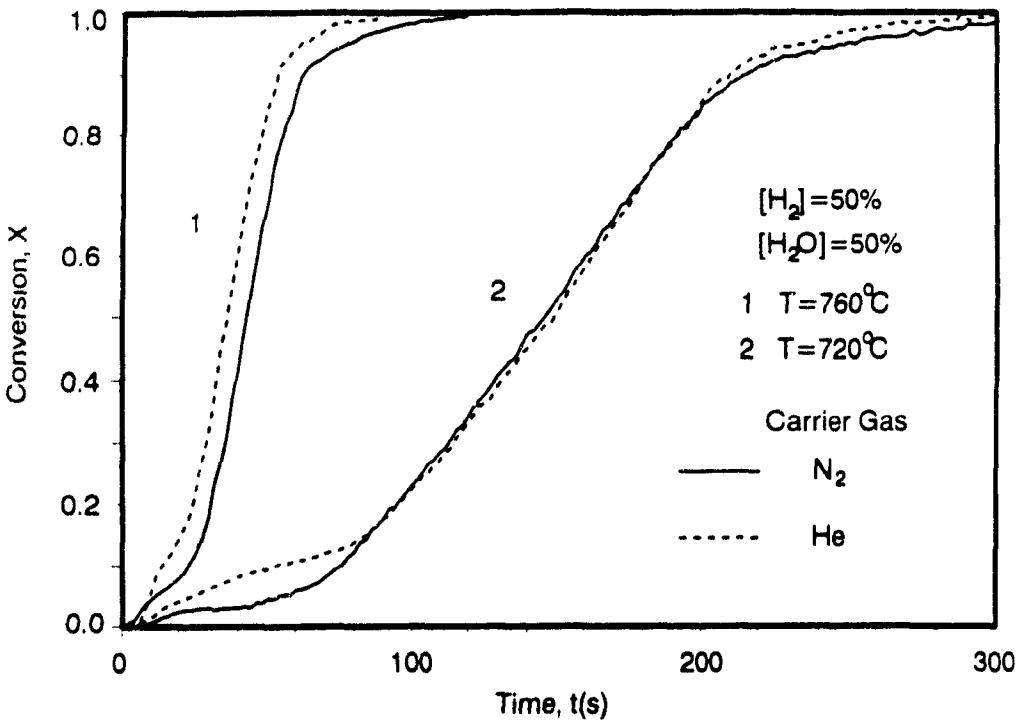

Figure 3(a) Influence of external mass-transfer

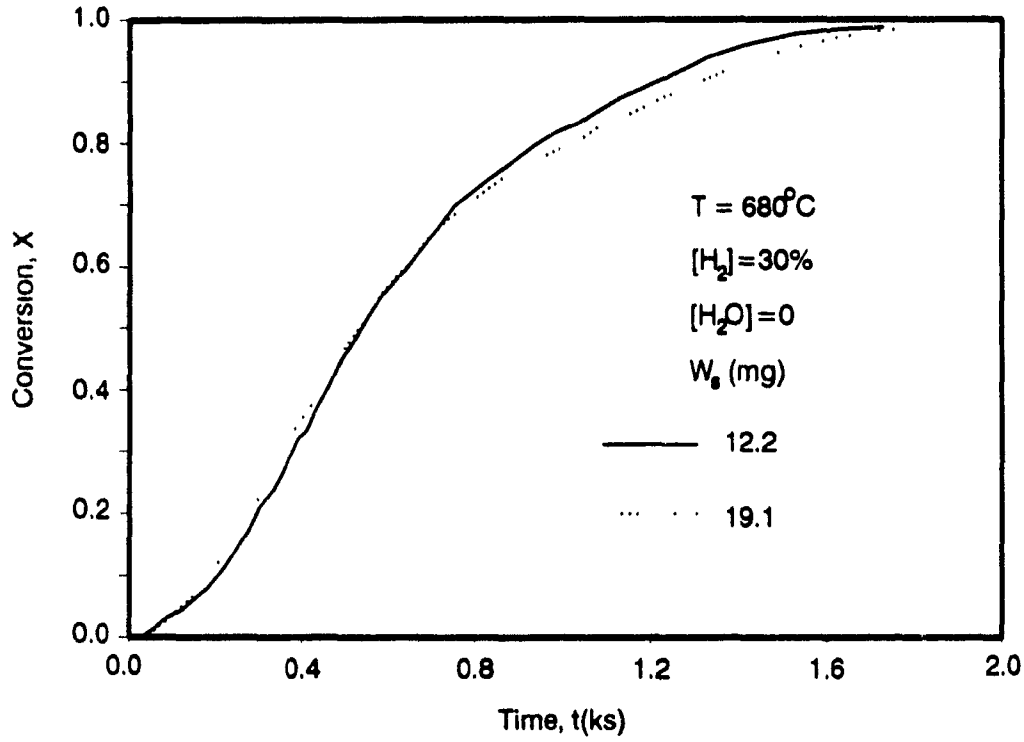

Figure 3(b) Influence of sample size

identified by using different carrier gases, since the external mass-transfer resistance with He as carrier gas is about one and half times smaller than that with N_2. The experimental results in Figure 3(a) with N_2 and He as carrier gases confirm that there is no mass-transfer resistance below 720°C. However, the kinetic data should be corrected for external mass transfer resistance above 720°C.

The effect of the size of the reduction sample on the reduction kinetics was also investigated. The conversion-time curves in Figure 3(b) obtained for two samples of 12 and 19 mg, respectively, at otherwise same conditions are not significantly different. This was taken as an indication that the sample size has no effect on the X-t curves over the range of the samples investigated.

KINETIC RESULTS AND DISCUSSION

Part 1 Reduction of Model Mixtures

The reduction experiments were performed in the temperature range of 630-750°C. The conversion-time curves in Figure 4 are sigmoidal in shape. Therefore the nucleation and growth kinetics given by equation (3) were first used to fit the data. The exponent n of Eq.(3) can be obtained from the slope of a plot of -ln(1-X) vs. t on a log-log scale, as is done in Figure 5. The fact that a straight line relationship is obtained for $X<0.6$, with approximately the same slope for all temperatures studied, supports the validity of the nucleation and growth model for the present reaction. The values of m obtained by straight line fitting of the data in Figure 5 for $X<0.6$, are listed in Table 4. The average value of m, 1.90, is very close to 2, which signifies that the nuclei growth is two- or one-dimensional, depending respectively on whether all nuclei are present at the start of reaction or are formed at a steady rate during reduction (Levenspiel, 1986). Therefore the reduction data were replotted, as shown in Figure 6(a), for three temperatures according to the kinetic equation:

$$[-\ln(1-X)]^{1/2} = k_1 t \qquad (13)$$

The reaction rate constant k_1, was obtained from the slope of the straight lines in Figure 6(a). The values of k_1 at m=2 are shown in Table 4. From the Arrhenius plot of k_1 in Figure 6(b), an apparent activation energy of 302

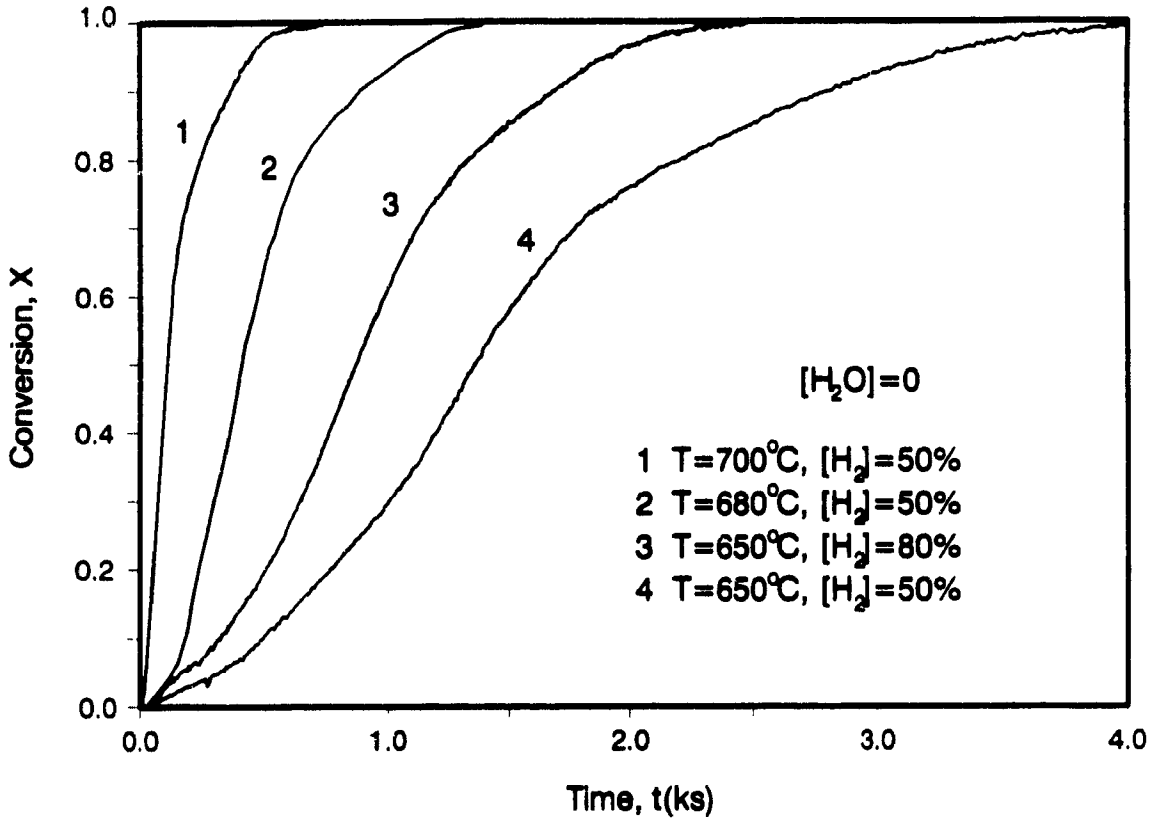

Figure 4 Typical reduction data

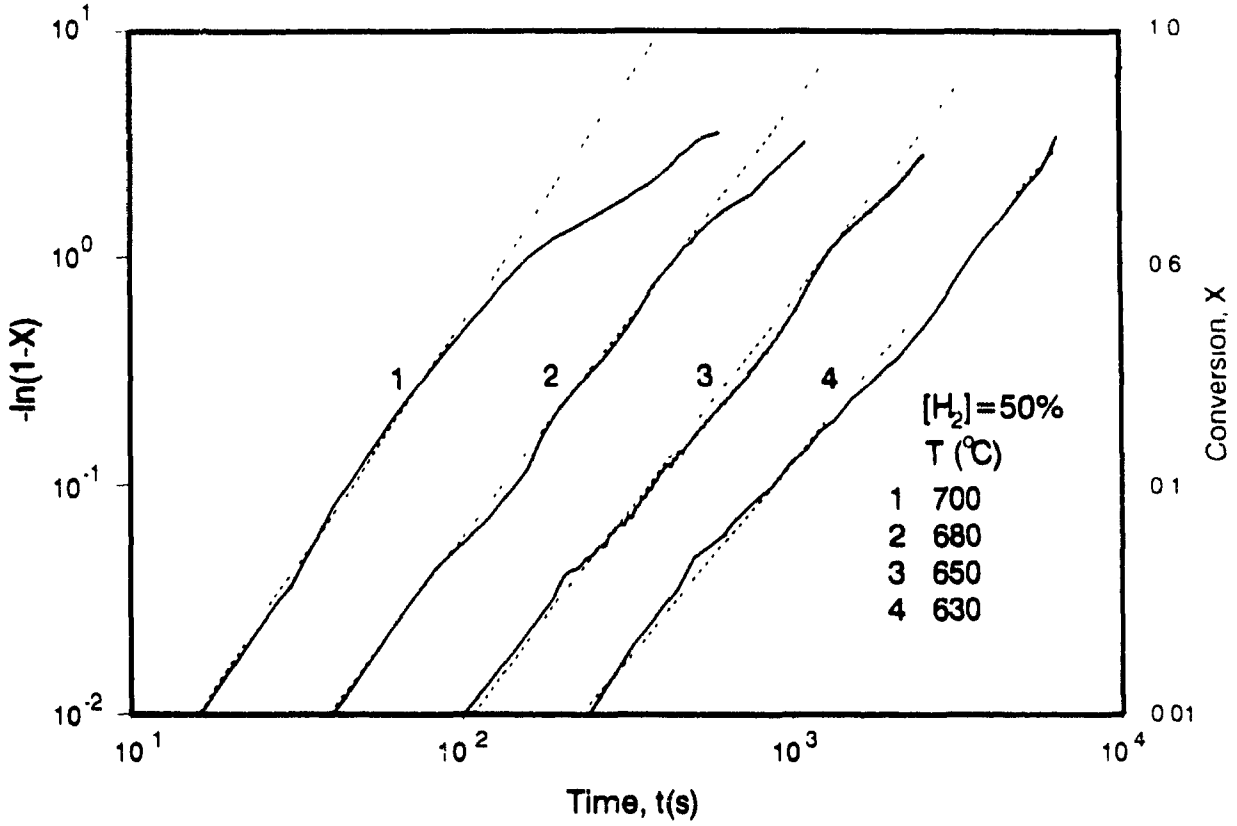

Figure 5 [-ln(1-X)] versus t

Table 4 Kinetic Parameters at Different Temperatures

T (℃)	630	650	680	700	720	750
m	1.86	1.83	1.88	1.94	1.93	1.98
k_1 ($\times 10^{3}$) (s^{-1})	0.31	0.66	2.23	6.76	10.64	16.14
t (s)	5593	2142	1084	621	363	189
D_e ($\times 10^{10}$) (cm^2/s)	0.05	0.10	0.20	0.35	0.62	1.20
t_b(s)	2326	994	260	2	-20	-35
a		0.70	0.71	0.68		

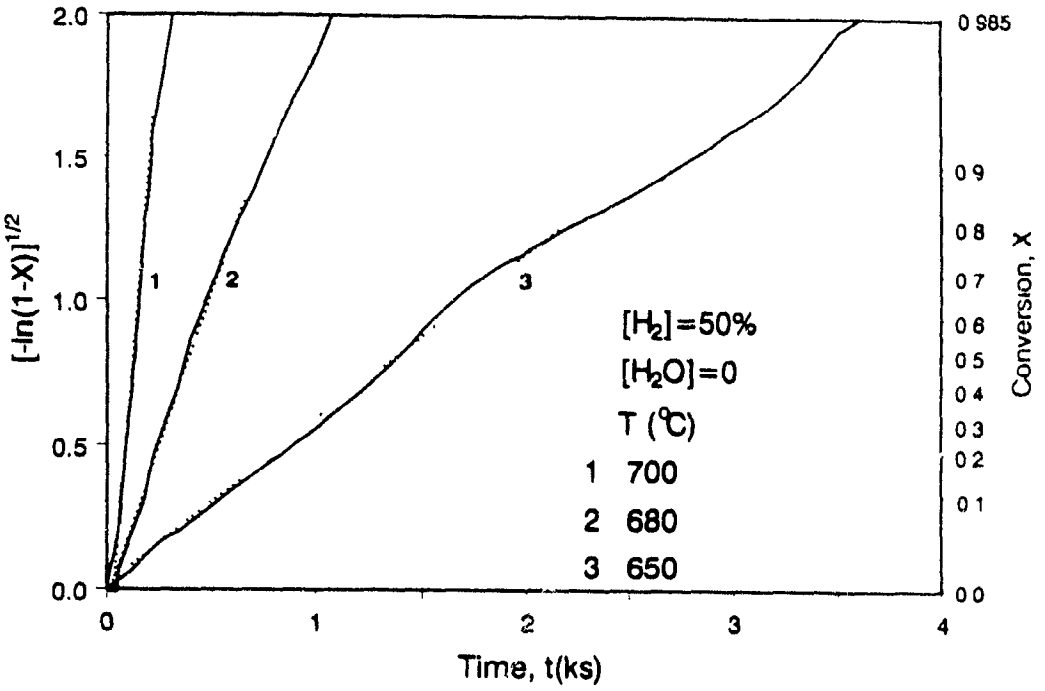

Figure 6(a) $[-\ln(1-X)]^{1/2}$ versus t

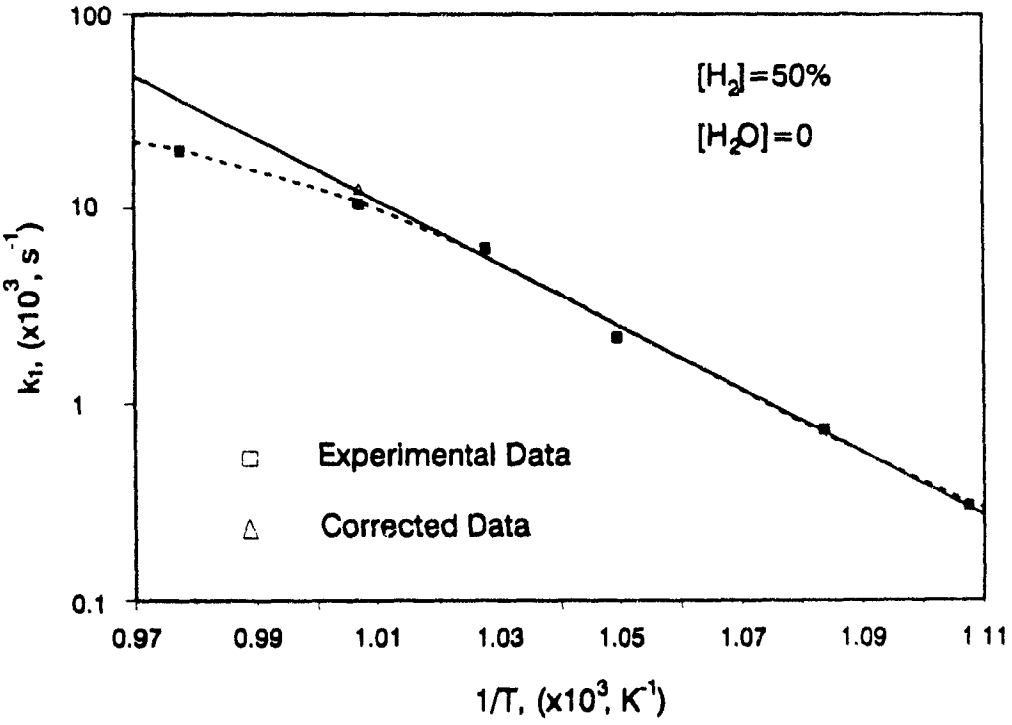

Figure 6(b) Arrhenius plot of rate constants

kJ/mol is obtained. It must be noted that the k_1 at 750°C was not used in the correlation of the data because of the mass-transfer resistance, while the value at 720°C was corrected for this effect. From Eq.(4) it follows that 1/2 $E_N + E_G = E$, where

$$E_N = RT^2(d\ln n_o/dT) \tag{14}$$

and

$$E_G = RT^2(d\ln k_s/dT) \tag{15}$$

The latter is the activation energy for the growth process and the former is the temperature dependence of n_o, the number of potential nucleus forming sites per unit volume. n_o is mostly determined by the extent of local deformation and the concentration of lattice defects. Since the original sample was treated above 900°C before reduction and the number of local deformations are mainly determined by the highest temperature during treatment, the influence of temperature on n_o is expected to be small. Assuming then that $E_N=0$, we obtain that the activation energy for nuclei growth is 302 kJ/mol.

In previous studies, Delmon and Roman (1973) obtained an activation energy for nucleation and growth kinetics of 142 kJ/mol (below 265°C) and 188 kJ/mol (above 265°C) for hydrogen reduction of NiO. El-Rahaiby and Rao (1979) found an activation energy for nucleation and growth kinetics of 237 kJ/mol for hydrogen reduction of iron oxide at 250-500°C. Thus the present activation energy for nucleus growth of 302 kJ/mol is higher but comparable to those in literature obtained for hydrogen reduction of metal oxide.

It can be seen in Figure 5 that the experimental data deviate from the nucleation and growth model when X>0.6. Accordingly, the shrinking core model [i.e. Eq.(5), (6) and (7)] was tried to describe the deceleratory period of reduction when X>0.6. It was found that reduction data were best fitted by the shrinking core model subject to product layer diffusion control [Eq.(6)] as can be seen in Figure 7. Contrary to Eq.(6), the linear region of the data points does not go through the origin because at low conversions the shrinking core model does not apply. The good linear relationship at high conversions is shown more clearly in Figure 8(a). The same transition from nucleation and growth kinetics to product-layer diffusion control was reported for the reduction of hematite to magnetite with CO by Et-Tabirou et al. (1988).

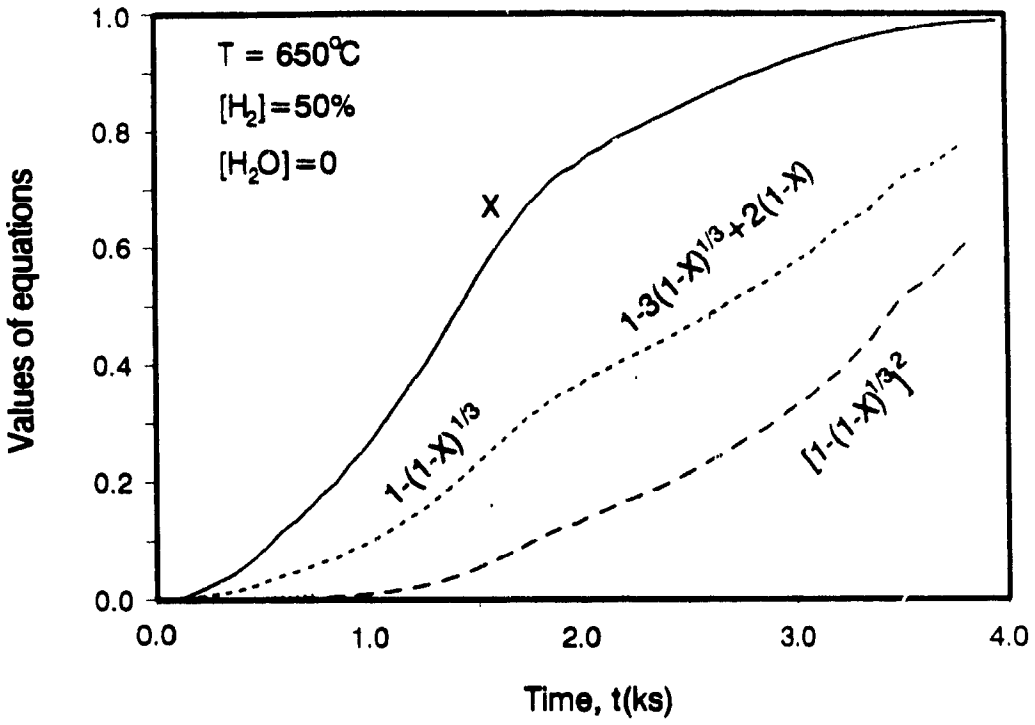

Figure 7 Fitting of the data to different forms of the shrinking core model

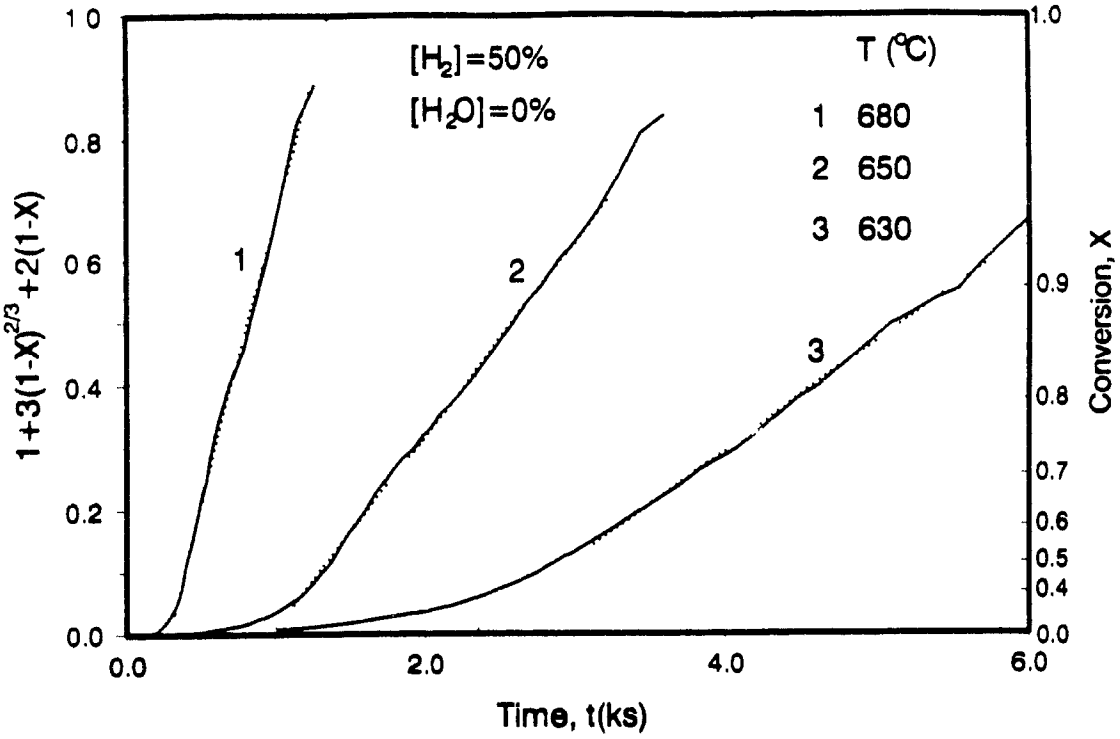

Figure 8(a) $1-3(1-X)^{2/3} + 2(1-X)$ versus t

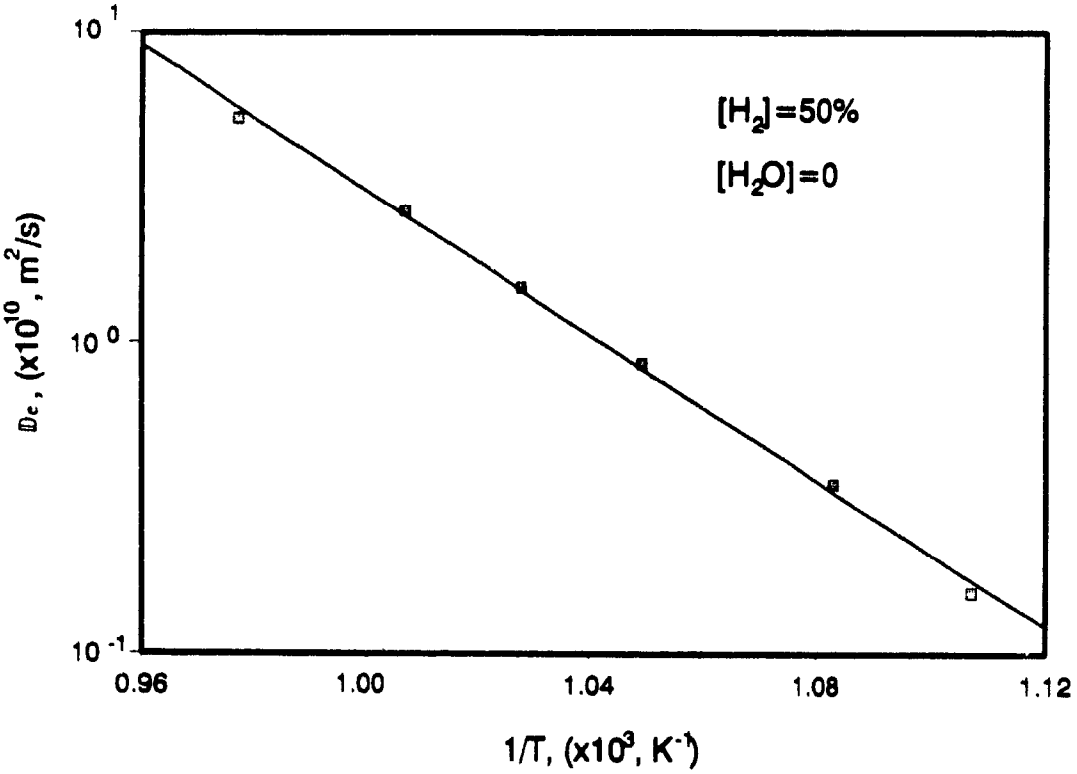

Figure 8(b) Arrhenius plot of effective diffusion coefficient, $\mathbb{D}_e$

The time for complete conversion of the particles, τ, was obtained by intersection of the straight lines in Figure 8(a) with $1-3(1-X)^{2/3}+2(1-X)=1.0$. The values of τ at different temperatures are listed in Table 4.

An initial time, t_b, can be defined as the time where the straight line fit of $1-3(1-X)^{2/3}+2(1-X)$ intersects with the horizontal axis at zero conversion. These values are also listed in Table 4. The fact that t_b is negative at the higher temperatures shows that this initial time has no physical significance. However t_b is needed for complete mathematical description of the reduction at high values of X, since the time, t, in Eq.(6) is now equal to $(t-t_b)$.

The effective diffusion coefficient $\mathbb{D}_e$ for the hydrogen diffusion through the product layer formed by reaction (8) is related to τ in Eq.(6) as (Levenspiel, 1986):

$$\mathbb{D}_e = \frac{d_p^2 \rho}{6 [H_2] \tau} \qquad (16)$$

where d_p is the average particle diameter (as 12.5 μm in this case because particle size distribution was measured), ρ, the molar density of Na_2SO_4 in the particles (3.0 g/cm^3) and $[H_2]$, the hydrogen concentration in the bulk of the gas. An Arrhenius plot in Figure 8(b) of the values of $\mathbb{D}_e$ listed in Table 4 gives an activation energy of 179 kJ/mol. This value is much higher than about 75-125 kJ/mol obtained for oxygen diffusion in metal oxides (Aronson et al., 1957). However a very high activation energy of 280 kJ/mol was also reported for CO diffusing through the reduced product layer of $FeTiO_3$ (El-Guindy and Davenport, 1970).

Surface area measurements were made on a sample before and after reduction at 700°C by N_2 adsorption with a Flowsorb II 2300 of Micromeritics. The specific surfaces of 0.95 and 0.70 m^2/g respectively (one point B.E.T. - surface aera), are close to that of the external surface of particles with the size of 2-3 μm. SEM pictures of particles showed that particle size is realy about 2-3 μm and there is no significant difference before and after reduction (see Figure 9). This indicates that reduction did not lead to particle disintegration or formation of a more porous product. This behavior is consistent with the small difference in molar density between Na_2SO_4 and Na_2S of respectively 5.40 and 4.20 cm^3/mol. Therefore it appears that after formation of an uninterrupted outer layer of sodium sulfide, the transport of hydrogen through the Na_2S lattice becomes rate-determining.

A comparison between the experimental results and the predictions with

(a) Sample before Reduction

(b) Partly reduced sample, X=35%

(c) Completely reduced sample

Figure 9 SEM pictures of the samples before and after reduction ($T=700°C$, $[H_2]=50\%$, $[H_2O]=0$)

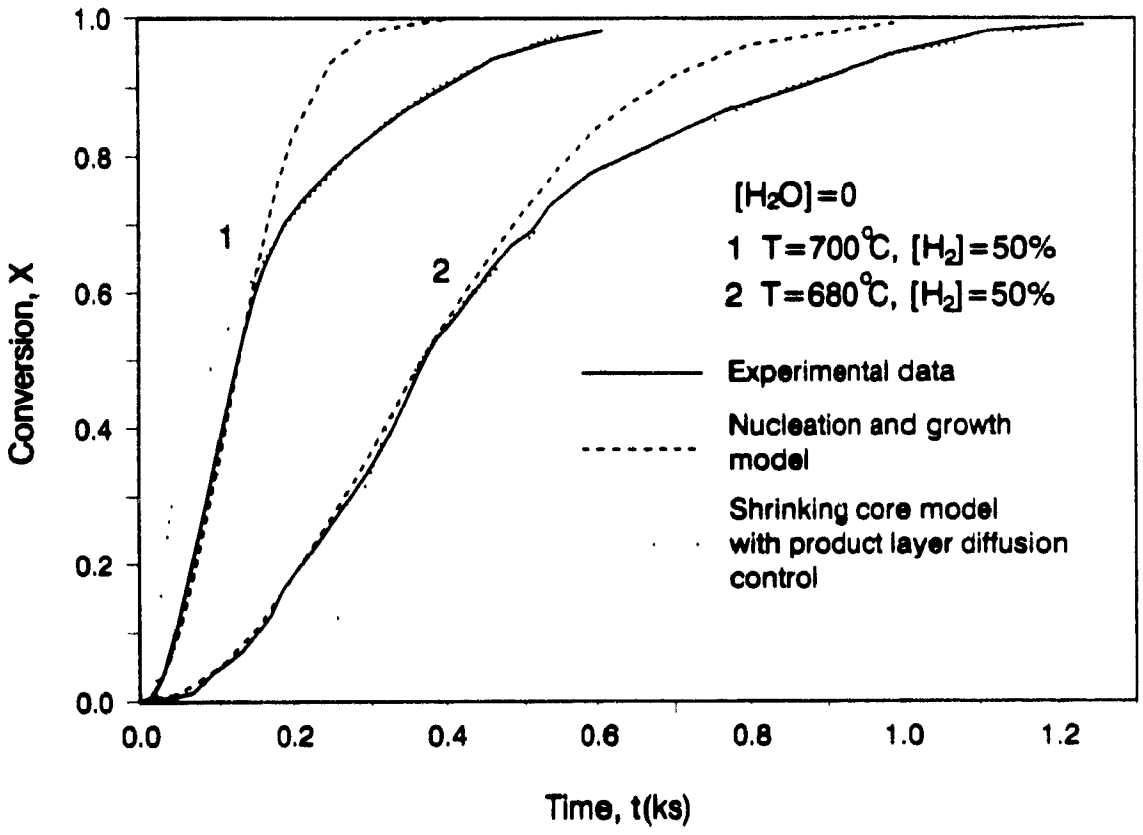

Figure 10 Comparison of model predictions and experimental data

the two models is shown in Figure 10. From this figure it can seen that reduction in the deceleratory period slows down more than expected from the nucleation and growth model. However when the rate determining step is changed from nucleation and growth to product layer diffusion, the reduction is well described at high conversions.

Influence of sodium sulfide

In order to confirm that the reduction starts with the formation of Na_2S nuclei, some Na_2S was added to the model mixture. A powder of $Na_2S{\cdot}9H_2O$ was dried at 500°C in N_2, ground (d_p<200 μm), and then mechanically mixed with the mixture of sodium sulfate and sodium titanate at a molar ratio Na_2S/Na_2SO_4 of 0.5. The time for total conversion is reduced by the addition of Na_2S as shown in Figure 11(a). A plot of $[-\ln(1-X)]^{1/2}$ versus time in Figure 11(b) shows that the data are still reasonably represented by the nucleation and growth model. The increase in the slope k_1 in Figure 11(b) suggests that the nuclei concentration, n_o, is increased, since it is unlikely that the intrinsic constant, k_4, in Eq.(4) is affected by surface contact with the Na_2S particles.

The same phenomenon was observed for the reduction of metal oxides such as NiO, Fe_2O_3 and $FeTiO_3$ (Lin, 1987; Zhao and Shadman, 1990). Nucleation and growth kinetics were also observed for these reductions, and addition of the metal product significantly shortened the total reduction time. Thus, in a practical reduction process, some recycling or back mixing of the product Na_2S would be advantageous, and a fluidized bed will be one of the preferred reactors for Na_2SO_4 reduction.

Influence of hydrogen concentration

The influence of the hydrogen concentration on the rate constant k_1 of the nucleation and growth model [Eq.(4)] is shown in Figure 12(a). The slope a, the reaction order in H_2 concentration in Eq.(4), is also listed in Table 4. The average value of the reaction order over the temperature range 650-700°C is about 0.70, indicating that the hydrogen concentration has a strong influence on reduction in the acceleratory period. The order of 0.70 and the relatively poor correlation of the data in Figure 12(a) suggest a complex reaction mechanism.

The mechanism proposed by Birk et al. (1971) for Na_2SO_4 reduction in the molten phase is

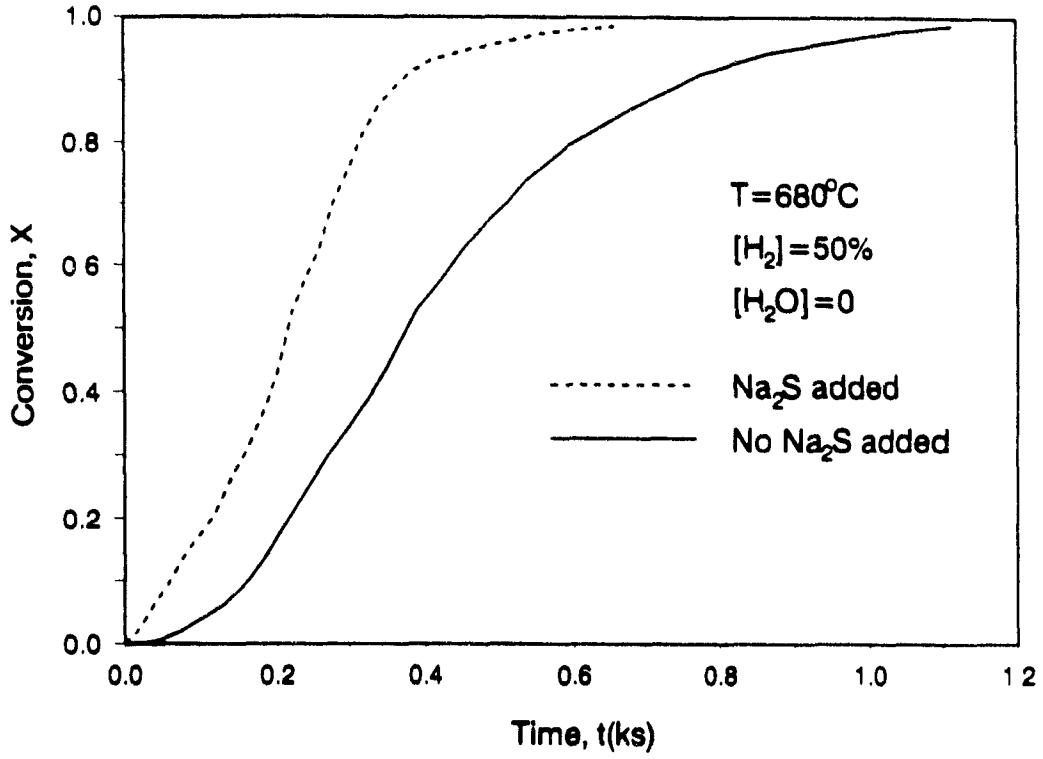

(a) Conversion, X, versus t

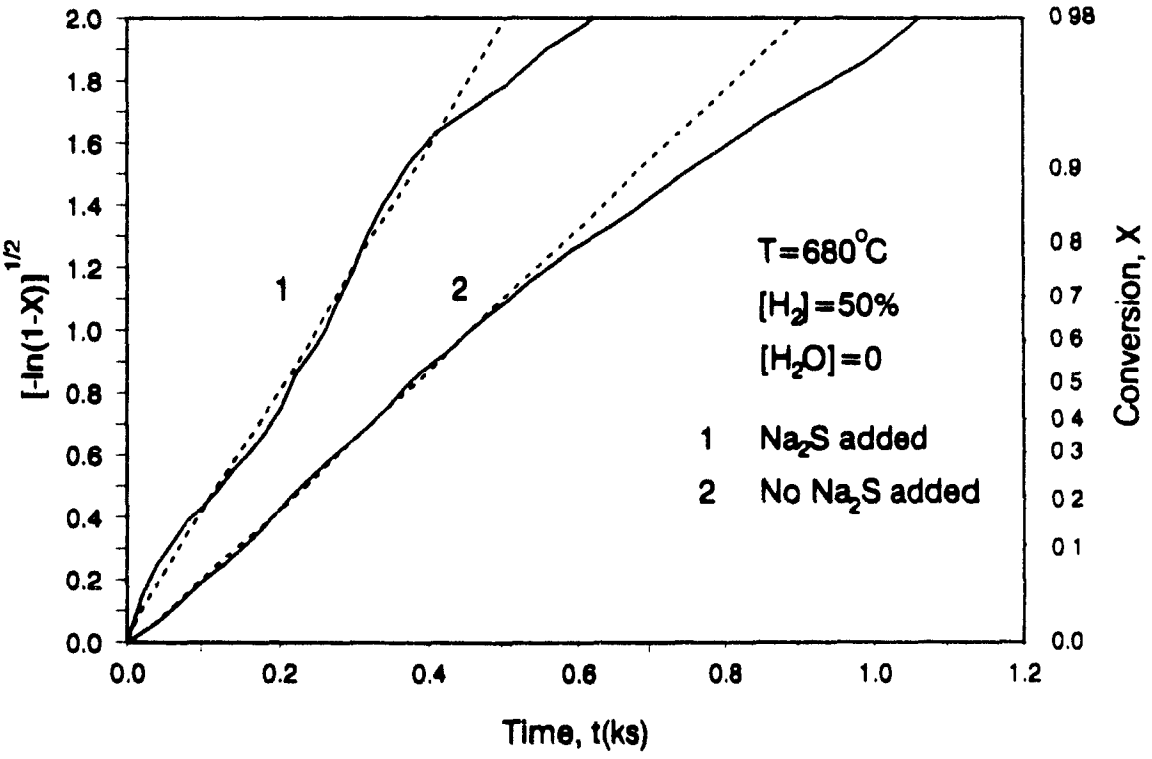

(b) $[-\ln(1-X)]^{1/2}$ versus t

Figure 11 Influence of Na_2S addition on reduction

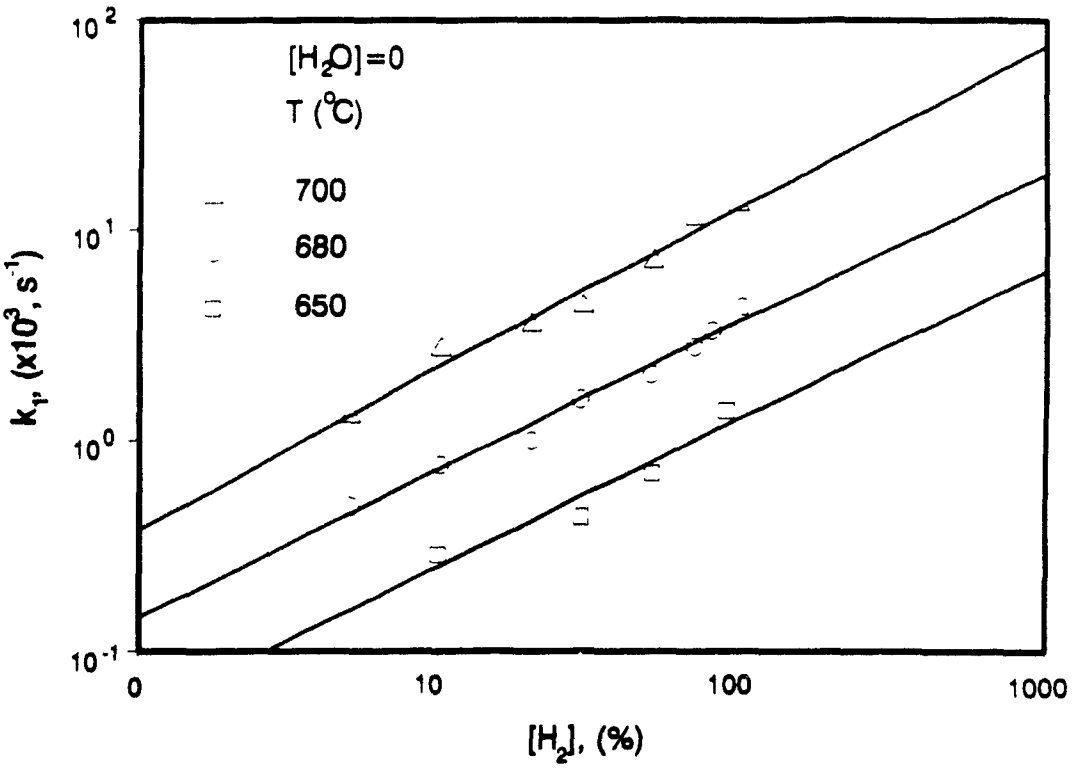

Figure 12(a) Influence of H_2 concentration on k_1

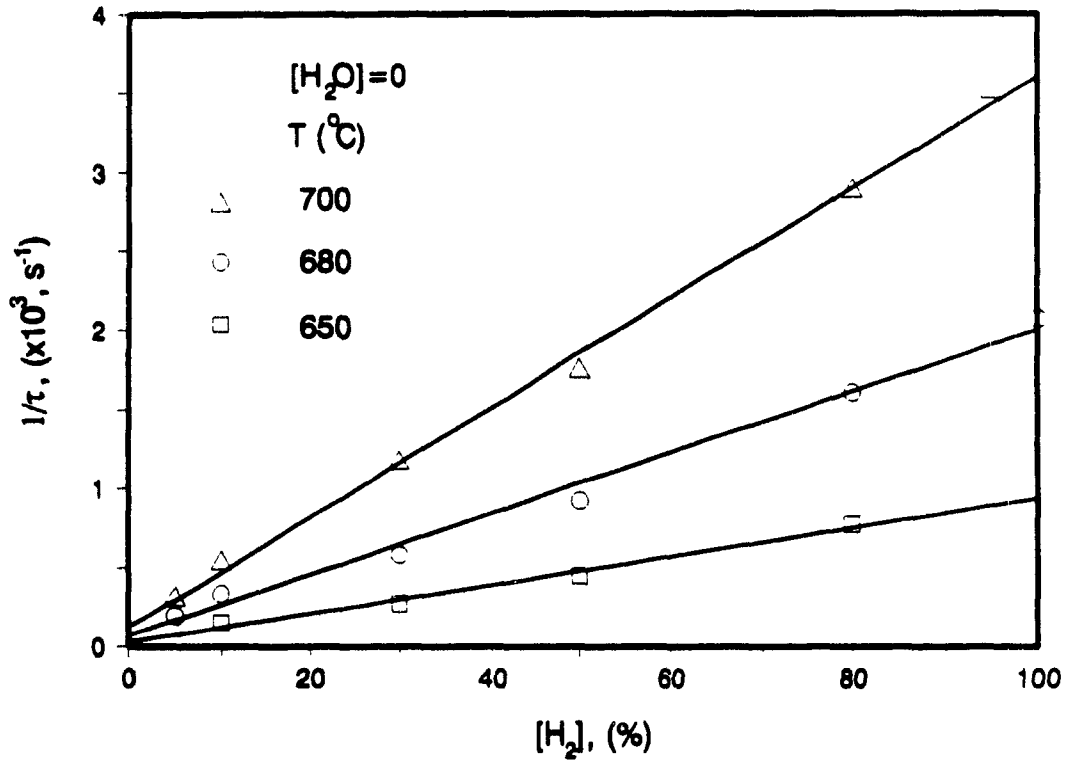

Figure 12 (b) Influence of H_2 concentration on τ

$$Na_2SO_4 + Na_2S = \text{Intermediates} \quad (17)$$

and $$\text{Intermediates} + H_2 = Na_2S + H_2O \quad (18)$$

This mechanism could explain the autocatalytic effect of Na_2S for homogeneous reduction. In the previous section it was shown that surface contact with Na_2S particles led to an increased reduction rate of Na_2SO_4. Therefore reactions (17) and (18) may also applicable to the present heterogeneous system where the intermediates formed by the solid-solid reaction between Na_2SO_4 and Na_2S are subsequently reduced by hydrogen to Na_2S. Also if reactions (17) and (18) are both rate controlling step, a reaction order in the H_2 concentration of less than 1.0 is obtained. The solid-solid reaction (17) would also be consistent with the high activation energy found for the present system. This kind of catalytically active product nuclei has been referred to as functional nuclei (Galwey 1980), and has been found to apply to the decomposition of copper formate (Galwey et al., 1974) and nickel formate (Brown et al., 1978).

Compared to published results, the reaction order in hydrogen concentration in the present case is very close to that found in many other hydrogen reduction studies. An order of 0.5 to 1.0 was found for hydrogen reduction of Fe_2O_3, UO_3, NiO and $CuSO_4$ (El-Rahaiby and Rao, 1979; Le Page and Fane, 1974; Delmon and Roman, 1973; Dhupe et al., 1987). For hydrogen reduction of Na_2SO_4 in the molten phase, Birk et al. (1972) found an order of 2/3.

The influence of hydrogen concentration on the inverse of the time for complete reduction, $1/\tau$, obtained from the diffusion limited period, is shown in Figure 12(b). The finding that $1/\tau$ is essentially proportional to the hydrogen concentration is in agreement with Eq.(16), thus confirming that diffusion of hydrogen through the product layer is the rate limiting step.

Influence of steam concentration

With increasing H_2O content of the reduction gas, a longer time was needed for nucleation as shown in Figure 13(a). The influence of steam content on k_1 and D_e, characteristic parameters for respectively the nucleation and growth, and diffusion controlled regimes, are displayed in Figure 13(b). These results show that although the nucleation is retarded by the presence of steam, subsequent growth of the nuclei as well as diffusion through the product layer is not appreciably affected.

According to Eq.(4), k_1 should not be affected by the steam concentration

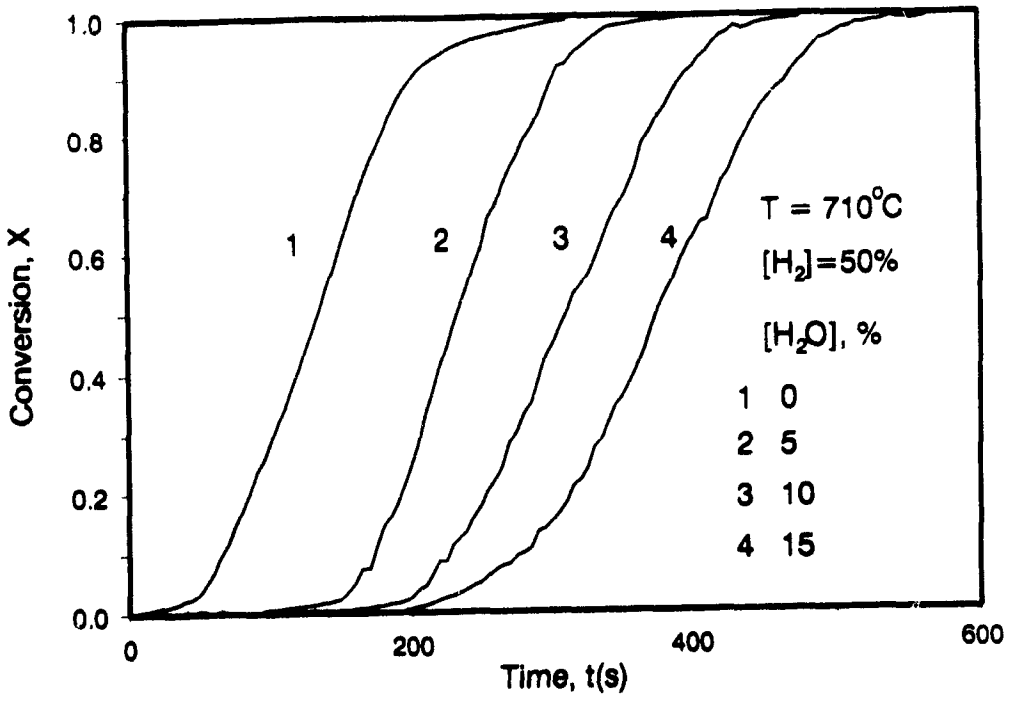

Figure 13(a) Influence of steam concentration on reduction

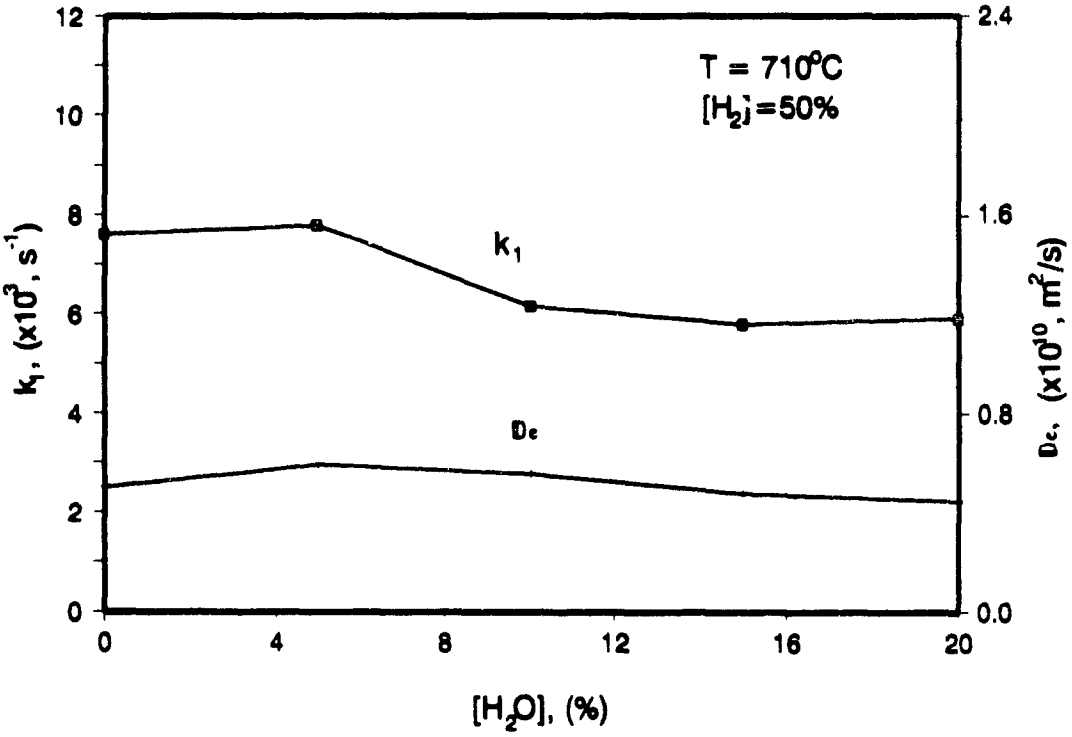

Figure 13(b) Influence of steam concentration on k_1 and $\mathbb{D}_e$

since the equilibrium constant of reaction (8) is very large (K_e=1.1x10^6). The small decrease in k_1 with increasing steam concentration might then be interpreted as a reduction of the number of active reaction sites, n_o in Eq.(4) by adsorption of steam on potential nucleation sites (Mckewan,1964). A similar explanation was given more recently by Hayes (1979 and 1981) for the increase in the rate of the hydrogen reduction of wustite with increasing steam pressure.

Concerning the nuclei formation reaction, it might be that Na_2S is formed by the following reactions:

$$Na_2SO_4 + H_2 = Na_2SO_3 + H_2O \quad (19)$$

$$Na_2SO_3 + 3\ H_2 = Na_2S + 3\ H_2O \quad (20)$$

and

$$4\ Na_2SO_3 = Na_2S + 3\ Na_2SO_4 \quad (21)$$

The formation of Na_2SO_3 as a first step is likely because Na_2SO_3 was identified by FTIR during the initial reaction stage in a recent study (Weston, 1986). The subsequent reduction of sodium sulfite by hydrogen is much easier than the sodium sulfate reduction as can be seen in Figure 14. Thermal decomposition of sodium sulfite via reaction (21) may also be important for the formation of Na_2S as was recently shown by Li (1989). However the nuclei formation can not only be explained by reaction (19) because the equilibrium constant is 0.08 at 710°C, which means that reaction (19) is thermodynamically impossible above 4% steam in 50% hydrogen. In this case the initiation must proceed according to reaction (8), which is kinetically very difficult. Thus nuclei formation in the presence of steam is very slow and full nuclei growth is delayed.

When sodium sulfide particles were added, the effect of steam on the induction time was eliminated without significantly affecting the reduction rate as can be seen in Figure 15. This lends further support to the model that the nuclei consist of Na_2S and their formation is strongly influenced by steam. The insensitivity of k_1 to the presence of steam with Na_2S addition also supports reaction (17) as the nuclei growth reaction because it involves only solids as reactants.

Influence of sodium titanate and titanium dioxide

The influence of sodium titanate on the sodium sulfate reduction was

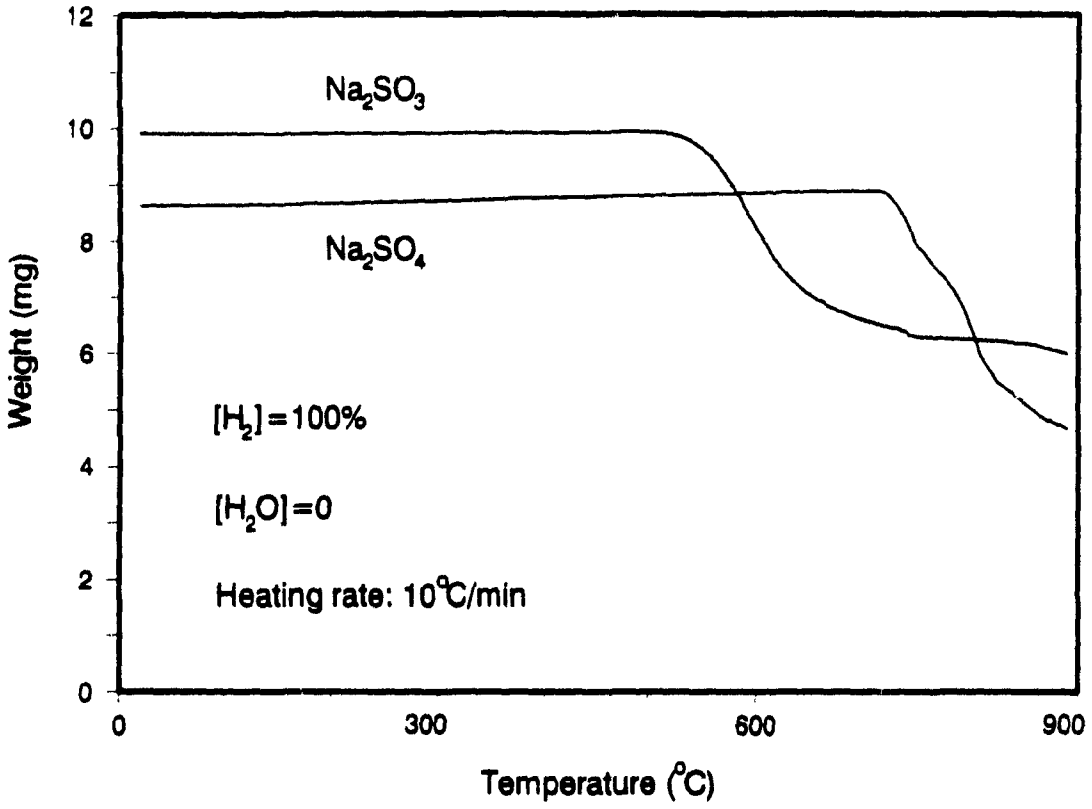

Figure 14 Comparison of reduction of pure Na_2SO_4 with Na_2SO_3

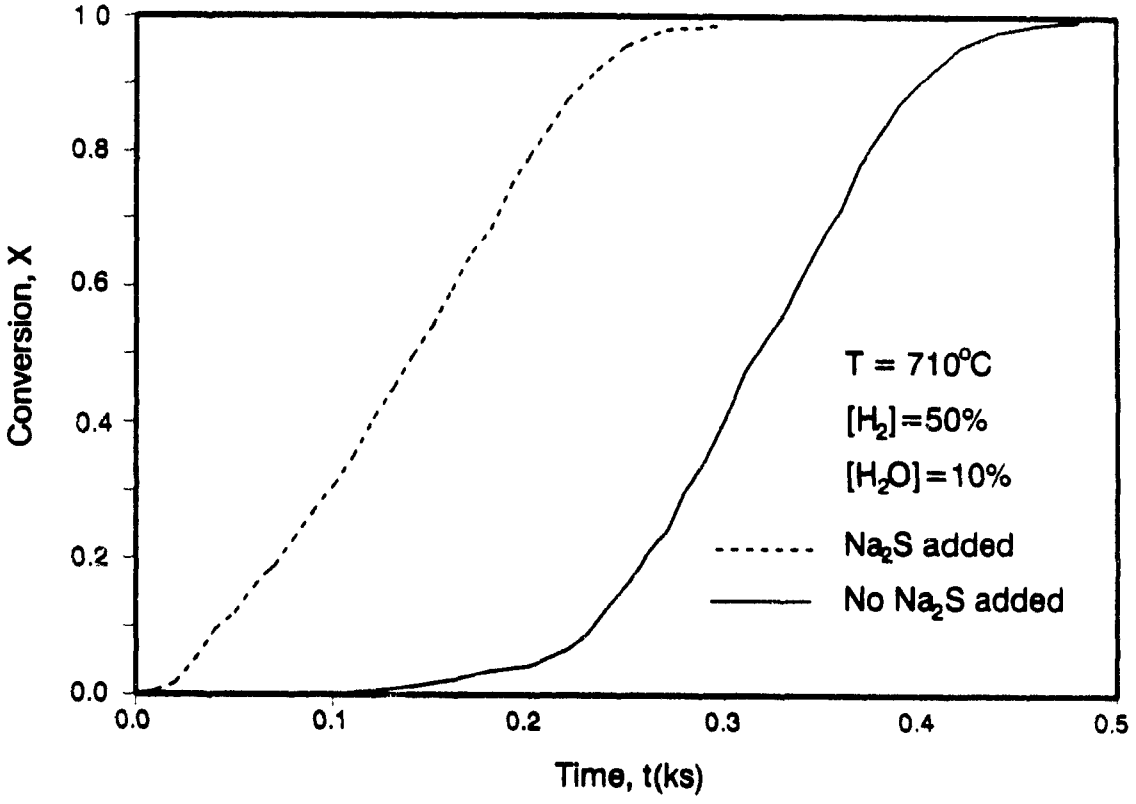

Figure 15 Influence of Na_2S addition on reduction in the presence of steam

studied by changing the molar fraction of sodium titanate, Y, in the model component mixture. The conversion time curves in Figure 16 show that the time for complete reduction time increases dramatically with decreasing Y, and that the reduction is incomplete when Y is smaller than 0.05. With pure Na_2SO_4 the final reduction is only about 20% after 3000 s.

It is interesting that the initial reduction of pure sodium sulfate proceeds at a reasonable rate but that subsequent further reaction is very slow. The characteristic reaction parameters in Figure 17 show that the influence of Y on De is much stronger than that on k_1. This suggests that in these cases a product layer is formed with a very low permeability for hydrogen which limits the reaction kinetics. As the thickness of Na_2S layer increases, the diffusion flux is progressively reduced, and complete reduction is only obtained after a very long reaction time. The same phenomenon has been observed for reduction of other compounds such as iron oxide (Szekely et al., 1976). The faster reduction with a higher molar fraction of sodium titanate can be explained by a more open structure of the product layer. This is also suggested by comparison of SEM pictures of the reduced samples in Figure 18, which show that the samples with sodium titanate (Y>0.25) are still powdered while the reduced sample of pure sodium sulfate reduction sample is sintered. Sintering of the sodium sulfide layer will lead to a dramatic decrease in the diffusion rate, while the porous structure will be retained up to complete sulfate reduction with a large fraction of high melting sodium titanate in the particles.

An interesting finding is that the reduction of a mixture of particles of pure Na_2SO_4 and pure sodium titanate (Y=0.75) is only slightly improved compared to that of pure sodium sulfate as shown in Figure 19(a). This confirms that major effect of sodium titanate is to improve the diffusion of hydrogen towards the reaction interface.

Metal oxides such as Fe_2O_3, NiO, CuO, and TiO_2 were previously reported to be reduction catalysts. This was tested for the present system by mixing 3% (by weight) TiO_2 with particles of sodium sulfate. The results in Figure 19(b), show that only a small improvement in reduction rate with TiO_2 addition especially when compared to the catalytic activity of 1.5% of Fe_2O_3, as will be shown later. The possible explanation for this is that good reduction catalysts are normally compounds which can be reduced themselves while TiO_2 is inert in H_2 at the present low temperatures.

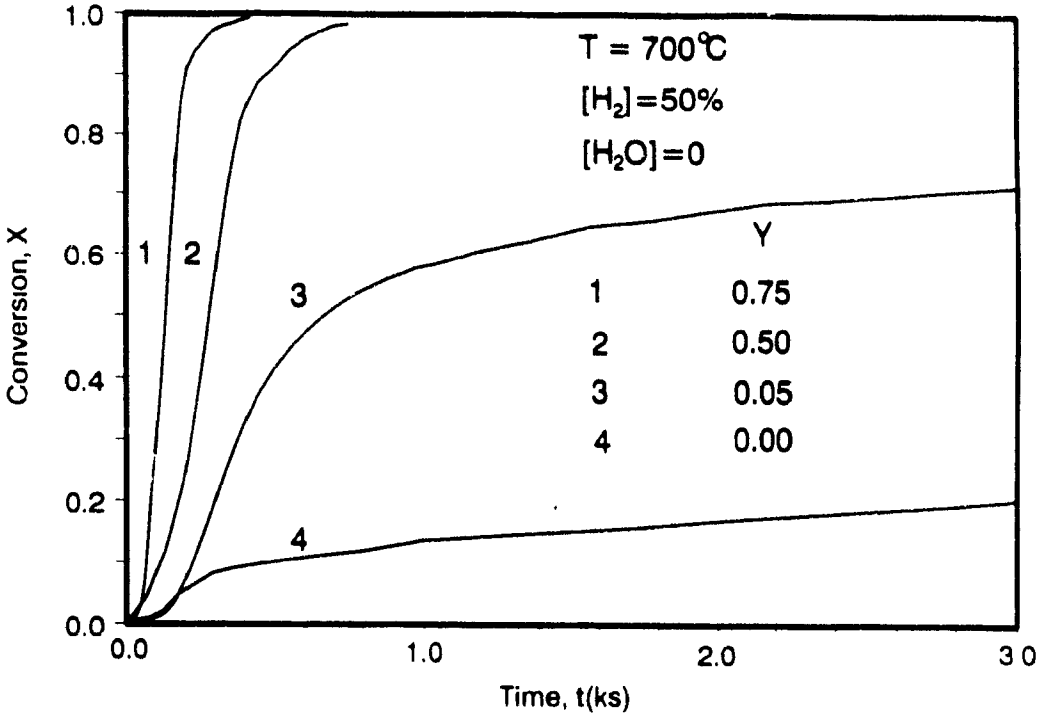

Figure 16 Influence of sodium titanate molar fraction, Y, on the conversion of Na_2SO_4

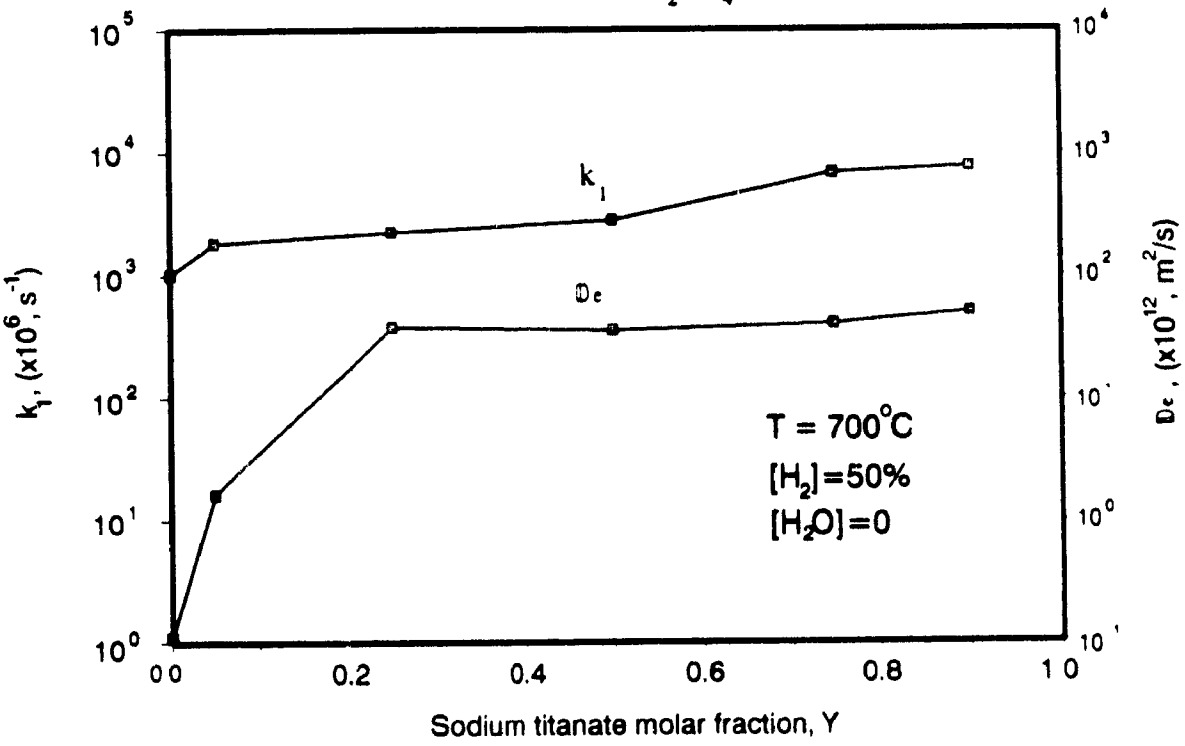

Figure 17 Influence of sodium titanate molar fraction, Y, on the rate constant, k_1, and effective coefficient, D_e.

(a) Pure sodium sulfate before reduction

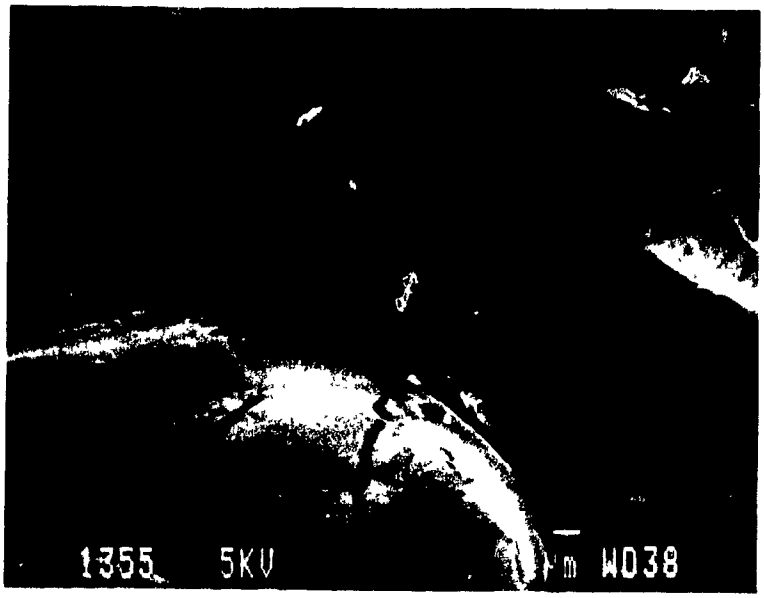

(b) sodium sulfate after reduced at 700°C for 5 minutes

Figure 18 SEM picture of pure sodium sulfate before and after reduction

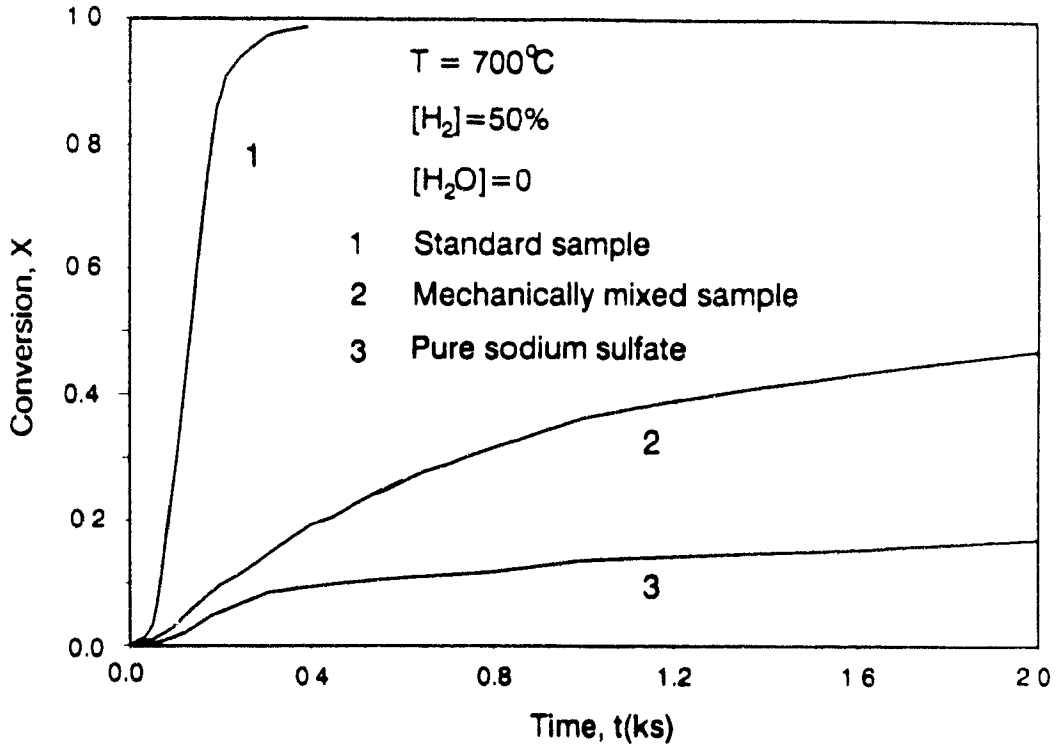

Figure 19(a) Influence of mixing on reduction

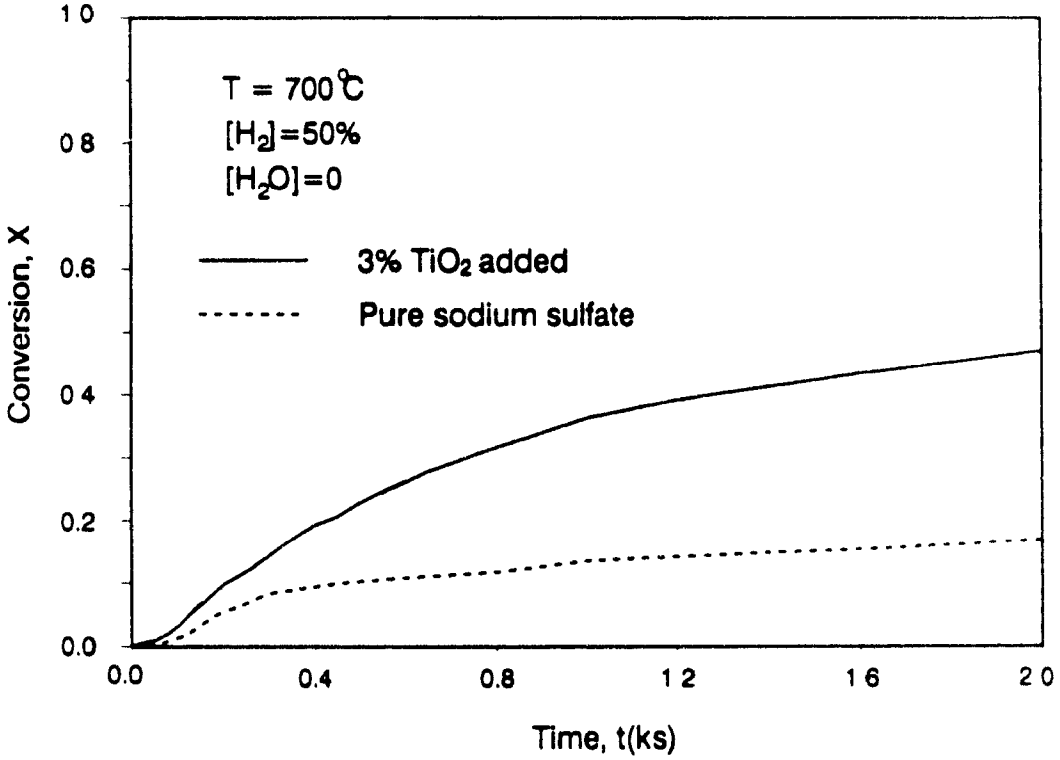

Figure 19(b) Influence of TiO_2 on reduction

Influence of iron oxide catalyst

Since iron oxide was reported to be the best catalyst for reduction of sodium sulfate, 1.5% by weight of iron oxide (d_p <25 μm) was ground with the standard mixture of Na_2SO_4 and $Na_2O{\cdot}TiO_2$ (i.e. 1:3 molar ratio). The results in Figure 20 show that the reduction with 1.5% iron oxide is about 10 times faster than obtained with the model mixture with 1.5% iron oxide, and only about two minutes are needed for 90% reduction at 680°C. The catalytic influence becomes significant at 660°C or higher as shown in Figure 21(a). It should be noted that the initial reduction of Na_2SO_4 with iron oxide is a slow process and that the length of the induction period is significantly reduced with increasing temperature. The reduction data are well fitted by the nucleation and growth model [Eq.(3)] with t replaced by $(t-t_i)$ over the conversion range of 0.2-0.85 as shown in Figure 21(b). The activation energy determined from the Arrhenius plot in Figure 21(c) of the reaction constant k_1 at the three temperatures of 660, 680, and 700°C is 239 kJ/mol. It must be pointed out however that the external mass-transfer resistance is significant for all three temperatures and thus the activation energy is a combination of kinetic and mass transfer effects. This might explain why the activation energy with Fe_2O_3 (239 kJ/mol) is lower than that without Fe_2O_3 (302 kJ/mol). The large difference in the reduction rates at 640°C and 660°C may be due to the difficulty of reducing iron oxide or its catalytic intermediate at 640°C.

The catalytic activity of iron oxide for reduction by H_2 was recognized by previous investigators. However its catalytic mechanism is not fully understood. Based on previous studies, there are at least two major mechanisms identified by which iron could catalyze the reduction: (i) reduced iron oxide can act as a heterogeneous (surface) catalyst; and ii) reduced iron can directly reduce sulfate or its reactive intermediate. The former mechanism was generally found for the reduction of metal oxides and other catalytic gas-solid reactions. The catalytic mechanism was explained by the easier formation of product nuclei because of the ability of these metals to activate hydrogen (Verhoeven and Delmon, 1966; Delmon, 1968). However this mechanism is unlikely for the present system because sulfide, is usually a very severe poison for surface catalysis.

The second type of mechanism could involve iron sulfide which is easily formed by the reaction of Fe_2O_3 with Na_2S or H_2S as found in Chapter 3. FeS thus reacts with Na_2SO_4 to form an intermediate, possibly $FeSO_4$, i.e.

$$FeS + Na_2SO_4 = Na_2S + FeSO_4 \qquad (22)$$

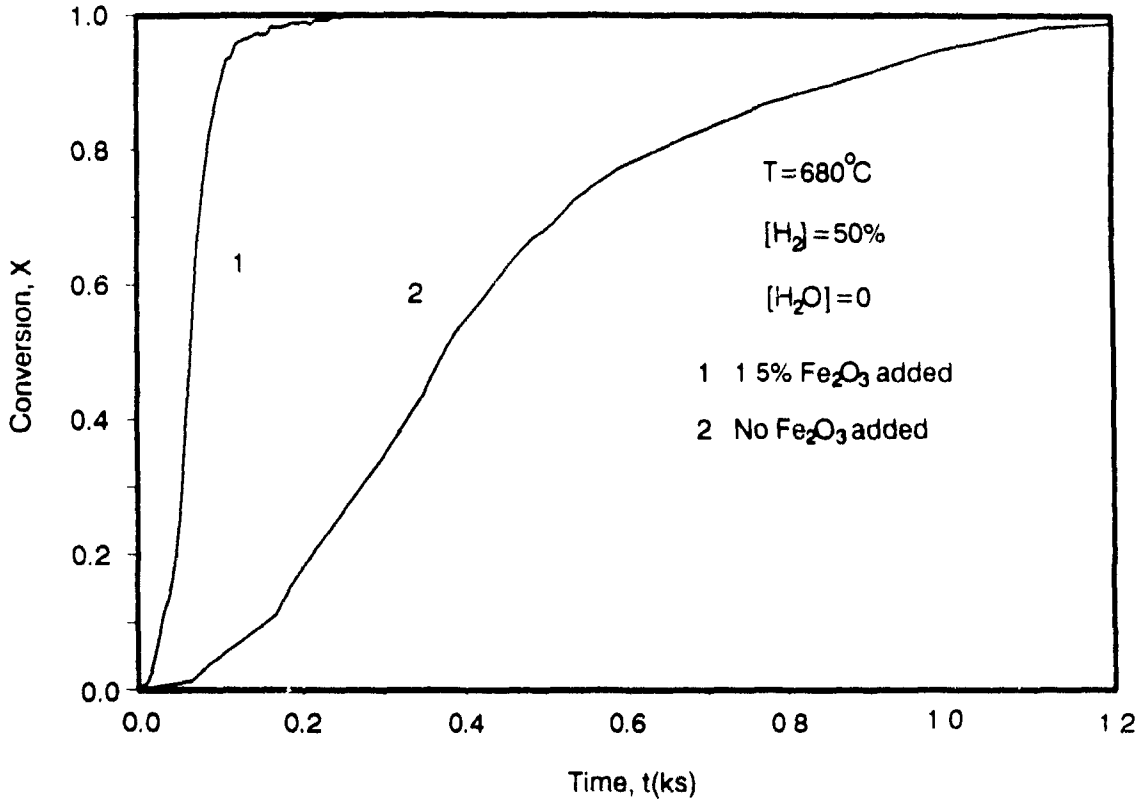

Figure 20 Influence of iron oxide on reduction

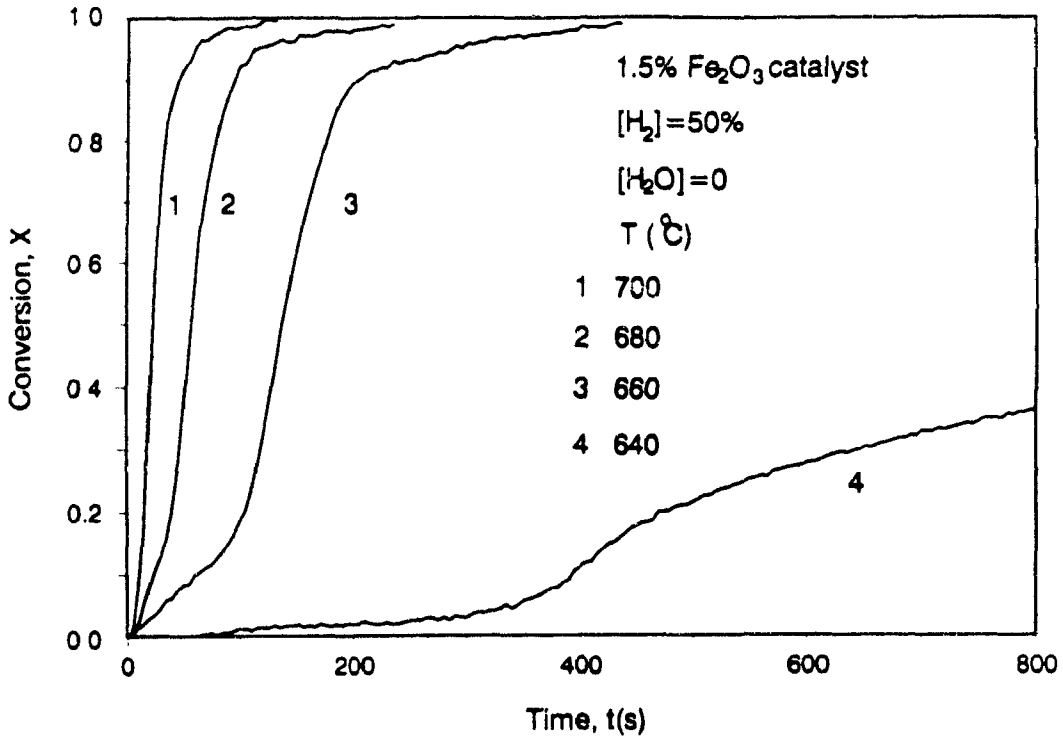

(a) X versus t

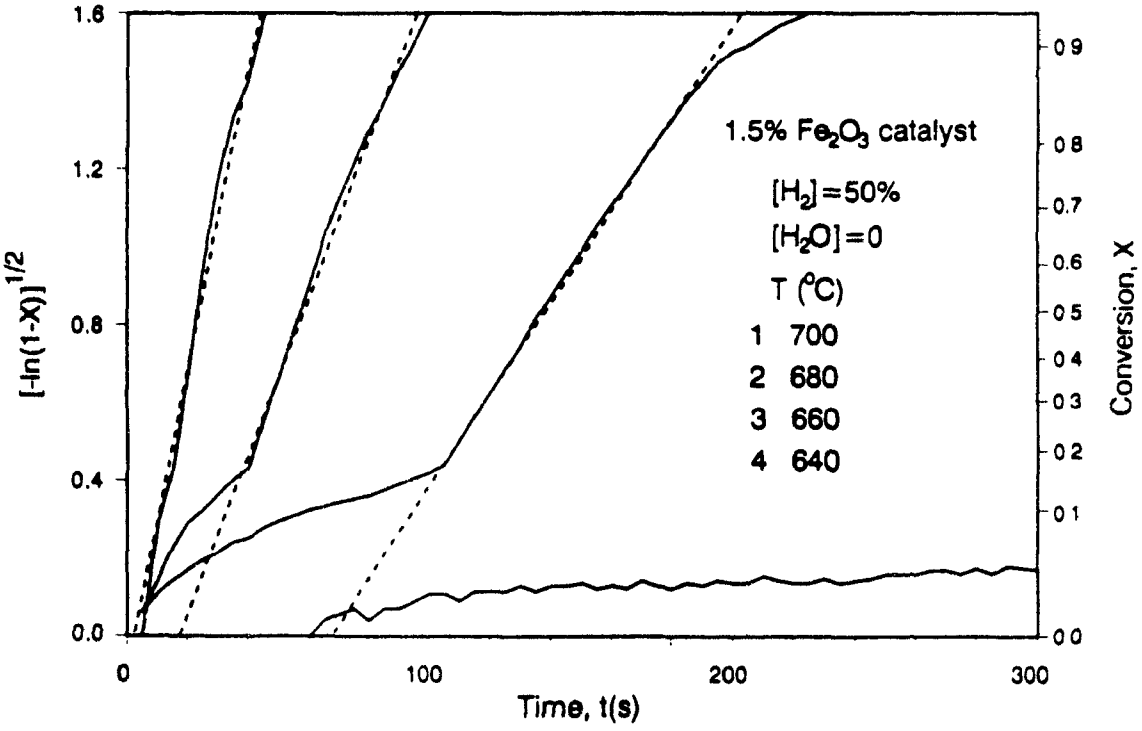

(b) $[-\ln(1-X)]^{1/2}$ versus t

Figure 21 Influence of iron oxide on reduction

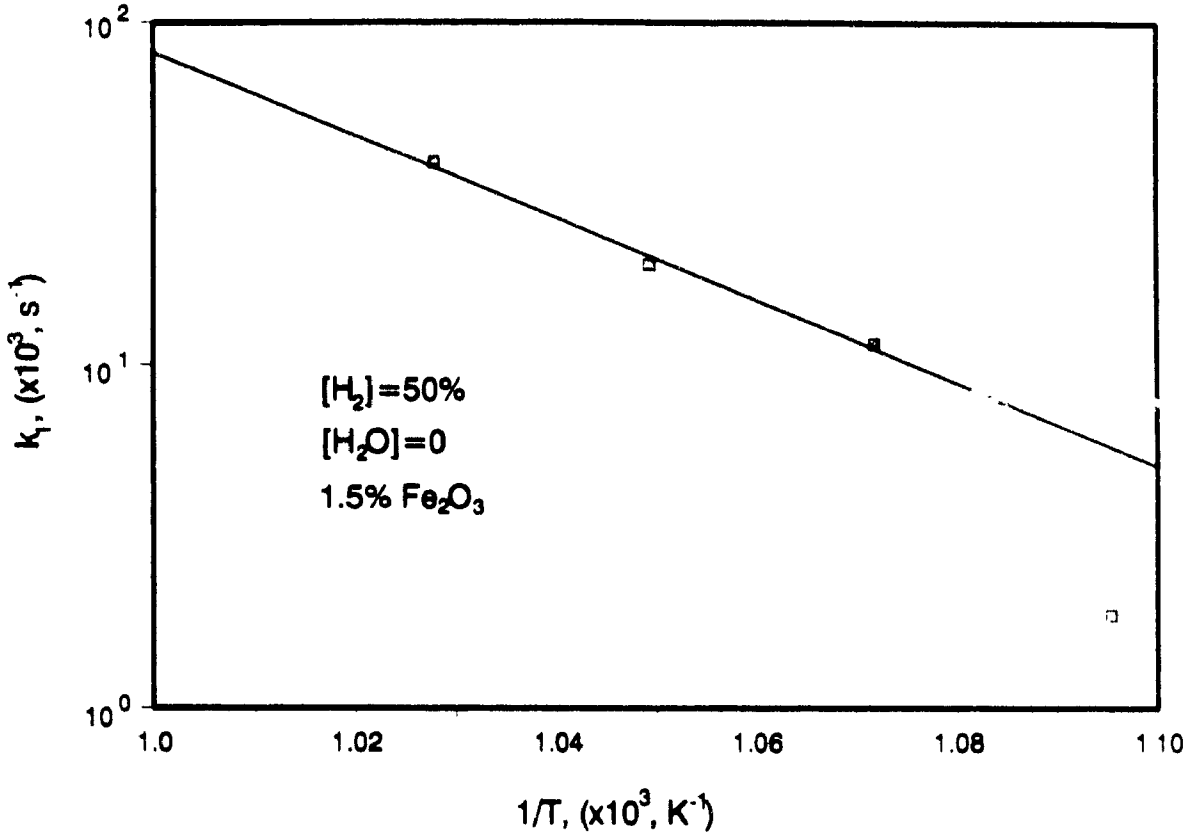

Figure 21(c) Arrhenius plot of reduction rate constants

Since $FeSO_4$ is not stable at high temperature and can easily be reduced to FeS, Reaction (22) would be followed by:

$$FeSO_4 + H_2 = FeS + H_2O \qquad (23)$$

This oxidation-reduction mechanism is supported by the evidence that FeS, $FeSO_4$ and other metal sulfur species are also good or even better catalysts than Fe_2O_3 for H_2 reduction of Na_2SO_4. The initial slow period with iron oxide could also be explained by the initial formation of FeS from iron oxide.

Since in practice, industrially produced TiO_2 will always contain some Fe_2O_3, the industrial reduction might actually benefit from the use of slightly impure TiO_2 as direct causticizing chemical.

Part II Reduction of Combusted Kraft Black Liquor

The combustion product of kraft black liquor with TiO_2 is mostly sodium titanate and sodium sulfate. However, industrial kraft black liquor contains some potassium and chlorine, and small amount of metals such as Al, Si and Fe. Moreover, its combustion product has probably a different morphological structure than that obtained by heating a model mixture of sodium carbonate, titanium dioxide and sodium sulfate. Thus it is expected that the reduction of the combustion product of kraft black liquor with TiO_2 will be different from that of the model mixture.

The reduction experiments of the kraft black liquor combustion product (Sample 1, see **Experimental** section) were performed in the temperature range of 630-720°C. Some typical sigmoid X-t data are shown in Figure 22 (a), which are very similar to those obtained with model mixtures of sodium titanate and sodium sulfate (Figure 4). Therefore the were replotted according to Eq.(3) in Figure 22(b). It shows that the data are well described up to 60-80% conversion by the nucleation and growth model. A very small induction period is found for the combustion product of kraft black liquor with TiO_2, compared to no induction time for the model mixture. The reaction constant, k_1, obtained from the slope of the straight lines, is plotted against reciprocal temperature in Figure 23. The activation energies of 283 and 276 kJ/mol for the nucleation and growth kinetics of respectively Sample 1 and Sample 2 are very close to that obtained earlier for the model mixture (302 kJ/mol), suggesting that the reaction mechanism is the same in all these cases. However, the absolute value of k_1 for Sample 1 is about one and half times

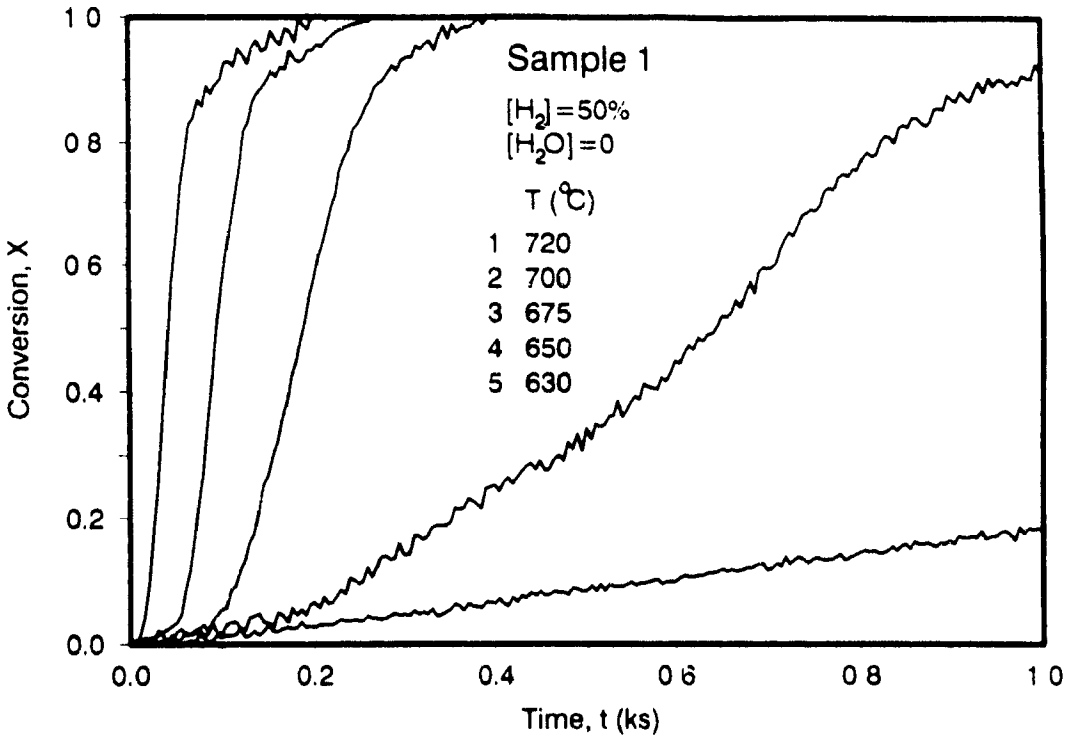

Figure 22(a) Reduction data of kraft black liquor mixed with TiO_2

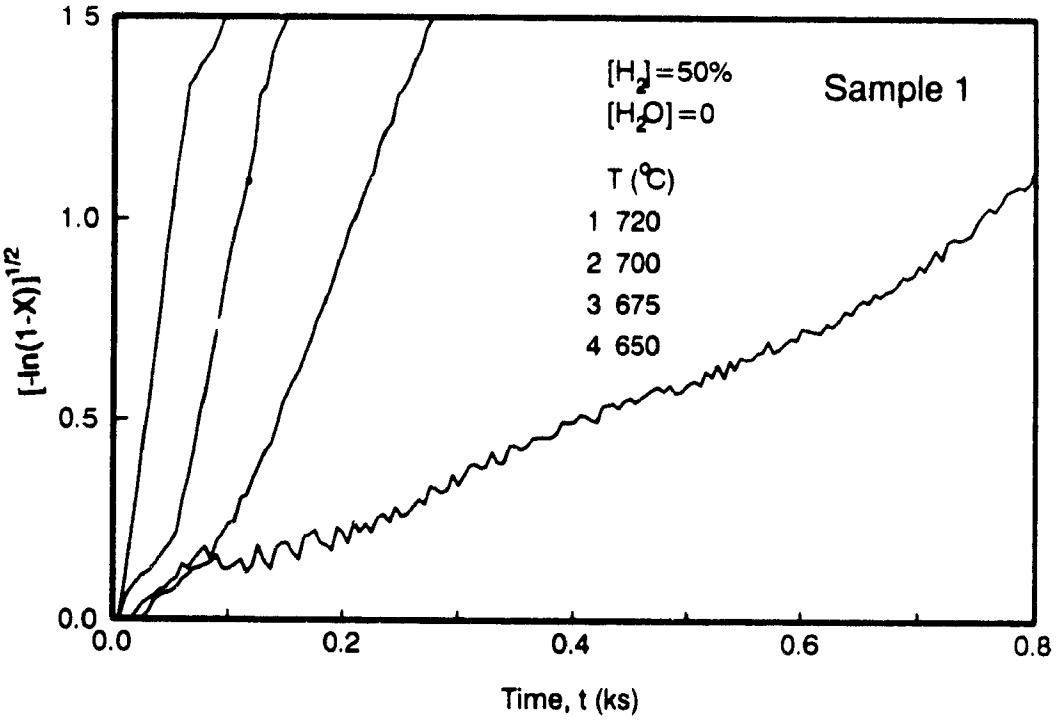

Figure 22(b) Fitting by nucleation and growth model

larger than that of Sample 2 at the same temperature. Compared with the model mixture, it is found that the reaction constant of sample 1 is about 3 times larger. There are three possible reasons which could explain the faster reduction of kraft black liquor. First, the black liquor combustion product contains a small amount of reduction catalysts such as Fe or other metals. The second reason might be that the distribution of Na_2SO_4 in sodium titanate is best in Sample 1, followed by Sample 2 and finally the model mixture. This is expected based on the preparation procedure for Samples 1 and 2, with TiO_2 burned with kraft black liquor in Sample 1 while Sample 2 is generated by heating TiO_2 and combusted kraft black liquor. The SEM-EDS mapping in Figure 24 shows a finer distribution of Na, S and Ti for Sample 1 compared to model mixture. Finally the surface area of combustion product of kraft black liquor (Sample 1) was found to be 4.21 m^2/g compared to 0.95 m^2/g for the model mixture. The higher surface area suggests a smaller effective particle size for the black liquor sample which might also explain the higher reduction rate.

Influence of hydrogen concentration

The influence of hydrogen concentration on the reduction of combusted kraft black liquor was analyzed in the same way as that of the model mixture. The influence of hydrogen concentration on the rate constant, k_1, is shown in Figure 25. It is found that k_1 is proportional to $[H_2]^{0.5}$. Thus the influence of the hydrogen concentration on the reduction of the kraft black liquor samples is somewhat smaller than that of model mixtures, for which an order in hydrogen concentration of 0.7 was obtained.

Influence of steam concentration

The influence of the steam concentration on the X-t curves for Sample 1 is shown in Figure 26. As can be seen, a longer initiation time was recorded for reduction with increasing steam concentration as shown in Figure 27(a). Furthermore it is also found that with increasing steam concentration, the nucleation and growth reaction rate constant decreases as shown in Figure 27(b). These results indicate that steam not only retards the formation of nuclei, but also decreases subsequent growth of the nuclei. This is different from the reduction of the model mixture, for which the steam concentration only affects the initiation time.

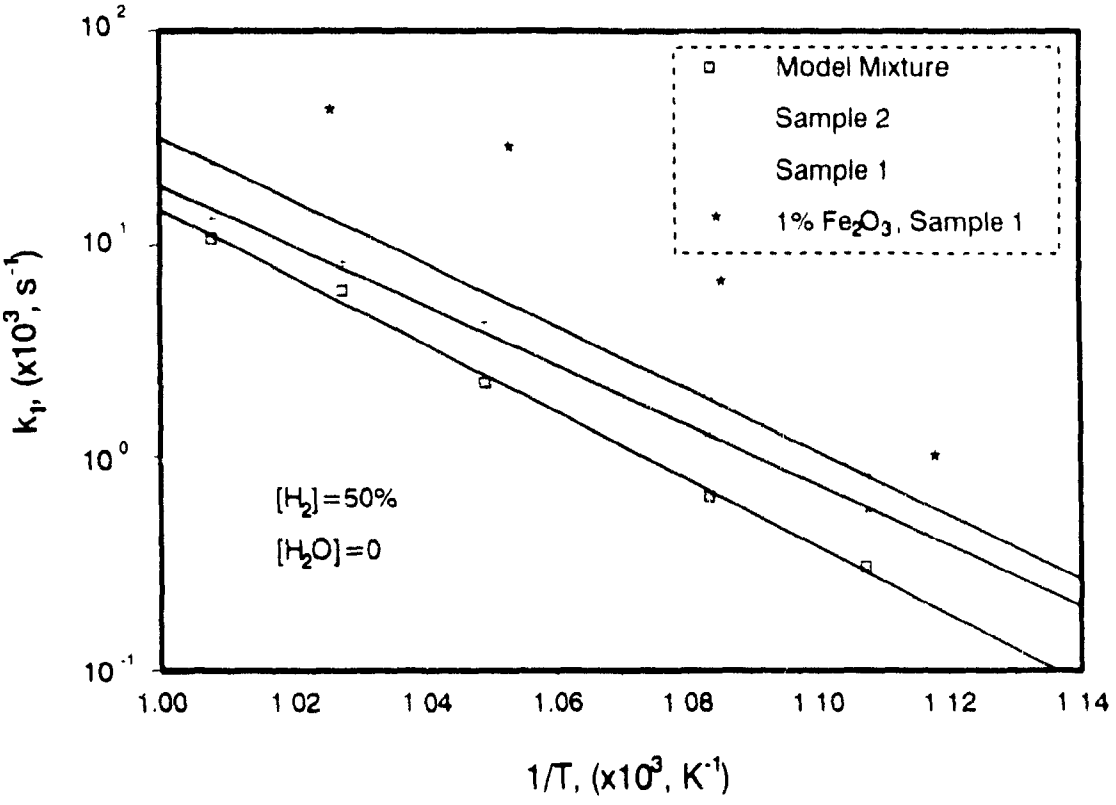

Figure 23 Arrhenius plot of reduction rate constants

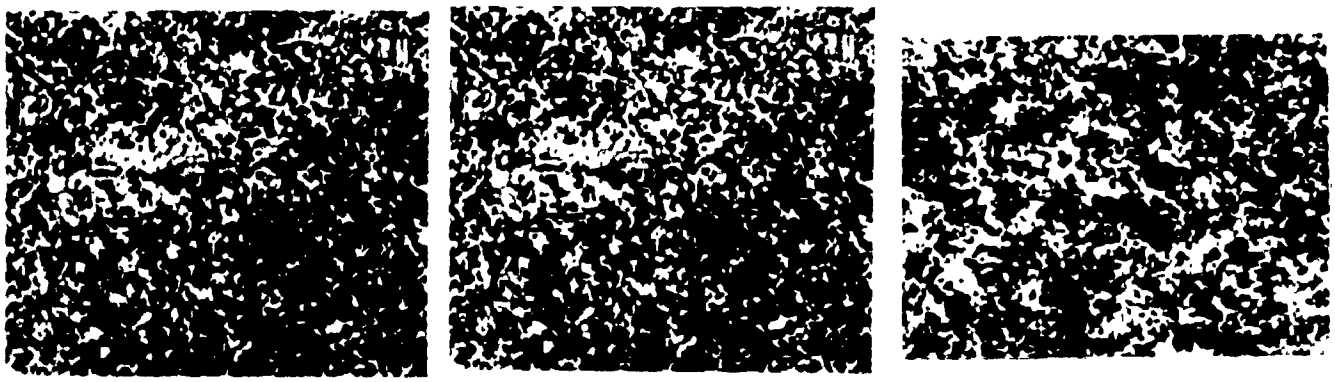

Na S Ti

(a) Kraft black liquor mixed with TiO_2 (Sample 1)

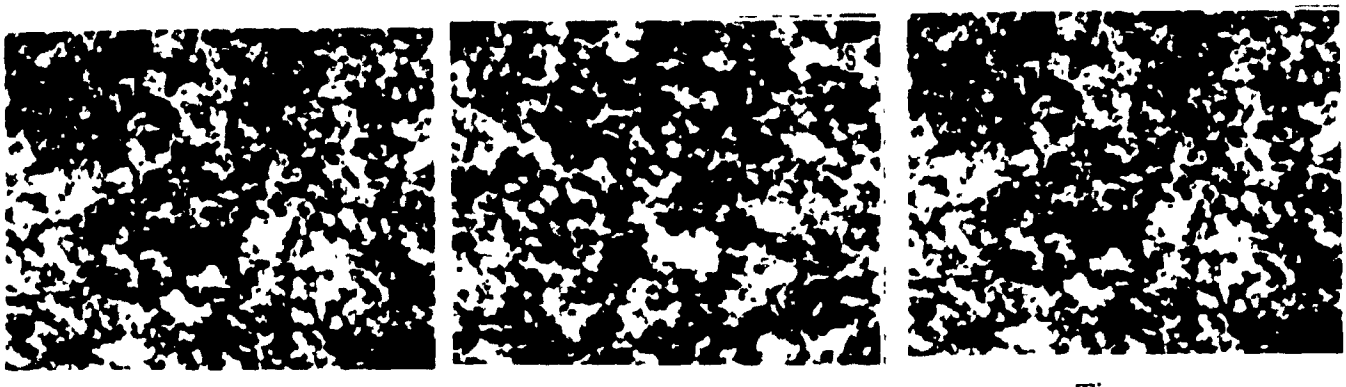

Na S Ti

(b) Model mixture

Figure 24 Elemental distribution from SEM-EDS mapping

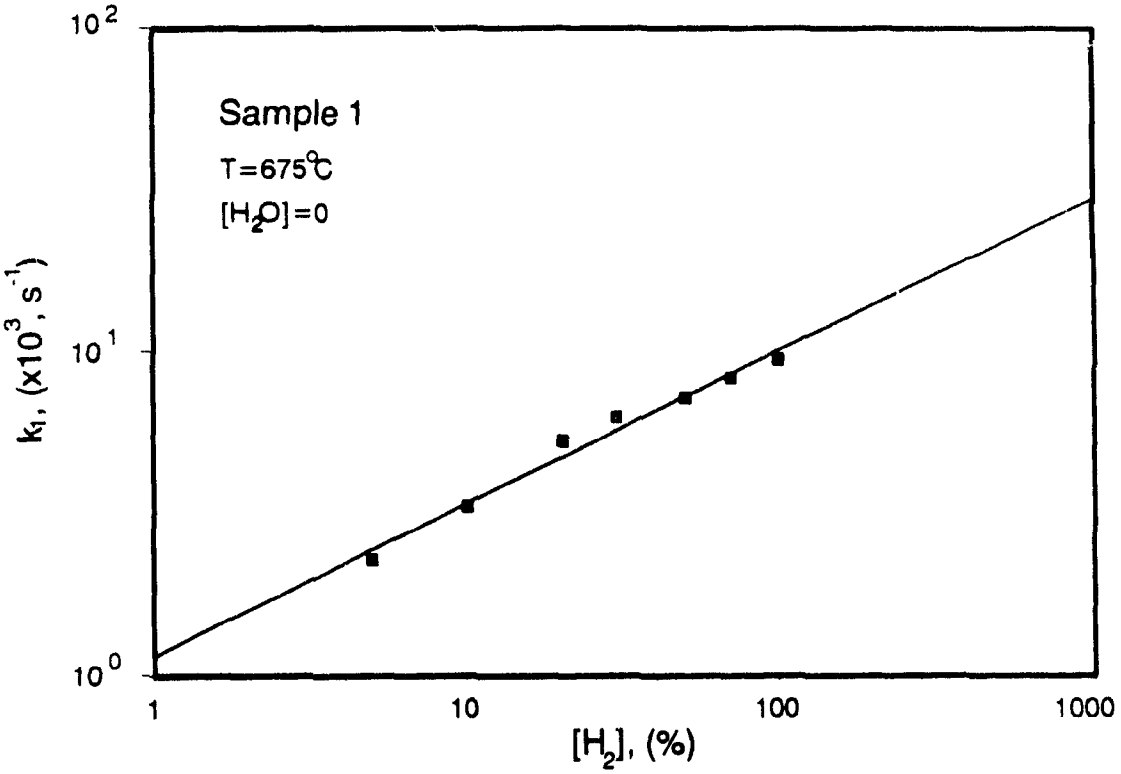

Figure 25 Influence of hydrogen concentration on k_1

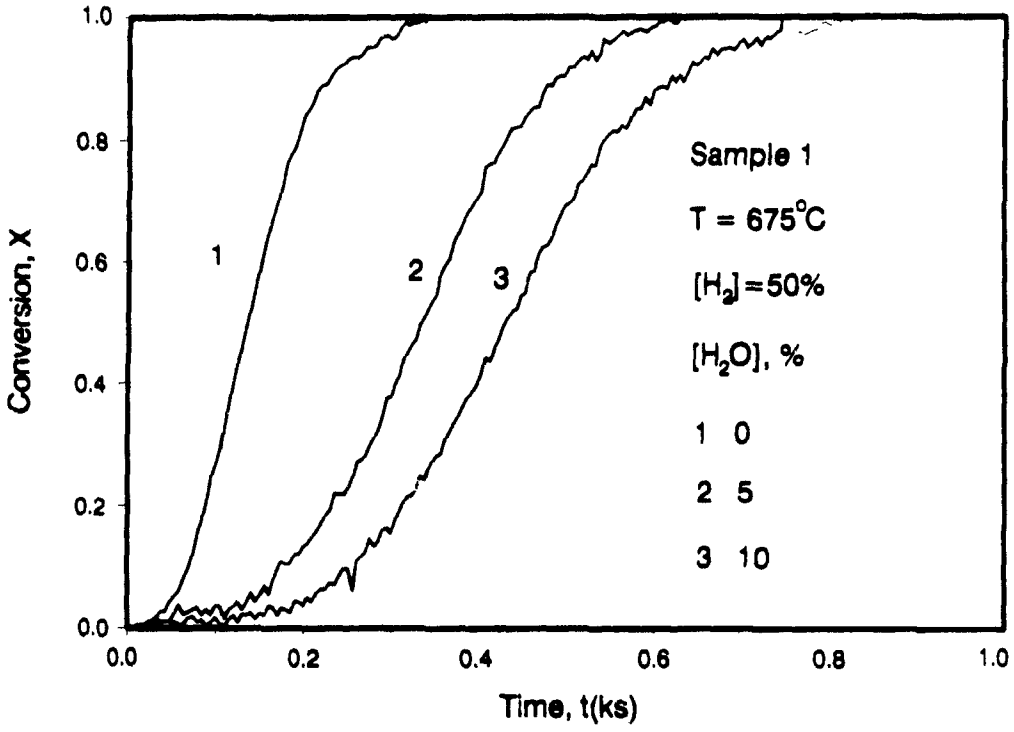

Figure 26 Influence of steam concentration on reduction

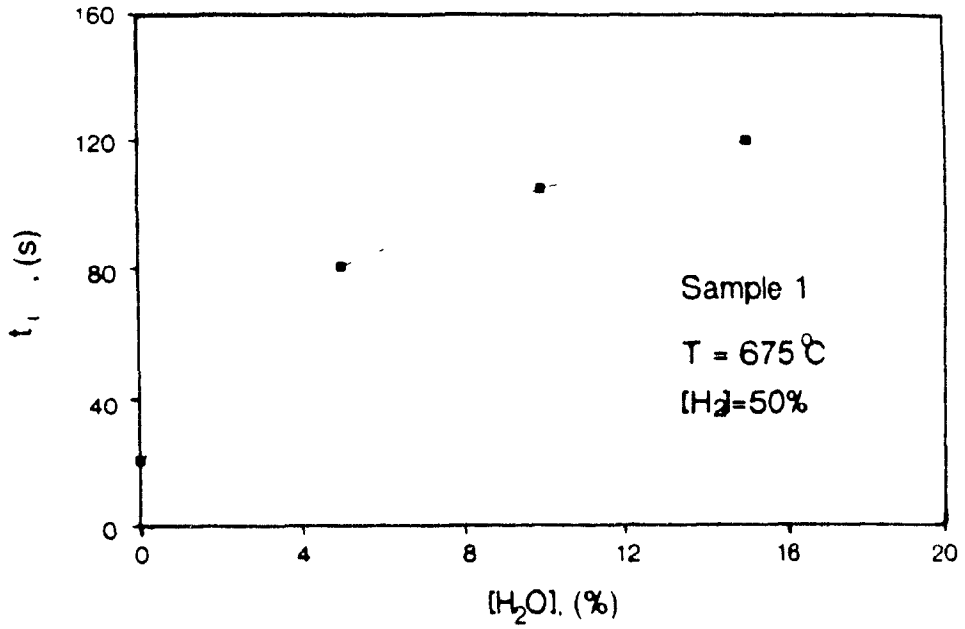

Figure 27(a) Influence of steam on t_1

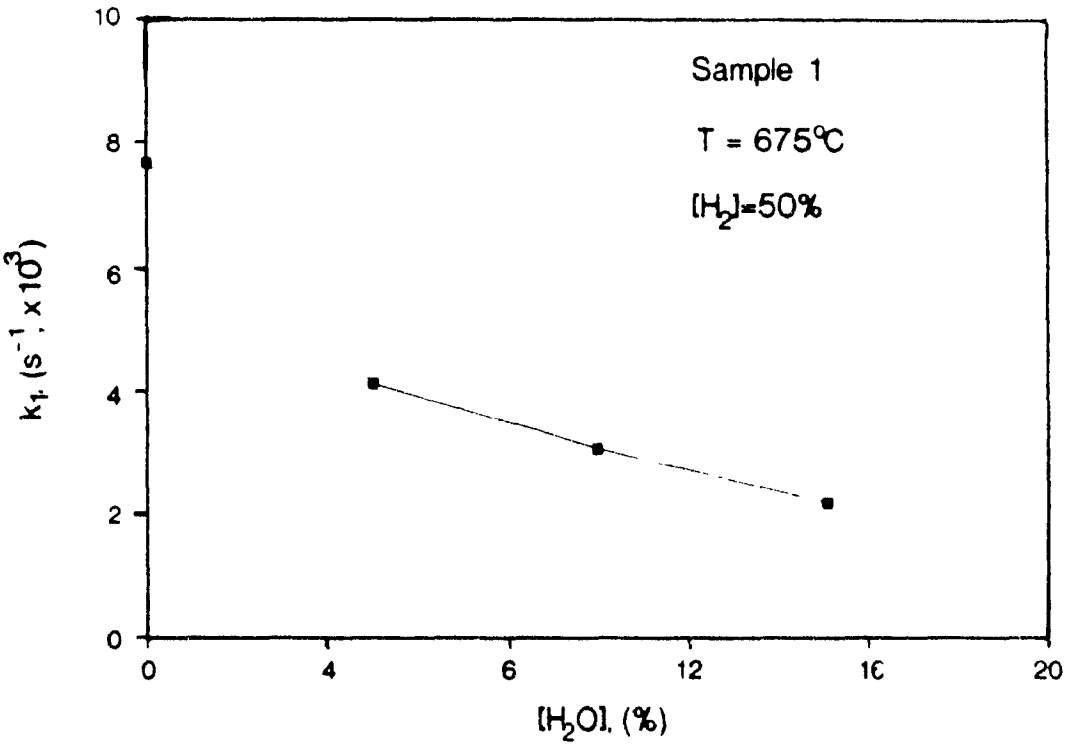

Figure 27(b) Influence of steam on, k_1

Influence of Iron Oxide Catalyst

Iron oxide was found to be a very good catalyst for the reduction of sodium sulfate mixed with sodium titanate. Therefore 1.5% (wt.) iron oxide (d_p <25μm) was mixed mechanically with Sample 1. It was again found that the presence of iron oxide dramatically accelerated the reduction of Na_2SO_4. The reduction data could also be described by the nucleation and growth model. The large increase in the reaction constant shown in Figure 23 confirms the catalytic effect of iron oxide. The non-linear relation between $\ln k_1$ and 1/T with addition of iron oxide can be explained by the strong external mass-transfer resistance at the higher temperatures.

The above reduction results indicate that direct causticized kraft black liquor sample can easily be reduced in the solid state, particularly when iron oxide is added as a catalyst.

CONCLUSION

The hydrogen reduction rate of sodium sulfate in a model mixture with sodium titanate is well described by the nucleation and growth model up to about 60% conversion, and by the shrinking core model with hydrogen diffusion control in the product layer above 60% conversion. The activation energies for the nucleation and growth period and diffusion controlled period are 302 and 179 kJ/mol, respectively. The nucleation and growth rate constant is proportional to $[H_2]^{0.7}$, while the rate constant in the diffusion controlled period is proportional to $[H_2]$. The presence of steam leads to a long induction time for the formation of nuclei. An increase in the sodium titanate molar fraction accelerates the reduction. The degree of mixing of Na_2SO_4 and sodium tiatante as determined by the preparation procedure of the model mixture has a large effect on the reduction behavior. The initial presence of sodium sulfide eliminates the induction period, even when steam is present in the reactant gas. Iron oxide (1.5% wt.) addition significantly accelerates the reduction.

The above kinetic models are also tested for samples of kraft black liquor heated and/or combusted with TiO_2. A faster reduction than that of the model mixture, and a nucleation and growth activation energy of about 280 kJ/mol are obtained for kraft black liquor samples.

NOMENCLATURE

a =Constant

d_c =Diameter of sample pan, m

d_p =Particle size, μm

E_N =Activation energy of n_o, J/mol

E_G =Activation energy of growth process, J/mol

$[H_2]$ =Hydrogen concentration, %

$[H_2O]$ =Steam concentration, %

k_1 =Nucleation and growth rate constant, s^{-1}

k_g =Film mass transfer coefficient, m/s

k_s =Intrinsic rate constant for interfacial reaction, s^{-1}

K_e =Equilibrium constant

M_H =Ratio of reaction rate to mass transfer rate.

m =Constant

N_{H_2} =Rate of hydrogen mass transfer, mole/(m^2s).

n_o =Initial concentration of nuclei.

P =Total pressure, atm.

P_{H_2} =Partial pressure of hydrogen, atm.

P_{H_2O} =Partial pressure of water, atm.

r_{max} =Maximum reaction rate, mol/(m^2s).

R =Universal gas constant, J/(mol K).

Sh =Sherwood Number ($=k_g d_c/\mathbb{D}$).

t =Time, s.

t_b =Time in shrinking core model, s.

t_i =Induction time, s.

T =Temperature, °C.

V =Gas velocity, m/s.

V_2 =Molar product volume, m^3/mol.

W =Weight, g.

X =Conversion.

Y =Molar fraction of sodium titanate.

Foreign Symbol

$\mathbb{D}$ =Diffusion coefficient, m^2/s

$\mathbb{D}_e$ =Effective diffusion coefficient, m^2/s.

ρ =Density, kg/m^3.

τ =Time for a complete conversion in shrinking core model, s.

REFERENCES

Adams, T.N. and W.J. Frederick, *Kraft Recovery Boiler — Physical and Chemical Processes*, American Paper Institute Inc., New York, N.Y , 1988.

Andersson, S., "Studies on Phase-Diagrams Na_2S-Na_2SO_4, Na_2CO_3-Na_2S-Na_2SO_4, Na_2CO_3-Na_2SO_4-NaOH, and Na_2CO_3-Na_2S-NaOH",*Chemica Scripta*,1982,20, p.164 -170.

Aronson, S, R B. Roof, Jr. and J. Belle, "Kinetic Study of the Oxidation of Uranium Dioxide", *The Journal of Chemical Physics*, 1957, 27, p.1.

Birk, J.R., C.M. Larsen, W.G. Vaox and R.D. Oldenkamp, "Hydrogen Reduction of Alkali Sulfide", *Ind Eng Chem , PDD*, 1971, 10(1), p.7.

Brown, M.E., B. Delmon, A.K. Galwey and M.J. McGinn, "Decomposition of Nickel Formate", *J Chim Phys* , 1978, 75, p.147.

Budnikoff, P.P. and E. Shilov, "The Reduction of Sodium Sulfate to Sodium Sulfide, Particularly by Hydrogen and Carbon Monoxide in the Presence of Catalysts", *Journal of the Society of Chemical Industry*, 1928, 6, p.111T.

Delmon, D. and A. Roman, "Kinetic Study of the Reduction of Nickel Oxide near its Antiferromagnetic-Paramagnetic Transition: Influence of the Magnetic Structure of the Reactant on the Kinetics of Nucleus Formation on Its Surface", *J Chem Soc. Faraday Trans.*, 1973, 69(1), p.941.

El-Guindy, M.I. and W.G. Davenport, "Kinetics and Mechanism of Ilmenite Reduction with Graphite", *Metallurgical Transactions*, 1970, 1, p.1729.

El-Rahaiby, S.K. and Y.K. Rao, "The Kinetics of Reduction of Iron Oxides at Moderate Temperatures", *Metallurgical Transactions*, 1979, 10B, p.251.

Et-Tabirou, M, B. Dupre and C. Gleitzer, "Hematite Single Crystal Reduction into Magnetite with CO-CO_2", *Metallurgical Transaction*, 1988, 79B, p.311.

Galwey, A.K., D.M. Jamieson and M.E. Brown, "Thermal Decomposition of Three Crystalline Modifications of Anhydrous Copper(II) Formate", *Journal of Chemistry*, 1974, 78(26), p.2664.

Geva, S., M. Farren, D.H. St. John, and P.C. Hayes, "The Effect of Impurity Elements on the Reduction of Wustite and Magnetite to Iron in CO/CO_2 and H_2/H_2O Gas Mixtures", *Metallurgical Transaction*, 1990, 21B, p.743.

Golikova, N.Y., et al. "Production of Highly Concentrated Sodium Sulfide in Fluidized Bed", *Tezizy Dokl Vses Nauchno-Tekh. Konf. Teknol*, 1976, p.173.

Harrison, L.G., "Reactions in Solid State", in *Comprehensive Chemical Kinetics* (C.H. Bamford and C.F.H. Tipper ed.), Vol.2, Elsevier, Amsterdam, 1969.

Hayes, P.C., "The Kinetics of Formation of H_2O and CO_2 during Iron Oxide

Reduction", *Metallurgical Transaction*, 1979, 10B, p 211-217

Hayes, P.C. and P. Grieveson, " The Effect of Nucleation and Growth on the Reduction of Fe_2O_3 to Fe_3O_4", *Metallurgical Transactions*, 1981, 12B, p 319.

Hough, G., *Chemical Recovery in the Alkaline Pulping Process*, TAPPI press, Atlanta, 1985.

Kiskilla, E., "Recovery of Sodium Hydroxide from alkaline Pulping Liquors by Smelt Causticizing, Part 2, Reaction Between Sodium Carbonate and Titanium Dioxide", *Paperi ja Puu Paper O Tra*, 1979, 61, p 394-401

Koga, Y. and [illegible]rison, "Reaction of Solids with Gases Other than Oxygen", in *Comprehensive Chemical Kinetics* (C.H. Bamford and C F H Tipper ed), Elsevier, Amsterdam, 1982, Vol.21, Chapter 2, p.119-149

Kunin, V.T. and I.P. Kirillov, "Reduction of Sodium Sulfate by Gaseous Reagents", *Izv Vyssh Ucheb Zaved , Khim Tekhnol (Russ)*, 1968, 11, p 569

Le Page, A.H. and A.G Fane, "The Kinetics of Hydrogen Reduction of UO_3 and U_3O_8 derived from Ammonium Diuranate", *J Inorg Nucl Chem* , 1974, Vol.36, p.87-92.

Levenspiel, O., *Chemical Reaction Engineering*, Wiley, New York, N.Y , Chapter 1-2, 1969.

Levenspiel, O., *Chemical Reactor omnibook*, OUS Bookstore Inc , Corvallis, Chapter 55.

Li, J., "Rate Processes During Gasification and Reduction of Kraft Black Liquor Char", *Ph D Thesis*, McGill University, Montreal, 1989.

Lin, C.I., "The Effect of Alkali Salt Catalyst on the Carbothermic Reduction of Nickel Oxide", *Metallurgical Transactions*, 1987, 19B, p 685.

McKewan, M., "Reactivity of Solids", *5th Int Symp.*, Munich, 1964, G Schwab ed., Elsevier, 1965, p.623

Nguyen, X.T., "Process to Regenerate Kraft Black Liquor", *Canadian Patent*, No. 1,193,406, 1985.

Nyman, C.J. and T.D. O'Brien, "Catalytic Reduction of Sodium Sulfate", *Industrial and Engineering Chemistry*, 1947, 39(8), p.1019.

Puttagunta, V. R., W. J. DeCoursey and N.N. Bakhshi, "Reduction of Sodium Sulfate with Hydrogen in a Fluidized Bed Reactor", *Can J of Chem Eng* , 1970, 48, p.73.

Sohn, H.Y. and S.K. Kim, "Intrinsic Kinetics of the Hydrogen Reduction of Copper Sulfate: Determination by a Nonisothermal Technique", *Metallurgical Transactions*, 1985, 16B, p.397.

Sohn, H.Y. and S. Won, "Intrinsic Kinetics of the Hydrogen Reduction of Cu_2S", *Metallurgical Transactions*, 1985, 16B, p.831.

Szekely, J., J.W Evans and H Y Sohn, *Gas-Solid Reactions*, Academic Press, New York, 1976, Chapter 8, p 338.

Weston, T.A., "The Regeneration of High Temperature Sulfur Dioxide Sorbents: The Carbon Monoxide Reduction of Supported Alkali Sulfates", *Ph D Thesis*, California Institute of Technology, 1986.

White, J.E.M. and A.H. White, "Manufacture of Sodium Sulfide: Reduction of Sodium Sulfate to Sodium Sulfide at Temperatures below 800°C", *Industrial and Engineering Chemistry*, 1936, 28(2), p.244.

Wolf, F. and H. Mathains, "Colorless Na_2S", *East German Patent*, No. 2,060, May, 1956 and No. 12,864, March, 1957.

Zhao, Y. and F. Shadman, "Kinetics and Mechanism of Ilmenite Reduction with Carbon Monoxide", *AIChE J*, 1990, 36(9), p.1433.

CHAPTER 7

CARBON MONOXIDE REDUCTION OF SODIUM SULFATE MIXED WITH SODIUM TITANATE

ABSTRACT

The solid state reduction kinetics by carbon monoxide of sodium sulfate mixed with sodium titanate are studied in a thermogravimetric system from 670-750°C. The conversion-time curves of the model mixtures are sigmoid-shaped and well described by the nucleation and growth model The activation energy is found to be 420 kJ/mol. The influence of the CO and CO_2 concentration, fraction of sodium titanate, initial presence of sodium sulfide and addition of iron oxide as a catalyst is investigated. Based on the experimental results, a reduction mechanism is proposed.

The reduction of the combustion product of kraft black liquor and TiO_2 is also studied. The results are very similar to those obtained with model mixtures. The main differences are that the reduction rate is faster and the activation energy is smaller at 244 kJ/mol.

INTRODUCTION

In one of the two proposed direct causticizing processes described in Chapter 3, a mixture of sodium sulfate and sodium titanate is produced by combustion of a mixture of kraft black liquor and TiO_2. The sodium sulfate in the combustion product must be reduced to sodium sulfide before it can be reused in the pulping process. Therefore the sulfate reduction is a critical separate step in this proposed direct causticizing process.

The reduction of sodium sulfate to sodium sulfide has been carried out routinely in industry for almost 175 years, First since the invention of the LeBlanc process in 1823 for the production of sodium sulfide, and later in the recovery furnace of the kraft pulping process. The reduction can be accomplished with several different reducing agents such as H_2, CO, C, CH_4 etc. (Meyer, 1965). Although considerable discrepancies concerning reduction temperatures and rates exist in the literature, temperatures between 750 and 900°C are frequently cited as ideal for reduction of pure sodium sulfate. Temperatures in the 600-700°C range have been utilized at the expense of longer reaction times, while temperatures above 900°C lead to significant side reactions. The most reactive conditions are obtained when there is intimate contact between the reducing agent and sodium sulfate. With gaseous reagents this is best achieved with Na_2SO_4 in the solid state. In this respect it should be noted that the eutectic melting point of a mixture of Na_2SO_4-Na_2S is 740°C (Andersson, 1982). However the presence of impurities or other compounds may significantly change the melting behavior.

Most of the recent reduction studies have been performed with Na_2SO_4 in the molten state (Birk et al., 1971; Sjoberg and Cameron, 1981; Cameron and Grace, 1983 and 1985; Li and van Heiningen, 1991). Of these, only Sjoberg and Cameron (1981) and Li and van Heiningen (1991) are concerned with reduction by CO. Sjoberg and Cameron (1981) reported that the reduction is kinetically controlled, zero order in sulfate, first order in CO and has an activation of 115 kJ/mol. Li and van Heiningen (1991), on the other hand, showed that the reaction is strongly limited by mass transfer of CO in the molten phase.

The studies of sodium sulfate reduction by CO in the solid state were reported many decades ago by Budnikoff and Shilov (1928) and White and White (1936), and most recently by Li and van Heiningen (1988). Budnikoff stated that sodium sulfate could not be reduced by CO below 850°C. However Li and van Heiningen(1988) found that CO reduction of sodium sulfate in a mixture with

sodium carbonate is relatively fast in the solid state below 760°C. White and White (1936) reported that the reduction by H_2 proceeds rapidly at 704°C as long as a solid state is present and that the CO reduction is slower than with H_2. It was also reported by Li and van Heiningen (1988) that the solid state reduction is described by solid-solid phase boundary reaction controlled kinetics, and is strongly retarded by CO_2 but not influenced by the CO concentration.

In Chapter 6, it was found that the hydrogen reduction of sodium sulfate mixed with sodium titanate is very fast below 750°C. Since CO is another commonly used reducing gas, it is the objective of this study to develop kinetic equations for the solid state reduction of sodium sulfate mixed with sodium titanate by CO. The influence of different parameters on the reduction will be presented and a mechanistic description of the reduction by CO will be proposed.

EXPERIMENTAL

Experimental Apparatus

The reduction experiments were performed in a thermogravimetric analysis (TGA) system. A schematic diagram of the experimental system with auxiliary gas preparation system is shown in Figure 1. The main components of this system are an electronic micro balance (Cahn Instruments, Inc., Model 1000), a quartz tube reactor, and a fixed furnace with PID controller. N_2 (99.99%) and He (99.995%) are zero grade quality, CO_2 is anaerobe grade (99.99%) and CO is ultra-high purity (99.99%). An oxygen trap is used for each gas line. Additionally, a CO_2, H_2O and hydrocarbon trap are used for the CO line because of the relatively low purity of CO.

A gas chromatograph with flame photometric detector (FPD) was used for analysis of sulfurous gases in the exhaust, while CO and CO_2 were determined continuously with infra-red (IR) CO and CO_2 analyzers. The reproducibility of the measurement of the concentration of sulfurous gases is within 5%. The inorganic ions in the solids, such as sulfate, sulfide, carbonate etc , were measured with an ion chromatograph (Dionex) equipped with a conductivity and electrochemical detector. The reproducibility for ion analysis is better than 5%. A high resolution scanning electron microscopy (SEM) was employed for examination of the particle surface of both partially and completely reduced

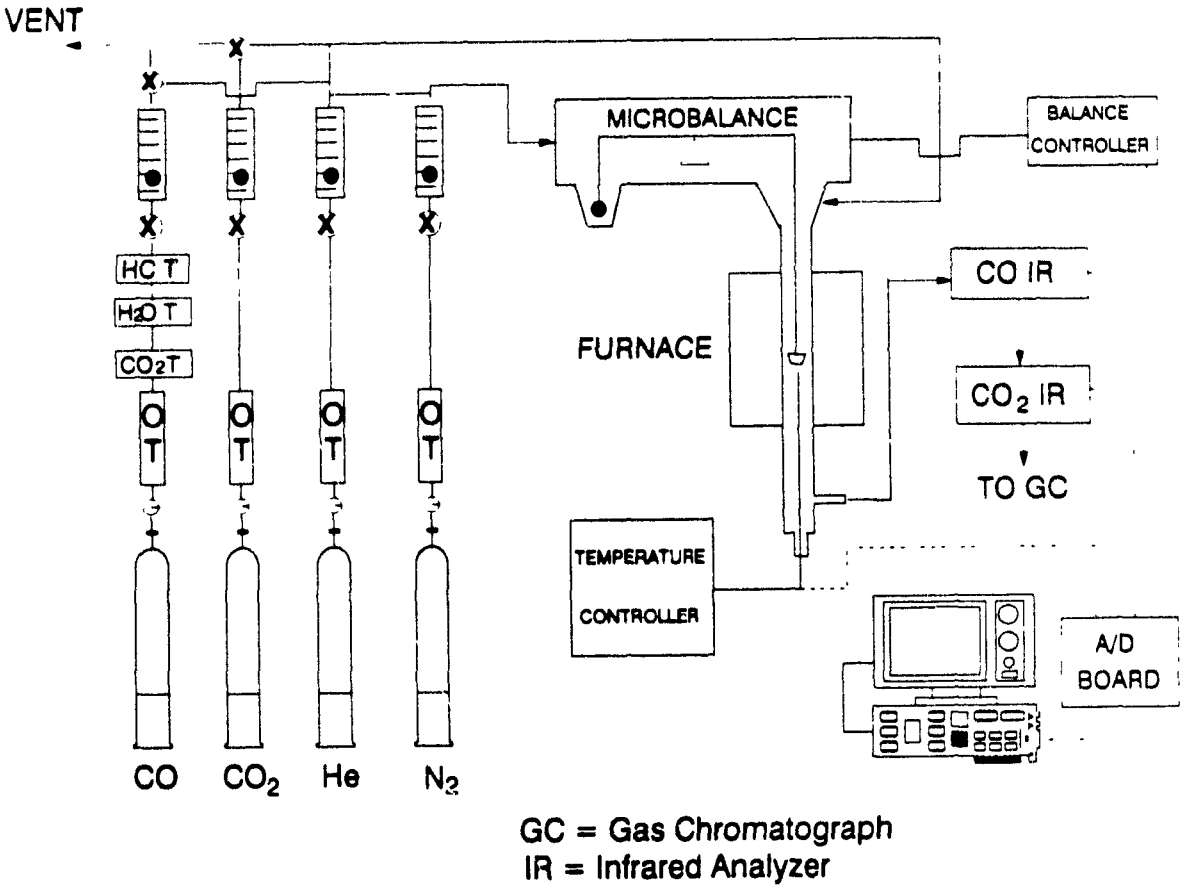

Figure 1 Experimental set-up of CO reduction

samples.

Sample preparation and experimental procedures

Three types of samples were prepared for the reduction experiments: i) a model mixture of sodium sulfate and sodium titanate, ii) the model mixture with 1.5% iron oxide, and iii) the combustion product of kraft black liquor and TiO_2. The model mixture was made as follows: reagent grade sodium sulfate and sodium carbonate (Na_2CO_3/Na_2SO_4=3:1 mol/mol, except when otherwise specified) were dissolved in deionized water, dried, ground, and then mixed mechanically with TiO_2 (d_p<10 μm). A TiO_2/Na_2CO_3 molar ratio of 1.25 was used, because it was found in Chapter 4 that $4Na_2O{\cdot}5TiO_2$ is the stable sodium titanate in CO_2 at the temperatures used in the present study. This mixture is put into a tube furnace at 900°C for 4 to 8 hours to obtain complete conversion of sodium carbonate. The resulting mixture of sodium titanate and sodium sulfate was ground to a particle size less than 25 μm. The second sample type was made by mechanically mixing 1.5% iron oxide (d_p<25 μm) with the previously described model mixture. The third sample type was made by keeping a mixture of TiO_2 (d_p<10 μm) and kraft black liquor (TiO_2/Na_2O=1·1 mol/mol) at 900°C in a tube furnace for 6 hours under an air atmosphere. The remaining salt mixture was then ground to a particle size less than 25 μm. All surfaces in contact with the sample during preparation were washed with deionized water to avoid contamination.

After adding 15-20 mg sample to the sample pan up to a bed height less than 1 mm, the TGA system is evacuated and refilled with N_2 or He to reduce the concentration of oxygen to a level below 10 ppm. Then under a He or N_2 flow of 300 scc/min, the furnace temperature was raised from 20°C to a final temperature at a heating rate of 25°C/min (except otherwise specified) CO and CO_2 were introduced to obtain the desired reduction atmosphere when a stable temperature was established. The sample weight, temperature, CO and CO_2 concentration were continuously recorded by a computerized data acquisition program. The total weight loss during reduction was normally 1.1 to 2.2 mg. At the end of an experiment the reactor was rapidly cooled and the sample immediately dissolved in deairated and deionized water to minimize reoxidation. Within a few minutes the sample is filtered, diluted and analyzed for its ion content by IC.

THERMODYNAMICS AND PRELIMINARY EXPERIMENTS

The following overall reactions may occur during the reduction of sodium sulfate by CO:

$$Na_2SO_4 + 4\ CO = Na_2S + 4\ CO_2 \qquad (1)$$

for which $\Delta G^\circ = -139.225 + 0.0297\ T$ kJ/mol

$$Na_2S + 2\ CO_2 = Na_2CO_3 + COS \qquad (2)$$

for which $\Delta G^\circ = -97.045 + 0.1338\ T$ kJ/mol, and

$$2\ CO = C + CO_2 \qquad (3)$$

for which $\Delta G^\circ = -170.000 + 0.174\ T$ kJ/mol

The Gibbs free energy of reaction (1) is -120 kJ/mol at 700°C indicating that this reaction is thermodynamically very favorable and may proceed at this temperature. However the Gibbs free energy of reaction (2) is 33 kJ/mol at 700°C and the formation of COS is strongly dependent on the concentration of CO_2, as was shown in Chapter 3. Reaction (3) is thermodynamically favorable below 750°C. However the kinetic limitations involved in the precipitation of the solid phase at lower temperatures are well documented (Powell, 1966) Some metals or their oxides are catalysts for this reaction.

Preliminary experiments show that reaction (3) is significant over the temperature range of 650 to 800 °C if a catalyst for carbon deposition is present. This was found earlier in the same TGA set-up by Li and van Heiningen (1988) who showed that a porcelain pan was coated with carbon and that the CO_2 concentration is one or two orders of magnitude higher than could be produced by reduction of sodium sulfate by CO. This indicated that reaction (3) took place inside the reactor tube and on the surface of the sample pan. Carbon decomposition on the surface of the sample pan was eliminated by using a high purity alumina (99.8%) pan. Duplicate experiments with a high purity alumina pan showed good reproducibility. The CO_2 production was still much larger than that formed by Na_2SO_4 reduction, because some carbon is still deposited on the surface of the thermocouple which is placed directly under the sample pan. Thus although the conversion of sulfate can be calculated from the measured

weight loss, it is not possible to use the CO_2 concentration in the exhaust for this purpose.

The sulfur mass balance after partial and complete reduction was good as indicated by the small percentage difference, ε_s, between the initial and final sulfur weight, respectively W_s^o and W_s^f shown in Table 1. This shows that the extent of progress of reaction (2) is very small. The COS concentration was also measured and found to be negligible (<5 ppm) below 750°C without the presence of CO_2. With CO_2 addition, the COS concentration was increased but still not large enough to represent a significant contribution to the measured weight loss. The measured weight loss, ΔW_L^E, was also in excellent agreement with the weight loss calculated from the initial weight of sulfate and the sulfide weight after reduction. It was found that the difference, ε_w, between ΔW_L^T and ΔW_L^E is less than 1% for all of the experiments except those with addition of CO_2. With CO_2 present, a small amount of sodium carbonate was detected in the reduced sample.

The reduction conversion, X, can be calculated from the measured weight loss as:

$$X = \frac{\Delta W}{W_0} \times \frac{142}{64} \qquad (4)$$

where ΔW is the weight loss recorded by the balance and W_0 is the weight of Na_2SO_4 in the initial sample.

Table 1 Mass Balances

Run No	T (°C)	[CO] (%)	[CO_2] (%)	W_s^o (mg)	W_s^f (mg)	ε_s (%)	ΔW_L^T (mg)	ΔW_L^E (mg)	ε_w (%)
1	750	50	0	0.87	0.86	-1.2	1.74	1.75	+0.7
2	750	50	4	0.72	0.69	-5.8	1.44	1.40	2.8
3	700	30	0	1.15	1.21	+5.2	2.30	2.29	0.4
4	670	50	0	0.95	0.98	+3.2	1.90	1.90	0

ROLE OF EXTERNAL MASS TRANSFER

As in Chapter 6, the maximum experimental reduction rate, r_{max}, was compared to the maximum rate of transfer of CO across the gas film surrounding the reduction sample, Nco.

The details of the calculation procedures can be found in Chapter 6. The values of Nco, r_{max}, and the mass transfer coefficient, k_g, at 50% CO and different temperatures are listed in Table 2. Since at temperatures less than or equal to 750°C, the ratio r_{max}/Nco is less than 5%, the external film mass transfer can be neglected up to 750°C.

Table 2 Evaluation of External Gas Film Mass-Transfer Resistance

Run NO	T (°C)	Carrier Gas	k_g (m/s)	N_{CO} (mol/m²s)	r_{max} (mol/m²s)	r_{max}/N_{CO} (%)
1	690	N_2	0 0484	1 948	0 004	0 22
		He	0 0993	3 996	0 004	0 11
2	710	N_2	0 0489	1 929	0 013	0 69
		He	0 1011	3 985	0 013	0 34
3	730	N_2	0 0493	1 906	0 031	1 60
		He	0 1030	3 977	0 034	0 85
4	750	N_2	0 0497	1 883	0 096	5 46
		He	0 1045	3 953	0 105	2 66
5	770	N_2	0 0500	1 858	0 235	12 1
		He	0 1066	3 961	0 293	7 44

The absence of a significant gas phase mass transfer resistance was verified experimentally by using different initial sample weights for reduction with 50% CO in helium at 720°C. The results in Figure 2 show a perfect agreement between the X-t curves obtained with initial weights of 11 and 23 mg. Since the actual CO consumption rate is different by more than a factor of 2, while Nco is the same for these two experiments, this confirms that the external and also the interparticle gas mass transfer resistance in the sample pan can be neglected.

Surprisingly, the results in Figure 2 also show that the reduction rate in N_2 is somewhat different from that obtained in He. Since N_2 has a significantly lower diffusivity and the gas stream is mainly heated by conduction rather than radiation, it might be that the difference between the X-t curves in He and N_2 are the result of small differences in gas and sample temperature. Because of the better heat and mass transfer rates in helium,

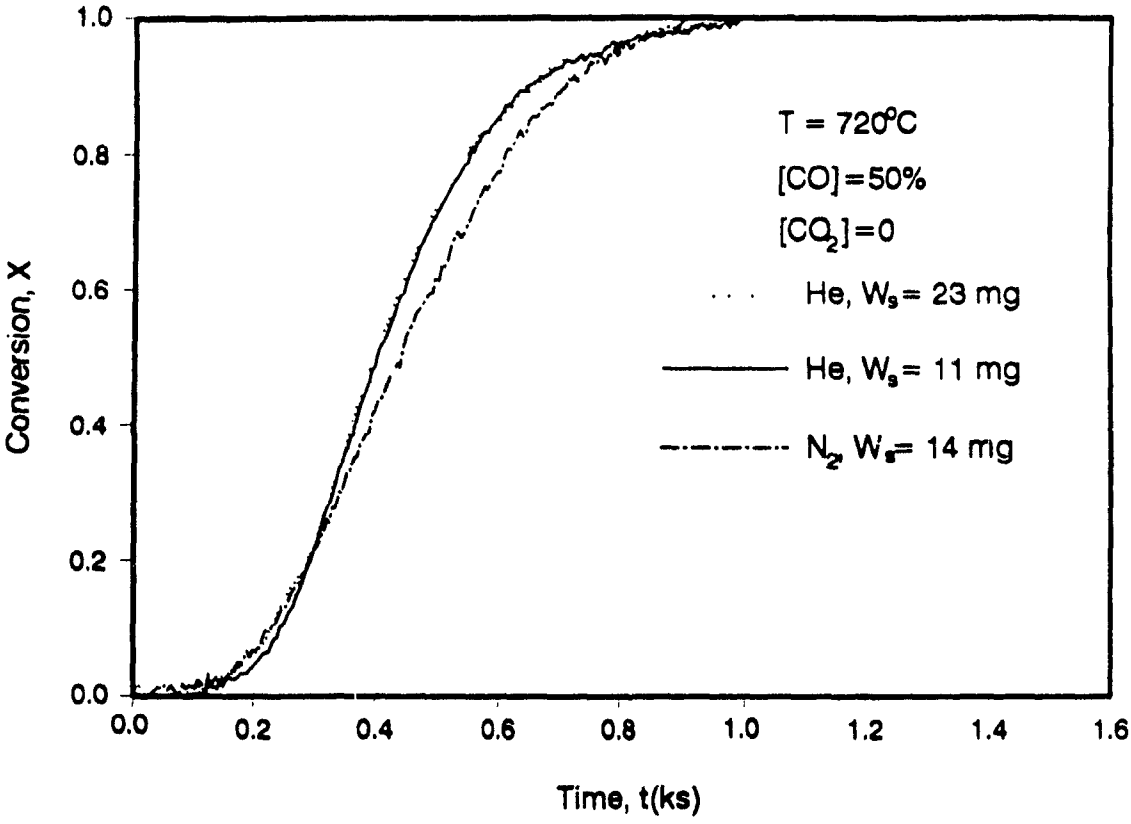

Figure 2 Influence of carrier gases and sample size on reduction

this gas was used as carrier gas in all further experiments.

RESULTS AND DISCUSSIONS

PART I. Reduction of Model Mixtures

An experiment with a temperature programed heating rate of 25°C/min under 100% CO in Figure 3 shows that the reduction starts at 650°C and is complete at 750°C. Above 850°C, the COS formation becomes significant, resulting in a large weight loss. Therefore isothermal kinetic measurements were made at six different temperatures in the range of 670 to 750°C. The conversion-time curves with 50% CO shown in Figure 4 are typical S-shaped. The time for complete reduction diminishes dramatically as the temperature is increased. As for the sulfate reduction by hydrogen (Chapter 6), one may identify three distinct regions in the X-t plots: (a) the induction, (b) the acceleration, and (c) the deceleration period. The induction period is most prominent at low temperatures. At 670°C, the induction period was about 750 seconds compared to only 50 seconds at 750°C. It will be shown that the induction period corresponds to the formation of Na_2S nuclei. During the acceleration period, these Na_2S nuclei grow continuously and there is a corresponding increase in the rate of reduction. Finally with excessive overlap and interpenetration of the Na_2S nuclei, the reduction rate tapers off and the deceleration period starts.

Evaluation of the rate constant, k_1, and induction time, t_i

Similar to the hydrogen reduction of sodium sulfate in Chapter 6, the CO reduction data were fitted according to the kinetic equation for the nucleation and growth model (Chapter 2):

$$[-\ln(1-X)]^{1/m} = k_1(t-t_i) \qquad (5)$$

The best fit of the reduction data was obtained with m=2. This corresponds to two dimensional or disk-like growth of the nuclei. A reasonably linear relationship was obtained as shown in Figure 5. The reaction rate constant, k_1, is equal to the slope of the straight lines. The induction time was determined by extrapolating the linear portion of the $[-\ln(1-X)]^{1/2}$ to zero time.

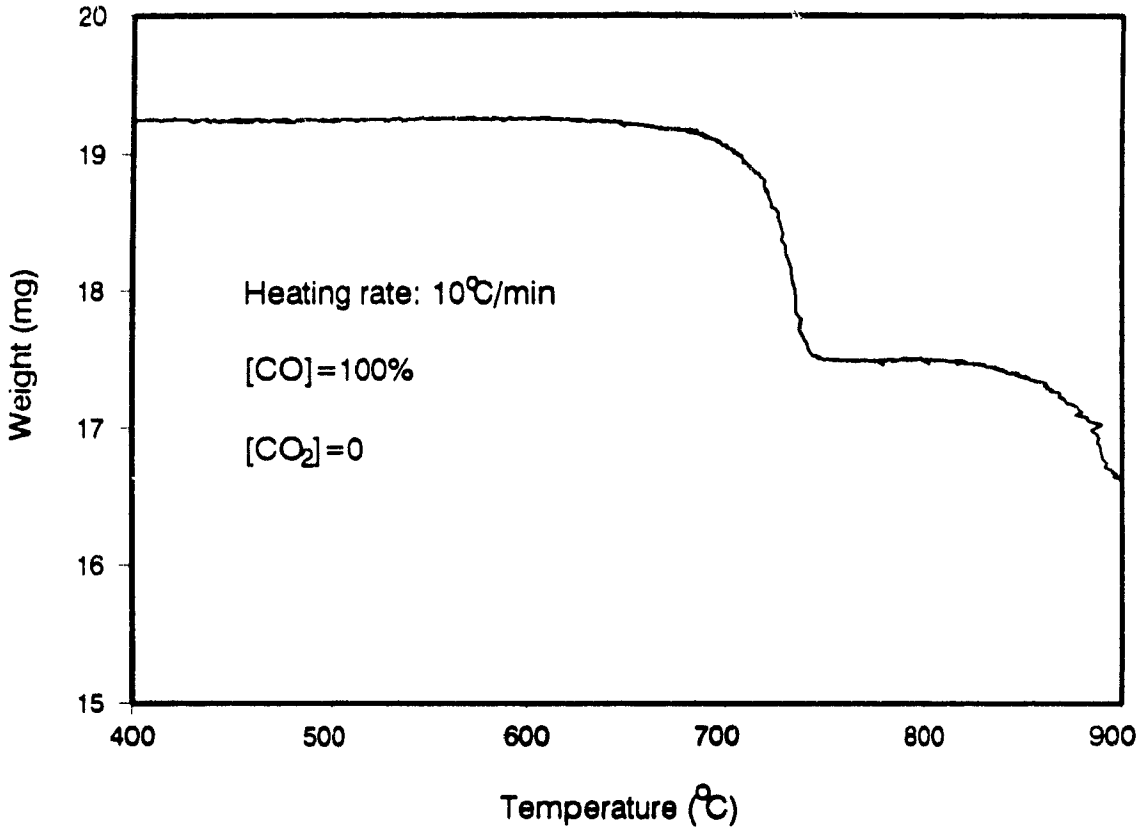

Figure 3 CO reduction as a function of temperature

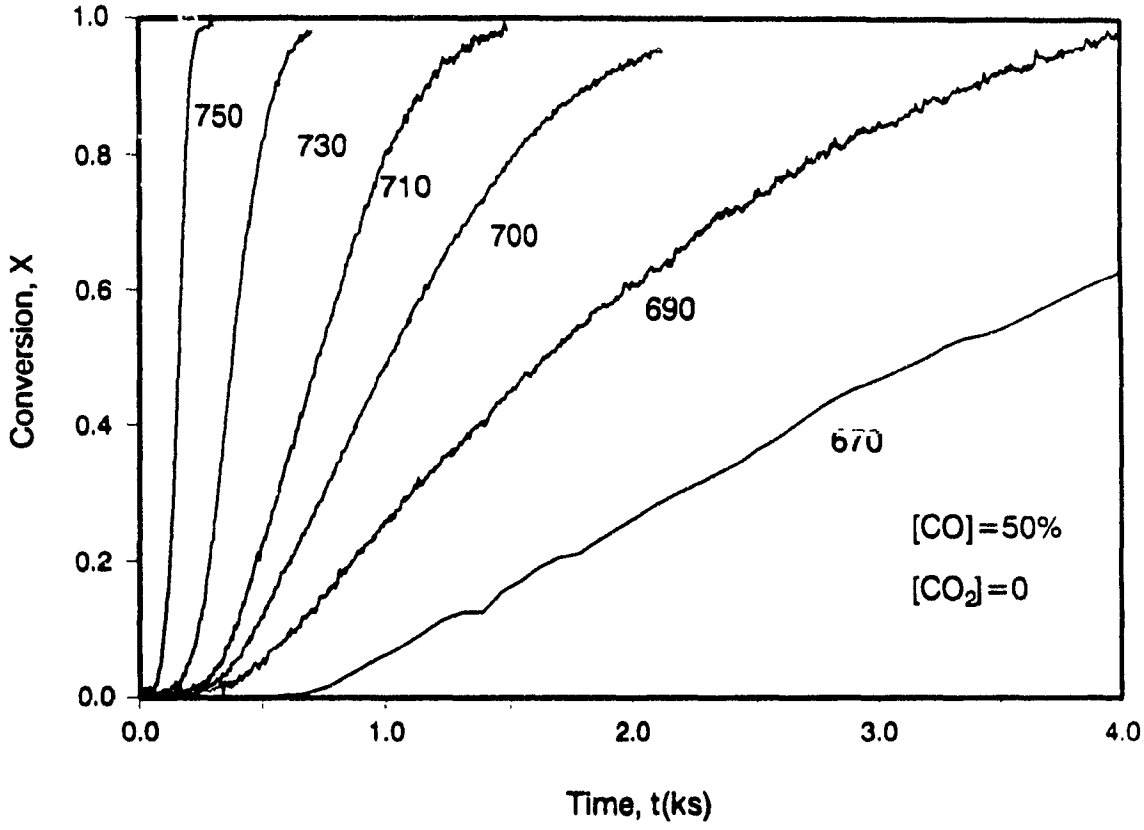

Figure 4 Influence of temperatures on reduction

Temperature-dependence of k_1 and t_1.

The rate constant k_1 for the reduction of sodium sulfate by 50% CO was determined at six temperatures varying from 670 to 750°C. An Arrhenius plot of the data in Figure 6 shows that the rate constant k_1 is a strong function of temperature. Regression analysis gave an activation energy of 420 kJ/mol. This is unusually high compared to 50-200 kJ/mol, the normal activation energy range of gas-solid reactions. Since the reduction of sodium sulfate probably proceeds in a few steps, this activation energy corresponds to the slowest of the steps involved. Such a high activation energy suggests that the rate controlling step may involve a solid-solid reaction, since it normally has a very high activation energy. Compared to the activation energy of 650 kJ/mol found by Li and van Heiningen (1988) for CO reduction of a mixture of sodium sulfate and sodium carbonate, the present activation energy is much lower. The difference may be explained by the fact that the experiments of Li and van Heiningen were performed with partly molten sulfide while the present reduction was conducted well below the melting point of the salt mixture. The present CO reduction data are also more temperature sensitive than the H_2 reduction (E_a=302 kJ/mol) as shown in Figure 6.

The induction times obtained from Figure 5 are plotted as $1/t_1$ against the inverse of temperature in Figure 7. The linear relationship between the inverse of induction time and temperature indicates that nuclei formation is an activated process. Regression analysis of the experimental data gives:

$$1/t_1 = 1.82 \times 10^7 \times \exp\left(-\frac{180{,}000}{R\,T}\right) \qquad (6)$$

The magnitude of the activation energy of 180 kJ/mol, suggests that the initial nuclei formation probably mainly involves the gas-solid reaction between CO and sodium sulfate.

Compared to the H_2 reduction without steam addition, for which the induction time is negligible, the reduction with only CO has a long induction period. This may be due to the formation of CO_2 from the disproportionation reaction of CO-[Reaction (3)] since later it will be shown that the presence of CO_2 strongly retards the nuclei formation.

Influence of sodium sulfide

It was reported that the sodium sulfate reduction by H_2 or CO is facilitated by the presence of sodium sulfide (Polyvyannyi and Demchenko,

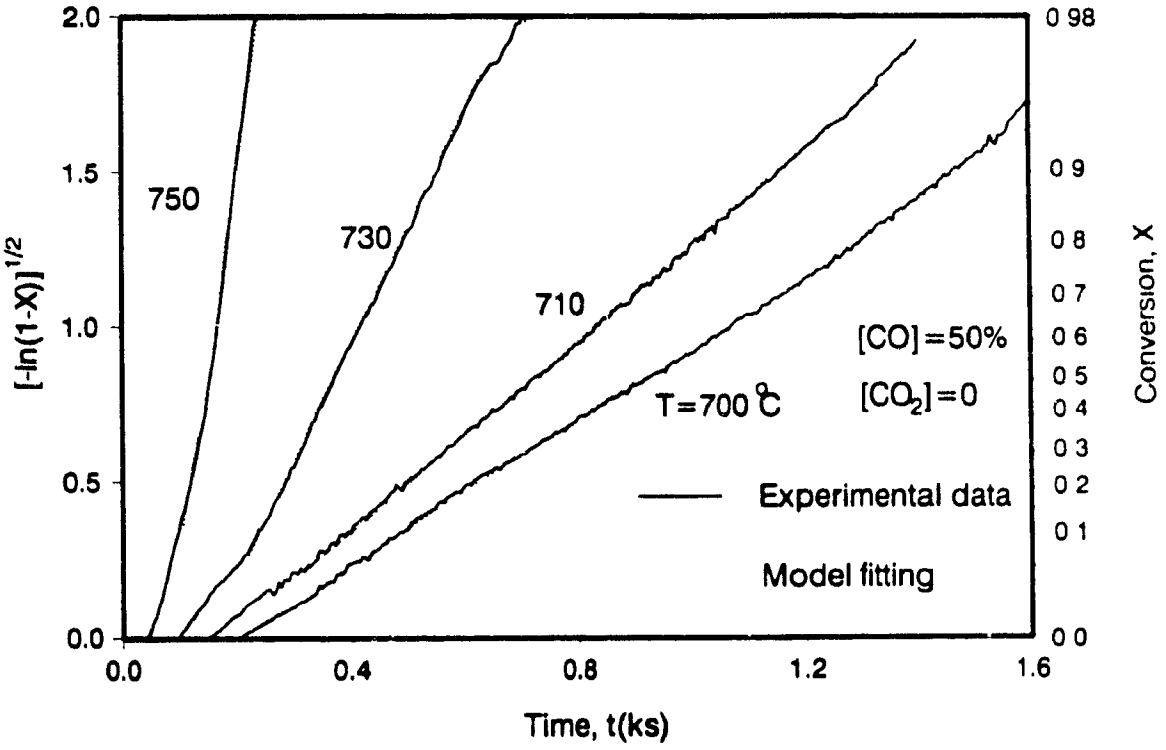

Figure 5 Data fitting by nucleation and growth kinetics

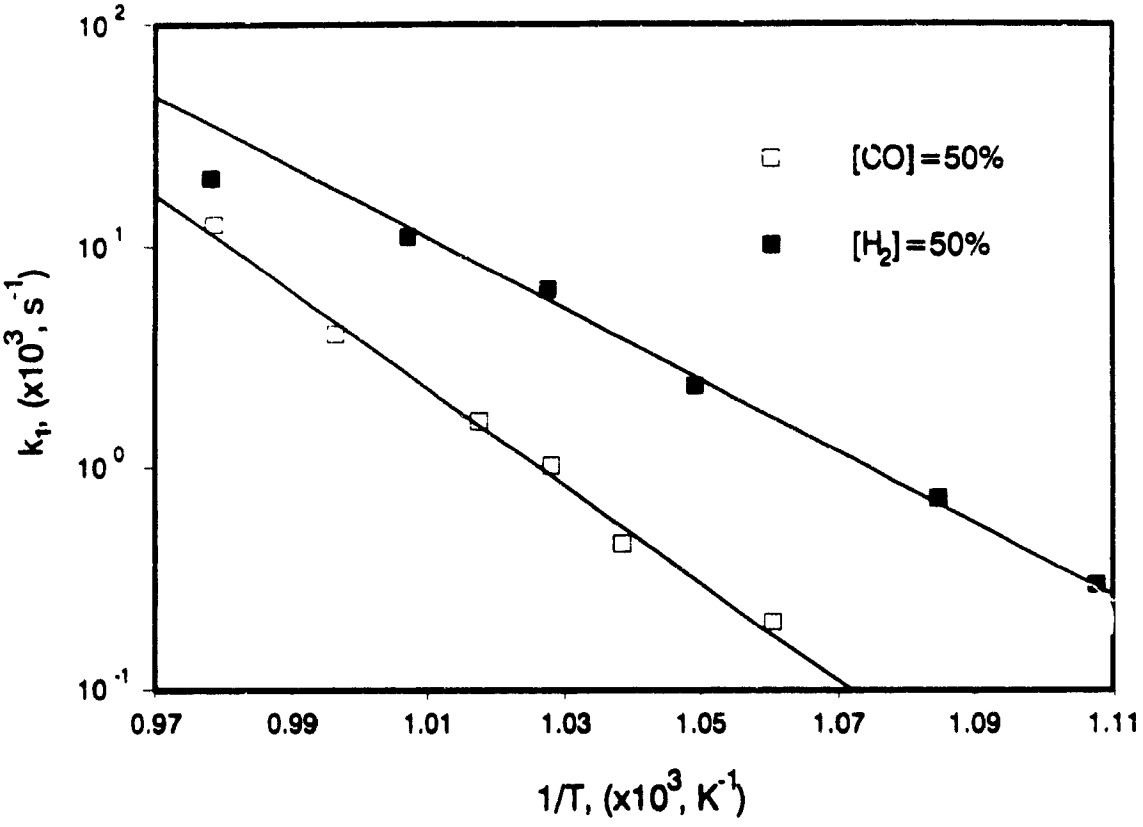

Figure 6 Arrhenius plot of rate constants

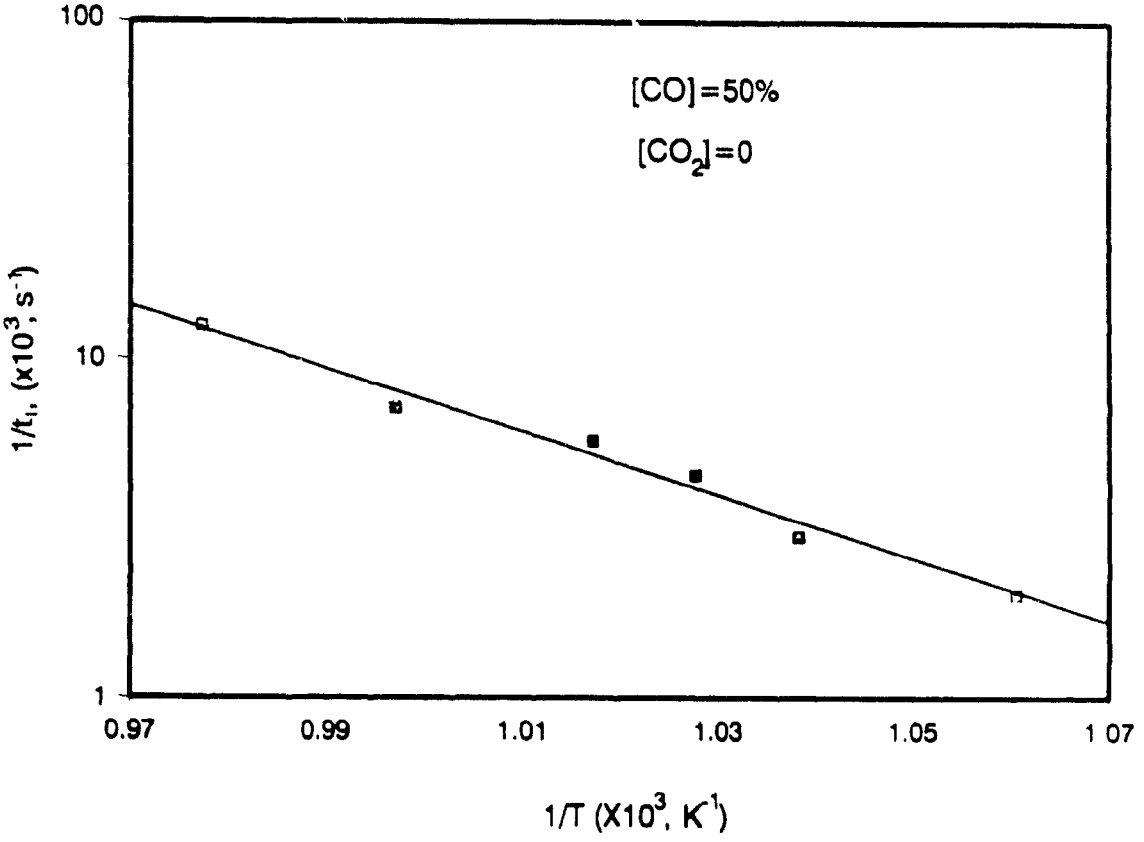

Figure 7 Influence of temperatures on induction time

1960; Birk et al., 1971; Li and van Heiningen, 1988; Chapter 6 of this thesis). Therefore some experiments were carried out with sodium sulfide particles added to the model mixture (molar ratio of Na_2S/Na_2SO_4=0.5). The results of these experiments in Figure 8(a) and 8(b) clearly show that the Na_2S addition completely eliminates the long induction time even with a relatively high concentration of CO_2 in the feed gas This behavior is similar to that found in Chapter 6 for the Na_2SO_4 reduction by H_2. The effect of the Na_2S addition on the initiation time and reaction constant is listed in Table 3. The nucleation and growth reaction constant obtained without CO_2 presence is not significantly affected by the addition of Na_2S. However, with the presence of CO_2, the rate constant is somewhat increased by the addition of Na_2S.

Table 3 Influence of Na_2S Addition on k_1 and t_1

No	[CO] (%)	[CO_2] (%)	T (°C)	t_i (s)		k_1 ($\times 10^3$ s^{-1})	
				Presence of sodium sulfide			
				No	Yes	No	Yes
1	50	0	700	186	0	0 95	0 93
2	50	9	720	399	42	2 98	3 93

The mechanism suggested for the catalytic effect of sodium sulfide by Birk et al. (1971) and Li and van Heiningen (1988) is:

$$Na_2SO_4 + Na_2S = \text{intermediate} \qquad (7)$$

whereby the intermediate is subsequently fast reduced to Na_2S by CO. Although the intermediate was not identified, polysulfide was proposed as a possible candidate in the earlier study of Birk et al., (1971). In the present case, Table 3 shows that the addition of Na_2S significantly reduces the induction time but has a much smaller or no influence on the rate constant, depending on the presence or absence of CO_2. Therefore, just as proposed for the effect of Na_2S addition for the Na_2SO_4 reduction by H_2, the present results suggests the addition of Na_2S provides the nuclei necessary for the initiation of the

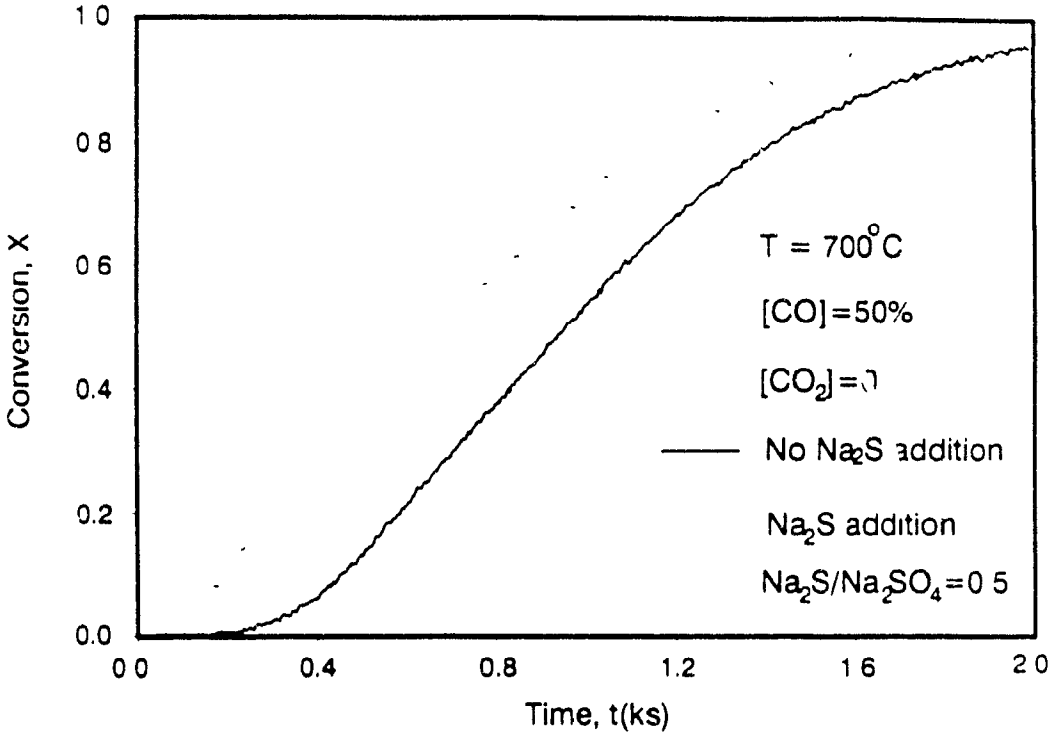

(a) Without the presence of CO_2

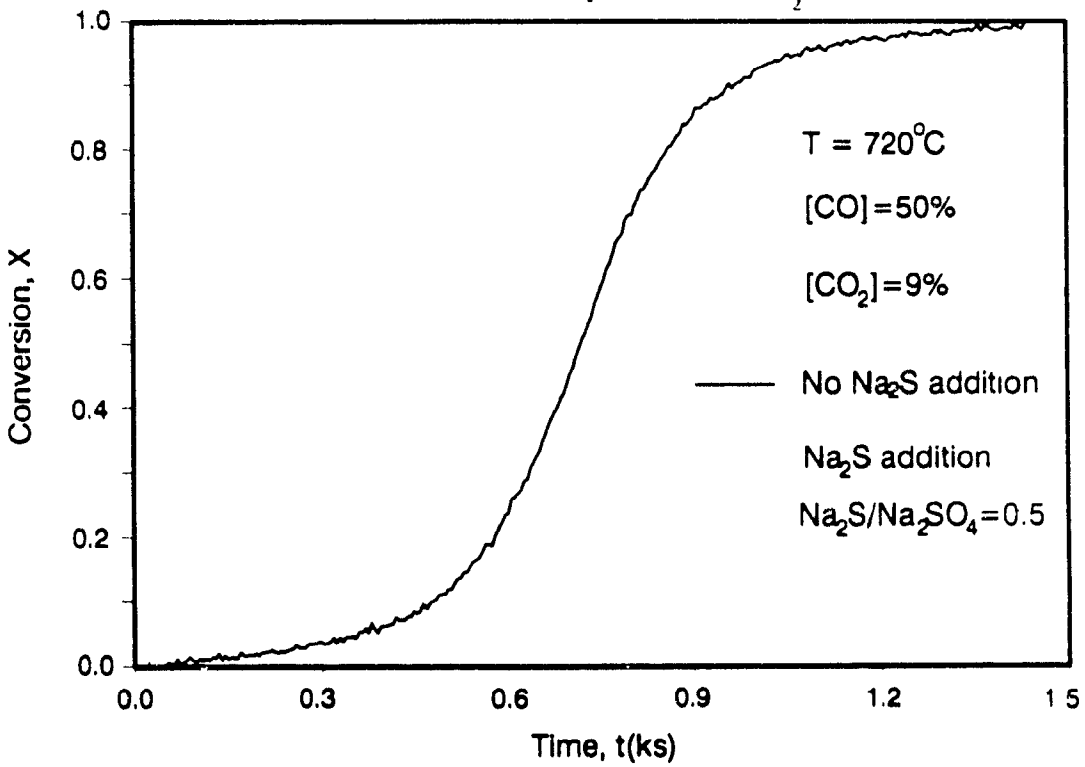

(b) With the presence of CO_2

Figure 8 Influence of sodium sulfide on reduction

reduction reaction. Thus the added Na_2S crystals, act as nuclei for the rapid growth of the Na_2S phase according to reaction (7), eliminating the formation stage of the nuclei This phenomenon has been observed for many metal oxide reductions, such as those of NiO, WO_3, etc (Roman and Delmon, 1973)

A practical consequence of the present result is that the reduction of sodium sulfate by CO is best achieved in a reactor with some backmixing, as for example in a fluidized bed, or with an external recycle of the sodium sulfide product.

Influence of CO concentration

The CO concentration has a significant influence on the reduction as shown in Figure 9. The influence of CO on the reaction rate constant, k_1, and the induction time, t_i, is shown in Figures 10(a) and 10(b), respectively. The inverse of induction time, $1/t_i$, varies linearly with CO concentration as shown in Figure 10(b) and this appears to support the earlier suggestion that the nuclei formation is due to the initial gas-solid reaction from Na_2SO_4 to Na_2SO_3. However the rate constant, k_1, is proportional to $[CO]^a$ with a= 0.57, 0.54, and 0.43, respectively for T =710, 730 and 750°C. A slightly larger broken reaction order of 0.7 was found for the hydrogen reduction of Na_2SO_4 in Chapter 6. The influence of the CO concentration becomes stronger when the temperature decreases, possibly because the suggested solid-solid reaction becomes more dominant at higher temperatures.

In Chapter 6 it was argued that the initial reduction of Na_2SO_4 by hydrogen proceeds with via Na_2SO_3 as intermediate. Similarly the onset of reduction by CO most likely proceeds according to the following initiation reaction:

$$Na_2SO_4 + CO = Na_2SO_3 + CO_2 \qquad (8)$$

Sodium sulfite is subsequently very fast further reduced by CO to sulfide or it decomposes to form sulfide and sulfate. This reaction would explain the strong influence of CO on the induction time as shown in Figure 10(b). It should be remembered, however, that other reaction besides reaction (8) determine the reduction rate after the induction period, since the temperature dependence of k_1 is larger than that normally found for gas-solid reactions, and k_1 is not proportional to the CO concentration. The existence of at least two parallel Na_2SO_4 conversion pathways may also explain the dependence of

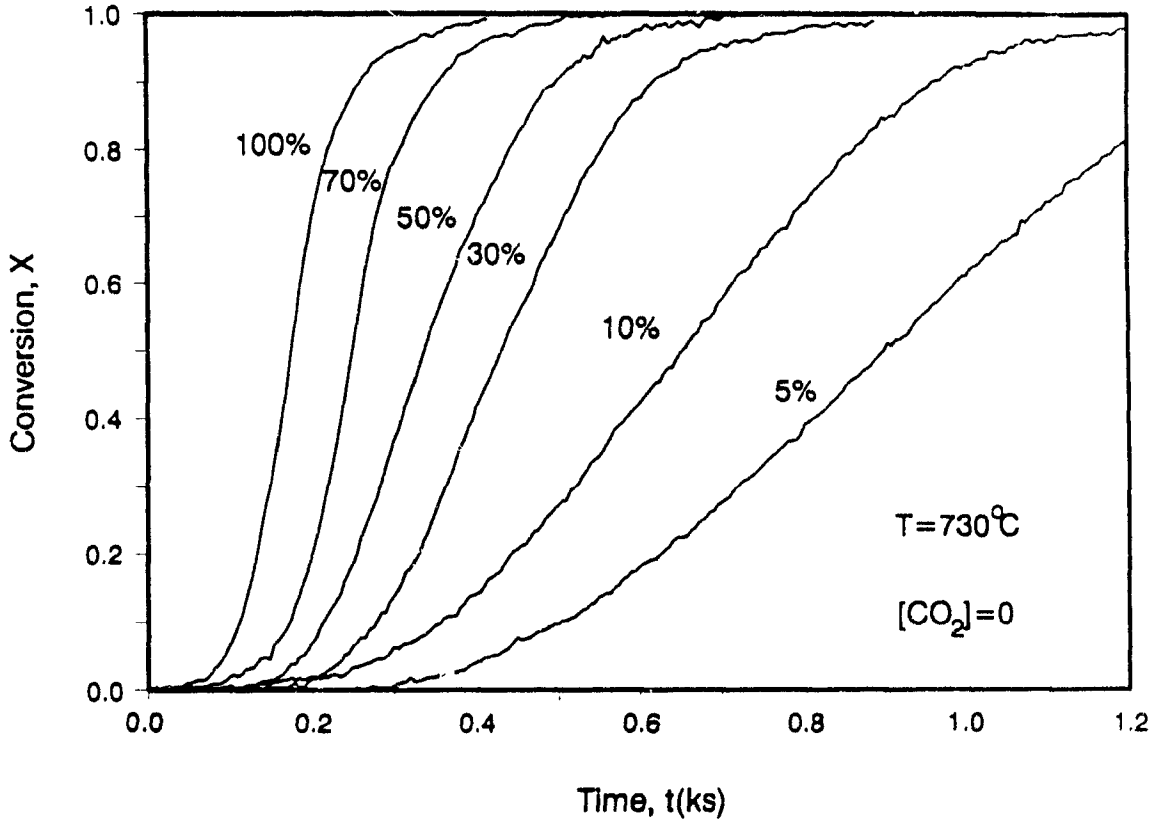

Figure 9 Influence of CO concentration on reduction

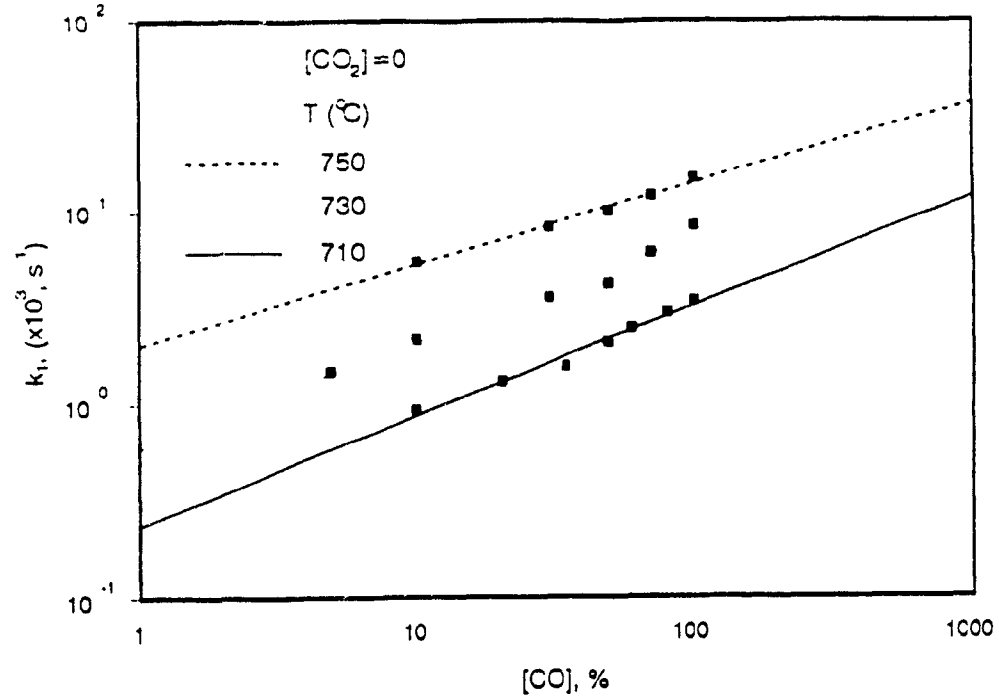

(a) k_1 versus [CO]

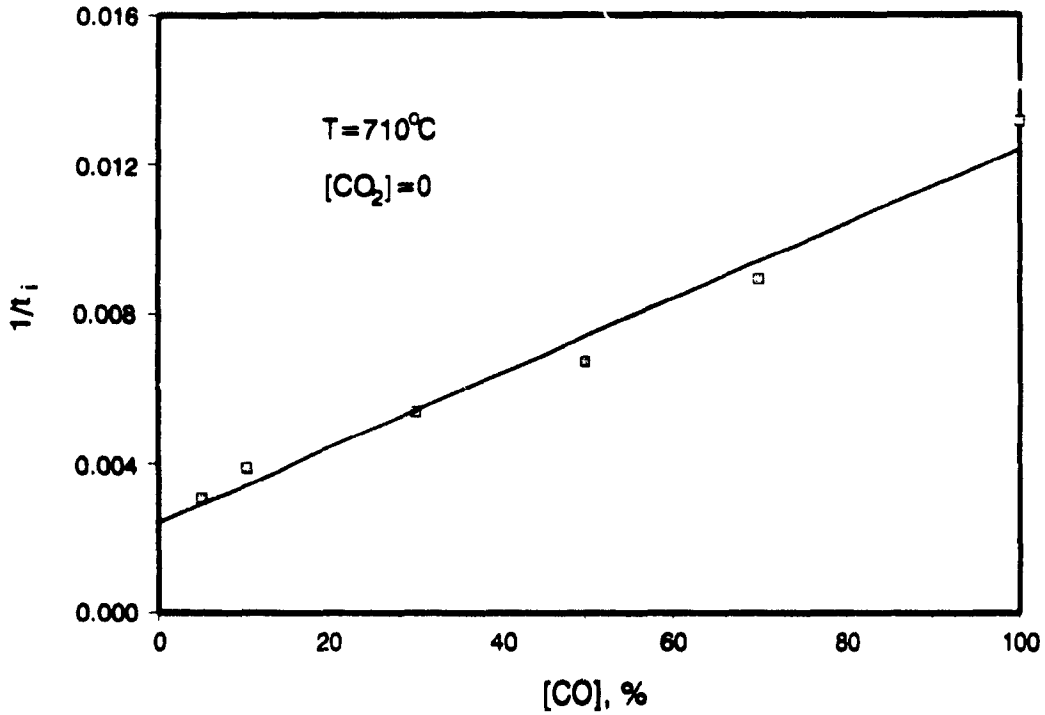

(b) $1/t_i$ versus [CO]

Figure 10 Influence of CO concentration on reduction

k_1 on the temperature and CO concentration.

Influence of CO_2 concentration

The effect of CO_2 concentration on the reaction constant and induction time is shown in respectively Figures 11(a) and 11(b). The induction time increases when the CO_2 concentration is increased. The initiation reaction, is more strongly retarded when the CO_2 concentration is larger than about 4%. The effect of CO_2 on the initiation can not be explained by its involvement in reaction (1), because this reaction has a large negative free energy and thus can be considered irreversible. In Chapter 6 it was suggested that the product gas may block the available nuclei sites. In the present case, the influence of CO_2 may also be explained by reaction (8) since this reaction has a small equilibrium constant of 0.098 at 720°C (i.e. at equilibrium when $[CO_2]$=5% and [CO]=50%). Thus it is thermodynamically impossible to form Na_2SO_3 according to reaction (8) when the $[CO_2]$ is larger than 5%. It is interesting to note that the decrease in $1/t_i$ with increasing $[CO_2]$ is stronger when $[CO_2]\geq 6\%$. However, in order to explain that initiation still occurs when $[CO]\geq 5\%$, another reaction must also be involved in the formation of the nuclei. As a possible reaction it is suggested that the following reaction:

$$Na_2SO_4 + 1/2\ C = Na_2SO_3 + 1/2\ CO_2 \qquad (9)$$

is involved. At 720°C, the equilibrium constant of this reaction is 0.17 $(atm)^{1/2}$, which is equivalent to an equilibrium concentration of CO_2 of 42% at 1 atmosphere total pressure. The small amount of carbon needed for reaction (9) is formed from the disproportion of CO according to reaction (3). It was speculated before that carbon may play a role as a catalyst in the reduction of sodium sulfate by CO (Budnikoff and Shilov, 1928). Since reaction (9) may be slower than reaction (8), the accelerated increase of the induction time above about 4% CO_2 in Figure 11(b) can be explained by that for CO>5% the nuclei are only formed by the slower reaction (9). Thus compared to the inhibiting effect of H_2O on the induction time when reducing sodium sulfate with H_2, the effect of CO_2 is more complex because the disproportionation of CO [reaction (3)] leads to an alternative reaction path for nuclei formation.

The effect of CO_2 on the rate constant of CO reduction, k_1, is very small and similar to that of H_2O on H_2 reduction of sodium sulfate.

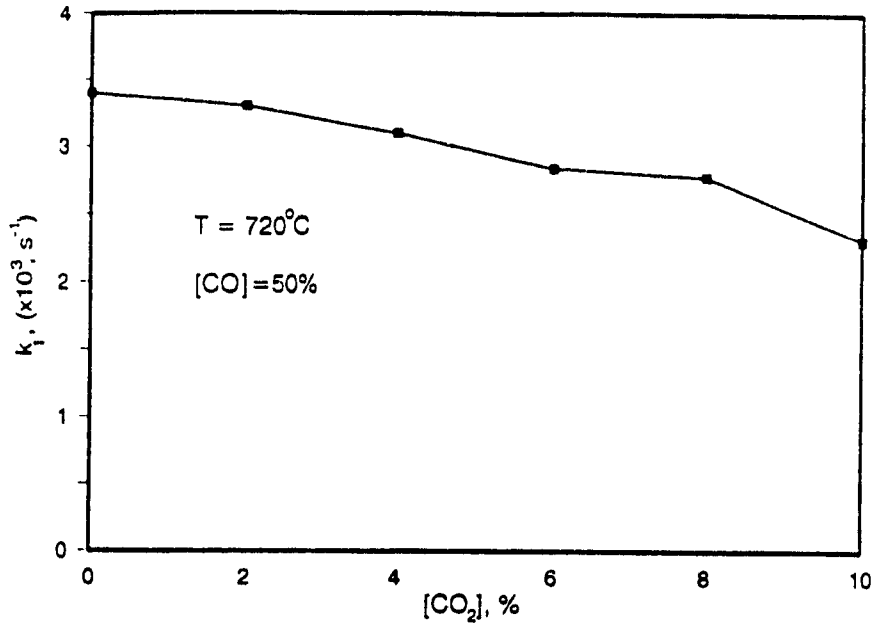

(a) k_1 versus $[CO_2]$

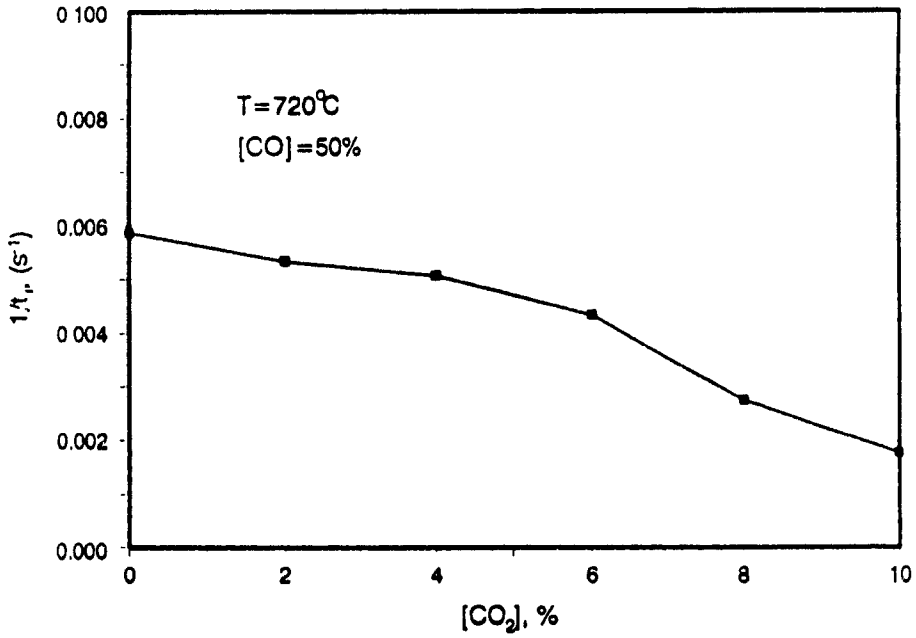

(b) $1/t_i$ versus $[CO_2]$

Figure 11 Influence of CO_2 concentration on reduction

Influence of sodium titanate molar fraction

Shown in Figure 12 are the Na_2SO_4 reduction results obtained with different molar fractions of sodium titanate. Also shown in Figure 12 is the reduction of pure sodium sulfate. It can be seen that the reduction of pure sodium sulfate initially proceeds reasonably fast, but than slows down dramatically after only a few percent conversion. SEM pictures of this reduced sample in Figure 13 shows that sintering has occurred after about 2 minutes at 720°C, i.e. significantly below the Na_2S-Na_2SO_4 eutectic melting point of 740°C. This sintering behavior restricts the access of CO to the reaction front. As the product layer increases in thickness, the CO flux is further reduced, making complete reduction extremely difficult. When mixed with more than 50% sodium titanate, the sulfate reduction is much faster and a complete reduction is achieved in a reasonable time. In this case the well dispersed mixture of sodium sulfate and high melting point sodium titanate does not sinter or melt as shown in Figure 14. Therefore the reduction could be completed in the solid state in the temperature range of 670-750°C. This is confirmed by the fact that similar to H_2 reduction, the CO reduction of a mixture of pure sodium sulfate and sodium titanate particles is not significantly improved because surface melting of the separate Na_2SO_4 still takes place.

The data in Figure 12 are fitted according to Eq.(5) and the kinetic equation for the shrinking core model with product layer diffusion control:

$$1-3(1-X)^{2/3}+2(1-X) = kt \qquad (10)$$

in respectively Figures 15(a) and 15(b). Figure 15(a) shows that only for a sodium titanate fraction of 75 and 95% the reduction is well described by the nucleation and growth model over a wide range of conversions with k_1 being respectively 1.60×10^{-3} s^{-1} and 1.25×10^{-3} s^{-1}. However for lower molar fraction of sodium titanate the reduction is described by the shrinking core model with product layer diffusion control [Figure 15(b)]. This effect of the molar fraction of sodium titanate is consistent with the improved access of CO to the reactant front provided by the non-sintering sodium titanate.

Proposed reduction mechanism

Based on the present experiments and evidences in literature, the following reaction mechanism is proposed for sodium sulfate reduction.

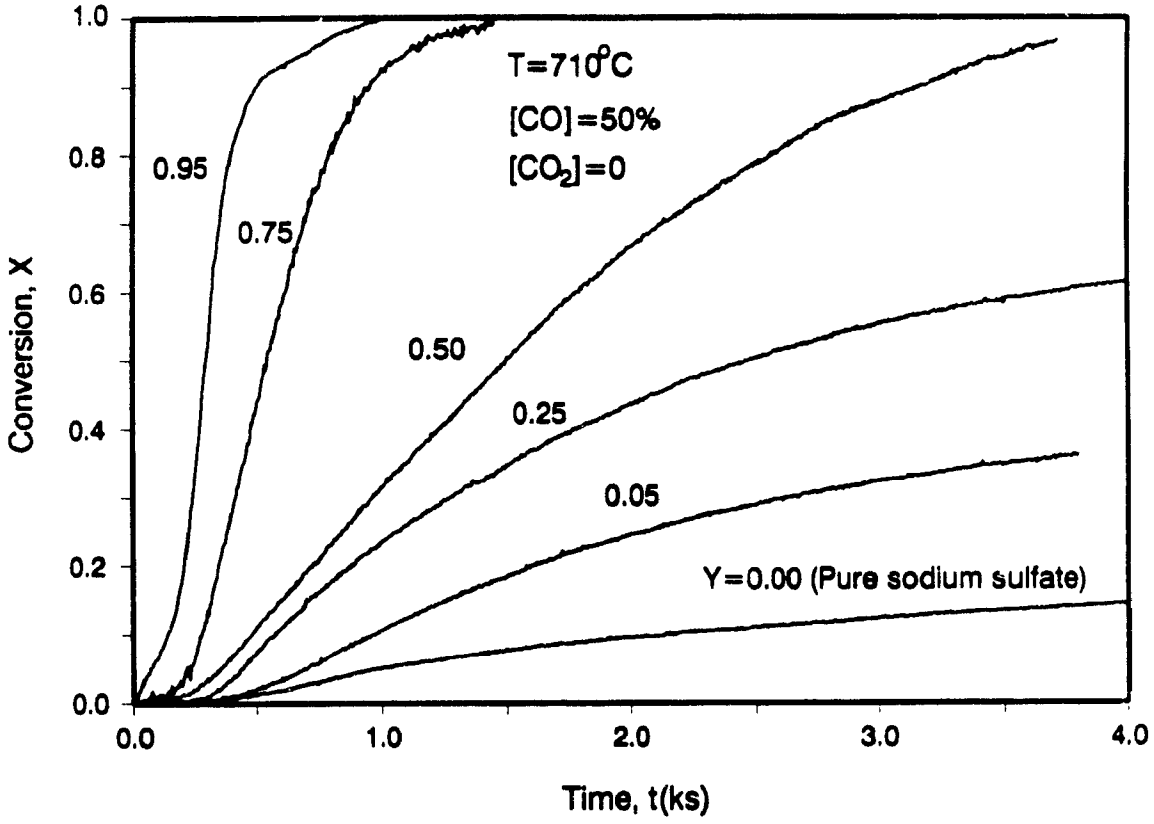

Figure 12 Influence of sodium titanate molar fraction on reduction

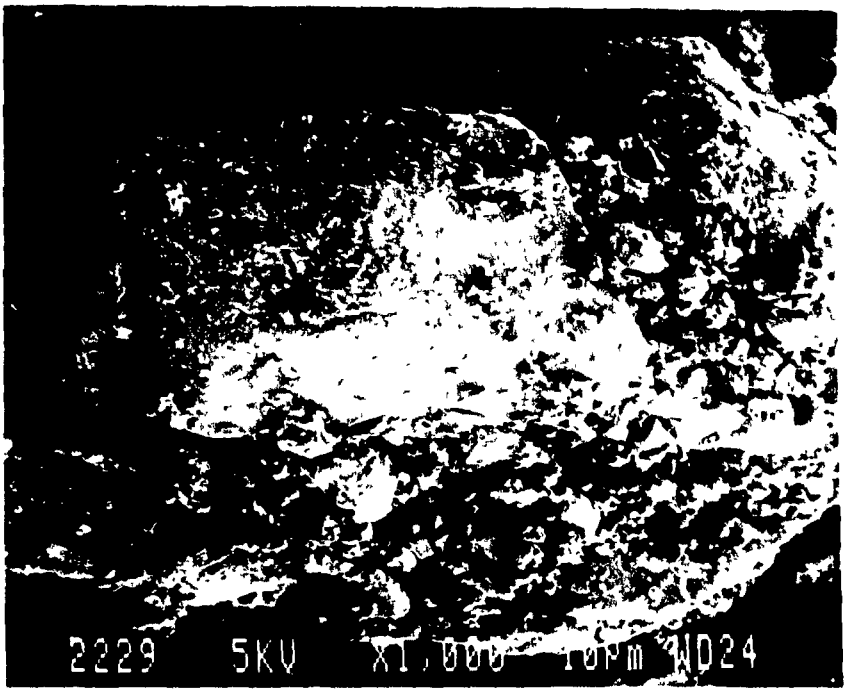

(a) Sample before reduction

(b) Sample after reduction at 720°C for 20 minutes

Figure 13 SEM pictures of the pure sodium sulfate before and after reduction

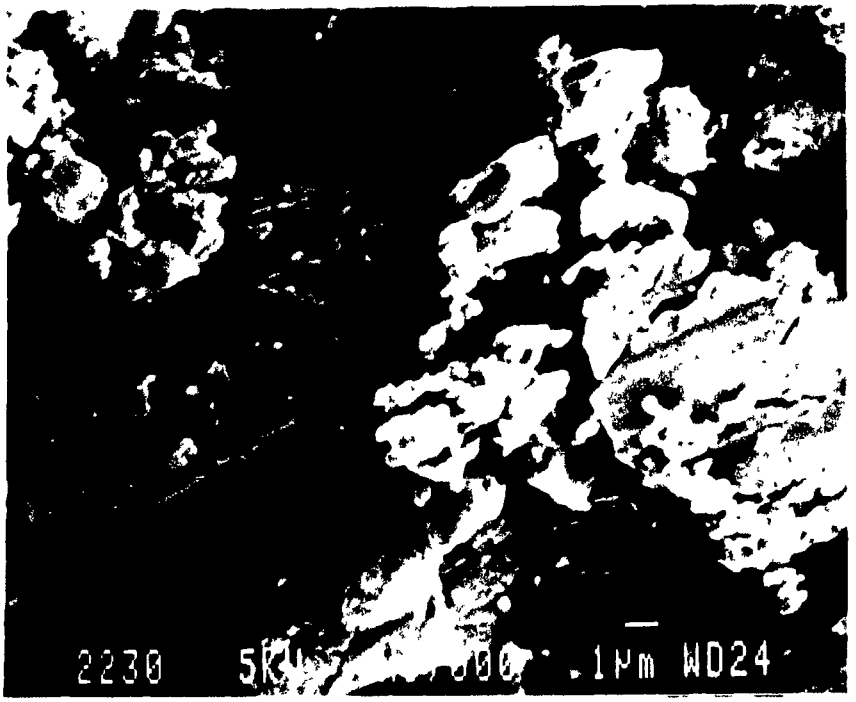

(a) Sample before reduction

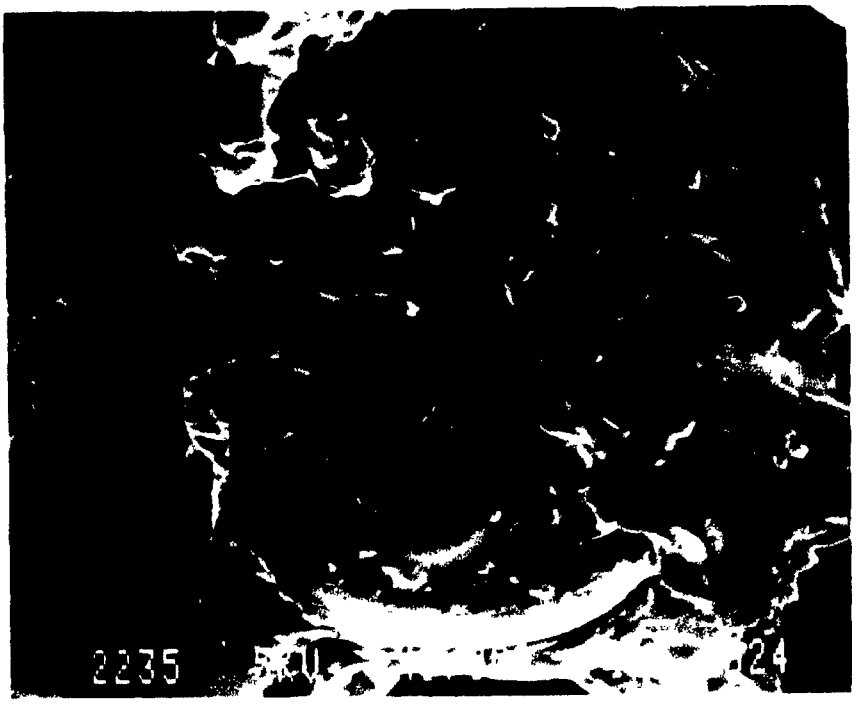

(b) Sample after reduction at 720°C for 30 minutes

Figure 14 SEM pictures of model mixture before and after reduction

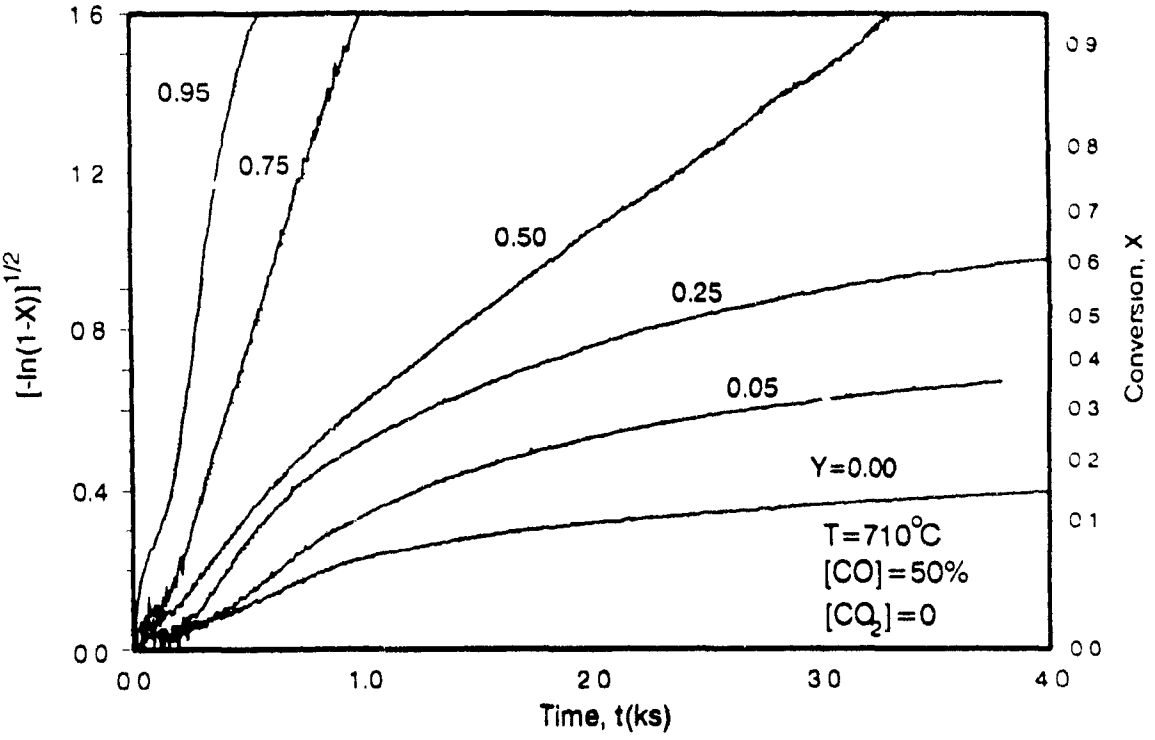

(a) $[\ln(1-X)]^{1/2}$ versus t

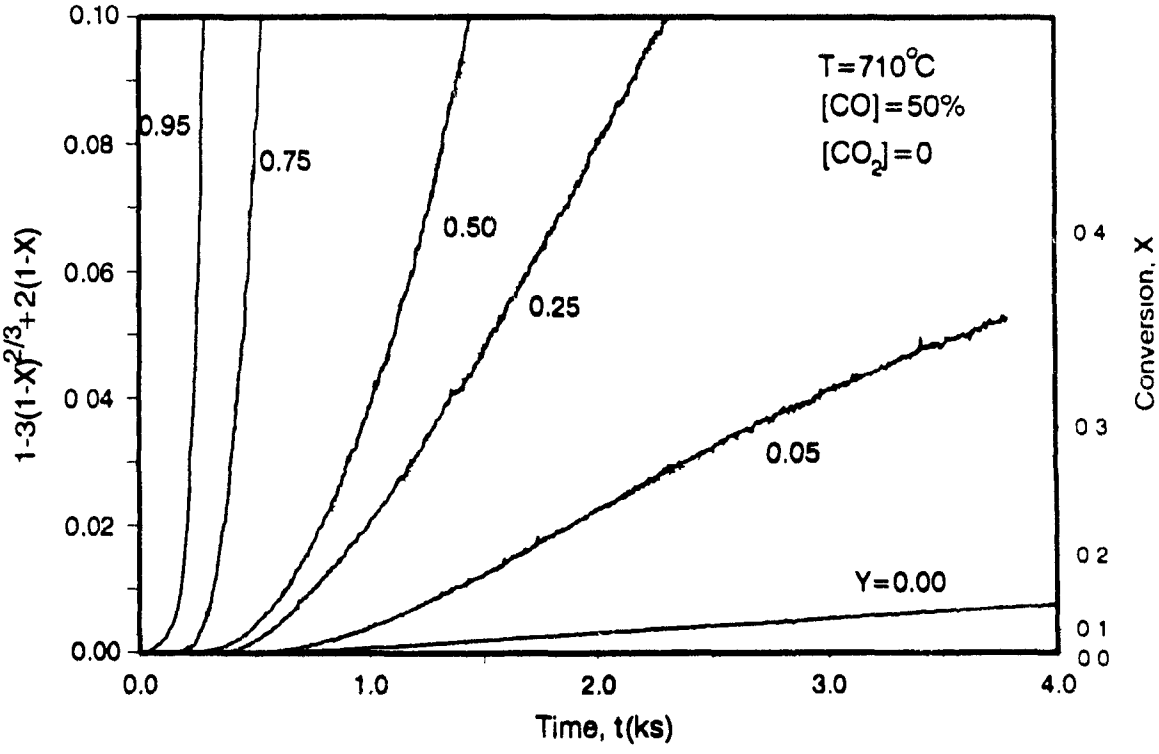

(b) $1-3(1-X)^{2/3} + 2(1-X)$ versus t

Figure 15 Model Fitting of the Data in Figure 12

In the induction period, sodium sulfate is most likely reduced to sodium sulfite by CO as

$$Na_2SO_4 + CO = Na_2SO_3 + CO_2 \quad (8)$$

When reaction (7) is thermodynamically unfavorable because of a high CO_2 concentration, Na_2SO_4 reduction by carbon is still possible via

$$Na_2SO_4 + 1/2\ C = Na_2SO_3 + 1/2\ CO_2 \quad (9)$$

Evidences for this reaction are the reduction experiments with carbon by Li (1989) of Na_2SO_4 mixed with Na_2CO_3 and the finding that carbon enhances the reduction of Na_2SO_4 both by H_2 and CO (Kunin et al., 1965). Sodium sulfite is subsequently rapidly further reduced by CO to sodium sulfide:

$$Na_2SO_3 + 3\ CO = Na_2S + 3\ CO_2 \quad (11)$$

or because Na_2SO_3 is unstable at high temperatures, it decomposes as:

$$4\ Na_2SO_3 = Na_2S + 3\ Na_2SO_4 \quad (12)$$

Both reaction (11) and (12) are thermodynamically very favorable with free energy of -138 and -195 kJ/mol, respectively. Evidences for the relative ease of reaction (11) and (12) are that the reduction of sodium sulfite by CO and decomposition of sodium sulfite were found to start at temperature as low as 600°C (Foerster and Kubel, 1924; Li, 1989). A very small amount of Na_2SO_3 was found during Na_2SO_4 reduction in Nyman and O'Brien's study (1947) and also detected by FTIR in the early stage of the reduction of sodium sulfate by Weston (1986). Since the induction time is strongly affected by the CO concentration, and its temperature dependence is in the range expected for gas-solid reaction, it seems likely that reaction (8) is the rate controlling step for the nuclei formation when the CO_2 concentration is low.

After formation of sufficient Na_2S nuclei or with the addition of Na_2S, the solid-solid reaction between Na_2S and Na_2SO_4 and the reduction of intermediates according to the following overall reactions:

$$Na_2S + Na_2SO_4 = \text{intermediates} \quad (7)$$

$$\text{Intermediates} + CO = Na_2S \qquad (13)$$

determine the overall conversion of Na_2SO_4 in the nucleation and growth period. The combination of these two reactions as rate controlling steps accounts for the high activation energy and the effect of CO on the reduction. Both reactions (7) and (13) are not significantly affected by the presence of CO_2.

PART II Iron Oxide Catalyzed Reduction

Several workers (White and White, 1936; Nyman and O'Brien, 1947; Bagbanly and Yu, 1961; Kunin et al., 1965; Birk et al., 1971) have studied the catalytic reduction of sodium sulfate. The catalysts investigated were iron compounds, copper compounds, nickel sulfide, platinum oxide, sodium sulfide, graphitized coal, sodium oxalate, sodium carbonate, lithium carbonate and potassium carbonate. 1.5% weight (or less) of iron added either as sulfate or as an oxide was demonstrated to be most effective. Therefore in the present work, 1.5% by weight of iron oxide was mixed mechanically with the model mixture. Although the COS concentration was somewhat higher with the presence of iron oxide, the side reaction (2) could still be neglected as was shown by analysis of both the solid and gas phases. In the presence of iron oxide, reduction was accelerated dramatically as can be seen in Figure 16. The reduction rate with iron oxide at 690°C was about 10 times higher than that without iron oxide. The induction time was also dramatically reduced. The kinetic results at different temperatures are shown in Figure 17. The iron oxide catalyzed reduction kinetics were also well fitted by the nucleation and growth model as shown in Figure 17(b). Regression analysis of the 4 lowest temperatures in the Arrhenius plot of the rate constants in Figure 18 gives an activation energy of 280 kJ/mol. The rate constant at 710°C was affected by mass transfer, since the ratio of the maximum CO consumption rate and the mass transfer rate, r_{max}/N_{CO} was 0.20. The addition of iron oxide reduced the activation energy considerably compared to 420 kJ/mol for uncatalyzed reaction. This indicates a possible change in the reduction mechanism as a result of the iron oxide addition.

There are at least two major ways by which iron or iron oxide could catalyze the reduction: (i) it can act as a heterogeneous (surface) catalyst or (ii) it or one of its reaction intermediates can directly reduce sulfate.

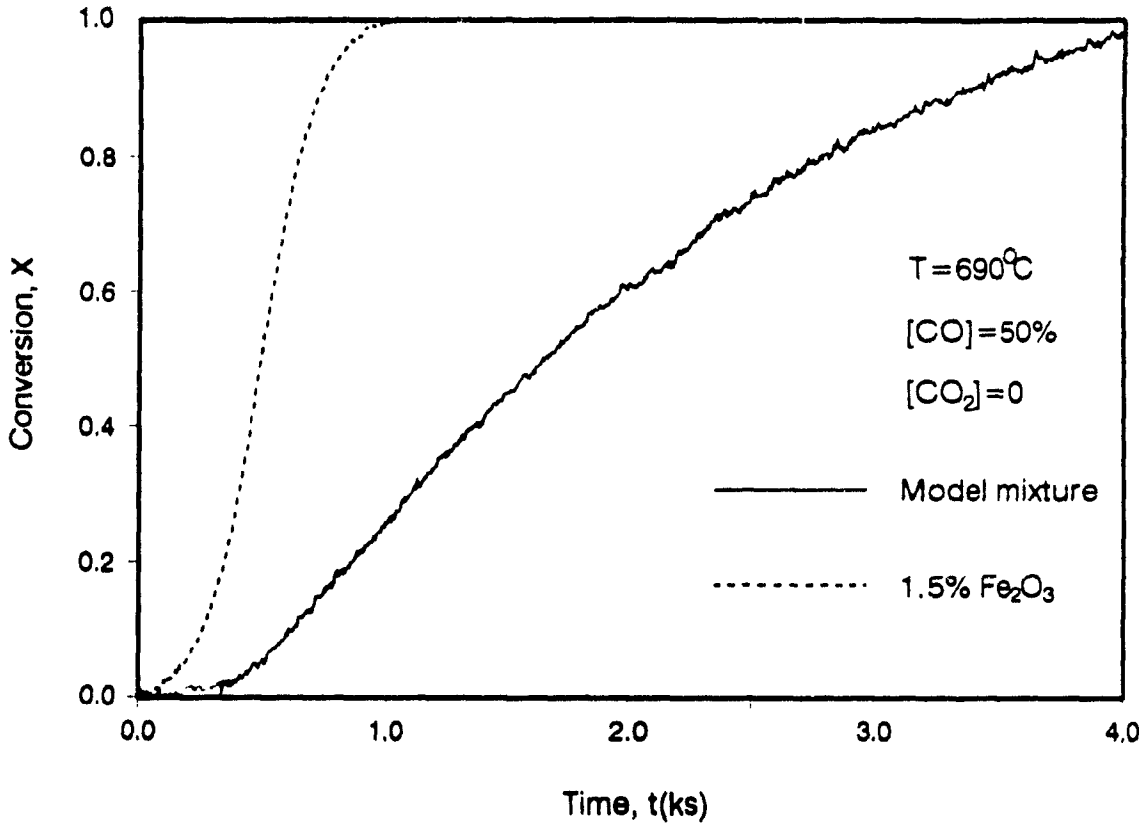

Figure 16 Influence of iron oxide addition on reduction

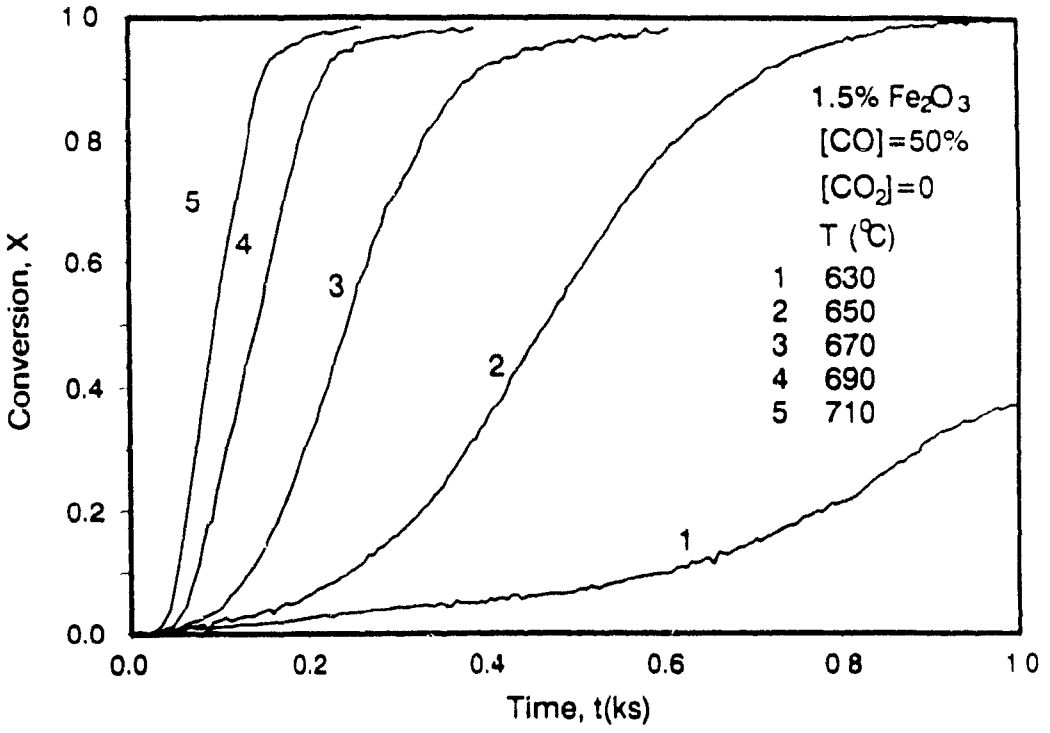

(a) X versus t

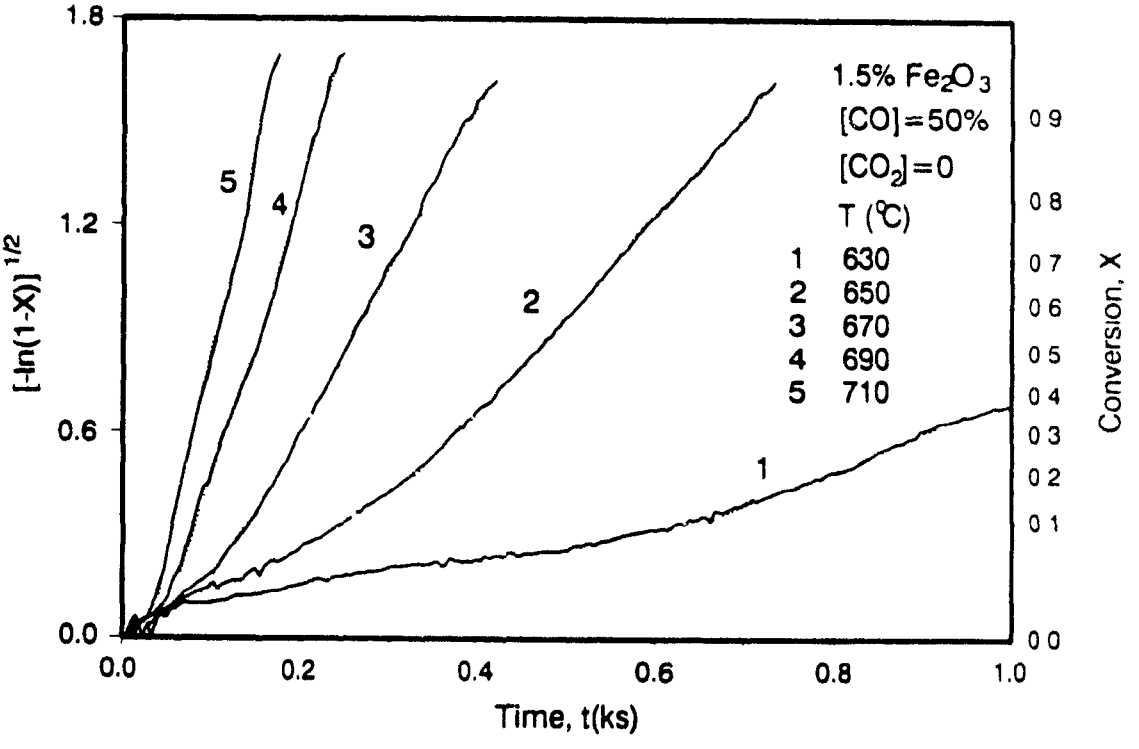

(b) $[\ln(1-X)]^{1/2}$ versus t

Figure 17 Iron oxide catalyzed reduction kinetics

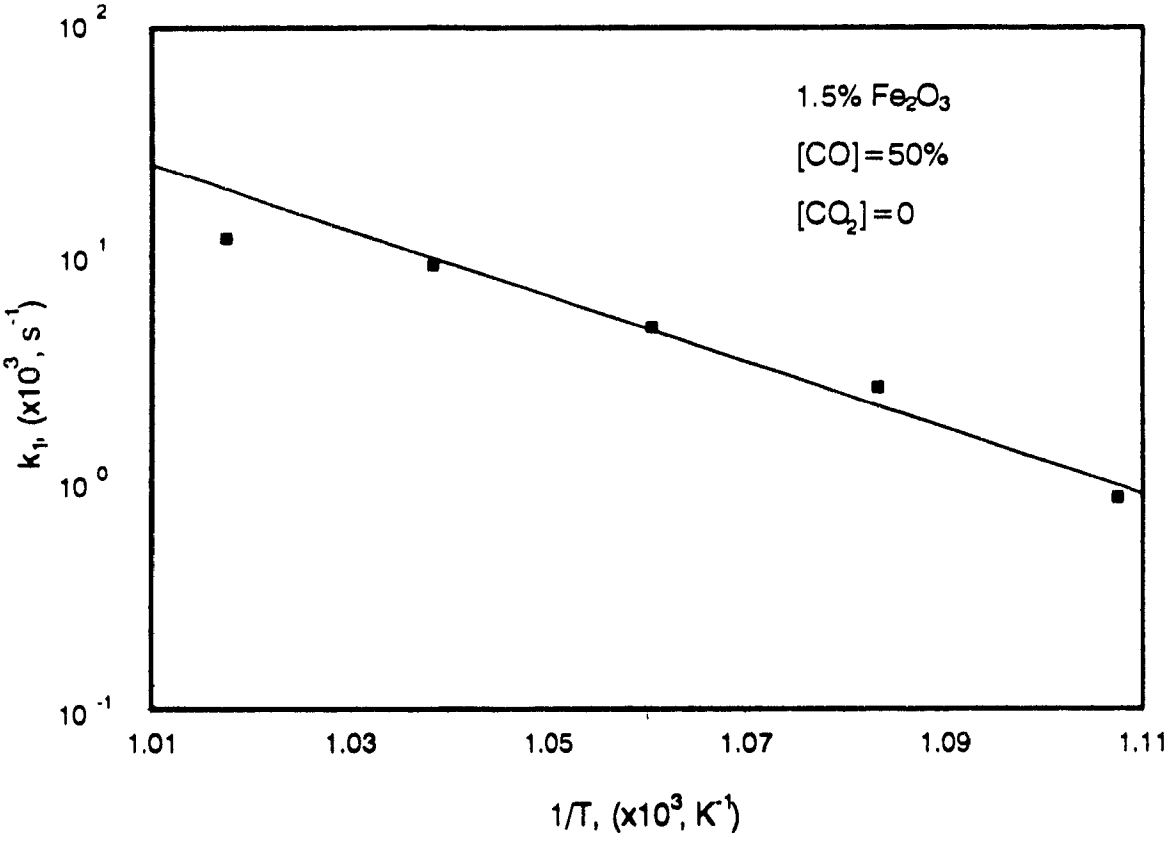

Figure 18 Arrhenius plot of rate constants with iron oxide addition

The former was widely found for the reduction of metal oxides and other catalytic gas-solid reactions, and was explained by the easier formation of product nuclei because of the ability of these metals to activate hydrogen (Delmon, 1969). In this interpretation, the foreign metals are thought to play the same role as the nuclei in the reduction. However this mechanism is unlikely in the present case, because sulfide, is usually a severe poison for surface catalysis. Therefore it seems more likely that the iron-containing species interacts with the sulfur-containing species. Since FeS is thermodynamically favorable at the present temperatures, the following mechanism is proposed similar to that for hydrogen reduction in Chapter 6.

$$FeS + Na_2SO_4 = Na_2S + FeSO_4 \quad (14)$$

$$FeSO_4 + CO = FeS + CO_2 \quad (15)$$

Or more generally, similar to the catalytic function of Na_2S via reaction (7), a catalytic mechanism can be formulated as:

$$FeS + Na_2SO_4 = \text{intermediate} \quad (16)$$

$$\text{intermediate} + CO = FeS + Na_2S + CO_2 \quad (17)$$

This mechanism is supported by the evidence that FeS, $FeSO_4$ and other metal sulfides or sulfates are just as good catalyst as iron oxide for the reduction (Birk et al., 1971).

PART III Reduction of Combusted Black Liquor Sample with TiO_2

In Chapter 6, it was found that the hydrogen reduction of kraft black liquor combusted with TiO_2, was much faster than that of the equivalent model mixture. Therefore the same experiments were repeated with CO. The preparation of the combusted kraft black liquor sample was given earlier in the experimental part of this chapter. The composition of kraft black liquor solids used for combustion is shown in Table 4. After complete combustion with TiO_2 in the tube furnace, the residue has a composition of approximately 20% (mole) sodium sulfate and 80% (mole) sodium titanate (as $4Na_2O.5TiO_2$).

Table 4 Elemental Composition of Kraft Black Liquor Solids

i) Main elements

Elements	Na	S	C	H	O	Cl	K
% (wt.)	22.90	2.90	31.67	2.64	33.04	0.16	1.46

ii) Other elements

Elements	Al	Si	Mn	Cr	Fe	Ti
ppm	1700	120	10.3	8	44	0

The reduction results of kraft black liquor combusted with TiO_2 are shown in Figure 19. The experimental data are very similar to those obtained with the model mixtures. The reduction results in Figure 19 are also well described by the nucleation and growth model and an activation energy of 244 kJ/mol is obtained as shown in Figure 20. Comparison with model mixture results shows that the reduction of kraft black liquor combusted with TiO_2 proceeds significantly faster. The faster reduction can be explained by two factors: i) the presence of impurities in kraft black liquor such as the metals, K, Al, Si, Fe, Cr, and Mn which could catalyze the reduction. ii) the distribution of sodium sulfate in combusted kraft black liquor is better than that in the model mixture. The explanation for the latter might be that the mixture of kraft black liquor and TiO_2 swells considerably, and sodium carbonate and sodium sulfate mixture, and even sodium titanate ($4Na_2O{\cdot}5TiO_2$) might melt as a result of the large heat release during the combustion. The better distribution of Na_2SO_4 in combusted kraft black liquor was confirmed by SEM-EDS mapping in Chapter 6.

IMPLICATIONS

The implication of the above reduction studies is that complete reduction of a mixture of kraft black liquor combusted with TiO_2 can be achieved in the

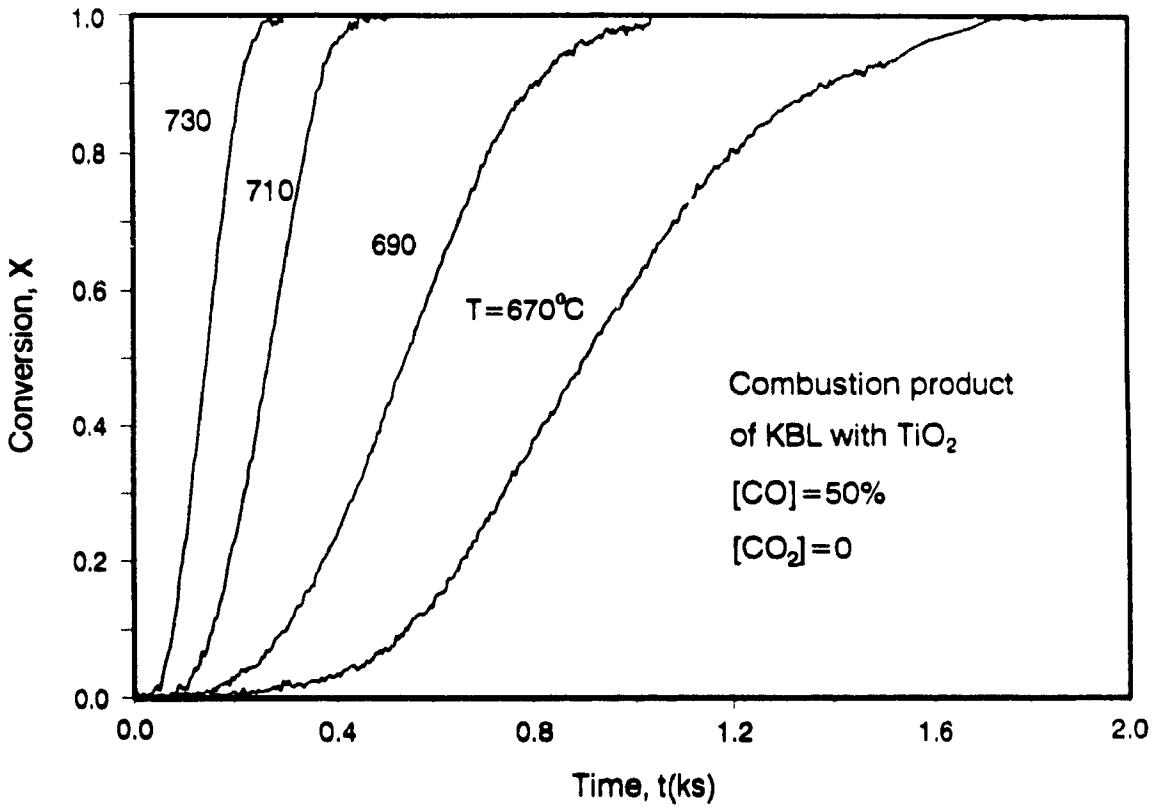

Figure 19 Reduction data of combusted kraft black liquor with TiO_2

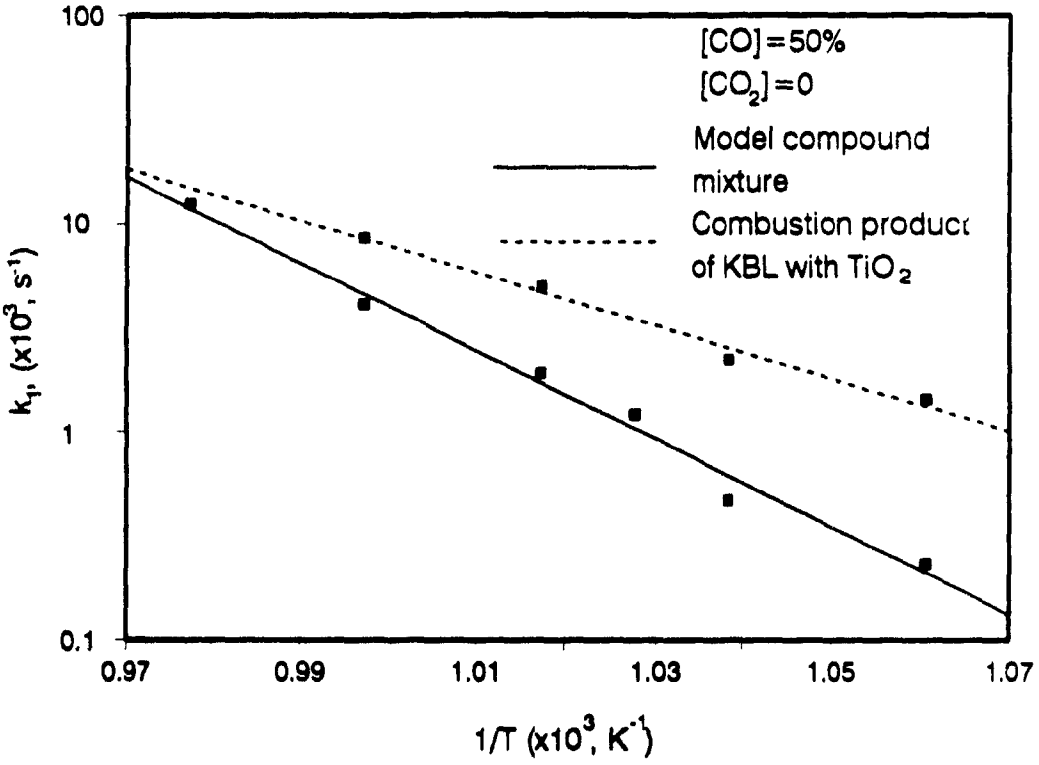

Figure 20 Arrhenius plot of rate constants of kraft black liquor sample

solid state over a temperature range of 650-750°C by CO. A fluidized bed reactor appears to be the ideal system to achieve complete reduction by CO and/or H_2 in a relatively short time in an industrial operation.

CONCLUSIONS

Complete reduction of sodium sulfate mixed with sodium titanate by CO is achieved in the solid state below 750°C. The CO reduction kinetics are well described by the nucleation and growth model. An activation energy of 420 kJ/mol is obtained for the reaction constant of the nucleation and growth kinetics. A reduction mechanism is proposed which includes both gas-solid and solid-solid reactions as rate controlling steps. The effect of the CO and CO_2 concentrations on the reduction is explained. The addition of sodium sulfide can eliminate the induction period for the formation of the nuclei. The reduction is catalyzed by iron oxide and the activation energy of the catalyzed reduction is 280 kJ/mol. The reduction of combusted kraft black liquor sample is faster than that of the model mixture and its activation energy is 244 kJ/mol.

NOMENCLATURE

a	=Power in a relationship between k_1 and [CO].
[CO]	=CO concentration, %.
$[CO_2]$	=CO_2 concentration, %.
d_p	=Particle size, μm.
E	=Activation energy, kJ/mol.
ΔG°	=Free energy change, J/mol.
ΔW_L^T	=Calcculated weight loss, mg.
ΔW_L^E	=Measured weight loss, mg.
k_1	=Rate constant, s^{-1}.
k_g	=Mass transfer coefficient, m/s.
K_e	=Equilibrium constant.
m	=Power in nucleation and growth model.
Nco	=Mass transfer rate of CO, mol/m^2s.
r_{max}	=Maximum reaction rate, mol/m^2s.
R	=Universal gas constant, J/mol K.
t	=Time, s.

t_i =Induction time, s.

T =Temperature, K.

W =Weight, mg.

W_0 =Initial weight, mg.

W_s =Sample weight, mg.

W_s^o =Sulfur weight in initial sample, mg.

W_s^o =Sulfur weight in reduced sample, mg.

X =Conversion.

Y =Sodium titanate molar fraction.

Greek symbols

ε_s =Percentage difference of sulfur mass, %.

ε_w =Percentage difference of weight loss, %.

REFERENCES

Andersson, S., "Studies on Phase-Diagrams Na_2S-Na_2SO_4, Na_2CO_3-Na_2S-Na_2SO_4, Na_2CO_3-Na_2SO_4-NaOH, and Na_2CO_3-Na_2S-NaOH", *Chemical Scripta*, 1982, 20, p.164-170.

Bagbanly, I.L., and F. Yu, "Reduction and Carbonization of a Mixture of Alkali Metals to Obtain the Na_2CO_3, Potash and Caustic alkalies", *Azerbaidzahn. Khin. Zhur.*, (Russ.), 111, 1959: Chem. Abstr. 55: 10,817c, 1961.

Birk, J.R., C.M. Larsen, W.G. Vaux and R.D. Oldenkamp, "Hydogen Reduction of Alkali Sulfate", *Ind. Eng. Chem. Proc. Des. Dev.*, 1971, 10(1), p.7.

Budnikoff, P.B., and E. Shilov, "The Reduction of Sodium Sulfate to Sodium Sulfide Particularly by Hydrogen and Carbon Monoxide in the Presence of Catalysts", *J. Soc. Chem. Ind.*, 1928, 6(4), p.111T.

Cameron, J.H. and T.M. Grace, "Kinetic Studies of Sulfate Reduction with Carbon", *Ind. Eng. Chem. Fundam.*, 1983, 22(4), p.486.

Cameron, J.H., and T.M. Grace, "Kinetic Study of Sulfate Reduction with Kraft Black Liquor Char", *Ind. Eng. Chem. Fundam.*, 1985, 24(4), p.443.

Dearnalery, R.I., D.H. Kerridge and D.J. Rogers, "Molten Lithium Sulfate -Sodium Sulfate-Potassium Sulfate Eutectic: Reactions of Some Sulfur Compounds", *Inorg. Chem.*, 1983, 22, p.3242.

Delmon, B., "Introduction â la Cinétique Hétérogène", *Technip Publ.*, Paris, 1969.

Foerster, V.F. and K. Kubel, "Reduction of Alkali sulfate", *Z. Anorg. Allge.*

Chem., 1924, 139, p.261.

Galwey, A.K., D.M. Jamieson and M.E. Brown, "Thermal Decomposition of Three Crystalline Modification of Anhydrous Copper(II) Formate", *J. Phys Chem.*, 1974, 78, p.2664.

Kunin, V.T., V.A. Nikitin and I.P. Kirillov, "Reduction of Na_2SO_4 by Products of the Pyrolysis of Petroleum Materials", *Izv Vysshikh Vchebn Zavedenii, Khim. I Khim. Tekhnol.*, 1965, 8(6), P.974, (Russian), Chem. Abstr., 64: 15,638 b, 1966.

Li, J. and A.R.P. van Heiningen, "Kinetics of Sodium Sulfate Reduction in the Solid State by Carbon Monoxide", *Chem Eng Sci.*, 1988, 43(8), p.2,079-2,085.

Li, J., and A.R.P. van Heiningen, "Effect of the Presence of a Molten Phase on the Rate of Sodium Sulfate Reduction by CO", submitted to *JPPS*, 1991.

Li, J., "Rate Processes during Gasification and Reduction of Black Liquor Char", *Ph.D. Thesis*, McGill University, Montreal, 1989.

Meyer, R.J., *Gmelins Handbook of Inorganic Chemistry*, 8th ed. (Ger.), Vol.21, p.184-205, Verlag Chemie Weinheim, Germany, 1965.

Nyman, C.J. and T.D. O'Brien, "Catalytic Reduction of Sodium Sulfate", *Ind. Eng. Chem*, 1947, 39, p.1,019.

Polyvyannyi, I.R. and R.S. Demchenko, R.S., "Reduction of Na_2SO_4", *Izvest Akad. Nauk. Kazakh.*, SSR, Ser. Met. Obogashchen. i Ogenuporov (Russ.), 1960, p.34, Chem. Abstr.: 55, 198e, 1961.

Powell, C.F., *Vapour Deposition*, C.F. Powell, J.H. Oxley, and J. M. Blocher, Jr., eds. p. 343, J. Wiley and Sons, N.Y., 1966.

Puttagunta, V.A., W.J. Decoursey and N.N. Bakhshi, "Reduction of Sodium Sulfate with Hydrogen in a Fluidized Bed Reactor", *Can. J. Chem. Eng.* 1970, 48(2), p.73.

Roman, A. and B. Dolmon, "Promotor and Carrier Effects in the Reduction of NiO/SiO_2", *Journal of Catalysis*, 1973, 30, p.333-342.

Sjoberg, M. and J. Cameron, "A Kinetic Study of Sodium Sulfate Reduction by Carbon Monoxide Gas", *AIChE Symposium Series*, 1981, 76, 200, p.35-40.

Weston, T.A., "The Regeneration of High Temperature Sulfur Dioxide Sorbents: The Carbon Monoxide Reduction of Supported Alkali Sulfate", *Ph. D Thesis*, California Institute of Technology, Ann Arbor, 1986.

White, J. F. M., and A. H. White, "Manufacture of Sodium Sulfide: Reduction of Sodium Sulfate to Sodium Sulfide at Temperatures below 800°C", *Ind. Eng. Chem.*, 1936, 28(2), p.244.

CHAPTER 8

GENERAL CONCLUSIONS

GENERAL SUMMARY

Kraft black liquor is the spent liquid formed during pulp production by digestion of wood in an aqueous solution of sodium hydroxide and sodium sulfide at elevated temperature and pressure. Recovery of the inorganic chemicals and thermal energy, by burning the concentrated black liquor, has been an integral part of alkaline pulping almost from the outset for economical and environmental reasons. Although the objective of chemical recovery is adequately achieved, there are major drawbacks associated with the present commercial recovery process. One of the potential less capital intensive, simpler, cleaner, and safer alternatives is the **Direct Causticizing Process** with an amphoteric metal oxide as causticizing agent. However, for development of this alternative technology, fundamental knowledge is needed of the chemical and physical processes which take place during the different process steps.

This thesis is concerned with the thermodynamic analysis of **Direct Causticizing Process** configurations and with the determination of the rate processes occurring during combustion and direct causticizing of kraft black liquor, as well as during reduction of sodium sulfate in this combustion product by H_2 and CO. A thermogravimetric analysis (TGA) and tube furnace system are the main experimental facilities used to determine the kinetics and mechanism of these reactions. Other supporting techniques include gas analysis by IR analyzer and gas chromatography, analysis of the ions by ion chromatography, and analysis of the solid samples by SEM, SEM-EDS and X-ray diffraction. Model mixtures and actual kraft black liquor samples are used in this study.

CONTRIBUTIONS TO KNOWLEDGE

1. A comprehensive thermodynamic analysis is performed of the direct causticization of kraft black liquor with amphoteric metal oxides. It is concluded that TiO_2 is the only technically viable metal oxide, and two process configurations are proposed for direct causticizing of kraft black liquor by TiO_2. The influence of temperature, TiO_2/Na_2O molar ratio and air ratio is established.

2. The kinetics and mechanism of CO_2 release from Na_2CO_3 by TiO_2 are determined. The formation of $4Na_2O{\cdot}5TiO_2$ is a fast reaction even in the solid state. Further reaction with Na_2CO_3 to $Na_2O{\cdot}TiO_2$ is a relatively slow reaction. The rate of $4Na_2O{\cdot}5TiO_2$ formation is well described by the solid-solid reaction model with product layer diffusion control. The influence of CO_2 and the presence of Na_2SO_4 on the Na_2CO_3 conversion is measured.

3. $Na_2O{\cdot}3TiO_2$ obtained after hydrolysis of $4Na_2O{\cdot}5TiO_2$ and $Na_2O{\cdot}TiO_2$ is even more reactive towards the Na_2CO_3 than TiO_2 at high temperature (above 775°C). The reaction kinetics of the reaction between Na_2CO_3 and $Na_2O{\cdot}3TiO_2$ are also described by the solid-solid reaction model with product layer diffusion control.

4. The addition of TiO_2 into kraft black liquor improves the combustion of kraft black liquor and reduces the sulfur emission. It also increases the melting point of the combusted product.

5. Simultaneous combustion and direct causticization of kraft black liquor can easily be achieved with a TiO_2/Na_2CO_3 molar ratio larger than 1.25, provided that sufficient heat is supplied. A high causticizing efficiency could be obtained with recycled $Na_2O{\cdot}3TiO_2$.

6. The hydrolysis of $Na_2O{\cdot}TiO_2$ and $4Na_2O{\cdot}5TiO_2$ yields a sodium hydroxide solution and a precipitate of $Na_2O{\cdot}3TiO_2$. The degree of hydrolysis is 66.6% and 58.0%, respectively for $Na_2O{\cdot}TiO_2$ and $4Na_2O{\cdot}5TiO_2$, in a agreement with thermodynamic analysis.

7. Sodium sulfate intimately mixed with sodium titanates can be

effectively reduced by H_2 or CO in the solid state below 750°C. Sodium sulfate in the combustion product of kraft black liquor and TiO_2 is even faster reduced because of the presence of trace quantities of catalytically active elements and the fine distribution of S, Na and Ti in the solids.

8. The reduction of sodium sulfate mixed with sodium titanates by H_2 or CO is accelerated by the initial presence of Na_2S and the addition of 1.5% iron oxide catalyst.

9. The reduction kinetics of sodium sulfate mixed with TiO_2 is well described by nucleation and growth model up to 60% conversion when H_2 is used as reducing agent and up to 95% conversion when CO is used. The H_2 reduction kinetics for conversion higher than 60% are well described by the shrinking core model with product layer diffusion control.

10. The reduction mechanism of Na_2SO_4 by H_2 and CO involves both gas-solid and solid-solid reactions. The initial nucleation is controlled by the conversion of Na_2SO_4 to Na_2SO_3. The subsequent nucleus growth is dominated by the solid-solid reaction of Na_2SO_4 and Na_2S.

11. The presence of H_2O and CO_2 retards the formation of Na_2S nuclei but does not significantly influence the subsequent growth of the Na_2S nuclei. Therefore with the initial addition of Na_2S, the influence of H_2O and CO_2 on the reduction of Na_2SO_4 is very small.

12. The difficulty to reduce pure sodium sulfate reduction with H_2 and CO is due to the formation of a liquid Na_2S layer which prevents further contact between Na_2SO_4 and the reducing gases. Since the presence of high melting sodium titanate prevents the formation of a continuous Na_2S layer, the reduction rate increases with increasing molar fraction of sodium titanate.

RECOMMENDATIONS AND SUGGESTIONS FOR FUTURE WORK

1. To determine the kinetics and the rate controlling step of the hydrolysis of $Na_2O{\cdot}TiO_2$ and $4Na_2O{\cdot}5TiO_2$ and the separation of $Na_2O{\cdot}3TiO_2$.

2. To study the influence of the particle size of TiO_2 or $Na_2O{\cdot}3TiO_2$ on

the direct causticizing of Na_2CO_3, on the reduction of Na_2SO_4 in the direct causticized product, and on the hydrolysis of the reduced mixture.

3. To study the mechamism of the rate processes mentioned in 2) using pellet samples.

4. To study the steam and CO_2 gasification of kraft black liquor mixed with TiO_2.

5. To study the influence of the TiO_2/Na_2CO_3 molar ratio on the reduction of Na_2SO_4 in the combustion product of kraft black liquor.

6. To study the reduction of sodium sulfate by a mixture of CO and H_2 or CH_4.

7. To compare the direct causticizing process with TiO_2 to the conventional recovery process using mass and energy balances and subsequent techno-economic analysis.

8. To study the combustion and direct causticizing, and reduction of kraft black liquor in a pilot fluidized bed.

9. To study the direct causticizing of kraft black liquor by ilmenite.

10. To study the effect of pressurization on the direct causticizing of kraft black liquor with TiO_2 in the gasification and combustion-reduction process configurations.

APPENDIX 1

Sh in Eq.(9) of Chapter 6 can be calculated from the following equation (Li, 1989):

$$\frac{Sh/Sc^{1/3} + 1.68}{1.63\ Re} = \{ 1 + [\frac{1.28}{Re^{0.6}} + \frac{1.1}{Re^{0.23}}]^n \}^{1/n} \qquad (1)$$

with n=6 when 0.3<Re<170. In Eq (1):

Sc: Schmidt number ($=\mu/(\rho D)$)

Re: Reynold Number ($=d_c V\rho/\mu$)

Sh: Sherwood Number ($=k_g d_c/D$)

The parameters in the non-dimensional groups are defined as:

$D_{a\text{-}m}$: the diffusion coefficient of "a" in the gas mixture, m^2/s.

d_c: the sample pan diameter (= 0.01 m in this study), m.

μ: the viscosity of the gas mixture, Pa/s.

ρ: the density of the gas mixture, kg/m^3.

V: the average gas velocity based on the reactor tube cross section, m/s.

The diffusion coefficient $D_{a\text{-}m}$ was calculated as (Treybal, 1968):

$$D_{a\text{-}m} = \frac{1-y_a}{\sum_{i=1}^{n} \frac{y_i}{D_{ai}}} \qquad (2)$$

where y is the mole fraction of each component in the mixture, D_{ai} is the binary diffusion coefficient of "a" and "i", which was calculated by Fuller's method (Fuller, 1966):

$$D_{ai} = \frac{10^3\ T^{1.75}\ (1/M_a + 1/M_i)^{1/2}}{P[(\sum_a (v_i)^{1/3} + (\sum_i (v_i)^{1/3}]} \qquad (3)$$

where M is molecular weight, T the absolute temperature in Kelvin, P pressure in atm and $\sum_a v_i$ the sum of the diffusion volumes. The viscosity of the feeding gas mixture was calculated by Eq.(4) proposed by Perry and Chilton (1969):

$$\mu_m = \frac{\sum y_i \mu_i (M_i)^{1/2}}{\sum y_i (M_i)^{1/2}} \qquad (4)$$

where μ_i is the viscosity of each component.

By means of Eq.(10) in Chapter 6 and Eq.(1), the values of k_g were found at all temperatures investigated and are shown in Table 3 of Chapter 6.

NOMENCLATURE

k_g =Filom mass transfer coefficient, m/s.
Ma =Molecular weight of component a, kg/mol.
M_i =Molecular weight of component i, kg/mol.
Re =Reynold Number ($=d_c V\rho/\mu$).
Sc =Schmidt number ($=\mu/(\rho \mathbb{D})$).
Sh =Sherwood Number ($=k_g d_c/\mathbb{D}$).
T =Temperature, °K.
y_a =Molar fraction of component a.
y_i =Molar fraction of component i.

Foreign Symbol

$\mathbb{D}_{ai}$ =Binary diffusion coefficient, m^2/s.
$\mathbb{D}_{a\text{-}m}$ =Diffusion coefficient of "a" in the gas mixture, m^2/s.
ρ =Density, kg/m^3.
μ =Viscosity, Pa/s.
μ_i =Viscosity of component i, Pa/s.
μ_m =Viscosity of gas mixture, Pa/s.
υ_i =Diffusion volume, m^3.

REFERENCES

Fuller, E.N., P.D. Schettler and J.C. Giddings, "A New Method for Prediction of Binary Gas-Phase Diffusion Coefficient", *Ind. Eng. Chem*, 1966, 58(5), p.18-27.

Li, J., "Rate Process during Gasification and Reduction of Kraft Black Liquor Char", *Ph.D. Thesis*, McGill University, Montreal.

Perry, R.H. and C.H. Chilton, *Chemical Engineers' Handbook*, 5th edition, McGraw-Hill, 1969, p.3-211 and 3-249.

Treybal, R.E., *Mass-Transfer Operation*, McGraw-Hill Book Company, N.Y., 2nd edition, 1968, p.24.